frontiers | Research Topics

Soil pollution, risk assessment and remediation

Edited by
Xiaokai Zhang, Williamson Gustave, Lizhi He
and Xing Yang

Published in
Frontiers in Environmental Science

ISSN 1664-8714
ISBN 978-2-8325-3139-6
DOI 10.3389/978-2-8325-3139-6

About Frontiers

Frontiers is more than just an open access publisher of scholarly articles: it is a pioneering approach to the world of academia, radically improving the way scholarly research is managed. The grand vision of Frontiers is a world where all people have an equal opportunity to seek, share and generate knowledge. Frontiers provides immediate and permanent online open access to all its publications, but this alone is not enough to realize our grand goals.

Frontiers journal series

The Frontiers journal series is a multi-tier and interdisciplinary set of open-access, online journals, promising a paradigm shift from the current review, selection and dissemination processes in academic publishing. All Frontiers journals are driven by researchers for researchers; therefore, they constitute a service to the scholarly community. At the same time, the *Frontiers journal series* operates on a revolutionary invention, the tiered publishing system, initially addressing specific communities of scholars, and gradually climbing up to broader public understanding, thus serving the interests of the lay society, too.

Dedication to quality

Each Frontiers article is a landmark of the highest quality, thanks to genuinely collaborative interactions between authors and review editors, who include some of the world's best academicians. Research must be certified by peers before entering a stream of knowledge that may eventually reach the public - and shape society; therefore, Frontiers only applies the most rigorous and unbiased reviews. Frontiers revolutionizes research publishing by freely delivering the most outstanding research, evaluated with no bias from both the academic and social point of view. By applying the most advanced information technologies, Frontiers is catapulting scholarly publishing into a new generation.

What are Frontiers Research Topics?

Frontiers Research Topics are very popular trademarks of the *Frontiers journals series*: they are collections of at least ten articles, all centered on a particular subject. With their unique mix of varied contributions from Original Research to Review Articles, Frontiers Research Topics unify the most influential researchers, the latest key findings and historical advances in a hot research area.

Find out more on how to host your own Frontiers Research Topic or contribute to one as an author by contacting the Frontiers editorial office: frontiersin.org/about/contact

Soil pollution, risk assessment and remediation

Topic editors
Xiaokai Zhang — Jiangnan University, China
Williamson Gustave — University of The Bahamas, Bahamas
Lizhi He — Zhejiang Agriculture and Forestry University, China
Xing Yang — Hainan University, China

Citation
Zhang, X., Gustave, W., He, L., Yang, X., eds. (2023). *Soil pollution, risk assessment and remediation*. Lausanne: Frontiers Media SA. doi: 10.3389/978-2-8325-3139-6

Table of contents

frontiers | Frontiers in Environmental Science

TYPE Editorial
PUBLISHED 18 July 2023
DOI 10.3389/fenvs.2023.1252139

OPEN ACCESS

EDITED AND REVIEWED BY
Oladele Ogunseitan,
University of California, Irvine,
United States

*CORRESPONDENCE
Williamson Gustave,
Williamson.Gustave@ub.edu.bs

RECEIVED 04 July 2023
ACCEPTED 07 July 2023
PUBLISHED 18 July 2023

CITATION
Zhang X, He L, Yang X and Gustave W (2023), Editorial: Soil pollution, risk assessment and remediation.
Front. Environ. Sci. 11:1252139.
doi: 10.3389/fenvs.2023.1252139

Editorial: Soil pollution, risk assessment and remediation

Xiaokai Zhang[1], Lizhi He[2], Xing Yang[3] and Williamson Gustave[4]*

[1]Institute of Environmental Processes and Pollution Control, School of Environmental and Civil Engineering, Jiangnan University, Wuxi, China, [2]Key Laboratory of Soil Contamination Bioremediation of Zhejiang Province, Zhejiang A & F University, Hangzhou, China, [3]Key Laboratory of Agro-Forestry Environmental Processes and Ecological Regulation of Hainan Province, College of Ecology and Environment, Hainan University, Haikou, China, [4]School of Chemistry, Environmental & Life Sciences, University of the Bahamas, Nassau, Bahamas

KEYWORDS

soil contamination, bioavailability, biogeochemistry, environmental toxicity, biochar

Editorial on the Research Topic
Soil pollution, risk assessment and remediation

Soil pollution is a global issue that poses serious threats to human and ecosystem health (Singh and Singh, 2020). Soils are crucial in providing numerous ecosystem services essential for sustaining life on Earth. However, the alarming reality is that we have been witnessing a rapid loss of the quality of our soils and the invaluable benefits they offer (Jie et al., 2002). For example, it has been estimated that 16.1% of soils are contaminated in China, as reported by the Chinese Ministry of Environmental Protection (MEP, 2014). Similar findings have been reported in the United States, where an estimated 294,000 sites require cleanup (USEPA, 2004), and in the United Kingdom, where it is estimated that 2% of the land area of England and Wales is contaminated (Environment Agency, 2009). These figures highlight the widespread nature of soil contamination and the urgent need for action to address this critical problem.

Anthropogenic activities are the primary source of soil contaminants. Both organic and inorganic pollutants can enter the soil matrix through various pathways, including the application of fertilizers and pesticides, improper disposal of wastewater, pharmaceuticals, plastics, and the burning of fossil fuels (Peña, 2022; Gautam et al., 2023). Once these pollutants have infiltrated the soil matrix, remediation becomes extremely challenging and costly. Moreover, they can pose significant health risks through the food chain. For instance, studies have demonstrated that heavy metals such as arsenic and cadmium reduce crop yields and severely impede crop quality and food security (Djahed et al., 2018; Yuan et al., 2021). Additionally, these organic and inorganic pollutants have been linked to serious illnesses in humans. Trace toxic metals like arsenic, lead, and cadmium have been associated with various types of cancers, while organic substances like polychlorinated biphenyls, polycyclic aromatic hydrocarbons, insecticides, and herbicides have been linked to various human diseases (Rahman et al., 2015).

To date, numerous studies have been conducted to address the soil pollution crisis by developing feasible risk assessment and remediation methods. Researchers have explored both biological and non-biological approaches to tackle this problem. The methods can be categorized as physical, chemical, and biological. Physical methods involve the physical removal, washing, encapsulation, and electrokinetic extraction contaminates in soil (Liu et al., 2018). Chemical methods include soil precipitation and solidification to immobilize and reduce pollutants bioavailability (Jiang et al., 2023). On the other hand, biological methods utilize plants and microorganisms to remove or transform pollutants into less toxic species. Among these approaches, biological methods are considered the most promising due to their ability to mitigate pollutants without generating secondary contaminants and their relative cost-effectiveness compared to physical methods (Gustave et al., 2022). Moreover, other techniques, such as the use of bioreporters, have focused on accurately assessing the risk posed by these contaminants (Zhang et al., 2022; Zhang et al., 2023).

Despite the significant amount of work that has been done on soil pollutant risk assessment and remediation, there is still a pressing need for further research in this field. Many existing methods are still in their infancy stages, and only a few have been implemented in real-world field settings. Additionally, there is a crucial requirement for more investigation into the risk assessment of soil and crop contamination resulting from these polluted soils. Recognizing this pressing need, a special focus was placed on this Research Topic, aiming to gather the latest studies that describe results pertaining to various areas, including but not limited to 1) Whole-cell bioreporter and biotic ligand model technology, 2) Bioavailability-based soil pollution risk assessment, 3) Utilization of biochar for soil remediation, 4) Investigation of biogeochemical behaviors of heavy metal(loid)s in soils, 5) Study of degradation, transformation, and immobilization of emerging organic pollutants in soils, and 6) Assessment of the impact of organic and/or inorganic soil amendments on the fate and transport of heavy metal(loid)s in agricultural soils.

A total of nine articles made significant contributions to the Research Topic, consisting of seven Original Research papers, one Brief Research Report, and one Review article. Xu et al. conducted a field study to investigate the effects of biochar and biochar-based fertilizers on soil properties, cadmium availability, and translocation in rice plants grown in cadmium-contaminated rice paddies. Similarly, Antonangelo et al. explored the potential of switchgrass and poultry litter biochar to immobilize and restrict the accumulation of heavy metals in ryegrass. Zhang et al. examined the use of various types of biochar, applied at low rates in the field, to mitigate cadmium contamination in *Brassica campestris* L. He et al. assessed the prevalence and risk of polycyclic aromatic hydrocarbons in top soils across China. Similarly, Maurin et al. presented a standardized extraction and analysis method to detect organic pollutants using samples from France. Dong et al. reported on the aggregation of organic amendments on bauxite residue particles and the associated mechanisms. Duan et al. focused on the effects of *Paenibacillus sabinae* and *Leptolyngbya* sp. RBD05 on the nutrient and chemical properties of saline-alkali soil. Lastly, Watson and Gustave assessed the potential risks associated with arsenic exposure from consuming market rice in The Bahamas, while Song et al. provided a review on the use of microalgae for wastewater remediation, soil improvement, and enhancement of crop quality.

Collectively, these studies greatly contribute to our understanding of soil pollution, its effects, and potential remediation strategies. Notably, the studies conducted by Xu et al., Zhang et al., and Antonangelo et al. provide valuable insights into the latest use of soil amendment, such as biochar, for effectively remediating cadmium and other trace toxic heavy metals. This is particularly crucial considering cadmium's ranking as the foremost heavy metal contaminant in Chinese soils (Zhao et al., 2015). Furthermore, the review by Song et al. and the studies by Duan et al. and Dong et al. shed further light on how microorganisms can play a vital role in bioremediation, establishing it as the most promising method. Additionally, other articles within this Research Topic present innovative standardized approaches for detecting organic pollutants, addressing a challenging issue that obstructs the accurate assessment of organic pollutants in soils. Lastly, the paper by Watson and Gustave unveils the extent of arsenic contamination in the market rice available in the Bahamas, a Small Island Developing State. While these articles have made significant contributions to our understanding of the subject, it is crucial to emphasize that substantial further research is required to tackle the pressing issue of soil pollution, mitigate associated human and ecological risks, and pave the way for effective solutions.

Author contributions

All authors listed have made a substantial, direct, and intellectual contribution to the work and approved it for publication.

Acknowledgments

We would like to extend our heartfelt appreciation to the numerous reviewers who generously volunteered their time to assist the authors in enhancing their manuscripts.

Conflict of interest

The authors declare that the research was conducted in the absence of any commercial or financial relationships that could be construed as a potential conflict of interest.

Publisher's note

References

Djahed, B., Taghavi, M., Farzadkia, M., Norzaee, S., and Miri, M. (2018). Stochastic exposure and health risk assessment of rice contamination to the heavy metals in the market of Iranshahr, Iran. *Food Chem. Toxicol.* 115, 405–412. doi:10.1016/j.fct.2018.03.040

Environment Agency (2009). *Reporting the evidence: Dealing with contaminated land in England and Wales: A review of progress from 2000–2007 with Part 2A of the environmental protection act*. Bristol, UK.

Gautam, K., Sharma, P., Dwivedi, S., Singh, A., Gaur, V. K., Varjani, S., et al. (2023). A review on control and abatement of soil pollution by heavy metals: Emphasis on artificial intelligence in recovery of contaminated soil. *Environ. Res.* 115592, 115592. doi:10.1016/j.envres.2023.115592

Gustave, W., Yuan, Z., Liu, F., and Chen, Z. (2021). Mechanisms and challenges of microbial fuel cells for soil heavy metal (loid) s remediation. *Sci. Total Environ.* 756, 143865. doi:10.1016/j.scitotenv.2020.143865

Jiang, M., He, L., Niazi, N. K., Wang, H., Gustave, W., Vithanage, M., et al. (2023). Nanobiochar for the remediation of contaminated soil and water: Challenges and opportunities. *Biochar* 5 (1), 2. doi:10.1007/s42773-022-00201-x

Jie, C., Jing, Z. C., Man, Z. T., and Zi, T. G. (2002). Soil degradation: A global problem endangering sustainable development. *J. Geogr. Scie.* 12, 243–252. doi:10.1007/bf02837480

Liu, L., Li, W., Song, W., and Guo, M. (2018). Remediation techniques for heavy metal-contaminated soils: Principles and applicability. *Sci. Total Environ.* 633, 206–219. doi:10.1016/j.scitotenv.2018.03.161

Ministry of Environmental Protection (MEP) (2014). *National soil contamination survey report*. Beijing, China: Ministry of Environmental Protection. Available at: http://www.mep.gov.cn/gkml/hbb/qt/201404/t20140417_270670.

Peña, A. (2022). A comprehensive review of recent research concerning the role of low molecular weight organic acids on the fate of organic pollutants in soil. *J. Hazard. Mat.* 434, 128875. doi:10.1016/j.jhazmat.2022.128875

Rahman, M. M., Dong, Z., and Naidu, R. (2015). Concentrations of arsenic and other elements in groundwater of Bangladesh and West Bengal, India: Potential cancer risk. *Chemosphere* 139, 54–64. doi:10.1016/j.chemosphere.2015.05.051

Singh, S. P., and Singh, M. K. (2020). "Soil pollution and human health," in *Plant responses to soil pollution*. Editors P. Singh, S. K. Singh, and S. M. Prasad (Singapore: Springer).

US Environmental Protection Agency (USEPA). (2004). *Cleaning up the nation's waste sites: Markets and technology trends*, Washington, DC

Yuan, H., Wan, Q., Huang, Y., Chen, Z., He, X., Gustave, W., et al. (2021). Warming facilitates microbial reduction and release of arsenic in flooded paddy soil and arsenic accumulation in rice grains. *J. Hazard. Mat.* 408, 124913. doi:10.1016/j.jhazmat.2020.124913

Zhang, X., Jiang, M., He, L., Niazi, N. K., Vithanage, M., Li, B., et al. (2023). Pandemic COVID-19 ends but soil pollution increases: Impacts and a new approach for risk assessment. *Sci. Total Environ.* 890, 164070. doi:10.1016/j.scitotenv.2023.164070

Zhang, X., Li, B., Schillereff, D. N., Chiverrell, R. C., Tefsen, B., and Wells, M. (2022). Whole-cell biosensors for determination of bioavailable pollutants in soils and sediments: Theory and practice. *Sci. Total Environ.* 811, 152178. doi:10.1016/j.scitotenv.2021.152178

Zhao, F. J., Ma, Y., Zhu, Y. G., Tang, Z., and McGrath, S. P. (2015). Soil contamination in China: Current status and mitigation strategies. *Environ. Sci. Technol.* 49 (2), 750–759. doi:10.1021/es5047099

frontiers | Frontiers in Environmental Science

TYPE Brief Research Report
PUBLISHED 04 October 2022
DOI 10.3389/fenvs.2022.1011785

Prevalence of arsenic contamination in rice and the potential health risks to the Bahamian population—A preliminary study

Carlton Watson[1]* and Williamson Gustave*,[2]

[1]Small Island Sustainability, University of The Bahamas, Nassau, Bahamas, [2]The School of Chemistry, Environmental & Life Sciences, University of The Bahamas, Nassau, Bahamas

Rice is among the most important staple foods worldwide. However, the consumption of rice and rice-based food products poses a potential health risk since rice is a paddy crop that is well known to accumulate high concentrations of arsenic (As) in its grain. In The Bahamas, although rice is heavily consumed, it is not grown locally. Instead, all the consumed rice and its derived products are imported. Recent food surveys in the major rice exporting countries have shown that a significant portion of their market rice products is contaminated with As. However, to date, the prevalence of As in the rice foods available in The Bahamas remains unknown. Therefore, in this study, we surveyed the occurrence of As in a selection of rice and rice products that were on sale in the Bahamian market. A total of 21 different rice brands were collected. The concentration of As and the potential health risk were estimated by target hazard quotient (THQ), hazard index (HI), and lifetime cancer risk (LCR). Our results showed that only the blue ribbon samples had an estimated inorganic arsenic (iAs) concentration above the World Health Organization (WHO) safety limits (200 μg/kg), which is based on global average consumption. However, when we factor for average rice consumption in The Bahamas, 79% of the rice samples had iAs concentration values indicative of carcinogenic risks and 57% had iAs concentration values that suggested non-carcinogenic health risks. Based on our results, we recommend urgent follow-up studies to further test rice varieties that show the greatest LCR and HI values and to also broaden the study to include more off-brand/generic varieties, cooked rice, and drinking water.

KEYWORDS

food safety, arsenic, risk assessment, Bahamas, contamination

Check for updates

OPEN ACCESS

EDITED BY
Debapriya Mondal,
St George's University of London,
United Kingdom

REVIEWED BY
Bhagwan Singh Chandravanshi,
Addis Ababa University, Ethiopia
Poonam Yadav,
Banaras Hindu University, India

*CORRESPONDENCE
Carlton Watson,
Carlton.watson@ub.edu.bs,
Cwatson1@gmail.com
Williamson Gustave,
Gutsavewill@hotmail.com,
Williamson.Gustave@ub.edu.bs

SPECIALTY SECTION
This article was submitted to
Toxicology, Pollution and the
Environment,
a section of the journal
Frontiers in Environmental Science

RECEIVED 04 August 2022
ACCEPTED 12 September 2022
PUBLISHED 04 October 2022

CITATION
Watson C and Gustave W (2022),
Prevalence of arsenic contamination in
rice and the potential health risks to the
Bahamian population—A
preliminary study.
Front. Environ. Sci. 10:1011785.
doi: 10.3389/fenvs.2022.1011785

1 Introduction

Rice is one of the world's most important staple foods on the international market and supplies more than 50% of the world's caloric intake (Clemens et al., 2013; Majumder and Banik, 2019). However, rice consumption poses a major health risk since the soils on which rice is normally grown are polluted with As (Zhao et al., 2014; Zeng et al., 2015; Liu et al., 2016). As an illustration, rice have been identified as a major route of dietary exposure to carcinogens such as As (Clemens et al., 2013; Gonzalez et al., 2020). Arsenic has been shown to induce a variety of serious health effects and has been linked to various cancers in humans (Majumder and Banik, 2019; Oberoi et al., 2019; Arcella et al., 2021).

In The Bahamas, rice is the main staple food and is imported from other countries. According to the most recently available trade data, in 2018, net imports of rice to The Bahamas were 7,172,780 kg. Since rice is not grown in The Bahamas per capita consumption is assumed to be approximately 18.6 kg (WITS, 2018). According to the United States Department of Agriculture (USDA), of the nearly 505.4 million tons of rice produced in 2021, the bulk was produced in Asia, and 149.0 million tonnes came from China (Childs, 2022; Childs and LeBeau, 2022). Though the United States of America (USA) only produced a small fraction of the rice, the US was ranked as the third largest exporter of rice, exporting $1.9 billion worth of rice in 2021 alone (USDA, 2021). Recent rice surveys have shown that a significant amount of rice exceeded the WHO standard for As (Zavala et al., 2008; Meharg et al., 2009; Rowell et al., 2014; Lee et al., 2018; Dai et al., 2022). As an illustration, Meharg et al. (2009) reported that polished white rice available in the American and French markets on average had 0.25 mg/kg and 0.28 mg/kg As in their gains, respectively. Moreover, similar results were obtained in a study carried out in Jamaica where the white and brown rice samples had As concentrations ranging from 0.110 to 0.487 mg/kg and 0.082–0.250 mg/kg, respectively (Antoine et al., 2012).

These results raise a serious concern about the potential risk of dietary exposure to As, especially from the consumption of rice among the Bahamian people. This is of particular importance given that plain rice, peas/bean, and rice are ranked among the most consumed staple foods in The Bahamas. Although market rice surveys have been conducted in other jurisdictions (Jorhem et al., 2008; Food and Agriculture Organization of the United Nations, 2014; Chen et al., 2018), to the best of our knowledge, a survey of As contamination in rice available in The Bahamas has not been carried out. Therefore, the main aims of this study were to investigate the prevalence of As contamination in market rice available on the Bahamian market and to estimate the associated As health risks. Thus, in this study, we tested 42 rice varieties on the Bahamian market for As. We also calculated the As target hazard quotient (THQ), hazard index (HI), and lifetime cancer risk (LCR) values for all samples based on WHO and/or the European Food Safety Authority (EFSA) standards. The findings of this study are anticipated to serve as a preliminary assessment of potential health risks associated with consuming Bahamian market rice.

2 Methods

2.1 Measurements

2.1.1 Sample collection

Imported rice samples were collected from the major grocery stores in New Providence Island including Super Value Food Store, Quality Supermarkets, John Chea Food Store, and Extra Value. A total of 71 samples were purchased, accounting for 21 different brands and 42 varieties (Supplementary Tables S1, S2). For the purpose of this study, we refer to "variety" as a particular brand and type; therefore, Mahatma long grain and Extra long grain would be considered as two different varieties.

2.1.2 Rice sample preparation

The bag was agitated, and a 10 g of rice sample was poured out into a clean Petri dish. The rice grains were ground and digested following the technique utilized by Williams et al. (2009). Briefly, 0.5 g of rice powder sample was digested using 10 ml of a 1:1 ratio of HNO_3 and H_2O_2 in a 50-ml polypropylene digestion tube. The samples were microwave digested in a MARS 6TM Microwave Digestion System (CEM, United States). First, the samples were heated to 55°C and held for 10 min, and then the temperature was increased to 75°C for 10 min. Lastly, the samples were heated to 95°C and digested at this temperature for 30 min. The digested samples were then filtered through a 0.45-µm filter and diluted with deionized water. To determine the As speciation, 1.5 g of ground rice powder was extracted with 15 ml of 0.28 M of HNO_3 at 95°C for 90 min in 50 ml of polypropylene. Heating blocks were used to maintain the samples at 95°C for 90 min**.**

2.1.3 Sample analysis

The total heavy metal and As concentrations of the rice samples were analyzed using inductively coupled plasma mass spectrometry (ICP-MS, NexION 300X, Perkin Elmer, US). The As speciation (to determine percentages of inorganic and organic arsenic) was determined using ion chromatography with inductively coupled plasma mass spectrometry (IC-ICP-MS) as described in the literature (Yuan et al., 2021). Briefly, the IC used in this study was equipped with a standard 25 µL sample loop and an anion-exchange column. The As species were separated using 20 mmol L^{-1} NH_4HCO_3 at pH 10 as the mobile phase at a flow rate of 1.0 ml min^{-1}. All standard curves were prepared in neutral conditions. A rice reference (GBW€080684) purchased from the National Research Centre of China was used to determine the accuracy of the analytical method. The rice sample recoveries of total As were within the range of 95.55–105.5% (n = 5).

2.2 Risk assessment analysis

2.2.1 Estimated daily intake

The EDI of the As by rice consumption was calculated using the following equation:

$$EDI = (C \times Con \times EF \times ED)/(Bw \times AT),$$

where C is the concentration of the As (μg/g) in the rice sample, Con is the daily average consumption of rice (g/person/day), EF is the exposure frequency (365 days/year), ED is the exposure duration (70 years), Bw is the average body weight (kg person^{-1}), and AT is the average time exposure for non-carcinogens (365 days ×70) (Antoine et al., 2012; Chen et al., 2018). An average body weight of 82.0 kg (based on reported BMI values for The Bahamas) (World Bank, 2022) was assumed.

2.3 Carcinogenic risk

2.3.1 Lifetime cancer risk

The potential of developing cancer is expressed in terms of LCR. The following equation was used to estimate the LRC:

$$\mathrm{LCR} = \mathrm{EDI} \times \mathrm{SF},$$

where SF is the cancer slope factor for a contaminant. This constant is proportional to the likelihood of a contaminant promoting cancer over a lifetime. It can be estimated from epidemiological studies or animal trials. In this study, the cancer slope factor used for iAs is 1.5 mg/kg per day. This value is a standard constant used in the absence of local epidemiological studies and was obtained from the Integrated Risk Information System (IRIS), which is prepared and maintained by the US Environmental Protection Agency (US Environmental Protection Agency-USEPA, 2007) (EPA, 2007). LCR values of below 1×10^{-4} are deemed acceptable according to US EPA standards (US Environmental Protection Agency-USEPA- National Center for Environmental Assessment, Office of Research and Development, 1986).

2.4 Non-carcinogenic risk

2.4.1 Target hazard quotient

The potential non-carcinogenic risks of As can be expressed as THQ, which is the ratio of EDI for As to its oral reference dose (RfD). The RfD varies for each element, and the value used for As was 0.3 μg/kg per day. The following equation was used to estimate the THQ:

$$THQ = EDI/RfD.$$

A THQ value less than one indicates that there is no significant risk of non-carcinogenic effects to the consumer. However, a THQ exceeding one indicates a potential risk of non-carcinogenic effects (US Environmental Protection Agency-USEPA- National Center for Environmental Assessment, Office of Research and Development, 1986; EPA, 2007).

2.4.2 Hazard index

The hazard index (HI) gives the cumulative effect of multiple metal/metalloid contaminants since rice grains may be contaminated with two or more contaminants; therefore, it is important to take into account the additive and/or interactive effects that may result from the exposure of two or more contaminants (Salama and Radwan, 2005; Dai et al., 2016; Brathwaite and Mohammed, 2018). However, our preliminary results indicate that the HI contribution from other metals was negligible, so we take HI to be approximately equal to $\mathrm{THQ}_{\mathrm{iAs}}$, that is:

$$HI = \sum_{n=1}^{i} THQ_n \approx THQ_{iAs} \ ,$$

where THQ_n is the THQ value of element n and $\mathrm{THQ}_{\mathrm{iAs}}$ equals the contribution from inorganic arsenic.

2.5 Statistical analysis

Statistical analysis was performed using Excel 2022 and Origin 2017 (Origin Lab Corporation, United States). Preliminary data processing was accomplished using Excel 2022, and the figure was drawn using Origin 2017.

3 Results and discussion

The aim of this study was to measure the As concentration and to estimate the associated As health risks of consuming different rice varieties available on the Bahamian market. Our results showed a large variation in As contaminants in rice grain across the Bahamian market, ranging from 4.85 to 269.4 μg kg^{-1} with an average of 88.4 μg kg^{-1}. A similar average As concentration of 87.0 μg kg^{-1} was reported by Praveena and Omar (2017) from Malaysia. As shown in Figures 1A and B, only one of the 42 rice varieties contained an estimated iAs concentration above the WHO (200 μg/kg body weight) safety limits after accounting for the organic As portion (Supplementary Figure S1) (Meharg et al., 2009; Moe et al., 2016). It is important to note that the sample containing iAs above the permissible limit was unpolished. The elevated As in the rice grain may be due to the presence of the bran layer and

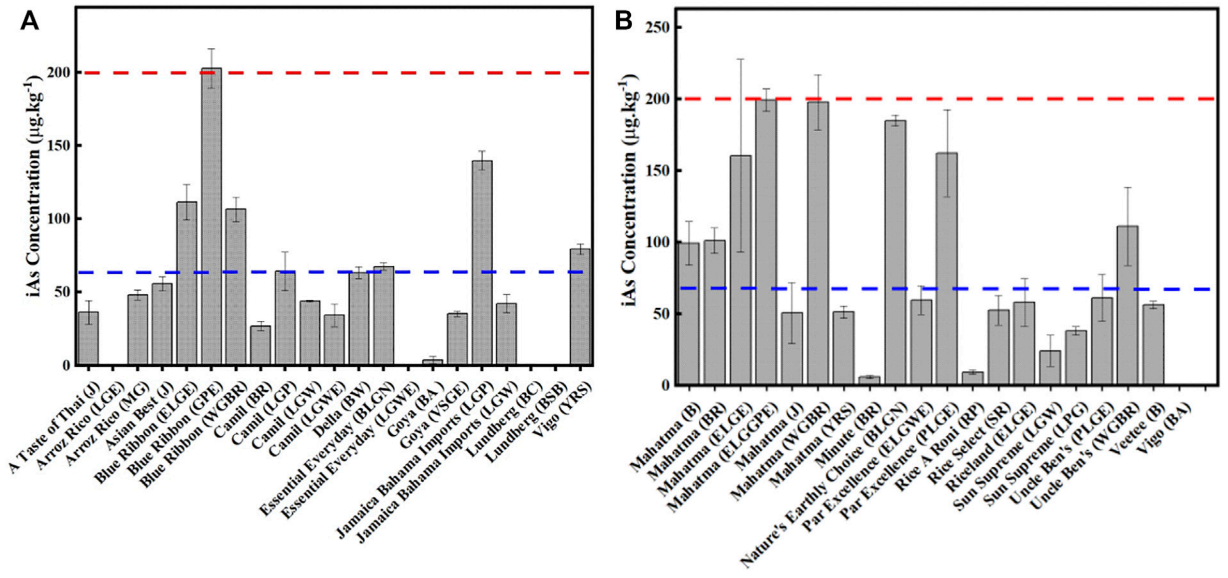

FIGURE 1
(A,B) Estimated inorganic arsenic (iAs) content in commonly found rice and rice products. The red line indicates the maximum threshold of iAs content as determined by WHO. The blue line indicates the average of the 42 rice varieties.

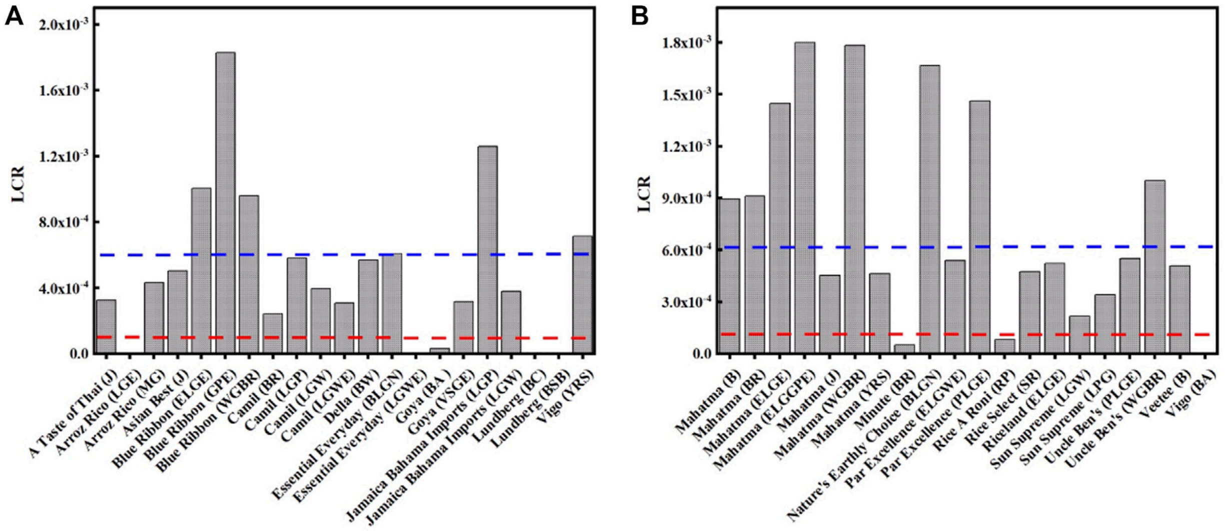

FIGURE 2
(A,B) Estimated lifetime cancer risk of various rice varieties based on a cancer slope function for iAs of 1.5 mg/kg per day. The red line denotes recommended threshold of 1.4 × 10^{-4}, and the blue line denotes the average value of 6 × 10^{-4} based on all LCR values for all 42 varieties.

cereal germ (Chen et al., 2018; Majumder and Banik, 2019). Previous studies have shown that a large portion of trace contaminants, especially As, is accumulated in the rice husk (Chen et al., 2018; Majumder and Banik, 2019). Thus, it is speculated that the unpolished rice had a higher concentration of As than the polished rice due to the presence of the husk. Although a large portion of the Mahatma rice brand (43%) contained total As above the maximum permissible limits established by WHO, it should be noted that 20–50% of the total As consisted of the non-toxic dimethylarsinic acid (DMA).

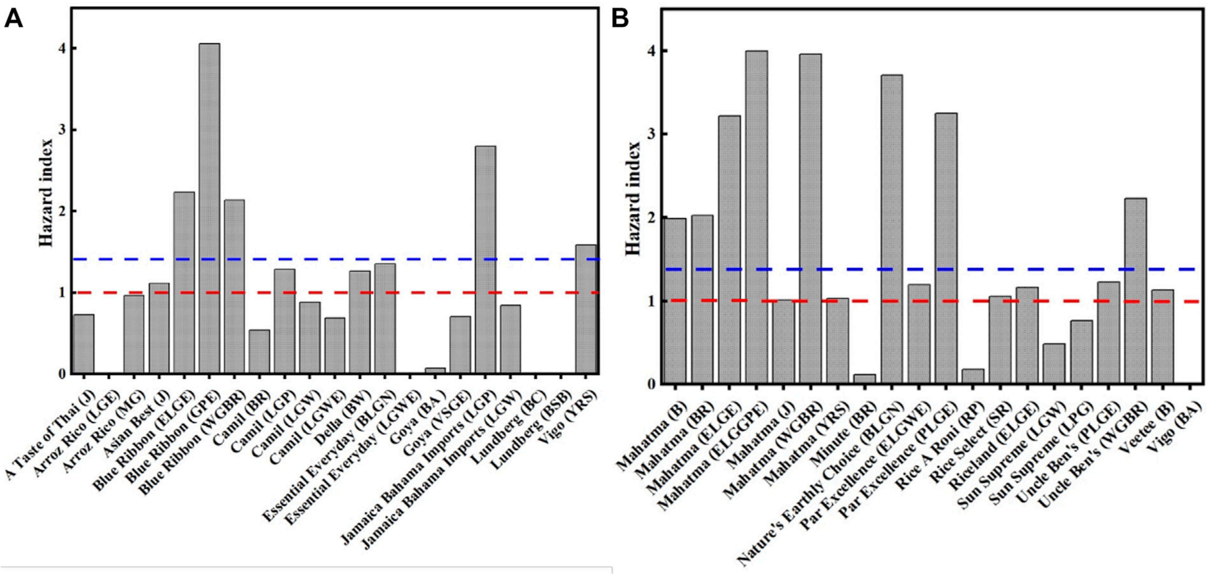

FIGURE 3
(A,B) Hazard index for all rice varieties under the assumption that HI ≈ THQ_{iAs}. The blue line indicates the average HI value of the overall 42 rice varieties. HI values above 1 indicate non-carcinogenic risks.

DMA has been reported to be less toxic to humans and is therefore not taken into consideration when estimating health risks associated with consuming rice (Moe et al., 2016). Thus, this significantly reduces the non-cancerogenic risk of consuming the Mahama rice product, since only iAs is considered when calculating such risks (Liao et al., 2018).

Rice is widely consumed in The Bahamas as one of the main staple foods, and this may pose a health risk as rice consumption is recognized as one of the main routes of human exposure to As. Therefore, increasing rice consumption will result in increased exposure and risk of As contamination to Bahamian consumers. Our preliminary results show that on average, an adult living in The Bahamas consumes 486.5 g of rice per day, which is comparable to what is consumed in China and East Asia (Qian et al., 2010; Fu et al., 2015; Dai et al., 2016; Liao et al., 2018). The EDI and THQ values for As are shown in Figures 2A and B and Figures 3A and B. Approximately 79% and 57% of the samples had carcinogenic and non-carcinogenic risk, respectively, above WHO/US EPA guidelines (Figures 2A and B and Figures 3A and B) for As. This discrepancy between iAs concentration and health risk is due to relatively high rice consumption in The Bahamas. Djahed et al. (2018) observed a similar carcinogenic risk in rice available in the city of Iranshahr, Iran market.

To be clear, in arriving at our values, we have assumed a constant iAs percentage of 75% of total As across all rice varieties. Although we have performed speciation measurements on multiple samples with iAs ranging from 40% to 97% (Supplementary Figure S1), we note the large variation in iAs speciation samples of the same brand varieties bought at different grocery stores. In two of the three cases where the same brand varieties were measured, iAs speciation percentages differed by approximately 20%. Given this, we have opted to use the constant 75% until further measurements with larger data sets can be performed. We cannot overemphasize the large uncertainties in arriving at our results and, therefore, the need to proceed with caution when interpreting these results and also the need for follow-up studies.

For example, the R*f*D, which is used to calculate non-carcinogenic risk, is an estimate with assumed uncertainties that could span an order of magnitude. Furthermore, the cancer slope factor used is subject to large uncertainties since it is based on a more than forty-year-old study of skin cancer in Taiwanese citizens (Tseng et al., 1968; Tseng, 1977). Although this value is commonly used to calculate broad carcinogenic risk, it is possible to determine better estimates for The Bahamas. However, this would require significant resources and long-term epidemiological studies. What is more achievable and useful in the short term is a national total diet study for The Bahamas.

This study is, to the best of our knowledge, the first of its kind in The Bahamas and served as a preliminary evaluation of As in various rice grains sold locally for potential health risks due to consumption. Although potential health risks were found, further studies should be conducted to corroborate these findings. It is also important to note that rice is just one source of As contaminants in staple foods. Additional studies of water and cereals are likely to reveal additional risks from those sources. Therefore, continuous monitoring and regular evaluation of the Bahamian marketed rice products, cereals, and water are recommended.

4 Conclusions and future prospects

Various brands of Bahamian marketed rice and rice products were investigated for their As content. Arsenic was determined to be the major contributor to human health risk. Our results showed that 2% of the samples had an estimated iAs concentration above the WHO (200 μg/kg) safety limits. Average As concentration values across all rice varieties suggest both carcinogenic and non-carcinogenic risks. However, these risks appear to be driven by consumption patterns rather than relatively high As contamination levels. This study is the first of its kind in The Bahamas and served as a preliminary evaluation of As in various rice grains sold locally for potential health risks due to consumption. Nonetheless, the results obtained here are subject to large uncertainties, and care should be exercised in the interpretation. Given the large incidences of obesity and cancer within The Bahamas, as well as the prevalence of rice in the Bahamian typical diet, follow-up studies would help to elucidate the role that rice, As, and other metalloids play in promoting disease and mortality in The Bahamas. In terms of immediate next action steps, we recommend the following:

1) Replicate parts of this study to focus on those varieties with the highest levels of inorganic arsenic. Similar results may justify the need for urgent action.
2) Expand the study to examine metal contaminants in cooked rice from various restaurants and eateries. This may give a more accurate representation of consumption levels of metal contaminants.
3) Conduct a survey to get a better understanding of the consumption patterns of rice and rice-based products. Rice products consumed by infants and children should be given particular attention since the effects of inorganic arsenic on infants and children have been shown to be more pronounced.
4) Expand the study to determine the effects of washing rice as well as cooking rice in a high water to rice ratio on levels of arsenic.
5) Conduct future studies on rice-based products especially those consumed by infants and children.

Data availability statement

The raw data supporting the conclusions of this article will be made available by the authors, without undue reservation.

Author contributions

CW and WG contributed to the design and implementation of the research, to the analysis of the results, and to the writing of the manuscript.

Funding

This work was financially supported by The Bahamas Agricultural Health and Food Safety Authority.

Acknowledgments

We are grateful to Patricia J. Johnson, Director of the Food Safety and Quality Unit, Bahamas Agricultural Health and Food Safety Authority, for her insightful comments and suggestions. The authors are also grateful to Chen Zheng and eBiogeochemistry Lab for analyzing the rice samples.

Conflict of interest

The authors declare that the research was conducted in the absence of any commercial or financial relationships that could be construed as a potential conflict of interest.

Publisher's note

Supplementary material

The Supplementary Material for this article can be found online at: https://www.frontiersin.org/articles/10.3389/fenvs.2022.1011785/full#supplementary-material

References

Antoine, J. M., Fung, L. A. H., Grant, C. N., Dennis, H. T., and Lalor, G. C. (2012). Dietary intake of minerals and trace elements in rice on the Jamaican market. *J. Food Compos. Analysis* 26 (1-2), 111–121. doi:10.1016/j.jfca.2012.01.003

Arcella, D., Cascio, C., and Gómez Ruiz, J. Á.European Food Safety Authority (EFSA) (2021). Chronic dietary exposure to inorganic arsenic. *EFSA J.* 19 (1), e06380. doi:10.2903/j.efsa.2021.6380

Brathwaite, J., and Mohammed, F. K. (2018). A preliminary health risk assessment of heavy metals in local and imported rice grains marketed in Trinidad and Tobago, WI. *Hum. Ecol. Risk Assess. An Int. J.* 26, 295–309. doi:10.1080/10807039.2018.1508328

Chen, H., Tang, Z., Wang, P., and Zhao, F. J. (2018). Geographical variations of cadmium and arsenic concentrations and arsenic speciation in Chinese rice. *Environ. Pollut.* 238, 482–490. doi:10.1016/j.envpol.2018.03.048

Childs, N. W., and LeBeau, B. (2022). *Rice outlook: February 2022*. USA: USDA. Available at: https://www.ers.usda.gov/webdocs/outlooks/103260/rcs-22b.pdf?v=7140.8.

Childs, N. W. (2022). *Rice outlook: May 2021*. USA: USDA. Available at: https://www.ers.usda.gov/webdocs/outlooks/101196/rcs-21d.pdf?v=2388.7.

Clemens, S., Aarts, M. G., Thomine, S., and Verbruggen, N. (2013). Plant science: The key to preventing slow cadmium poisoning. *Trends Plant Sci.* 18 (2), 92–99. doi:10.1016/j.tplants.2012.08.003

Dai, H., Song, X., Huang, B., and Xin, J. (2016). Health risks of heavy metals to the general public in Hengyang, China, via consumption of rice. *Hum. Ecol. Risk Assess.Int. J.* 22 (8), 1636–1650. doi:10.1080/10807039.2016.1207156

Dai, J., Tang, Z., Gao, A. X., Planer-Friedrich, B., Kopittke, P. M., Zhao, F. J., et al. (2022). Widespread occurrence of the highly toxic dimethylated monothioarsenate (DMMTA) in rice globally. *Environ. Sci. Technol.* 56 (6), 3575–3586. doi:10.1021/acs.est.1c08394

Djahed, B., Taghavi, M., Farzadkia, M., Norzaee, S., and Miri, M. (2018). Stochastic exposure and health risk assessment of rice contamination to the heavy metals in the market of Iranshahr, Iran. *Food Chem. Toxicol.* 115, 405–412. doi:10.1016/j.fct.2018.03.040

EPA (2007). Arsenic, inorganic (CASRN 7440-38-2).

Food and Agriculture Organization of the United Nations. (2014). Rice market monitor. Available from: http://www.fao.org/economic/RMM. Accessed September 1, 2014.

Fu, Q. L., Li, L., Achal, V., Jiao, A. Y., and Liu, Y. (2015). Concentrations of heavy metals and arsenic in market rice grain and their potential health risks to the population of Fuzhou, China. *Hum. Ecol. Risk Assess.Int. J.* 21 (1), 117–128. doi:10.1080/10807039.2014.884398

González, N., Josep, C., Antoni, R., Bosch, J., Timoner, I., and Castell, V. (2020). Dietary exposure to total and inorganic arsenic via rice and rice-based products consumption. *Food Chem. Toxicol.* 141, 111420.

Jorhem, L., Åstrand, C., Sundström, B., Baxter, M., Stokes, P., Lewis, J., et al. (2008). Elements in rice from the Swedish market: 1. cadmium, lead and arsenic (total and inorganic). *Food Addit. Contam. Part A* 25 (3), 284–292. doi:10.1080/02652030701474219

Lee, S. G., Lee, Y. S., Cho, S. Y., Chung, M. S., Cho, M., Kang, Y., et al. (2018). Monitoring of arsenic contents in domestic rice and human risk assessment for daily intake of inorganic arsenic in Korea. *J. Food Compos. Analysis* 69, 25–32. doi:10.1016/j.jfca.2018.02.004

Liao, N., Seto, E., Eskenazi, B., Wang, M., Li, Y., and Hua, J. (2018). A comprehensive review of arsenic exposure and risk from rice and a risk assessment among a cohort of adolescents in Kunming, China. *Int. J. Environ. Res. Public Health* 15 (10), 2191. doi:10.3390/ijerph15102191

Liu, G., Wang, J., Zhang, E., Hou, J., and Liu, X. (2016). Heavy metal speciation and risk assessment in dry land and paddy soils near mining areas at southern China. *Environ. Sci. Pollut. Res.* 23 (9), 8709–8720. doi:10.1007/s11356-016-6114-6

Majumder, S., and Banik, P. (2019). Geographical variation of arsenic distribution in paddy soil, rice and rice-based products: A meta-analytic approach and implications to human health. *J. Environ. Manag.* 233, 184–199. doi:10.1016/j.jenvman.2018.12.034

Meharg, A. A., Williams, P. N., Adomako, E., Lawgali, Y. Y., Deacon, C., Villada, A., et al. (2009). Geographical variation in total and inorganic arsenic content of polished (white) rice. *Environ. Sci. Technol.* 43 (5), 1612–1617. doi:10.1021/es802612a

Moe, B., Peng, H., Lu, X., Chen, B., Chen, L. W., Gabos, S., et al. (2016). Comparative cytotoxicity of fourteen trivalent and pentavalent arsenic species determined using real-time cell sensing. *J. Environ. Sci.* 49, 113–124. doi:10.1016/j.jes.2016.10.004

Oberoi, S., Devleesschauwer, B., Gibb, H. J., and Barchowsky, A. (2019). Global burden of cancer and coronary heart disease resulting from dietary exposure to arsenic, 2015. *Environ. Res.* 171, 185–192. doi:10.1016/j.envres.2019.01.025

Praveena, S. M., and Omar, N. A. (2017). Heavy metal exposure from cooked rice grain ingestion and its potential health risks to humans from total and bioavailable forms analysis. *Food Chem. x.* 235, 203–211. doi:10.1016/j.foodchem.2017.05.049

Qian, Y., Chen, C., Zhang, Q., Li, Y., Chen, Z., and Li, M. (2010). Concentrations of cadmium, lead, mercury and arsenic in Chinese market milled rice and associated population health risk. *Food control.* 21 (12), 1757–1763. doi:10.1016/j.foodcont.2010.08.005

Rowell, C., Kuiper, N., Al-Saad, K., Nriagu, J., and Shomar, B. (2014). A market basket survey of as, Zn and Se in rice imports in Qatar: health implications. *Food Chem. Toxicol.* 70, 33–39. doi:10.1016/j.fct.2014.04.041

Salama, A. K., and Radwan, M. A. (2005). Heavy metals (cd, pb) and trace elements (cu, zn) contents in some foodstuffs from the Egyptian market. *Emir. J. Food Agric.* 17, 34–42. doi:10.9755/ejfa.v12i1.5046

Tseng, W. P., Chu, H., How, S. W., Fong, J. M., Lin, C. S., and Yeh, S. H. U. (1968). Prevalence of skin cancer in an endemic area of chronic arsenicism in Taiwan. *J. Natl. Cancer Inst.* 40 (3), 453–463.

Tseng, W. P. (1977). Effects and dose-response relationships of skin cancer and Blackfoot disease with arsenic. *Environ. health Perspect.* 19, 109–119. doi:10.1289/ehp.7719109

United States Department of Agriculture (2021). U.S. Rice exports in 2021. Available at: https://www.fas.usda.gov/commodities/rice

US Environmental Protection Agency-USEPA- National Center for Environmental Assessment, Office of Research and Development (1986). Guidelines for the health risk assessment of chemical mixtures *(Fed Reg 51: 34014–25.* Washington, DC: US EPA Federal Registry.

US Environmental Protection Agency-USEPA (2007). *Concepts, methods and data sources for cumulative health risk assessment of multiple chemicals, exposures and effects: A resource document*. Cincinnati, OH: US EPA Federal Registry. (EPA/600/R-06/013F).

Williams, P. N., Lei, M., Sun, G., Huang, Q., Lu, Y., Deacon, C., et al. (2009). Occurrence and partitioning of cadmium, arsenic and lead in mine impacted paddy rice: Hunan, China. *Environ. Sci. Technol.* 43 (3), 637–642. doi:10.1021/es802412r

WITS 2018 The Rice imports by country in 2018. Available at: https://wits.worldbank.org/trade/comtrade/en/country/BHS/year/2018/tradeflow/Imports/partner/ALL/product/1006

World Bank 2022 Gender statitics. Available at: https://databank.worldbank.org/reports.aspx?source=283&series=SH.STA.OB18.MA.ZS

Yuan, Z. F., Gustave, W., Boyle, J., Sekar, R., Bridge, J., Ren, Y., et al. (2021). Arsenic behavior across soil-water interfaces in paddy soils: coupling, decoupling and speciation. *Chemosphere* 269, 128713. doi:10.1016/j.chemosphere.2020.128713

Zavala, Y. J., Gerads, R., Gürleyük, H., and Duxbury, J. M. (2008). Arsenic in rice: II. Arsenic speciation in USA grain and implications for human health. *Environ. Sci. Technol.* 42 (10), 3861–3866. doi:10.1021/es702748q

Zeng, F., Wei, W., Li, M., Huang, R., Yang, F., and Duan, Y. (2015). Heavy metal contamination in rice-producing soils of Hunan Province, China and potential health risks. *Int. J. Environ. Res. Public Health* 12 (12), 15584–15593. doi:10.3390/ijerph121215005

Zhao, F. J., Ma, Y., Zhu, Y. G., Tang, Z., and McGrath, S. P. J. E. (2014). Soil contamination in China: Current status and mitigation strategies. *Environ. Sci. Technol.* 49 (2), 750–759. doi:10.1021/es5047099

Frontiers in Environmental Science

TYPE Review
PUBLISHED 12 October 2022
DOI 10.3389/fenvs.2022.1035332

OPEN ACCESS

EDITED BY
Xiaokai Zhang,
Jiangnan University, China

REVIEWED BY
Ahmed Abdelhafez,
The New Valley University, Egypt
Jianhua Fan,
East China University of Science and
Technology, China

*CORRESPONDENCE
Qingshan Xu,
ljchber@163.com
Pengfei Cheng,
chengpengfei@nbu.edu.cn

SPECIALTY SECTION
This article was submitted
to Soil Processes,
a section of the journal
Frontiers in Environmental Science

RECEIVED 02 September 2022
ACCEPTED 27 September 2022
PUBLISHED 12 October 2022

CITATION
Song X, Bo Y, Feng Y, Tan Y, Zhou C,
Yan X, Ruan R, Xu Q and Cheng P (2022),
Potential applications for
multifunctional microalgae in
soil improvement.
Front. Environ. Sci. 10:1035332.
doi: 10.3389/fenvs.2022.1035332

Potential applications for multifunctional microalgae in soil improvement

Xiaotong Song[1], Yahui Bo[1], Yanzhang Feng[1], Yinghong Tan[2], Chengxu Zhou[1], Xiaojun Yan[3], Roger Ruan[4], Qingshan Xu[2]* and Pengfei Cheng[1]*

[1]College of Food and Pharmaceutical Sciences, Ningbo University, Ningbo, Zhejiang, China, [2]Lijiang Cheng Hai Bao Er Biological Development Co., Ltd., Lijiang, Yunnan, China, [3]Key Laboratory of Marine Biotechnology of Zhejiang Province, Ningbo University, Ningbo, Zhejiang, China, [4]Center for Biorefining, and Department of Bioproducts and Biosystems Engineering, University of Minnesota-Twin Cities, Saint Paul, MN, United States

Soil is the basis of agricultural production, and the quality of soil directly affects crop quality and yield. Microalgae can carry out photosynthesis, carbon and nitrogen fixation, and produce large amounts of valuable biomass coupled with wastewater treatment. Also, microalgae can produce plant hormones and other high-value products, which can promote plant growth, improve soil fertility, soil ecological health, and control crop diseases. This research reviews the characteristics of microalgae in improving soil health, discusses the situation of microalgae in controlling soil pollutants, elaborates on the technical application of microalgae in alleviating soil problems, and proposes potential applications of microalgae in ecological environment. Also, resource utilization of multifunctional microalgae is discussed, to provide a theoretical basis for the application of microalgae in soil improvement.

KEYWORDS

microalgae, soil fertility, characteristic pollutants, crop diseases, ecological environment protection

Introduction

Soil is the basic substance of the earth's ecosystem, and an indispensable resource for economic and social development. Soil health is an important part of ecosystem health. As we know, the health soil can grow various products that benefit human health, it can improve the quality of water and the atmosphere, and has a certain degree of anti-pollution capability (Jun et al., 2018). Soil pollution is a 'centralized', 'complex' and 'explosive' problem, and would reduce the soil quality and productivity of cultivated land and thus directly endangers food safety, ecological security, and human health (Nematollahi et al., 2020). It also pollutes groundwater through water conservancy, which seriously damages the stability of soil ecosystems (Perez-Lucas et al., 2019).

Algae include macroalgae and microalgae, while microalgae are a class of low-grade organisms, small in size, simple in structure, but with high photosynthetic efficiency. Microalgae are widely distributed in different habitats, such as soil, oceans, rivers, lakes, and even extreme environments (high salinity, low pH, high temperature, etc.) (Jun et al., 2016; Little et al., 2021). About 40,000 different species of microalgae exist on earth and account for about 20%–30% of the unknown algae in the world (Dahiya, 2015). Microalgae include eukaryotes such as diatoms and green algae, and prokaryotes such as cyanobacteria, which offer the following advantages as soil biofertilizer, owing to their specific characteristics: 1) They can prevent nutrient loss by slowly releasing nitrogen, phosphorus, and potassium to meet the growth needs of plants (Coppens et al., 2016; Sasaki et al., 2020). 2) They also contain trace elements and substances that promote plant growth, such as plant hormones, vitamins, carotenoids, amino acids, and antifungal substances (Silva et al., 2019). These substances can promote crop growth and improve soil fertility. 3) Microalgae reproduce quickly and can be cultivated on a large scale, and their biomass can be directly used for soil inoculation without polluting the surrounding environment. They can also reclaim damaged soil, such as desertified soil and saline-alkali land (Wu et al., 2022).

In recent years, the overuse of fossil fuels has greatly increased energy consumption, as well as the adverse impact of industrial waste on the environment. Apart from industrial waste, agricultural waste is also a major cause of water pollution. Compared with other physical and chemical treatment methods, microalgae biotechnology is a promising method with important potential, to address the energy crisis and wastewater treatment (Randrianarison and Ashraf, 2017; Wollmann et al., 2019).

Moreover, carbon neutrality has become a consensus goal in the global response to climate change, but many challenges to achieve this goal still exist. The novel microalgae can use solar energy to efficiently fix CO_2 through photosynthesis; they can convert and fix organic carbon through heterotrophic assimilation and convert them into biofuels, biomaterials, and biofertilizers to replace the use of fossil fuels, plastics, and fertilizers. In agricultural production, different pollutants from wastewater including pesticides, fertilizers, and rural domestic garbage, which contaminates the soil because of the lack of fixed pollution emission points. The use of microalgae could purify different types of wastewaters, and harvest microalgal biomass as a fertilizer (Wuang et al., 2016; Das et al., 2019), and greatly reduce production costs (Tang et al., 2020). Moreover, it can improve soil quality through its own growth, promoting microbial decomposition, improving the transformation and circulation of soil materials, enhancing soil fertility, and providing more usable materials for crops.

Therefore, this review focuses on three aspects: 1) microalgae cultivation for the improvement of soil ecological health, 2) using microalgae to control diseases and soil pollutants and reduce soil crop diseases, and 3) employing microalgae for the wastewater treatment and their resource utilization. This review is to provide a scientific basis for improving soil problems in agriculture, and to provide reference for the resource application of wastewater treatment with microalgae.

Microalgae cultivation improves soil ecological health

Farmland are susceptible to the loss of soil fertility due to large-scale intensive farming, which may lead to soil degradation of cultivatable land. Amongst other soil microbiota, the novel microalgae alone account for about 27% of the total biomass in agricultural land (Abinandan et al., 2019). Moreover, cyanobacteria are more suitable as soil biological indicators for land use and have the potential to improve soil health and fertility (Chamizo et al., 2018) (Table 1). Green algae and cyanobacteria produce abundant organic matter during climate change (Grzesik and Romanowska, 2015), increase soil organic carbon by releasing exopolysaccharides (EPSs) during algal cell decomposition, and become a readily available form of carbon, required for the growth of soil microbiota (Tiwari et al., 2019).

Microalgae improve soil physicochemical properties

Soil microorganisms, including bacteria, fungi, viruses and microalgae, that distribute in different soil layers and are invisible to the naked eye. They promote the decomposition of soil organic matter and the transformation of nutrients through oxidation, nitrification, and nitrogen fixation, and have remarkable impacts on soil formation, material circulation, and fertility evolution. In addition to nitrogen and carbon fixation, microalgae can secrete a variety of active substances, such as carotenoids, proteins, fatty acids, plant hormones, extracellular polysaccharides (EPSs), vitamins and antibiotics. Plant hormones are a class of small molecules that act as chemical messengers to coordinate the activities of agricultural crops and higher plant cells (Raza et al., 2019). They play important roles in plant growth and development, while EPSs can provide nutrients for soil microorganisms, increase soil organic carbon and thus affect soil properties (Redmile-Gordon et al., 2020).

On the other hand, microalgae can enhance the stability of soil aggregates with the increment of organic matter, nitrogen, phosphorus and pH (6.5–8.5) in the soil (Redmile-Gordon et al., 2020). Stable soil aggregates are an important factor in maintaining soil fertility, which provide suitable pores for plant growth and nutrients absorption. A rank soil aggregate structure can increase soil oxygen content and water holding capacity. It was reported that organic soil aggregates mainly formed of algal filaments and EPSs after cyanobacteria were inoculated into the soil for 6 weeks (Malam Issa et al., 2007). Yilmaz et al. studied the effect of different microalgal biofertilizer on the stability of soil aggregates, and found that the retention of the available water and plant root growth could be improved by inoculating Chlorella sp. alone or in combination with vermiculite (Yilmaz and Sönmez, 2017). Previous research

TABLE 1 Improvement of soil health and fertility with different microalgae. Adapted with the permission from Taylor & Francis Online (Abinanda et al., 2019).

Soil type	Major soil characteristics	Cyanobacterial/microalgal inoculants	Soil fertility improvement	Reference
Silt loam soil	Poor micronutrient availability	*Anabaena sp.* and *Providencia sp*	Iron concentration in soil was >2–3 folds	Manjunath et al. (2016)
Desert soil	Low organic carbon and total nitrogen	*Microcoleus vaginatus Gom*	>5-Fold increments of soil organic carbon and total nitrogen based original content	Shubin et al. (2017)
Sterile soil	Low nutrients	*Chlorella sp.*, *Scenedesmus sp*	Microbial biomass carbon	Renuka et al. (2016)
Clay loam	Low nitrogen	*Chlorella vulgaris*	Improved nitrogen and soil enzyme activities	Dineshkuma et al. (2018)
Ferruginous tropical soil	Poor soil aggregation	*Nostoc sp*	Improvement of aggregate stability	Yadav et al. (2021)
Glade soil	Poor nutrients and hydrophysical parameters	*Tribonema minus*, *Choricystisminor*, and *Klebsormidium subtile*	*Tribonema minus*, *Choricystisminor*, and *Klebsormidium subtile*	Lichner al., (2013)

reported that alkali-hydrolyzed nitrogen, soil organic matter, available phosphorus and potassium, increased considerably after watering cucumber, tomato, pepper and radiant cowpea with different concentrations of microalgae liquid fertilizer, and the enzyme activity in soil such as protease, catalase, etc. also increased in varying degrees (Alobwede et al., 2019; Deepika and Mubarakali, 2020).

Microalgae, including prokaryotes and eukaryotes have a range of unique and valuable properties to cope with challenging agricultural scenarios (Rizwan et al., 2018; Kato and Hasunuma, 2021). Microalgae are beneficial for soil nutrient cycling, as they can improve nutrient utilization and produce biologically active substances (Ekinci et al., 2019; Ronga et al., 2019); while some other microalgae produce biofuels or other high value chemicals, such as EPSs, which improve soil structure and soil quality (Renuka et al., 2018).

Microalgae improve soil microbial community structure

Microalgae as the potential organic carbon have a wide range of agricultural uses (Renuka et al., 2018). The depletion of soil organic carbon leads to a decrease in soil fertility and is an important factor in farmland degradation (Stavi and Lal, 2015). Microalgae convert carbon (including organic carbon) into sugars through photosynthesis, which also affect soil microbial community structure, and thus improve soil aggregation and stability (Marks et al., 2019). Moreover, the multifunctional microalgae, especially for the cyanobacteria, can secrete plant hormones and active substances to further control pathogens and pests (Garcia-Gonzalez and Sommerfeld, 2016; Chanda et al., 2019). The biomass accumulated by the microalgae, can be converted into nutrients that can be used by other plants (Coppens et al., 2016; Alobwede et al., 2019).

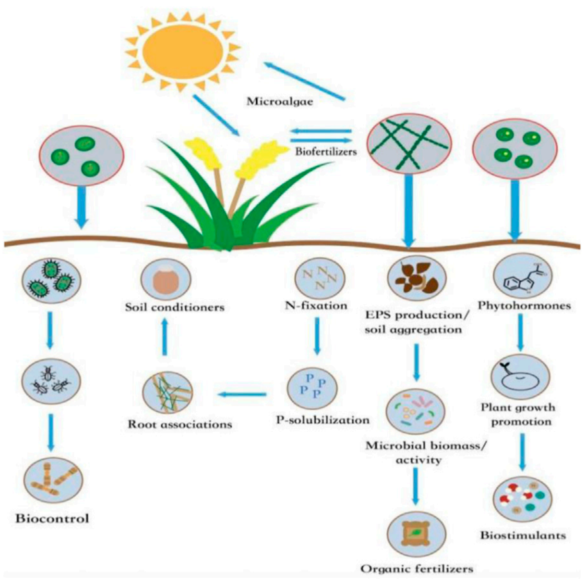

FIGURE 1
The beneficial mechanism of microalgae on soil and plants improvement. Permission from ELSEVIER (Alvarez et al., 2021).

The use of active microalgae-derived biofertilizers can improve the microbial ecosystem of the soil, plant growth, nutrient use efficiency, simultaneous tolerance to abiotic stress and reduce the utilize of chemical fertilizers (Ronga et al., 2019; Yoder and Davis, 2020). During the growth of some microalgae species, the contents of intracellular and extracellular polysaccharides increase considerably, which can fix more carbon in the soil; therefore, increase the dissolved organic carbon (DOC) and total carbon (TC) (Jiajun et al., 2019). Whether microalga-derived biostimulants are used alone or mixed with traditional biological fertilizers, they can promote

TABLE 2 Chemical compounds found in microalgae have potential as biopesticides. Adapted with the permission from Taylor & Francis Online (Costa et al., 2018).

Microalga	Activity	Metabolite	Extraction method	Identification/ quantification method	Reference
Anabaena laxa	Antimicrobial	Laxaphycin B and laxaphycin C	Fractionation of the extract by successive gel filtration	High performance liquid chromatography (HPLC)	Hernandez-Carlos and Gamboa-Angulo., (2011)
Anabaena sp	Larvicidal	Anatoxin-a	Ultrasonic disintegration of the microalgae cell wall	GC/MS	Mejean et al. (2014)
Calothrix sp	Insecticide	Eremophilone	Essential oil obtained by vacuum distillation	GC/MS	Yasinet al., (2018)
Chlorella vulgaris	Antifungal	Phenolic compounds	Extraction using FolinCiocalteu reagent	HPLC	Mofeed and El-Bilawy, (2020)
Fischerella sp	Antimicrobial	Ambiguine isonitrile	Extraction using methanol/H_2O	HPLC	Albarano et al. (2020)
Lyngbya sp	Larvicidal	Pahayokolides	Extraction using methanol/H_2O	Unrealized	Pattanayak et al. (2021)

the activity of soil nitrogenase (Cai et al., 2017). The synergetic effects of microalgal biomass on soil and plants would provide a basis for the application of microalgae in crop production (Alvarez et al., 2021) (Figure 1).

Microalgae control specific pollutants that can cause plant diseases in soil

In agricultural production, biochemical pesticides are selected to control pests through non-toxic mechanisms, but high concentrations of pesticides or fertilizers could poison weeds and cause various growth abnormalities, such as root growth inhibition and carbon assimilation. Degradation of the microtubule system and membrane directly contributes to weed death (Mfarrej and rara, 2019). Therefore, the development of microbial pesticides that use organic matter, such as algae, bacteria or fungi has become necessary. Cyanobacteria are regarded as one of the main biological agents for the management of soil diseases and the control of pathogenic fungi in plants (Stavi and Lal, 2015). They produce bioactive compounds called secondary metabolites (Mager and Thomas, 2011), antifungal and antimicrobial activities are toxic to nematodes (Marks et al., 2019). Various species and genera of microalgae are potential producers of secondary metabolites owing to their biological control and insecticidal properties. Chemical compounds found in microalgae that have potential as biopesticides are listed in Table 2 (Costa et al., 2018).

Heavy metals

Heavy metals, such as chromium (Cr), arsenic (As), cadmium (Cd), mercury (Hg) and lead (Pb), are carcinogenic, and toxic even in trace amounts. They persist in the food chain, leading to bioaccumulation and thus posing a threat to human health and environmental ecology (Leong and Chang, 2020). Using microalgae in the remediation of heavy metals has become an emerging trend owing to their abundant resources, low price, high removal efficiency and eco-friendliness. Compared to higher plants, fast growth, simple and non-toxic process are also the main advantages for microalgae (Leong and Chang., 2020). Table 3 shows the ability of microalgae for the removal of heavy metals from aqueous solutions.

The adsorption process of microalgae not only releases free radicals against heavy metals, but also synthesizes antioxidants such as glutathione reductase, superoxide dismutase (SOD), peroxidase, ascorbate peroxidase, catalase, etc. (Upadhyay et al., 2016). As endogenous antioxidants, GSH and ASC play key roles in reducing both free radicals and reactive oxygen species (ROS) (Devars et al., 2000). Microalgae secrete high levels of ASC, which acts as a hydroxide-philic reducing buffer and is responsible for protecting cellular components from oxidative threats. ASC exerts a protective effect on microalgae by regulating the activity of ascorbic acid glutathione (ASC-GSH) pathway and metalloenzymes while maintaining the balance of ROS elimination and generation. Furthermore, high levels of GSH can protect microalgal cells by scavenging free radicals, providing tolerance, promoting PCs and ASC synthesis, and restoring substrates for other antioxidants (Gomez-Jacinto et al., 2015).

In detail, heavy metal removal with microalgae through two-stage action: biosorption and bioaccumulation (Figure 2). Biosorption is the fast passive adsorption outside the cell, while bioaccumulation is an active and slow transport process. Microalgal cell wall components include organic proteins, polysaccharides, lipids as well as cellular macromolecules such as peptides and exopolysaccharides, with various functional groups to bind heavy metals (Priatni et al., 2018). Moreover, laminar, carboxyl, monomeric alcohol and deodorizing sulfates of macromolecular clusters from microalgae can also be formed to attract cations and anions of different heavy metals (Pradhan et al., 2019; Leong and Chang., 2020).

TABLE 3 The ability of microagae for the removal of heavy metals from aqueous solutions (Leong and Chang, 2020).

Microalgae strains	Heavy metal	Temp (˚C)	Optimal pH	Initial metal conc. (mg/L)	Biomass conc. (g/L)	Time (min)	Max. Sorption (mg/g)	Removal Efficiency (%)	Reference
Ulothrix cylindricum	As	20	6	10	4	60	2.45	98	Tuzen et al. (2009)
Immobilized Chlorella sp	Cd	-	6	10	1.3	-	15.51	92.5	Shen et al. (2018)
Scenedesmus quadricauda	Cr	25	6	100	2	120	-	98.3	Shokri Khoubestani et al.(2015)
Phormidium sp	Pb	25	5	10	4	40	2.305	92.2	Das et al. (2016)
Spirogyra sp	Hg	4	4	1	3	30	0.253	76	Rezaee et al. (2006)

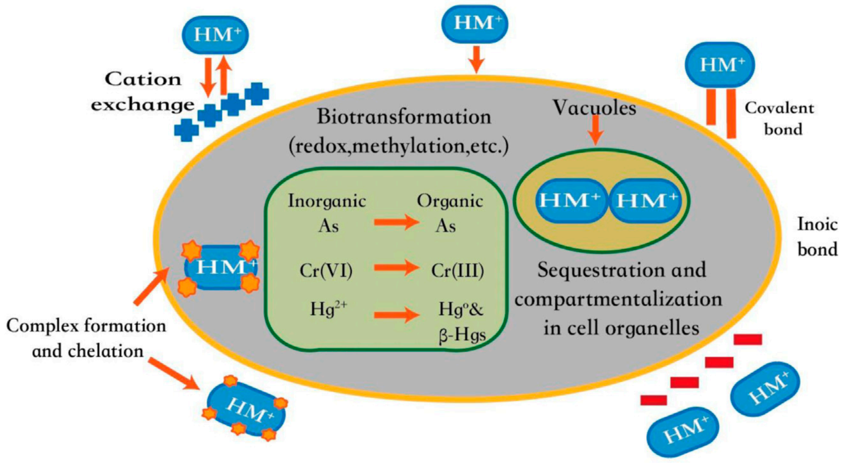

FIGURE 2
Mechanism of Removal of Heavy Metals by Microalgae. Adapted with the permission from ELSEVIER (Leong and Chang, 2020).

Organic pesticides

It was found that the organophosphorus pesticide malathion can inhibit the growth of *Aspergillus oryzae* and *Nostoc muscorum* in paddy fields; however, the nitrogen-fixing cyanobacteria could degrade malathion and utilize them as a source of phosphorus (Ibrahim et al., 2014). Amongst them, *Candida grisea* has the highest biodegradability (91%). Hangjun et al. found that Anabaena PD-1 isolated from rice fields could tolerate polychlorinated biphenyls (PCBs) (Hangjun et al., 2015), and low-chlorinated PCBs are more easily degraded by the algae than their highly chlorinated counterparts. Meta-trichlorodiphenyls, tetrachlorobiphenyls and para-trichlorodiphenyls are more susceptible to dechlorination degradation than their ortho-chlorinated counterparts. In addition, the algae can also degrade dioxin-like PCBs. After 25 days of treatment, the degradation rates of 12 dioxin-like PCB compounds ranged from 37.4% to 68.4%, indicating that the algae can be used for the *in-situ* bioremediation of PCB-contaminated paddy soil. Tiwari et al. found that Scytonema sp. BHUS-5 could remove and degrade methyl parathion and use the phosphorus after degradation (Tiwari et al., 2017). Abdel-Aty et al. found that Anabaena sphaerica has the ability to remove diurons, and when the initial diuron concentration was 40 mg/L and the pH was 3, adding 1 g/L Anabaena sp. could remove diuron with the rate of 80% in 80 min (Abdel-Aty et al., 2017).

Antibiotics

Antibiotics are the chemical substances produced during the metabolism of microorganisms that can inhibit the growth and activity of other microorganisms at low concentrations (Sherpa et al., 2015). Antibiotics are widely used in aquaculture, soil and crop planting (Chuah et al., 2016). It was reported that antibiotics have shown a powerful effect in inhibiting the reproduction, sterilization and bacteriostasis of aquatic bacteria (Lijian et al., 2020). It is accustomed to add different types of antibiotics to the algal fluid to achieve sterilization or bacteriostasis. Different antibiotic treatments can also be used in different growth stages of microalgae. Haematococcus pluvialis was sterilized with 8 different antibiotics and the antibacterial effect of adding griseofulvin in the early stage was the best, but the antibacterial effect of adding penicillin in the middle and late stage was more obvious (Kiki et al., 2020).

However, the applications of antibiotics are to inhibit the growth of bacteria in the process of microalgal culture, but the use of antibiotics also has an impact on the growth rate, algal cell density, and chlorophyll content (Dantas et al., 2019; Shan et al., 2020). The effect of antibiotics on algae is dual; they may be used as a poison to inhibit the growth of algae, it can also induce toxic irritant effects at specific concentrations; so as to activate protease and induce gene expression, etc., and further to promote the growth of microalgae.

Microalgae remove antibiotics in contaminated soil mainly through biosorption, bioaccumulation and biodegradation, and then achieve the purpose of degradation, thereby restoring soil fertility. Aseptic microalgal culture is very important in its genetic, biochemical, physiological, and taxonomic studies (Ananthi et al., 2018). It shows an effect in sterilization, as antibiotics inhibit the growth and reproduction of bacteria (Xiaoyu et al., 2022). Microalgae are more resistant to antibiotics than bacteria; hence, obtaining sterile algae by selectively using one or more antibiotics for aseptic treatment (Sandhya and Vijayan, 2019).

Microplastics

The problem of microplastic pollution in the soil has attracted global attention. Many reports have been conducted on microplastics, especially on the effect of the water and soil environment. As primary producers, microalgae play an important role in aquatic ecosystems and can maintain the balance of aquatic ecosystems (Nickelsen, 2017; Yokota et al., 2017). Previous studies have found that microplastics can act as substrates for the growth of Raphidocelis subcapitata and promote the growth of the algae (Canniff and Hoang, 2018). Microalgae are sensitive to toxic substances and all changes in microalgae will ultimately affect the structure and function of aquatic ecosystems (Guo et al., 2016; Cai et al., 2017).

At present, plastics are made from chemicals derived from fossil fuels, particularly ethylene and propylene. However, lipids, proteins, and carbohydrates are important raw materials for bioplastic synthesis. Microalgae are rich in these substances; therefore, they become an important source of bioplastic raw materials. The main used in the industrial-scale production of bioplastics contain polylactic acid (PLA), polyhydroxybutyrates (PHBs), polyhydroxyalkanoates (PHAs), starch plastics, protein and cellulosic plastics (Laurens et al., 2017). Calothrix sp., Synechocystis sp., Nostoc sp., Oscillatoria sp., and Spirulina sp. are expected to be used for PHAs production, whereas photoautotrophic Scenedesmus sp. can be used for PLA production (Chaofan et al., 2019). Nutrient-limiting increase PHA and PHB production but without affecting microalgal growth (Kamravamanesh et al., 2018).

Microalgae biotechnology improves soil diseases

Microalgae biotechnology is based on the biology and engineering principles to study algal breeding, algal cell culture, and algal harvest and the treatment of water and nutrients. The established microalgae biotechnology involves carbon sequestration, emission reduction, large-scale cultivation, environmental remediation, bait and feed, functional or high value products (Alam et al., 2020). Moreover, the microalgae biotechnological potential in the maintenance of soil fertility and health are greatly useful and worth expecting.

Saline soil application

To date, about 99.13 million hm^2 of saline-alkali land are present in China, especially in Gansu, Ningxia, Xinjiang and other provinces and regions in the northwest region. In detail, the soil affected by salinization in Gansu province is close to 30,000 hm^2, especially in Hexi and Yanhuang irrigation areas. The area of soil salinization is increasing annually because of unreasonable irrigation. The annual loss of grains exceeds 100 million kg (Lili and Baoshan, 2021). Cyanobacteria play an important role in the improvement of saline soil. They can improve the contents of nutrients and contribute to the chelation of harmful sodium ions in the soil. The EPSs secreted by cyanobacteria have a tendency to chelate cations. EPSs have negatively charged groups, such as uric acid (Kumar et al., 2018), reduces the availability of Na+ in soil solution by binding to Na+. Nisha et al. isolated several salt- and drought-tolerant cyanobacteria from saline-alkali land and used cyanobacteria as biological fertilizer to improve saline soil, potassium, magnesium cation exchange capacity and soil water-holding energy and also decrease sodium ions and electrical conductivity. Saline-tolerant algae can survive in high-salinity environments and can be considered for application as biological bacterial fertilizers in saline-alkali soils.

In saline soils, the application of fungi Arbuscular mycorrhiza and green algae can increase pH, bacterial biomass carbon, root density, carbon mineralization, soil microbes and soil aggregate formation (Al-Maliki and Ebreesum, 2020). However, Gehringer et al. found that the inoculation of nitrogen-fixing cyanobacteria in high salinity soils can reduce wheat biomass and nutrient content, which may be due to the adsorption of nutrients by algal extracellular polymers, making them unable to be absorbed by plants (Gehringer et al., 2010). This finding indicates that nitrogen-fixing cyanobacteria may not be suitable for wheat in saline-alkali soil but are beneficial to soil fixation. Saline soils are usually low in nitrogen, carbon, and phosphorus; have high electrical conductivity and contain some toxic ions, which greatly limit plant growth (Munns et al., 2020).

Desertification soil application

Nitrogen-fixing cyanobacteria have been used in desertification soil control in the form of biological crusts in Northwest China and have achieved good results. However, the adaptation mechanism of nitrogen-fixing cyanobacteria to such extreme environmental conditions has not been fully elucidated. The researchers measured organic matter, soil texture, nitrogen, phosphorus, temperature, and solar irradiance in Brazil and found that Leptolyngbya sp. has better biocrust under drought conditions (De Lima et al., 2021). Wu et al. found that the shape, species and Colour composition of artificial algal crusts increased with the growth of crusts, and available nitrogen, phosphorus and soil moisturnd also increased (Wu et al., 2022). It shows that the artificial inoculation of biological crusts can improve soil fertility and micro-ecological environment of the topsoil. It was revealed that the tolerance of Lentinula boryana to drought stress could be expressed by the levels of intracellular proline, SOD and carotenoids (Prasanna et al., 2014).

Cyanobacteria act as an important protective role in biological soil crusts (BSCs) in arid and semi-arid regions; however, the cyanobacteria, green algae, and mosses are lesser concern in the wetter agricultural soils of eastern North America. Unlike the traditional BSCs growth pattern in semi-arid areas, the substrate growth in agricultural soils is frequent, short-lived and rapid (Xin and Bruns, 2019). Therefore, cyanobacteria, as renewable C and N resources and have a role in enhancing soil resilience, and have broad prospects in soil applications. Phylogenetic mapping showed that all typical members of the cyanobacterial circle were eutrophic and many of them were nitrogen-fixing bacteria. As assessed with qPCR, nitrogen fixation genes are actually several orders of magnitude more abundant than in bulk biocrust soils. In contrast, competition for CO2, low organic carbon concentrations, and light define a fraction of OTUs separated from cyanobacteria (Couradeau et al., 2019).

Nitrogen-fixing cyanobacteria may also promote desert plant growth and drought resistance. Some cyanobacteria can secrete active compounds which help in promotion of plant growth. Research showed that these active compounds have potential to reduce abiotic stress in crops (Gr et al., 2021). Moreover, cyanobacteria can improve soil quality and alleviate salinity stress and drought resistance with a wide application.

Microalgae wastewater treatment and soil improvement resource utilization

Traditional wastewater treatment has gone from backward and expensive. They simply transfer contaminants from the water, which also cause secondary pollution. Microalgal wastewater treatment is a biological process that removes pollutants while also fixing CO_2, and the harvested microalgal biomass can be made into various high valuable products (Jacob et al., 2021). However, advanced methods are required to avoid the adverse effects of different pollutants when use of microalgal biomass based on the wastewater treatment for the improvement of soil (Wu et al., 2022). The characteristic pollutants in wastewater can affect the growth and metabolism of microalgae. Exogenous carbon can effectively increase the growth rate of microalgae and thus improve the removal effect of nitrogen and phosphorus, it also increases the cost of treatment and operation. Swine wastewater is rich in organic matter and afford an effective carbon for the growth of microalgae that can eliminate the cost of carbon supply and simultaneously reduce the organic matter. The researchers designed a comprehensive process for the treatment of digested manure wastewater for advanced treatment and resource recovery (Shubin et al., 2017). It is concluded that the activated carbon adsorption combined with microalgae purification can remove nutrients in wastewater with high efficiency. However, the resource utilization of microalgae after wastewater treatment can improve the economy. Some studies have shown that cyanobacteria polysaccharides in desert soil can play an important role in sand surface stability and soil nutrient retention (Xu et al., 2013). Water retention and structure protection abilities were considerably positively correlated with the content of total carbohydrates and macromolecular carbohydrates in the crust when watering the active microalgae. This indicates that the EPSs from microalgae can play a key role in soil remediation. Microalgae could accumulate 30%–80% of lipids, particularly triacylglycerols. Most algal strains, such as Chlorella, produce fatty acids in the range of C16–C18, whereas the carbon chain of biodiesel is concentrated in C14–C18; therefore, it is suitable for biodiesel production. Carbohydrates are one of the components of microalgal biomass and can be directly used to produce bioethanol. Studies have shown that algae grown in wastewater have the potential to accumulate carbohydrates; therefore, carbohydrate-rich biomass can be cultivated in soil to reduce the cost of microalgae production. In addition, many studies have shown that cultivating microalgae with agricultural wastewater can produce valuable compounds i.e., proteins, carbohydrates, pigments, vitamins, etc., which can be used to further produce cosmetics, food, feed, and/or medicine (Alvarez et al., 2021).

Conclusion

Soil health is an important segment of ecological environment. However, soil pollution deteriorates the soil quality and productivity of cultivated land and thus directly endangers food safety and human health. Photosynthetic microalgae can improve soil physicochemical properties, soil microbial community structure, and recycling with their multiple active chemicals. Likewise, microalgae can control much pollutants of underlying factors for soil deterioration, such as heavy metals, pesticides, antibiotic, and microplastics, with their particular cell structure or functional group. Moreover, utilization of microalgal biomass after wastewater treatment has a sustainable prospect in saline soil and desertification soil application.

Author contributions

XS: Methodology, Data curation, Formal analysis, Investigation, Software, Visualization, Writing—original draft. YB and YF: Data curation, Formal analysis, Investigation, Writing—original draft. YT, CZ, and XY: Conceptualization, Writing—review & editing, Funding acquisition. RR and QX: Conceptualization, Funding acquisition, Project administration, Resources, Supervision, Writing—review & editing. PC: Conceptualization, Methodology, Data curation, Formal analysis, Investigation, Software, Visualization, Writing—original draft, Writing—review & editing, Funding acquisition.

Funding

This research was supported in part by grants from the National Natural Science Foundation of China (32170369), the Natural Science Foundation of Zhejiang Province (LZJWY22B070001), the Yunnan Key Laboratory of Microalgae (202105AG070013), University of Minnesota MnDrive Environment Program (MNE12), and University of Minnesota Center for Biorefining.

Conflict of interest

Authors YT and QX were employed by the company Lijiang Cheng Hai Bao Er Biological Development Co., Ltd.

The remaining authors declare that the research was conducted in the absence of any commercial or financial relationships that could be construed as a potential conflict of interest.

Publisher's note

References

Abdel-Aty, A. M., Ammar, N. S., Ghafar, H. H. A., and Ali, R. K. (2013). Biosorption of cadmium and lead from aqueous solution by fresh water alga Anabaena sphaerica biomass. *J. Adv. Res.* 4 (4), 367–374. doi:10.1016/j.jare.2012.07.004

Abinandan, S., Subashchandrabose, S. R., Venkateswarlu, K., and Megharaj, M. (2019). Soil microalgae and cyanobacteria: The biotechnological potential in the maintenance of soil fertility and health. *Crit. Rev. Biotechnol.* 39 (8), 981–998. doi:10.1080/07388551.2019.1654972

Al-Maliki, S., and Ebreesum, H. (2020). Changes in soil carbon mineralization, soil microbes, roots density and soil structure following the application of the arbuscular mycorrhizal fungi and green algae in the arid saline soil. *Rhizosphere* 14, 100203. doi:10.1016/j.rhisph.2020.100203

Alam, M. A., Jingliang, X., and Zhongming, W. (2020). *Microalgae biotechnology for food, health and high value products*. Singapore: Springer, 81–123.

Albarano, L., Esposito, R., Ruocco, N., and Costantini, M. (2020). Genome mining as new challenge in natural products discovery. *Mar. Drugs* 18 (4), 199. doi:10.3390/md18040199

Alobwede, E., Leake, J. R., and Pandhal, J. (2019). Circular economy fertilization: Testing micro and macro algal species as soil improvers and nutrient sources for crop production in greenhouse and field conditions. *Geoderma* 334, 113–123. doi:10.1016/j.geoderma.2018.07.049

Alvarez, A. L., Weyers, S. L., Goemann, H. M., Peyton, B. M., and Gardner, R. D. (2021). Microalgae, soil and plants: A critical review of microalgae as renewable resources for agriculture. *Algal Res.* 54, 102200. doi:10.1016/j.algal.2021.102200

Ananthi, V., Prakash, G. S., Rasu, K. M., Gangadevi, K., Boobalan, T., Raja, R., et al. (2018). Comparison of integrated sustainable biodiesel and antibacterial nano silver production by microalgal and yeast isolates. *J. Photochem. Photobiol. B Biol.* 186, 232–242. doi:10.1016/j.jphotobiol.2018.07.021

Cai, Z., Xiaohua, C., Jiangtao, W., and Liju, T. (2017). Toxic effects of microplastic on marine microalgae skeletonema costatum: Interactions between microplastic and algae. *Environ. Pollut.* 220, 1282–1288. doi:10.1016/j.envpol.2016.11.005

Canniff, P. M., and Hoang, T. C. (2018). Microplastic ingestion by Daphnia magna and its enhancement on algal growth. *Sci. Total Environ.* 633, 500–507. doi:10.1016/j.scitotenv.2018.03.176

Chamizo, S., Mugnai, G., Rossi, F., Certini, G., and De Philippis, R. (2018). Cyanobacteria inoculation improves soil stability and fertility on different textured soils: Gaining insights for applicability in soil restoration. *Front. Environ. Sci.* 6, 49. doi:10.3389/fenvs.2018.00049

Chanda, M. J., Merghoub, N., and El Arroussi, H. (2019). Microalgae polysaccharides: The new sustainable bioactive products for the development of plant bio-stimulants? *World J. Microbiol. Biotechnol.* 35, 177. doi:10.1007/s11274-019-2745-3

Chaofan, Z., Show, P. L., and Ho, S. H. (2019). Progress and perspective on algal plastics–a critical review. *Bioresour. Technol.* 289, 121700. doi:10.1016/j.biortech.2019.121700

Chuah, L. O., Effarizah, M. E., Goni, A. M., and Rusul, G. (2016). Antibiotic application and emergence of multiple antibiotic resistance (MAR) in global catfish aquaculture. *Curr. Environ. Health Rep.* 3 (2), 118–127. doi:10.1007/s40572-016-0091-2

Coppens, J., Grunert, O., Van Den Hende, S., Vanhoutte, I., Boon, N., Haesaert, G., et al. (2016). The use of microalgae as a high-value organic slow-release fertilizer results in tomatoes with increased carotenoid and sugar levels. *J. Appl. Phycol.* 28 (4), 2367–2377. doi:10.1007/s10811-015-0775-2

Costa, O. Y., Raaijmakers, J. M., and Kuramae, E. E. (2018). Microbial extracellular polymeric substances: Ecological function and impact on soil aggregation. *Front. Microbiol.* 9, 1636. doi:10.3389/fmicb.2018.01636

Couradeau, E., Giraldo-Silva, A., De Martini, F., and Garcia-Pichel, F. (2019). Spatial segregation of the biological soil crust microbiome around its foundational cyanobacterium, Microcoleus vaginatus, and the formation of a nitrogen-fixing cyanosphere. *Microbiome* 7 (1), 55–12. doi:10.1186/s40168-019-0661-2

Dahiya, A. (2015). Algae biomass cultivation for advanced biofuel production. *Bioenergy*, 219–238. doi:10.1016/B978-0-12-407909-0.00014-6

Dantas, D. M. D. M., Oliveira, C. Y. B. D., Costa, R. M. P. B., Carneiro-da-Cunha, M. D. G., Gálvez, A. O., and Bezerra, R. D. S. (2019). Evaluation of antioxidant and antibacterial capacity of green microalgae Scenedesmus subspicatus. *Food Sci. Technol. Int.* 25 (4), 318–326. doi:10.1177/1082013218825024

Das, D., Chakraborty, S., Bhattacharjee, C., and Chowdhury, R. (2016). Biosorption of lead ions (Pb2+) from simulated wastewater using residual biomass of microalgae. *Desalin. Water Treat.* 57 (10), 4576–4586. doi:10.1080/19443994.2014.994105

Das, P., Quadir, M. A., Thaher, M. I., Alghasal, G. S. H. S., and Aljabri, H. M. S. J. (2019). Microalgal nutrients recycling from the primary effluent of municipal wastewater and use of the produced biomass as bio-fertilizer. *Int. J. Environ. Sci. Technol. (Tehran).* 16 (7), 3355–3364. doi:10.1007/s13762-018-1867-8

De Lima, N. M. M., Munoz-Rojas, M., Vazquez-Campos, X., and Branco, L. H. Z. (2021). Biocrust cyanobacterial composition, diversity, and environmental drivers in two contrasting climatic regions in Brazil. *Geoderma* 386, 114914. doi:10.1016/j.geoderma.2020.114914

Deepika, P., and MubarakAli, D. (2020). Production and assessment of microalgal liquid fertilizer for the enhanced growth of four crop plants. *Biocatal. Agric. Biotechnol.* 28, 101701. doi:10.1016/j.bcab.2020.101701

Devars, S., Aviles, C., Cervantes, C., and Moreno-Sanchez, R. (2000). Mercury uptake and removal by Euglena gracilis. *Arch. Microbiol.* 174 (3), 175–180. doi:10.1007/s002030000193

Dineshkumar, R., Kumaravel, R., Gopalsamy, J., Sikder, M. N. A., and Sampathkumar, P. (2018). Microalgae as bio-fertilizers for rice growth and seed yield productivity. *Waste Biomass Valorization* 9 (5), 793–800. doi:10.1007/s12649-017-9873-5

Ekinci, K., Erdal, I., Uysal, O., Uysal, F. O., Tunce, H., and Doğan, A. (2019). Anaerobic digestion of three microalgae biomasses and assessment of digestates as biofertilizer for plant growth. *Environ. Prog. Sustain. Energy* 38 (3), e13024. doi:10.1002/ep.13024

Garcia-Gonzalez, J., and Sommerfeld, M. (2016). Biofertilizer and biostimulant properties of the microalga Acutodesmus dimorphus. *J. Appl. Phycol.* 28 (2), 1051–1061. doi:10.1007/s10811-015-0625-2

Gehringer, M. M., Pengelly, J. J., Cuddy, W. S., Fieker, C., Forster, P. I., and Neilan, B. A. (2010). Host selection of symbiotic cyanobacteria in 31 species of the Australian cycad genus: Macrozamia (Zamiaceae). *Mol. Plant. Microbe. Interact.* 23 (6), 811–822. doi:10.1094/MPMI-23-6-0811

Gomez-Jacinto, V., Garcia-Barrera, T., Gomez-Ariza, J. L., Garbayo-Nores, I., and Vílchez-Lobato, C. (2015). Elucidation of the defence mechanism in microalgae Chlorella sorokiniana under mercury exposure. Identification of Hg-phytochelatins. *Chem. Biol. Interact.* 238, 82–90. doi:10.1016/j.cbi.2015.06.013

Gr, S., Yadav, R. K., Chatrath, A., Gerard, M., Tripathi, K., Govindsamy, V., et al. (2021). Perspectives on the potential application of cyanobacteria in the alleviation of drought and salinity stress in crop plants. *J. Appl. Phycol.* 33 (6), 3761–3778. doi:10.1007/s10811-021-02570-5

Grzesik, M., and Romanowska-Duda, Z. (2015). Ability of cyanobacteria and green algae to improve metabolic activity and development of willow plants. *Pol. J. Environ. Stud.* 24 (3), 1003–1012. doi:10.15244/pjoes/34667

Guo, J., Selby, K., and Boxall, A. B. (2016). Comparing the sensitivity of chlorophytes, cyanobacteria, and diatoms to major-use antibiotics. *Environ. Toxicol. Chem.* 35 (10), 2587–2596. doi:10.1002/etc.3430

Hangjun, Z., Xiaojun, J., Liping, L., and Wenfeng, W. (2015). Biodegradation of polychlorinated biphenyls (PCBs) by the novel identified cyanobacterium Anabaena PD-1. *PLoS ONE* 10 (7), e0131450. doi:10.1371/journal.pone.0131450

Hernandez-Carlos, B., and Gamboa-Angulo, M. M. (2011). Metabolites from freshwater aquatic microalgae and fungi as potential natural pesticides. *Phytochem. Rev.* 10, 261–286. doi:10.1007/s11101-010-9192-y

Ibrahim, W. M., Karam, M. A., El-Shahat, R. M., and Adway, A. A. (2014). Biodegradation and utilization of organophosphorus pesticide malathion by cyanobacteria. *Biomed. Res. Int.* 1-6, 392682. doi:10.1155/2014/392682

Jacob, A., Ashok, B., Alagumalai, A., Chyuan, O. H., and Le, P. T. K. (2021). Critical review on third generation micro algae biodiesel production and its feasibility as future bioenergy for IC engine applications. *Energy Convers. Manag.* 228, 113655. doi:10.1016/j.enconman.2020.113655

Jiajun, H., Hongcheng, G., Yiyun, X., Min-tian, G., Shiping, Z., Tsang, Y. F., et al. (2019). Using a mixture of microalgae, biochar, and organic manure to increase the capacity of soil to act as carbon sink. *J. Soils Sediments* 19 (11), 3718–3727. doi:10.1007/s11368-019-02337-z

Jun, C., Yan, W., Benemann, J. R., Xuecheng, Z., Hongjun, H., and Song, Q. (2016). Microalgal industry in China: Challenges and prospects. *J. Appl. Phycol.* 28 (2), 715–725. doi:10.1007/s10811-015-0720-4

Jun, W., Jian, L., Leiming, L., Xiuyun, M., and amd Yongming, L. (2018). Pollution, ecological-health risks, and sources of heavy metals in soil of the northeastern Qinghai-Tibet Plateau. *Chemosphere* 201, 234–242. doi:10.1016/j.chemosphere.2018.02.122

Kamravamanesh, D., Kovacs, T., Pflügl, S., Druzhinina, I., Kroll, P., Lackner, M., et al. (2018). Increased poly-β-hydroxybutyrate production from carbon dioxide in randomly mutated cells of cyanobacterial strain Synechocystis sp. PCC 6714: Mutant generation and characterization. *Bioresour. Technol.* 266, 34–44. doi:10.1016/j.biortech.2018.06.057

Kato, Y., and Hasunuma, T. (2021). Metabolic engineering for carotenoid production using eukaryotic microalgae and prokaryotic cyanobacteria. *Adv. Exp. Med. Biol.* 1261, 121–135. doi:10.1007/978-981-15-7360-6_10

Kiki, C., Rashid, A., Wang, Y., Li, Y., Zeng, Q., Yu, C. P., et al. (2020). Dissipation of antibiotics by microalgae: Kinetics, identification of transformation products and pathways. *J. Hazard. Mat.* 387, 121985. doi:10.1016/j.jhazmat.2019.121985

Kumar, D., Kastanek, P., and Adhikary, S. P. (2018). Exopolysaccharides from cyanobacteria and microalgae and their commercial application. *Curr. Sci.* 115 (2), 234–241. doi:10.18520/cs/v115/i2/234-241

Laurens, L. M., Markham, J., Templeton, D. W., Christensen, E. D., Van Wychen, S., Vadelius, E. W., et al. (2017). Development of algae biorefinery concepts for biofuels and bioproducts; a perspective on process-compatible products and their impact on cost-reduction. *Energy Environ. Sci.* 10 (8), 1716–1738. doi:10.1039/C7EE01306J

Leong, Y. K., and Chang, J. S. (2020). Bioremediation of heavy metals using microalgae: Recent advances and mechanisms. *Bioresour. Technol.* 303, 122886. doi:10.1016/j.biortech.2020.122886

Lichner, L., Hallett, P. D., Drongova, Z., Czachor, H., Kovacik, L., Mataix-Solera, J., et al. (2013). Algae influence the hydrophysical parameters of a sandy soil. *Catena* 108, 58–68. doi:10.1016/j.catena.2012.02.016

Lijian, L., Liang, W., Qin, X., Siyu, X., Wenting, L., Sen, L., et al. (2020). Use of microalgae based technology for the removal of antibiotics from wastewater: A review. *Chemosphere* 238, 124680. doi:10.1016/j.chemosphere.2019.124680

Lili, L., and Baoshan, W. (2021). Protection of halophytes and their uses for cultivation of saline-alkali soil in China. *Biology* 10 (5), 353. doi:10.3390/biology10050353

Little, S. M., Senhorinho, G. N., Saleh, M., Basiliko, N., and Scott, J. A. (2021). Antibacterial compounds in green microalgae from extreme environments: A review. *Algae* 36 (1), 61–72. doi:10.4490/ALGAE.2021.36.3.6

Mager, D. M., and Thomas, A. D. (2011). Extracellular polysaccharides from cyanobacterial soil crusts: A review of their role in dryland soil processes. *J. Arid. Environ.* 75 (2), 91–97. doi:10.1016/j.jaridenv.2010.10.001

Malam Issa, O., Défarge, C., Le Bissonnais, Y., Marin, B., Duval, O., Bruand, A., et al. (2007). Effects of the inoculation of cyanobacteria on the microstructure and the structural stability of a tropical soil. *Plant Soil* 290 (1), 209–219. doi:10.1007/s11104-006-9153-9

Manjunath, M., Kanchan, A., Ranjan, K., Venkatachalam, S., Prasanna, R., Ramakrishnan, B., et al. (2016). Beneficial cyanobacteria and eubacteria synergistically enhance bioavailability of soil nutrients and yield of okra. *Heliyon* 2 (2), e00066. doi:10.1016/j.heliyon.2016.e00066

Marks, E. A., Montero, O., and Rad, C. (2019). The biostimulating effects of viable microalgal cells applied to a calcareous soil: Increases in bacterial biomass, phosphorus scavenging, and precipitation of carbonates. *Sci. Total Environ.* 692, 784–790. doi:10.1016/j.scitotenv.2019.07.289

Mejean, A., Paci, G., Gautier, V., and Ploux, O. (2014). Biosynthesis of anatoxin-A and analogues (anatoxins) in cyanobacteria. *Toxicon* 91, 15–22. doi:10.1016/j.toxicon.2014.07.016

Mfarrej, M. F. B., and Rara, F. M. (2019). Competitive, sustainable natural pesticides. *Acta Ecol. Sin.* 39 (2), 145–151. doi:10.1016/j.chnaes.2018.08.005

Mofeed, J., and El-Bilawy, E. H. (2020). Toxicity and disruptive impacts of fenhexamid fungicide against the green alga, Chlorella vulgaris. *Egypt. Acad. J. Biol. Sci. F. Toxicol. Pest Control* 12 (1), 45–57. doi:10.21608/EAJBSF.2020.78133

Munns, R., Passioura, J. B., Colmer, T. D., and Byrt, C. S. (2020). Osmotic adjustment and energy limitations to plant growth in saline soil. *New Phytol.* 225 (3), 1091–1096. doi:10.1111/nph.15862

Nematollahi, M. J., Keshavarzi, B., Zaremoaiedi, F., Rajabzadeh, M. A., and Moore, F. (2020). Ecological-health risk assessment and bioavailability of potentially toxic elements (PTEs) in soil and plant around a copper smelter. *Environ. Monit. Assess.* 192 (10), 639–719. doi:10.1007/s10661-020-08589-4

Nickelsen, K. (2017). The organism strikes back: Chlorella algae and their impact on photosynthesis research, 1920s–1960s. *Hist. Philos. Life Sci.* 39 (2), 9–22. doi:10.1007/s40656-017-0137-2

Pattanayak, S., Das, S., and Biswal, G. (2021). Crop disease control through application of algal biopesticides: Alternate route map in organic farming. *Biopestic. Org. Farming*, 123–126. doi:10.1201/9781003027690-30

Perez-Lucas, G., Vela, N., El Aatik, A., and Navarro, S. (2019). Environmental risk of groundwater pollution by pesticide leaching through the soil profile. Pesticides. In ed L. Marcelo and S. Sonia, *Anthropogenic. Activities and the health of our the environment.* 1–28. doi:10.5772/intechopen.82418

Pradhan, D., Sukla, L. B., Mishra, B. B., and Devi, N. (2019). Biosorption for removal of hexavalent chromium using microalgae Scenedesmus sp. *J. Clean. Prod.* 209, 617–629. doi:10.1016/j.jclepro.2018.10.288

Prasanna, R., Sood, A., Ratha, S. K., and Singh, P. K. (2014). Cyanobacteria as a green option for sustainable agriculture. *Cyanobacteria* 9, 145–166. doi:10.1002/9781118402238.ch9

Priatni, S., Ratnaningrum, D., Warya, S., and Audina, E. (2018). Phycobiliproteins production and heavy metals reduction ability of Porphyridium sp. *IOP Conf. Ser. Earth Environ. Sci.* 160, 012006. doi:10.1088/1755-1315/160/1/012006

Randrianarison, G., and Ashraf, M. A. (2017). Microalgae: A potential plant for energy production. *Geol. Ecol. Landscapes* 1 (2), 104–120. doi:10.1080/24749508.2017.1332853

Raza, A., Mehmood, S. S., Tabassum, J., and Batool, R. (2019). "Targeting plant hormones to develop abiotic stress resistance in wheat. Wheat. Production," in *Changing. Environments.* (Singapore: Springer), 557–577.

Redmile-Gordon, M., Gregory, A. S., White, R. P., and Watts, C. W. (2020). Soil organic carbon, extracellular polymeric substances (EPS), and soil structural stability as affected by previous and current land-use. *Geoderma* 363, 114143. doi:10.1016/j.geoderma.2019.114143

Renuka, N., Guldhe, A., Prasanna, R., Singh, P., and Bux, F. (2018). Microalgae as multi-functional options in modern agriculture: Current trends, prospects and challenges. *Biotechnol. Adv.* 36 (4), 1255–1273. doi:10.1016/j.biotechadv.2018.04.004

Rezaee, A., Ramavandi, B., Ganati, F., Ansari, M., and Solimanian, A. (2006). Biosorption of mercury by biomass of filamentous algae Spirogyra species. *J. Biol. Sci.* 6 (4), 695–700. doi:10.3923/jbs.2006.695.700

Rizwan, M., Mujtaba, G., Memon, S. A., Lee, K., and Rashid, N. (2018). Exploring the potential of microalgae for new biotechnology applications and beyond: A review. *Renew. Sustain. Energy Rev.* 92, 394–404. doi:10.1016/j.rser.2018.04.034

Ronga, D., Biazzi, E., Parati, K., Carminati, D., Carminati, E., and Tava, A. (2019). Microalgal biostimulants and biofertilisers in crop productions. *Agronomy* 9 (4), 192. doi:10.3390/agronomy9040192

Sandhya, S. V., and Vijayan, K. K. (2019). Symbiotic association among marine microalgae and bacterial flora: A study with special reference to commercially important isochrysis galbana culture. *J. Appl. Phycol.* 31 (4), 2259–2266. doi:10.1007/s10811-019-01772-2

Sasaki, M., Takagi, A., Ota, S., Kawano, S., Sasaki, D., and Asayama, M. (2020). Coproduction of lipids and extracellular polysaccharides from the novel green alga Parachlorella sp. BX1. 5 depending on cultivation conditions. *Biotechnol. Rep.* 25, e00392. doi:10.1016/j.btre.2019.e00392

Shan, C., Jiayuan, L., Wenbo, F., Mingzhe, Y., Zhang, W., Houtao, X., et al. (2020). Biochemical responses of the freshwater microalga Dictyosphaerium sp. upon exposure to three sulfonamides. *J. Environ. Sci.* 97, 141–148. doi:10.1016/j.jes.2020.05.018

Shen, Y., Zhu, W., Li, H., Ho, S. H., Chen, J., Xie, Y., et al. (2018). Enhancing cadmium bioremediation by a complex of water-hyacinth derived pellets immobilized with Chlorella sp. *Bioresour. Technol.* 257, 157–163. doi:10.1016/j.biortech.2018.02.060

Sherpa, R. T., Reese, C. J., and Aliabadi, H. M. (2015). Application of iChip to grow "uncultivable" microorganisms and its impact on antibiotic discovery. *J. Pharm. Pharm. Sci.* 18 (3), 303–315. doi:10.18433/j30894

Shokri Khoubestani, R., Mirghaffari, N., and Farhadian, O. (2015). Removal of three and hexavalent chromium from aqueous solutions using a microalgae biomass-derived biosorbent. *Environ. Prog. Sustain. Energy* 34 (4), 949–956. doi:10.1002/ep.12071

Shubin, L., Li, W., Haijian, Y., Delu, Z., and Chunxiang, H. (2017). A new biofilm based microalgal cultivation approach on shifting sand surface for desert cyanobacterium Microcoleus vaginatus. *Bioresour. Technol.* 238, 602–608. doi:10.1016/j.biortech.2017.04.058

Silva, G. H., Sueitt, A. P. E., Haimes, S., Tripidaki, A., van Zwieten, R., and Fernandes, T. V. (2019). Feasibility of closing nutrient cycles from black water by microalgae-based technology. *Algal Res.* 44, 101715. doi:10.1016/j.algal.2019.101715

Stavi, I., and Lal, R. (2015). Achieving zero net land degradation: Challenges and opportunities. *J. Arid. Environ.* 112, 44–51. doi:10.1016/j.jaridenv.2014.01.016

Tang, D. Y. Y., Khoo, K. S., Chew, K. W., Tao, Y., Ho, S. H., and Show, P. L. (2020). Potential utilization of bioproducts from microalgae for the quality enhancement of natural products. *Bioresour. Technol.* 304, 122997. doi:10.1016/j.biortech.2020.122997

Tiwari, B., Singh, S., Chakraborty, S., Verma, E., and Mishra, A. K. (2017). Sequential role of biosorption and biodegradation in rapid removal degradation and utilization of methyl parathion as a phosphate source by a new cyanobacterial isolate Scytonema sp. BHUS-5. *Int. J. Phytoremediation* 19 (10), 884–893. doi:10.1080/15226514.2017.1303807

Tiwari, O. N., Bhunia, B., Mondal, A., Gopikrishna, K., and Indrama, T. (2019). System metabolic engineering of exopolysaccharide-producing cyanobacteria in soil rehabilitation by inducing the formation of biological soil crusts: A review. *J. Clean. Prod.* 211, 70–82. doi:10.1016/j.jclepro.2018.11.188

Tuzen, M., Sari, A., Mendil, D., Uluozlu, O. D., Soylak, M., and Dogan, M. (2009). Characterization of biosorption process of As(III) on green algae Ulothrix cylindricum. *J. Hazard. Mat.* 165 (1), 566–572. doi:10.1016/j.jhazmat.2008.10.020

Upadhyay, A. K., Mandotra, S. K., Kumar, N., Singh, N. K., Singh, L., and Rai, U. N. (2016). Augmentation of arsenic enhances lipid yield and defense responses in alga Nannochloropsis sp. *Bioresour. Technol.* 221, 430–437. doi:10.1016/j.biortech.2016.09.061

Wollmann, F., Dietze, S., Ackermann, J. U., Bley, T., Walther, T., Steingroewer, J., et al. (2019). Microalgae wastewater treatment: Biological and technological approaches. *Eng. Life Sci.* 19 (12), 860–871. doi:10.1002/elsc.201900071

Wu, W., Ke, T., Zhou, X., Li, Q., Tao, Y., Zhang, Y., et al. (2022). Synergistic remediation of copper mine tailing sand by microalgae and fungi. *Appl. Soil Ecol.* 175, 104453. doi:10.1016/j.apsoil.2022.104453

Wuang, S. C., Khin, M. C., Chua, P. Q. D., and Luo, Y. D. (2016). Use of Spirulina biomass produced from treatment of aquaculture wastewater as agricultural fertilizers. *Algal Res.* 15, 59–64. doi:10.1016/j.algal.2016.02.009

Xiaoyu, W., Meiyin, W., Lei, Z., Yongdong, D., Yang, H., Chenda, Y., et al. (2022). ALA_PDT promotes ferroptosis-like death of Mycobacterium abscessus and antibiotic sterilization via oxidative stress. *Antioxidants* 11 (3), 546. doi:10.3390/antiox11030546

Xin, P., and Bruns, M. A. (2019). Development of a nitrogen-fixing cyanobacterial consortium for surface stabilization of agricultural soils. *J. Appl. Phycol.* 31 (2), 1047–1056. doi:10.1007/s10811-018-1597-9

Xu, Y., Rossi, F., Colica, G., Deng, S., De Philippis, R., and Chen, L. (2013). Use of cyanobacterial polysaccharides to promote shrub performances in desert soils: A potential approach for the restoration of desertified areas. *Biol. Fertil. Soils* 49 (2), 143–152. doi:10.1007/s00374-012-0707-0

Yadav, P., Gupta, R. K., Singh, R. P., Yadav, P. K., Patel, A. K., and Pandey, K. D. (2021). "Role of cyanobacteria in green remediation," in *Sustainable environmental clean-up* (Amsterdam, Netherlands: Elsevier), 187–210. doi:10.1016/B978-0-12-823828-8.00009-8

Yasin, D., Fatma, T., Zafaryab, M., Ahmad, N., Aziz, N., and Rizvi, M. M. A. (2018). Exploring the bio-efficacies of methanolic extracts of Nostoc muscorum and Calothrix brevissima with their Characterization Using GC-MS. *Nat. Prod. J.* 8 (4), 305–316. doi:10.2174/2210315508666180807095636

Yilmaz, E., and Sönmez, M. (2017). The role of organic/bio–fertilizer amendment on aggregate stability and organic carbon content in different aggregate scales. *Soil Tillage Res.* 168, 118–124. doi:10.1016/j.still.2017.01.003

Yoder, N., and Davis, J. G. (2020). Organic fertilizer comparison on growth and nutrient content of three kale cultivars. *HortTechnology* 30 (2), 176–184. doi:10.21273/HORTTECH04483-19

Yokota, K., Waterfield, H., Hastings, C., Davidson, E., Kwietniewski, E., and Wells, B. (2017). Finding the missing piece of the aquatic plastic pollution puzzle: Interaction between primary producers and microplastics. *Limnol. Oceanogr. Lett.* 2 (4), 91–104. doi:10.1002/lol2.10040

frontiers | Frontiers in Environmental Science

TYPE Original Research
PUBLISHED 22 November 2022
DOI 10.3389/fenvs.2022.1035960

OPEN ACCESS

EDITED BY
Xing Yang,
Hainan University, China

REVIEWED BY
Viraj Gunarathne,
University of Wuppertal, Germany
Ali El-Naggar,
Ain Shams University, Egypt

*CORRESPONDENCE
Dan Liu,
liudan@zafu.edu.cn

SPECIALTY SECTION
This article was submitted to Toxicology, Pollution and the Environment,
a section of the journal
Frontiers in Environmental Science

RECEIVED 03 September 2022
ACCEPTED 27 October 2022
PUBLISHED 22 November 2022

CITATION
Xu M, Luo F, Tu F, Rukh G, Ye Z, Ruan Z and Liu D (2022), Effects of stabilizing materials on soil Cd bioavailability, uptake, transport, and rice growth.
Front. Environ. Sci. 10:1035960.
doi: 10.3389/fenvs.2022.1035960

Effects of stabilizing materials on soil Cd bioavailability, uptake, transport, and rice growth

Meizhen Xu[1], Fei Luo[1], Feng Tu[1], Gul Rukh[2], Zhengqian Ye[3], Zhongqiang Ruan[3] and Dan Liu[3]*

[1]Chengbang Ecological Environment Co Ltd., Hangzhou, China, [2]Department of Chemistry, The Islamia College University Peshawar, Peshawar, Pakistan, [3]Key Laboratory of Soil Contamination Bioremediation of Zhejiang Province, Zhejiang A and F University, Hangzhou, China

Cadmium, a widespread toxic heavy metal in farmland soils, is harmful to human health. A field experiment was conducted to investigate the effects of biochar and biochar-based fertilizers on soil pH, organic matter, and available Cd, as well as rice Cd uptake and translocation. The results showed that rice biomass was significantly increased after both the application of biochar and high rate of biochar-based fertilizers at the tillering stage. The biomass and plant height of rice were improved at filling and maturity stages. Soil pH was significantly increased with the application of biochar but not with the biochar-based fertilizer. The amendments of biochar and biochar-based fertilizers had no significant ($p < 0.05$) influence on soil organic matter content. The concentration of available Cd in soil and the concentration of Cd in rice were decreased with the application of different amounts of biochar and biochar-based fertilizers in the mature stage. However, this effect was much greater under biochar amendment. Compared to the control, the concentration of available Cd in soil was reduced by 33.09% with the low application rate of biochar, while that was reduced by 18.06% with the high application rate of biochar. The lowest bioaccumulation factor was due to the high concentration of biochar and biochar-based fertilizers. It is concluded that biochar and biochar-based fertilizers particularly at a high addition rate are appropriate for decreasing Cd mobility and improve soil quality for contaminated paddy soils. The study showed a method for the safe production of rice in Cd-polluted farmlands by using a high application rate of biochar or carbon-based fertilizers.

KEYWORDS

biochar, biochar-based fertilizer, Cd, rice, farmland soils

1 Introduction

Heavy metal pollution of agricultural soil can be due to industrial wastes and the application of agricultural chemicals, such as fertilizers and pesticides (Jin et al., 2019). This seriously affects quality and yield of agricultural products, which further poses a threat to human health (Yan et al., 2016; Shang et al., 2019). The major heavy metals in contaminated soils are Cd, Pb, Cu, and As, among which Cd is the most common heavy metal in agricultural soils. Rice, one of the main food crops in China, accounts for 55% of the annual grain consumption in China (Ye et al., 2012). Rice planted in Cd-contaminated soils can result in Cd accumulation in rice grains (Cai et al., 2019; Huang et al., 2019) and further enter into the human body through the food chain (Long et al., 2019). Accumulation of Cd in the human body can lead to a series of diseases, such as anemia, organ damage, and progression of cancer in humans (Zhong et al., 2017). Therefore, soil Cd pollution is a critical issue in the rice-growing area of China.

The *in situ* remediation technology of Cd is one of the most widely used agricultural soil remediation technologies (Xu et al., 2019). The amendments currently used widely for remediating Cd-contaminated soils can promote plant growth and reduce risk of soil pollution (Beesley and Marmiroli 2011; Bolan et al., 2014). However, different amendments derived from different materials can immobilize soil Cd to reduce its environmental risk in various ways (Abad-Valle et al., 2016; Kai et al., 2017). Among the passivators, biochar is a commonly used amendment to reduce Cd in agricultural soils to ensure safe production of rice (Hamid et al., 2020; Yang et al., 2021). Biochar-based fertilizers are also an eco-friendly fertilizer that are based on biochar in addition to the organic or inorganic fertilizers (Nyambishi et al., 2017). The application of biochar in the soil can improve soil's physical structure, improve soil's acidity by increasing soil pH, and enhances the water-holding capability and soil fertility, thus ultimately increasing the crop yield (Mansoor et al., 2021; Mohamed et al., 2021). Biochar has a large specific surface area and a strong adsorption capacity for heavy metals, which can be used to reduce the bioavailability of heavy metals (Tian et al., 2021). Previous research showed that biochar could significantly reduce the concentration of acid-soluble Cd in soils by increasing soil pH, thus consequently increasing the Cd immobilization (Xu et al., 2022). Meanwhile, the biochar is effective for promoting plant growth and reducing Cd accumulation (Albert et al., 2021; Wang et al., 2022), showing that the 1% application rate of biochar reduced the Cd concentrations of rice grains by 29.3–35.2%. Biochar derived from different raw materials and produced under different conditions can affect the remediation efficiency of Cd-contaminated agricultural soils (El-Naggar et al., 2021; El-Naggar et al., 2022).

The application of biochar and biochar-based fertilizers to polluted agricultural soils displayed a great practical significance for preventing soil nutrient loss and alleviating agricultural non-point source pollution (Lv et al., 2021). We hypothesized that the application of biochar and biochar-based fertilizers can reduce the transport of Cd from the soil to plant and the accumulation of Cd in rice grains through decreasing the bioavailability of Cd in soil. In this study, a field experiment was conducted to study the effects of the application rate of biochar and biochar-based fertilizers on chemical properties of soil, soil Cd availability, and its uptake by rice, as well as the growth of rice in a Cd-contaminated rice-growing soil. This study aims to search for an effective method for decreasing Cd uptake and clarify the effects of biochar and biochar-based fertilizers on heavy metal immobilization and rice growth.

2 Materials and methods

2.1 Test materials

The tested soil was the paddy soil, with a pH of 5.56, organic matter of 2.3%, available N of 126 mg kg^{-1}, available P of 4.58 mg kg^{-1}, available K of 110 mg kg^{-1}, and total Cd of 0.42 mg kg^{-1}.

Biochar was produced from wood chips under an oxygen-limited condition; the material was heated to 450°C at a heating rate of 20°C/min with a retention time of 2 h in a muffle furnace and then taken out and left until the oven temperature dropped to room temperature. A biochar-based fertilizer was produced by mixing biochar and calcium magnesium phosphate fertilizer ($P_2O_5 \geq 12\%$) at a 1:9 ratio. The properties of biochar and biochar-based fertilizer are presented in Table 1.

2.2 Experimental design

The experiment was conducted in the Jinhua Economic Development Zone (119°21′26″, 29°3′33”). Five treatments were set for this experiment: CK, soil without amendment (control); T1, low biochar (4500 kg hm^{-1}); T2, high biochar (9000 kg hm^{-1}); T3, low biochar-based fertilizer (2250 kg hm^{-1}); and T4, high biochar-based fertilizer (4500 kg hm^{-1}). Each treatment had three replicates. In the field experiment, the random block arrangement design was adopted with a plot area of 5m × 8m each. The ridge covered by a plastic film served as spacing between plots.

The rice variety (Yongyou 1540) at the three-leaf stage was transplanted to the field on 2 July 2020 and was harvested on 25 October 2020. The method of base fertilizer + top dressing was used for rice fertilization in all treatments. The base fertilizer was a compound fertilizer (with the contents of N, P, and K of 15-15-15), which was applied at the rate of 450 kg hm^{-2}, and the fertilizer was applied with top dressing (300 kg hm^{-2}) at the tillering stage.

2.3 Sample collection and analysis

The samples of both rice plants and soils were collected at tillering, booting, filling, and maturity stages, respectively. Five samples were collected as a mixed sample from each plot with a depth of 0–20 cm. The harvested plants were washed three times with deionized water, heated at 105°C for 30 min, and then dried at 65°C to be of constant weight. Rice plants were divided into roots, stems, leaves, and brown rice, as well as carrying out the

TABLE 1 Characteristics of biochar and biochar-based fertilizer.

Property	Biochar	Biochar-based fertilizer
pH	10.42	8.27
Organic matter (%)	42.5	38.4
Ash (%)	12.9	11.2
Electrical conductivity (ds m^{-1})	0.38	0.31
Total Cd (mg kg^{-1})	Not detected (<0.05)	0.03

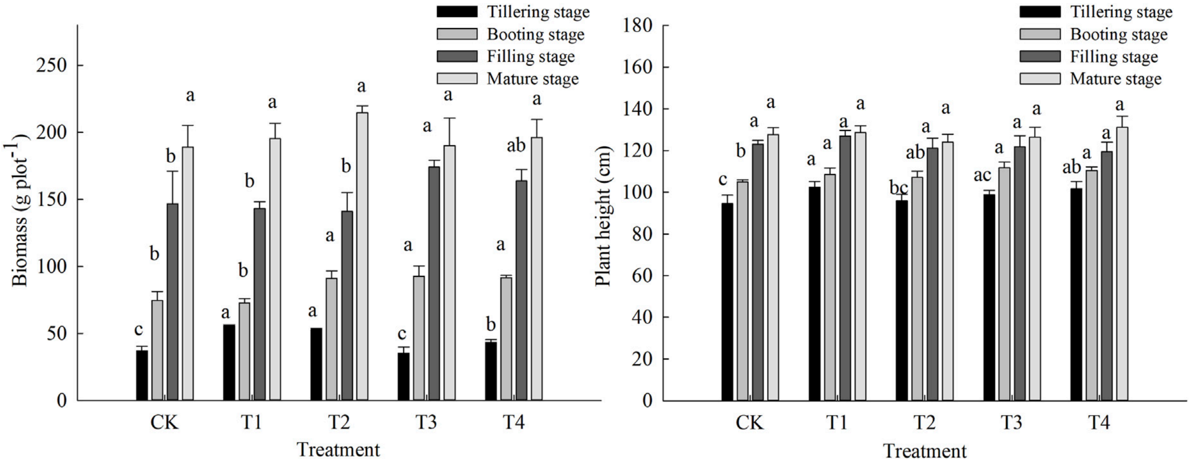

FIGURE 1
Effects of biochar and biochar-based fertilizer on biomass and plant height. Data points and error bars represent mean ± S.D. of three replicates (n = 3). Different letters indicate a significant difference between different treatments in the same period ($p < 0.05$).

determination of dry weight of each part and plant height. The Cd content of each part was determined with digestion of 0.3 g sample with a mixture of HNO_3 and $HClO_4$.

The harvested soils were air-dried and passed through 2-mm and 0.149-mm sieves for chemical analysis. We determined their chemical properties such as pH value (soil/water ratio of 1:2.5), organic matter (potassium dichromate volumetric method), available N (alkaline diffusion method), available P (molybdenum antimony anti-colorimetric method), available K (flame photometer), and total Cd content (Xu et al., 2021). Available Cd contents in soils (extracted by 0.1 M $CaCl_2$ after shaking for 4 h at 1:20 w/v) were determined according to Xu et al. (2021). The soil and plant Cd contents were analyzed by atomic absorption spectroscopy (Shimadzu AA-7000, Japan). The number of certified reference material was GBW 07405 (GSS-5) for verification of soil analysis. The quality control showed the spiked recoveries of Cd between 90% and 110%. The Cd accumulation in terms of bioaccumulation factor (BCF) and translocation factor (TF) were determined as follows: BCF = [Cd concentration in rice tissues]/[Cd total concentration in soil]; TF = [Cd concentration in the stem (leaf, husk, and brown rice)]/[Cd concentration in the root].

2.4 Statistical analysis of data

Statistical analysis was conducted using SPSS 21.0. The values were reported as mean and standard deviation of three independent replicates. The difference was statistically significant at $p < 0.05$ using one-way ANOVA and LSD. The graphical work was carried out using SigmaPlot software v.12.5.

3 Results

3.1 Plant height and the biomass of rice tissues

Figure 1 displays that the biomass of rice at the tillering stage was significantly increased by 50.63%, 42.57%, and 17.13% after

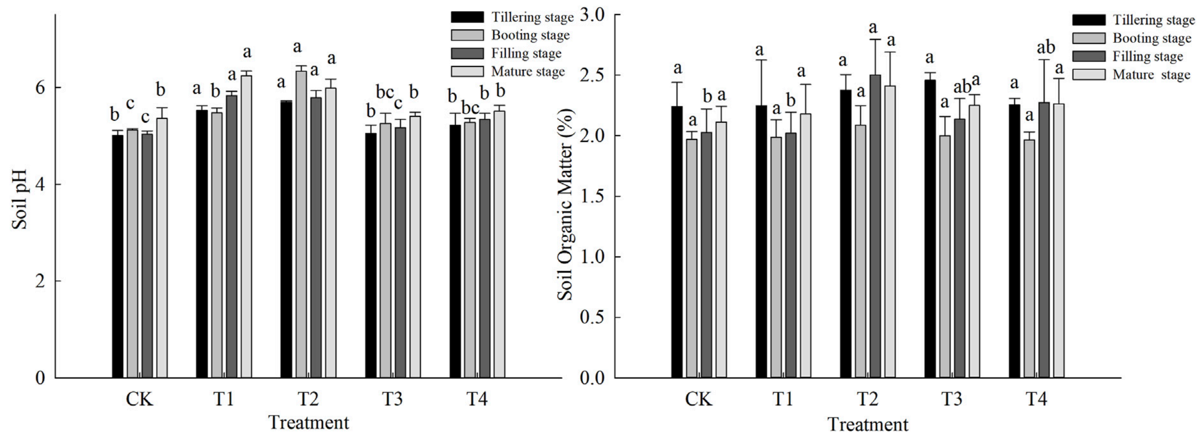

FIGURE 2
Variation in soil pH and organic matter after the addition of different amounts of biochar and biochar-based fertilizer. Data points and error bars represent mean ± S.D. of three replicates ($n = 3$). Different letters indicate a significant difference between different treatments in the same period ($p < 0.05$).

the application of low and high biochar and high biochar-based fertilizer compared to the control, respectively. The biomass of rice at booting and filling stages was increased by 24.30%, 18.63%, 22.86%, and 11.59% with different amounts of the biochar-based fertilizer compared to the control, respectively. The biomass of rice at maturity stages did not exhibit a significant increase with biochar and biochar-based fertilizer treatments compared to the control (Figure 1). The height of the rice plant was enhanced after the addition of biochar and biochar-based fertilizer at tillering and booting stages. There was no significant variation in plant height during filling and maturity stages.

3.2 Dynamic changes of soil properties

Figure 2 indicates that biochar treatment significantly increased soil pH by 0.49 unit compared to CK ($p < 0.05$) at the maturity stage. There was no change in soil pH after the application of the biochar-based fertilizer. The higher pH value was found in biochar-treated soils than those treated with the biochar-based fertilizer. The treatments of biochar and biochar-based fertilizer showed no significant improvement in soil organic matter (OM) compared to the control (Figure 2).

3.3 Effects of different stabilizing materials on available Cd in soil

The concentration of available Cd in soil was reduced by biochar and biochar-based fertilizer, except for the low biochar-based fertilizer at the booting stage (Figure 3). The low application of biochar significantly reduced the concentrations of available Cd in soil by 26.26% compared to those in the control at the tillering stage. The available Cd concentrations in T1, T2, T3, and T4 were reduced by 33.09%, 21.12%, 11.94%, and 19.94% in comparison with those in the control at the maturity stage, respectively. The biochar showed more significant effects on Cd immobilization in soils than the biochar-based fertilizer.

3.4 Effects of different stabilizing materials on Cd uptake and translocation in rice

The concentrations of Cd in rice were decreased with the application of stabilizing materials (Figure 4). The concentrations of Cd in roots, stems, and brown rice were significantly decreased by 19.45%, 24.95%, and 18.06% in T2 treatment and 11.78%, 25.15%, and 14.45% in T4 treatment compared to those in the control. There was no significant difference in Cd concentration of roots with low application amendment (T1 and T3 treatments) in comparison with the control.

The bioconcentration factors and translocation factors of Cd in rice were reduced by different stabilizing materials (Table 2). The BCF size of Cd in rice was $BCF_{root} > BCF_{stem} > BCF_{leaf} > BCF_{husk} > BCF_{brown\ rice}$ in all treatments. The BCF of Cd in rice in all treatments was in the sequence of: CK > low biochar > low biochar-based fertilizer > high biochar-based fertilizer > high biochar. The TF of Cd in rice was $TF_{root\text{-}shoot} > TF_{root\text{-}leaf} > TF_{root\text{-}husk} > TF_{root\text{-}brown\ rice}$.

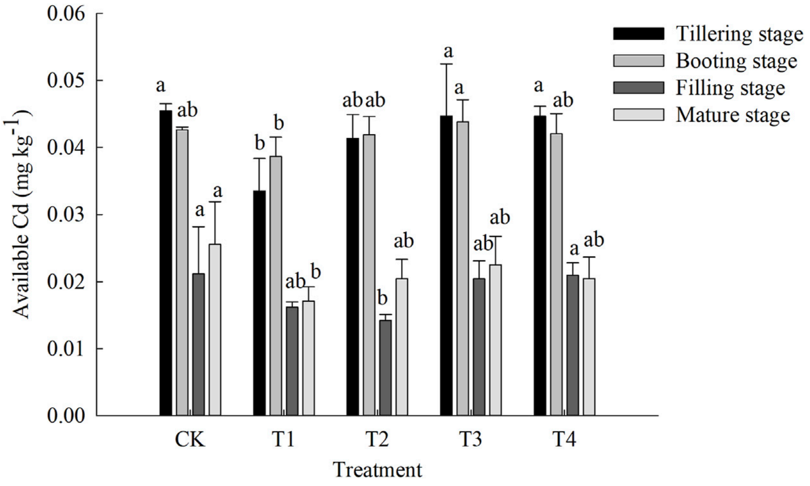

FIGURE 3
Concentrations of available Cd in soil with different stabilizing materials. Data points and error bars represent mean ± S.D. of three replicates (n = 3). Different letters indicate a significant difference between different treatments in the same period ($p < 0.05$).

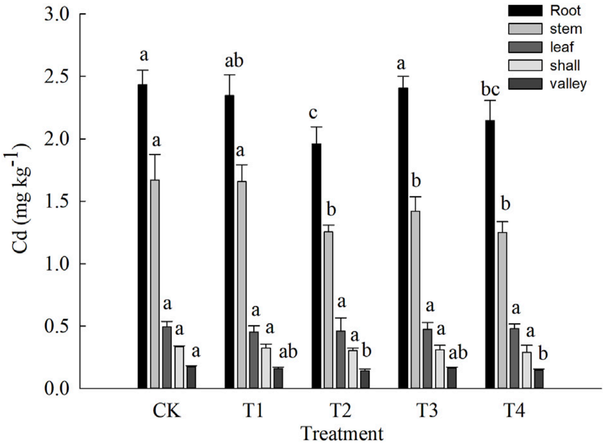

FIGURE 4
Concentrations of Cd in rice with different stabilizing materials. Data points and error bars represent mean ± S.D. of three replicates (n = 3). Different letters indicate a significant difference between different treatments in the same period ($p < 0.05$).

4 Discussion

Figure 2 exhibits the increase in soil pH and organic matter with the application of different stabilizing materials, and the highest pH value was recorded by treatments of biochar compared to the biochar-based fertilizer. This may be due to the higher pH of biochar (10.42) than that of the biochar-based fertilizer (8.27). The increase in soil pH and organic carbon may affect the bioavailability of Cd. The activated functional groups of stabilizing materials (such as -OH, C-O, and CO_3^{2-}) might immobilize Cd ions in soil by precipitation, adsorption, ion exchange, or electrostatic methods (Ahmad et al., 2014; Liu et al., 2020). Previous research showed that the amendment of biochar could release free radical ions such as OH^-, HPO_4^{2-}, and CO_3^{2-}, which may precipitate with Cd and form compounds such as $Cd(Ca_{10-x}Cd_x\ (PO_4)_6(OH)_2$, $CdCO_3$, $Cd_3(PO_4)_2$, and K_4CdCl_6, thus reducing the bioavailability of Cd (Lei et al., 2019). In addition, the oxygen-containing functional groups (such as -OH, -COOH, and C=O) on the biochar surface could also complex with Cd in soil, increasing the Cd immobilization (Rocco et al., 2018). In this study, the decrease in available Cd concentrations in stabilizing materials may be explained by the increase in soil pH. The immobilization of Cd in soil with the amendments further decreased the translocation of Cd from soil to plants. Previous research also reported that the application of biochar (5%) to soil contaminated by heavy metals reduced Cd, Pb, and Zn mobility and availability and hence decreasing the accumulation of metals in different parts of *Phaseolus vulgaris* L (Lomaglio et al., 2018).

The results showed that Cd mainly accumulated in roots, followed by stems and leaves. The transportation route is root–stem–leaf–grain, and the application of stabilizing materials reduced the Cd accumulation in plant roots and rice grains. This suggests that the reduction of Cd transfer from the root to stem in biochar treatment may lead to the decrease in Cd accumulation in grains (Chen et al., 2016). Root–stem translocation is the main factor determining Cd accumulation in grains of rice (Yu and Zhou 2009). In this study, the transport factors from the above ground to grain of rice under high-biochar treatment increased, but the Cd concentration in rice still decreased significantly. This can be explained that the Cd

TABLE 2 Translocation factors and bioconcentration factors of Cd in rice.

Treatment	BCF					TF			
	Root	Stem	Leaf	Husk	Brown rice	Root-stem	Root-leaf	Root-husk	Root-brown rice
CK	5.40 ± 0.26a	3.71 ± 0.45a	1.09 ± 0.10a	0.76 ± 0.01a	0.40 ± 0.02a	0.687 ± 0.078a	0.204 ± 0.028a	0.139 ± 0.008a	0.072 ± 0.006a
T1	5.22 ± 0.37ab	3.69 ± 0.30a	1.00 ± 0.11a	0.71 ± 0.07a	0.36 ± 0.02ab	0.708 ± 0.071ab	0.194 ± 0.034a	0.138 ± 0.006a	0.069 ± 0.005a
T2	4.36 ± 0.30c	2.78 ± 0.12b	1.02 ± 0.24a	0.67 ± 0.05a	0.31 ± 0.03b	0.643 ± 0.072abc	0.234 ± 0.041a	0.155 ± 0.017a	0.073 ± 0.004a
T3	5.36 ± 0.21a	3.16 ± 0.26b	1.04 ± 0.12a	0.69 ± 0.08a	0.36 ± 0.02ab	0.59 ± 0.033bc	0.197 ± 0.022a	0.129 ± 0.02a	0.068 ± 0.002a
T4	4.78 ± 0.36bc	2.78 ± 0.19b	1.07 ± 0.08a	0.64 ± 0.12a	0.33 ± 0.01b	0.583 ± 0.021c	0.224 ± 0.003a	0.135 ± 0.024a	0.07 ± 0.003a

mobilization in the soil was reduced, and the transfer rate of Cd from soil to the part of the plant above the ground will be reduced (Rizwan et al., 2012). Our results were in accordance with the previous researche studies (Bian et al., 2013; Yao et al., 2021). Since the reduction in Cd concentration in edible parts of plants is the key to produce safe food in Cd-contaminated soils (Rizwan et al., 2016), the amendments in this study showed potential effect on remediation of heavy metal-contaminated soil.

The biomass of rice was increased significantly after the application of biochar as stabilizing materials at the tillering stage (Figure 1). This may be due to the increase in soil organic carbon which can control the bioavailability of Cd through forming organic matter–metal complexes (Chiang et al., 2006). Meanwhile, the results showed that the soil organic matter was higher in the biochar treatment than that in the biochar-based fertilizer treatment, which may be due to the higher C storage of biochar than that of the biochar-based fertilizer (Albert et al., 2021). It has been reported that the increase in soil organic carbon with the amendment of biochar and biochar-based fertilizer also provided the carbon resource to microorganisms, promoting the soil microorganism abundance and stimulating soil enzyme activity (Yan et al., 2019). Some studies also show that biochar can improve nitrogen efficiency and promote rice growth by adsorbing and slowly releasing nitrogen (Spokas et al., 2012). This further improved the soil fertility and enhanced the growth of rice (Mansoor et al., 2021). In addition, Cd may reduce the plant cell-wall constituents, inhibit mitosis, and damage the Golgi apparatus of plants which reduced the plant growth (Kachout et al., 2010), while biochar can decrease the detrimental influence of heavy metals, for example, increasing the plant chlorophyll content (Abbas et al., 2017b). In addition, plants could also mediate the transformation, mobility, and bioavailability of heavy metals, which may be due to the interactions of plant, soil, and microbes (Park et al., 2011). Thus, the amendment of biochar not only promoted the plant growth through increasing organic carbon content or nitrogen efficiency which enhanced the interactions of plant and soils but also increased the Cd immobilization in soil through reducing the Cd accumulation and transport of cadmium in plants, increasing the rice yield and food safety (Zhang et al., 2013; Abbas et al., 2017a).

5 Conclusion

The biomass of rice increased with the application of different amounts of biochar and carbon-based fertilizers, while the height of the rice plant increased with the application of low biochar and high carbon-based fertilizer at the mature stage. The concentration of available Cd in soil was reduced with the application of biochar and biochar-based fertilizer. This may be due to the improvement of soil properties, like the increase in soil pH and organic carbon content, which further reduced the BCF of Cd at the high application rate of soil amendments. Although the translocation of Cd from the root to stem showed no significant difference with the addition of biochar, the decrease in Cd accumulation in the root still decreased the Cd accumulation in grains. It is concluded that biochar and biochar-based fertilizer with a high application rate in this study not only improve Cd-contaminated soils but also provide practical significance for future field experiments.

Data availability statement

The raw data supporting the conclusion of this article will be made available by the authors, without undue reservation.

Author contributions

MX and DL contributed to the conception and design of the study. FL and FT organized the database. ZR performed the statistical analysis. MX wrote the first draft of the manuscript. GR, ZY, DL, and MX wrote the sections of the manuscript. All authors contributed to manuscript revision, read, and approved the submitted version.

Funding

The study was financially supported by a grant from the Natural Science Foundation of Zhejiang Province (No. LZ20C160003) and Key Research and Development Project of Zhejiang Province (No. 2022C0222).

Conflict of interest

Authors MX, FL, and FT were employed by the Chengbang Ecological Environment Co. Ltd.

The remaining authors declare that the research was conducted in the absence of any commercial or financial relationships that could be construed as a potential conflict of interest.

Publisher's note

References

Abad-Valle, P., Álvarez-Ayuso, E., Murciego, A., and Pellitero, E. (2016). Assessment of the use of sepiolite amendment to restore heavy metal polluted mine soil. *Geoderma* 280, 57–66. doi:10.1016/j.geoderma.2016.06.015

Abbas, T., Rizwan, M., Ali, S., Adrees, M., Zia-ur-Rehman, M., Qayyum, M. F., et al. (2017a). Effect of biochar on alleviation of cadmium toxicity in wheat (*Triticum aestivum* L.) grown on Cd-contaminated saline soil. *Environ. Sci. Pollut. Res.* 25, 25668–25680. doi:10.1007/s11356-017-8987-4

Abbas, T., Rizwan, M., Ali, S., Zia-ur-Rehman, M., Qayyum, M. F., Abbas, F., et al. (2017b). Effect of biochar on cadmium bioavailability and uptake in wheat (*Triticum aestivum* L.) grown in a soil with aged contamination. *Ecotoxicol. Environ. Saf.* 140, 37–47. doi:10.1016/j.ecoenv.2017.02.028

Ahmad, M., Rajapaksha, A. U., Lim, J. E., Ming, Z., Bolan, N., Mohan, D., et al. (2014). Biochar as a sorbent for contaminant management in soil and water: A review. *Chemosphere* 99, 19–33. doi:10.1016/j.chemosphere.2013.10.071

Albert, H. A., Li, X., Jeyakumar, P., Wei, L., Huang, L., Huang, Q., et al. (2021). Influence of biochar and soil properties on soil and plant tissue concentrations of Cd and Pb: A meta-analysis. *Sci. Total Environ.* 755, 142582–142627. doi:10.1016/j.scitotenv.2020.142582

Beesley, L., and Marmiroli, M. (2011). The immobilisation and retention of soluble arsenic, cadmium and zinc by biochar. *Environ. Pollut.* 159 (2), 474–480. doi:10.1016/j.envpol.2010.10.016

Bian, R., Chen, D., Liu, X., Cui, L., Li, L., Pan, G., et al. (2013). Biochar soil amendment as a solution to prevent Cd-tainted rice from China: Results from a cross-site field experiment. *Ecol. Eng.* 58 (13), 378–383. doi:10.1016/j.ecoleng.2013.07.031

Bolan, N., Kunhikrishnan, A., Thangarajan, R., Kumpiene, J., Park, J., Makino, T., et al. (2014). Remediation of heavy metal(loid)s contaminated soils – to mobilize or to immobilize? *J. Hazard. Mater.* 266, 141–166. doi:10.1016/j.jhazmat.2013.12.018

Cai, L. M., Wang, Q. S., Luo, J., Chen, L. G., Zhu, R. L., and Wang, S. (2019). Heavy metal contamination and health risk assessment for children near a large Cu-smelter in central China. *Sci. Total Environ.* 650 (1), 725–733. doi:10.1016/j.scitotenv.2018.09.081

Chen, D., Guo, H., Li, R., Li, L., Pan, G., Chang, A., et al. (2016). Low uptake affinity cultivars with biochar to tackle Cd-tainted rice—A field study over four rice seasons in hunan, China. *Sci. Total Environ.* 541, 1489–1498. doi:10.1016/j.scitotenv.2015.10.052

Chiang, P. N., Wang, M. K., Chiu, C. Y., and Chou, S. Y. (2006). Effects of cadmium amendments on low-molecular-weight organic acid exudates in rhizosphere soils of tobacco and sunflower. *Environ. Toxicol.* 21 (5), 479–488. doi:10.1002/tox.20210

El-Naggar, A., Chang, S. X., Cai, Y., Lee, Y. H., Wang, J., Wang, S.-L., et al. (2021). Mechanistic insights into the (im) mobilization of arsenic, cadmium, lead, and zinc in a multi-contaminated soil treated with different biochars. *Environ. Int.* 156, 106638. doi:10.1016/j.envint.2021.106638

El-Naggar, A., Chen, Z., Jiang, W., Cai, Y., and Chang, S. X. (2022). Biochar effectively remediates Cd contamination in acidic or coarse-and medium-textured soils: A global meta-analysis. *Chem. Eng. J.* 442, 136225. doi:10.1016/j.cej.2022.136225

Hamid, Y., Tang, L., Hussain, B., Usman, M., and Yang, X. (2020). Organic soil additives for the remediation of cadmium contaminated soils and their impact on the soil-plant system: A review. *Sci. Total Environ.* 707, 136121–136137. doi:10.1016/j.scitotenv.2019.136121

Huang, Y., Wang, L., Wang, W., Li, T., He, Z., and Yang, X. (2019). Current status of agricultural soil pollution by heavy metals in China: A meta-analysis. *Sci. Total Environ.* 651 (2), 3034–3042. doi:10.1016/j.scitotenv.2018.10.185

Jin, G., Fang, W., Shafi, M., Wu, D., and Liu, D. (2019). Source apportionment of heavy metals in farmland soil with application of APCS-MLR model: A pilot study for restoration of farmland in shaoxing city Zhejiang, China. *Ecotoxicol. Environ. Saf.* 184, 109495. doi:10.1016/j.ecoenv.2019.109495

Kachout, S. S., Mansoura, A. B., Leclerc, J., Mechergui, R., Rejeb, M., and Ouerghi, Z. (2010). Effects of heavy metals on antioxidant activities of: Atriplex hortensis and A. Rosea. *Electron. J. Environ. Agric. Food Chem.* 9 (3), 444–457.

Kai, Y., Jian, X., Jiang, X., Liu, C., and Lu, J. (2017). Stabilization of heavy metals in soil using two organo-bentonites. *Chemosphere* 184, 884–891. doi:10.1016/j.chemosphere.2017.06.040

Lei, S., Shi, Y., Qiu, Y., Che, L., and Xue, C. (2019). Performance and mechanisms of emerging animal-derived biochars for immobilization of heavy metals. *Sci. Total Environ.* 646, 1281–1289. doi:10.1016/j.scitotenv.2018.07.374

Liu, G., Meng, J., Huang, Y., Dai, Z., and Xu, J. (2020). Effects of carbide slag, lodestone and biochar on the immobilization, plant uptake and translocation of as and Cd in a contaminated paddy soil. *Environ. Pollut.* 266 (1), 115194. doi:10.1016/j.envpol.2020.115194

Lomaglio, T., Hattab-Hambli, N., Miard, F., Lebrun, M., Morabito, D., and Trupiano, D. (2018). Cd, Pb, and Zn mobility and (bio)availability in contaminated soils from a former smelting site amended with biochar. *Environ. Sci. Pollut. Res.* 25 (26), 25744–25756. doi:10.1007/s11356-017-9521-4

Long, X., Phla, B., Xfja, B., and Pjc, C. (2019). Health risk assessment and spatial distribution characteristics of heavy metal pollution in rice samples from a surrounding hydrometallurgy plant area in No. 721 uranium mining, East China. *J. Geochem. Explor.* 207, 106360. doi:10.1016/j.gexplo.2019.106360

Lv, G., Yang, T., Chen, Y., Hou, H., Liu, X., Li, J., et al. (2021). Biochar-based fertilizer enhanced Cd immobilization and soil quality in soil-rice system. *Ecol. Eng.* 171, 106396. doi:10.1016/j.ecoleng.2021.106396

Mansoor, S., K Our, N., Manhas, S., Zahid, S., Ahmad, P., and Sharma, V. (2021). Biochar as a tool for effective management of drought and heavy metal toxicity. *Chemosphere* 271 (4), 129458. doi:10.1016/j.chemosphere.2020.129458

Mohamed, B. A., Ellis, N., Chang, S. K., Bi, X., and Chen, W. (2021). Engineered biochars from catalytic microwave pyrolysis for reducing heavy metals phytotoxicity and increasing plant growth. *Chemosphere* 271, 129808. doi:10.1016/j.chemosphere.2021.129808

Nyambishi, T. J., Gwenzi, W., Chaukura, N., and Nyamande, M. (2017). Synthesis and nutrient release patterns of a biochar-based N-P-K slow-release fertilizer. *Int. J. Environ. Sci. Technol. (Tehran).* 15 (5), 405–414. doi:10.1007/s13762-017-1399-7

Park, J. H., Lamb, D., Paneerselvam, P., Choppala, G., Bolan, N., and Chung, J.-W. (2011). Role of organic amendments on enhanced bioremediation of heavy metal (loid) contaminated soils. *J. Hazard. Mater.* 185 (2-3), 549–574. doi:10.1016/j.jhazmat.2010.09.082

Rizwan, M., Meunier, J. D., Miche, H., and Keller, C. (2012). Effect of silicon on reducing cadmium toxicity in durum wheat (Triticum turgidum L. cv. Claudio W.)

grown in a soil with aged contamination. *J. Hazard. Mater.* 209-210, 326–334. Mar.30). doi:10.1016/j.jhazmat.2012.01.033

Rizwan, M., Ali, S., Abbas, T., Zia-Ur-Rehman, M., Hannan, F., Keller, C., et al. (2016). Cadmium minimization in wheat: A critical review. *Ecotoxicol. Environ. Saf.* 130, 43–53. doi:10.1016/j.ecoenv.2016.04.001

Rocco, C., Seshadri, B., Adamo, P., Bolan, N. S., Mbene, K., and Naidu, R. (2018). Impact of waste-derived organic and inorganic amendments on the mobility and bioavailability of arsenic and cadmium in alkaline and acid soils. *Environ. Sci. Pollut. Res.* 25, 25896–25905. doi:10.1007/s11356-018-2655-1

Shang, E., Xu, E., Zhang, H., and Huang, C. (2019). Temporal-spatial trends in potentially toxic trace element pollution in farmland soil in the major grain-producing regions of China. *Sci. Rep.* 9 (1), 19463. doi:10.1038/s41598-019-55278-5

Spokas, K. A., Novak, J. M., and Venterea, R. T. (2012). Biochar's role as an alternative N-fertilizer: Ammonia capture. *Plant Soil* 350 (1), 35–42. doi:10.1007/s11104-011-0930-8

Tian, X., Wang, D., Chai, G., Zhang, J., and Zhao, X. (2021). Does biochar inhibit the bioavailability and bioaccumulation of as and Cd in co-contaminated soils? A meta-analysis. *Sci. Total Environ.* 762, 143117. doi:10.1016/j.scitotenv.2020.143117

Wang, J., Yuan, R., Zhang, Y., Si, T., Li, H., Duan, H., et al. (2022). Biochar decreases Cd mobility and rice (Oryza sativa L.) uptake by affecting soil iron and sulfur cycling. *Sci. Total Environ.* 836, 155547. doi:10.1016/j.scitotenv.2022.155547

Xu, W., Hou, S., Amankhan, M., Chao, Y., Dan, L., and Zebin, R. (2021). Effect of water and fertilization management on Cd immobilization and bioavailability in Cd-polluted paddy soil. *Chemosphere* 276, 130168. doi:10.1016/j.chemosphere.2021.130168

Xu, W., Shafi, M., Penttinen, P., Hou, S., Liu, D., and Ma, J. (2019). Bioavailability of heavy metals in contaminated soil as affected by different mass ratios of biochars. *Environ. Technol.* 41 (9), 3329–3337. doi:10.1080/21622515.2019.1609096

Yan, S., Niu, Z., Zhang, A., Yan, H., Zhang, H., He, K., et al. (2019). Biochar application on paddy and purple soils in southern China: Soil carbon and biotic activity. *R. Soc. open Sci.* 6 (7), 181499. doi:10.1098/rsos.181499

Yan, W., Liu, D., Peng, D., Mahmood, Q., Chen, T., Wang, Y., et al. (2016). Spatial distribution and risk assessment of heavy metals inthe farmland along mineral product transportation routes in Zhejiang, China. *Soil Use Manag.* 32, 338–349. doi:10.1111/sum.12268

Yang, X., Li, J., Liang, T., Yan, X., Zhong, L., Shao, J., et al. (2021). A combined management scheme to simultaneously mitigate as and Cd concentrations in rice cultivated in contaminated paddy soil. *J. Hazard. Mater.* 416, 125837. doi:10.1016/j.jhazmat.2021.125837

Yao, Y., Zhou, H., Yan, X. L., Yang, X., and Liao, B. H. (2021). The Fe_3O_4-modified biochar reduces arsenic availability in soil and arsenic accumulation in indica rice (Oryza sativa L.). *Environ. Sci. Pollut. Res.* 28, 18050–18061. doi:10.1007/s11356-020-11812-x

Ye, X., Ma, Y., and Bo, S. (2012). Influence of soil type and genotype on Cd bioavailability and uptake by rice and implications for food safety. *J. Environ. Sci.* 24 (9), 1647–1654. doi:10.1016/s1001-0742(11)60982-0

Yu, Z., and Zhou, Q. (2009). Growth responses and cadmium accumulation of Mirabilis jalapa L. under interaction between cadmium and phosphorus. *J. Hazard. Mater.* 167 (1-3), 38–43. doi:10.1016/j.jhazmat.2008.12.082

Zhang, Z., Solaiman, Z. M., Meney, K., Murphy, D. V., and Rengel, Z. (2013). Biochars immobilize soil cadmium, but do not improve growth of emergent wetland species Juncus subsecundus in cadmium-contaminated soil. *J. Soils Sediments* 13 (1), 140–151. doi:10.1007/s11368-012-0571-4

Zhong, B., Chen, J., Shaff, M., Guo, J., Wang, Y., Wu, J., et al. (2017). Effect of lead (Pb) on antioxidation system and accumulation ability of Moso bamboo (Phyllostachys pubescens). *Ecotoxicol. Environ. Saf.* 138, 71–77. doi:10.1016/j.ecoenv.2016.12.020

frontiers | Frontiers in Environmental Science

TYPE Original Research
PUBLISHED 16 January 2023
DOI 10.3389/fenvs.2022.1114335

Field verification of low-level biochar applications as effective ameliorants to mitigate cadmium accumulation into *Brassica campestris* L from polluted soils

Youchi Zhang[1], Shuang Liu[2], Shanna Lin[1], Brian J. Reid[1,3], Frederic Coulon[4] and Chao Cai[1]*

[1]Key Lab of Urban Environment and Health, Institute of Urban Environment, Chinese Academy of Sciences, Xiamen, China, [2]Zhongke Dingshi Environmental Engineering Co., Ltd, Beijing, China, [3]School of Environmental Sciences, University of East Anglia, Norwich, United Kingdom, [4]School of Water, Energy and Environment, Cranfield University, Cranfield, United Kingdom

Check for updates

OPEN ACCESS

EDITED BY
Lizhi He,
Zhejiang Agriculture and Forestry University, China

REVIEWED BY
Hanbo Chen,
Shenyang Agricultural University, China
Boling Li,
Suzhou University of Science and Technology, China

*CORRESPONDENCE
Chao Cai,
✉ ccai@iue.ac.cn

SPECIALTY SECTION
This article was submitted to Toxicology, Pollution and the Environment, a section of the journal Frontiers in Environmental Science

RECEIVED 02 December 2022
ACCEPTED 29 December 2022
PUBLISHED 16 January 2023

CITATION
Zhang Y, Liu S, Lin S, Reid BJ, Coulon F and Cai C (2023), Field verification of low-level biochar applications as effective ameliorants to mitigate cadmium accumulation into *Brassica campestris* L from polluted soils.
Front. Environ. Sci. 10:1114335.
doi: 10.3389/fenvs.2022.1114335

Introduction: Cadmium (Cd) has been recognized as a significant contributor to the pollution of farmland soils in China, and biochars have been reported to be effective in mitigating soil Cd pollution. However, most studies have been conducted in laboratory or greenhouse settings, not at a field scale, and the biochars used have been applied at unrealistically high amounts (>10 t/ha).

Methods: In this research, three biochars: rice straw biochar (RSB), pig manure biochar (PMB) and rice husk biochar (RHB) were produced from readily available farm residues. Then the effects at low-level application (1.8 and 3.6 t/ha) on Cd were investigated in a field experiment cropped with rape (*Brassica campestris* L.).

Results: Batch adsorption experiments indicated Cd adsorption capacity of three biochars followed the order of RSB (43.5 mg/g) > PMB (33.3 mg/g) > RHB (24.4 mg/g). Field experiment indicated biochar amendments could slightly change soil pH and cation exchange capacity (CEC); yet led to considerable and significant decreases in extractable Cd concentrations [reductions of: 43%–51% (PMB), 29%–35% (RSB) and 17%–19% (RHB)]. Reduced extractable Cd correlated with lower Cd concentrations in rape plants. PMB and RSB were more effective in decreasing Cd phytoaccumulation into edible parts of rape (>68% reduction) than RHB.

Discussion: Low-level application of PMB or RSB could efficiently decrease the phytoaccumulation of Cd from soils into crops. These results demonstrate the reality of biochar-based remediation solutions to contribute to the mitigation of diffuse Cd contamination in farmland. The results also highlight the need to trail biochars in the presence of the soil to be targeted for remediation.

KEYWORDS

biochar, cadmium, field application, farmland, Brassica

Highlights

- Low application rates, 1.8 t/ha of biochar reduced Cd bioavailability in field soils
- Doubling field application rates of biochar increased Cd immobilization by 10%
- PMB and RSB amendment resulted in lower Cd concentrations in rape than RHB

1 Introduction

Due to industrialization and urbanization, soil cadmium (Cd) pollution is a global issue. Often this pollution is localized in areas of industrial activity (Liao et al., 2015). However, long range transport from industrial sources and the use of tainted water resources for irrigation have resulted in farmland accumulating high levels of contaminants (Khan et al., 2021). In China the latest official soil surveys conclude that 19.4% of national farmland soils (based on the sampling points) has been contaminated (MEP, 2014). Cd, along with mercury (Hg), arsenic (As), copper (Cu), lead (Pb), chromium (Cr), zinc (Zn) and nickel (Ni), are recognized to be priority risk drivers. Cd can migrate from contaminated soils to food crops, which can significantly increase human health risk associated with Cd poisoning (Xiao et al., 2018). There is therefore an urgent need to develop efficient and scalable techniques for the remediation of farmland diffusely polluted with potentially toxic elements (PTEs).

Biochar is the product of the pyrolysis of organic solid wastes under anoxic or limited oxygen conditions (Gao et al., 2022). Several types of biochars have been reported to be efficient in immobilizing heavy metals through mechanisms such as adsorption, surface precipitation and electrostatic interaction (Alam et al., 2018). Biochar influence on Cd availability has been extensively studied over the last decade. For example, Rehman et al. (2018), Li et al. (2019) and Bashir et al., 2018 all reported decreases in Cd bioavailability and reduced Cd accumulation into plants following biochar application to soil. In addition, biochars have been reported to improve soil properties, enhance soil fertility and increase crop yields (Rehman et al., 2018). Thus, biochar amendment is considered as a cost-effective strategy for soil improvement and pollution abatement.

However, most of these studies were conducted in laboratory or greenhouse settings (Rees et al., 2014; Mohamed et al., 2017; Bashir et al., 2018). There is to date little information and guidance on field-scale *in situ* applications of biochar. Moreover, where field trial results have been reported they have shown inconsistent outcomes (O'Connor et al., 2018); these different outcomes being attributed to variable field conditions and contrasting biochar properties. The properties of biochars can be varied widely according to feedstock type used and the pyrolysis conditions applied (Tomczyk et al., 2020; Zong et al., 2021). In addition, after being applied to soils, different biochar types give rise to contrasting changes to the soil properties such as pH and cation exchange capacity (CEC) (Yuan et al., 2021). These soil factors further influence metal ion behaviour. Xiao et al. (2019) produced wheat straw biochar (WS500) and rice straw biochar (RS500) at 500°C, and found the pH, ash content and CEC of two biochars were differed. After applied into two alkaline soils, the decrease of concentration of DTPA extracted Cd in WS500 treatments were kept higher than those in RS500 treatments, and the Cd accumulation into ryegrass grew in WS500 amend soils were 1.04–1.17 times as those in RS500 amended soils.

There are also issues pertaining to the realism of biochar application rates applied into field soils in many of the published reports (Rajkovich et al., 2012; Cui et al., 2016). Many authors have used biochar at very large application amounts, for example, 10–40 t ha^{-1} (Cui et al., 2016; O'Connor et al., 2018). In a few studies, application rates of biochar have been even higher (equivalent to more than 90 t/ha; Rajkovich et al., 2012; Rondon et al., 2007). Given the limit availability of biochar resource and the associated cost of biochar application, such large rates of biochar application at a field scale would likely be unfeasible. Importantly, it has been reported that decreases in metal availability, following biochar application, are not proportional to the amount of biochar applied (Bian et al., 2014); and, in Jeffery's meta-analysis (1,483 studies), a poor relationship between biochar application rate and crop yield was reported ($r^2 = .1$; Jeffery et al., 2011). It might therefore be concluded that high application rates of biochar may not be necessary to achieve desired outcomes. Thus, there is a need to evaluate biochar efficacy to mitigate Cd phytoaccumulation using low application rates of biochar under field relevant conditions.

In this study, three biochars including rice straw biochar (RSB), rice husk biochar (RHB) and pig manure biochar (PMB) were prepared and evaluated for their Cd adsorption capacities in the laboratory. The biochars were then used, in a field experiment at two low application rates (1.8 and 3.6 t/ha), under a crop of rape (*Brassica campestris* L.), to: 1) evaluate their influence upon the accumulation of Cd from field soils into the rape roots and edible parts; 2) explore the mechanisms influencing Cd phytoaccumulation, and; 3) provide evidence to assist the selection of biochar feedstock and biochar application rate for utilization to abate risks associated with Cd pollution in farmland soils.

2 Materials and methods

2.1 Biochar preparation

Rice straw biochar (RSB), rice husk biochar (RHB) and pig manure biochar (PMB) were produced using pilot-scale biochar pyrolysis equipment (L 4.5 m × W .8 m × H 2 m). The pyrolysis equipment comprised a pyrolysis chamber, a heating chamber, a feedstock supply system and a biochar output system. The equipment had an overall production capacity of 20 ton per year. Feedstocks were pyrolyzed in the pyrolysis chamber at 500°C for 1 h under limited oxygen conditions. Thereafter, the biochars were ground through a 2 mm sieve. The physico-chemical properties of the three biochars were assessed using methods described in previous work (Zhang and Luo, 2014). Cd adsorption capacities of the biochars were characterized using batch equilibration adsorption experiments (Zhang and Luo, 2014; Zhang et al., 2019) (full details are provided in the supporting information). Briefly, biochar (50 mg) was shaken with $Cd(NO_3)_2$ solution (5 mL) with Cd^{2+} concentration of 25 mol/L–500 mol/L at 25°C at 150 rpm for 48 h. Thereafter the suspensions were collected, and the concentration of Cd measured by inductively coupled plasma optical emission spectrometer (ICP-OES) (Optima 7000DV; PerkinElmer Inc.).

2.2 Field study

The field experiment was conducted on an upland farm located in Zhouzai village (24°23′26.08″N, 117°43′26.25″E), Zhangzhou city, Fujian province in southern China. The concentration of Cd in local soil was .38 mg/kg. This Cd concentration of soils exceeded the regulatory limit for agricultural soils (.30 mg/kg; MEP, 2018). Thus, the Cd concentration was less than twice of the value of regulatory limit, which suggests the experimental soil was not heavily polluted. In China, such marginal exceedance is far more common, than heavy pollution in polluted farmland soils (Teng et al., 2014).

In November 2016, soil (0–20 cm) was ploughed. Biochars were then spread on the soil surface, and thoroughly mixed with the soils using a tillage machine (1GQN-120; Weifang shengxuan machines corporation). The applications of biochar were 0, 1.8 and 3.6 t/ha. Each treatment was produced in triplicate. The area of each plot was 4 m^2. Two weeks after biochar application, the land was rolled, and rape (*Brassica campestris* L.) seeds were sown. Irrigation and fertilizer management were performed according to the conventional practices of the local farmers and were identical on all plots, in which the metal concentrations of fertilizers used in the experiment fitted the requirement of limit value of Chinese standard of ecological index of arsenic, cadmium, lead, chromium and mercury for fertilizers (AQSIQ, 2009).

2.3 Sampling and analysis

In January 2017, the rape plants were harvested. Three composite rape samples, each consisting of 10 plants randomly selected from each plot, were collected (resulting in nine composite rape samples for each treatment regime). Following their transfer to the laboratory, the rape samples were washed with deionized water. Thereafter, the rape samples were cut into two parts (the edible part and the root), and dried in the oven at 90°C. For the analysis of Cd concentrations in the plants, subsamples of the edible part, or root, were crushed, ground, and passed through a .2 mm sieve. Samples of the edible part or root were then digested with HNO_3 (65%, Merck, EMSURE™) using a protocol modified from Zhu et al. (2008). For quality control, plant reference material (GBW 10015; purchased from the National Research Center for Standards in China) was digested and measured alongside the experimental samples, as were reagent blanks. The concentration of Cd in the digestates were analysed using an inductively coupled plasma mass spectrometry (ICP-MS 7500cx; Agilent Inc.). Concentrations of Cd were reported on a dry weight basis. The recovery of Cd from the reference material was 108%–113%. Details of quality control of ICP-MS measurement were described in the Supplementary materials.

Nine soil samples (0–20 cm) were collected from each treatment (3 samples drawn from each plot replicate). Soil samples were air-dried in the laboratory at room temperature, and then ground and passed through a 2 mm sieve. Subsamples of soils were ground and passed through a .15 mm sieve. The pH of soil samples was measured using a pH meter at the ratio of 1 g soil: 2.5 mL deionized water. The CEC of soil was measured using the NH_4OAc-NaOAc method (U.S. Environmental Protection Agency 1986). The concentrations of available Cd in soils were determined using a .01 mol/L $CaCl_2$ extraction method (Houba et al., 1996). Briefly, soil samples were extracted with .01 mol/L $CaCl_2$ solution at the ratio of 1 g soil : $CaCl_2$ solution (10 mL). After 2 h shaking, the suspensions were centrifuged, and the concentrations of Cd in the supernatant were measured using inductively coupled plasma mass spectrometry (ICP-MS 7500cx; Agilent Inc.).

2.4 Data management and statistic analysis

The data were analysed using Microsoft Excel (Microsoft Corp., United States), OriginLab OriginPro 2018 software (OriginLab Corp., United States) and IBM SPSS Statistics 22.0 software (IBM Corp., United States). The fitting of batch adsorption data was performed with OriginLab 2018 software. Statistical analysis of the data was performed with IBM SPSS Statistics 22.0 software. Significant differences among treatments were analysed using one-way analysis of variance (ANOVA) (at $p < .05$ level).

3 Results

3.1 Biochar characterisation

Properties varied across the three biochar types (Table 1). pH was always alkaline and ranged between 9.87 and 10.7; RSB had the highest pH (10.7). Carbon content in RSB or RHB was much higher than the content in PMB, while N and O contents in PMB were the highest amongst the three biochars (1.51% and 20%, respectively). The surface topography and pore structure of the biochars also varied (Table 1; Supplementary Figures S1, S2). The surface area of biochars followed the order of RSB > PMB >> RHB, and the average pore volume of biochars followed the order of PMB = RSB >>> RHB. Based on these chemical and physical properties, it was hypothesised that the RSB (with high pH, high carbon content and high surface area) would offer the best performance for Cd immobilisation (Chen et al., 2011; Shen et al., 2017; O'Connor et al., 2018).

Results of the batch equilibrium experiment indicated that Cd adsorption capacity of the three biochars followed the order: RSB > PMB > RHB (Figure 1; Supplementary Table S1). Cd adsorption onto both PMB and RHB were better fitted by the Freundlich isotherm model (rather than Langmuir isotherm model), while the RSB was fitted well with both the Langmuir and Freundlich isotherm models (Supplementary Table S1). As fitted by the Langmuir isotherm model, the saturation adsorption capacity of RSB, PMB and RHB were 43.5 mg/g, 33.3 mg/g and 24.4 mg/g, respectively. In addition, based on the fitting results, it was concluded that Cd adsorption onto the three biochars was likely attributable to chemical adsorption on heterogeneous surfaces (Zhang and Luo 2014). The value of 1/n in the Freundlich isotherm model followed the order of RSB < PMB < RHB. Since 1/n represented the adsorption affinity of metal ions onto adsorbent, this result confirmed that the adsorption of Cd^{2+} ion onto RSB was the greatest, while RHB showed lowest affinity for Cd ions.

3.2 Effects of biochar amendment on the properties of field soils

The pH in biochar amended soils were increased (Figure 2A). However, no significant difference ($p > .05$) in soil pH were observed among three biochar treatments.

The CEC in the PMB and RSB amended soils were slightly higher, but not significantly different ($p > .05$), to that in the control (Figure 2B). In contrast, soil amended with RHB had a lower CEC (20.0 cmol/kg–20.3 cmol/kg), and it was not significantly different ($p > .05$) from that in the control.

Available Cd concentration in the control soil was 21.5 ± 1.9 μg/kg. Following biochar amendment, the available Cd concentrations were significantly lowered in all treatments ($p < .05$). However, greatest reductions in bioavailable Cd in soil were observed with PMB amendment (43% and 51% reduction at 1.8 and 3.6 t/ha) and RSB amendment (29% and 35% reduction at 1.8 and 3.6 t/ha) (Figure 3).

TABLE 1 Biochar properties[‡].

	PMB	RSB	RHB
pH	9.87 ± .01 c	10.7 ± .2 a	10.0 ± .1 b
pH$_{zpc}$	9.48	9.53	8.91
C (%)	20.5 ± .6 b	41.7 ± .7 a	42.2 ± .1 a
N (%)	1.51 + .03 a	1.06 + .03 b	.62 + .01 c
O (%)	20.1 ± .7 a	12.0 ± 1.0 b	11.1 ± .4 b
H (%)	1.25 ± .03 c	2.01 ± .07 b	2.95 ± .05 a
Ash (%)	67.9 ± .4 a	35.9 ± .4 b	34.7 ± .2 b
Surface topography and pore structure			
BET surface area (m^2/g)	4.13	4.92	2.28
Average pore volume (m^3/g)	.014	.012	.006
Average pore size (nm)	12.7	9.45	9.72
Surface functional groups			
Carboxyl group (mmol/kg)	.25 + 0.001 b	.63 + .13 a	.25 + .001 b
Phenolic group (mmol/kg)	.50 + .25 b	.38 + .18 b	1.17 + .14 a
Lactonic group (mmol/kg)	.75 + .01 b	.87 + .13 b	1.33 + .14 a
Total acid functional group (mmol/kg)	1.50 + .25 b	1.88 + .18 b	2.75 + .25 a
Total base functional group (mmol/kg)	2.38 + .13 b	7.75 + .01 a	.50 + .001 c

[‡] Dissimilar letters indicated significant differences ($p < .05$) among three biochars for a given measurement.

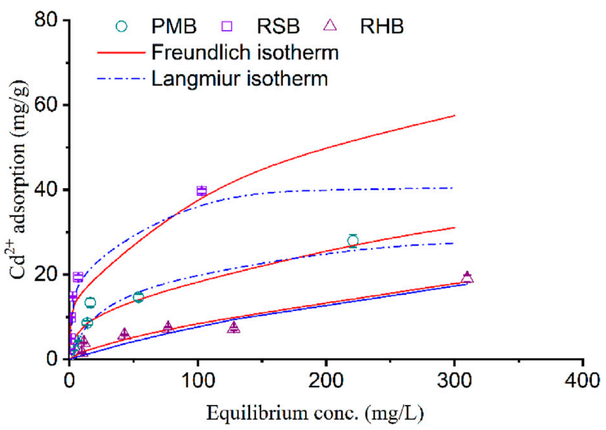

FIGURE 1
Adsorption isotherm of Cd^{2+} ions onto PMB (circles), RSB (squares) and RHB (triangles).

3.3 Effects of biochar amendment on the growths of rape plants in filed

Biochar amendment influenced the growth of rape plants. Increases in dry weight of edible parts (Supplementary Figure S3A) and dry weight of roots (Supplementary Figure S3B) were observed in all instance following biochar amendment. However, these increases in biomass were marginal, and none were significantly different ($p > .05$) when compared to the control (except for the dry weight of root, in the treatment with 1.8 t/ha amendment of PMB).

3.4 Effects of biochar amendment on Cd accumulation into plants

In all instances, biochar amendment resulted in a decrease in the concentration of Cd in rape plants (Figure 4). For the edible part of rape (Figure 4A), the concentrations of Cd in the treatments with PMB and RSB were significantly ($p < .05$) decreased; these levels being 68%–70% of the control value. In the RHB treatments, the Cd concentrations were approximately 89% of the control value, which were higher than the concentrations in treatment with PMB or RSB amendment.

Regarding Cd concentrations in roots (Figure 4B), the Cd concentrations in the treatments with PMB, RSB and RHB were all observed to decrease. Where application rate was equivalent, no significant differences ($p > .05$) were observed across the three biochar types.

4 Discussion

The physico-chemical properties of three biochars were different. PMB contained lower C and higher N than RSB and RHB prepared from plant residues, which was in agreement with previous reports (Zornoza et al., 2016; Bashir et al., 2018). Such differences have previously been attributed to differences in the element composition of feedstocks (Zhao et al., 2013). In addition, the three biochars had different surface topography and pore structure, where PMB and RHB offer higher pore structures than RHB. This finding is in good agreement with previous literature highlighting that contrasting feedstock sources produced biochars with different physical and chemical properties (Tomczyk et al., 2020).

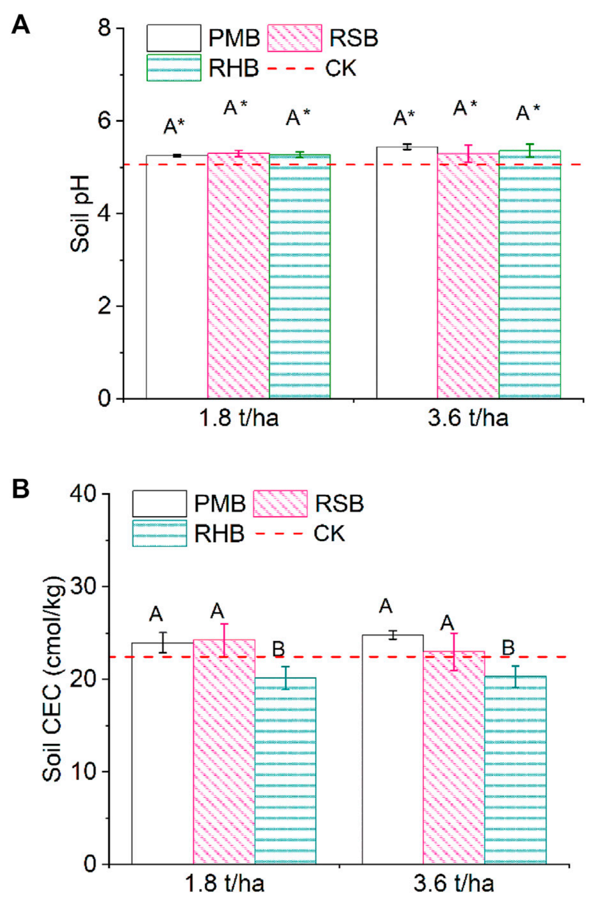

FIGURE 2
Changes in the properties of soil and soil amended with biochars **(A)** soil pH and **(B)** CEC. "*" indicates a value to be significantly different to the control (CK) value ($p < .05$).

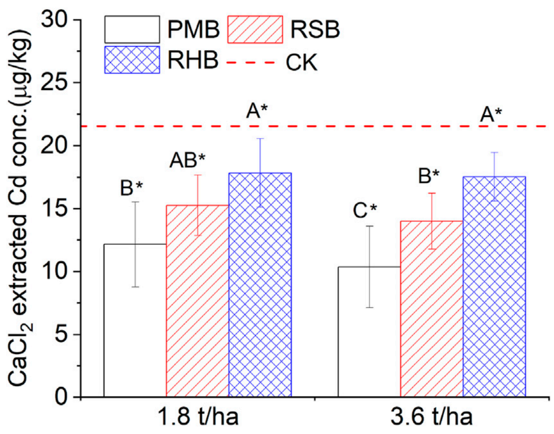

FIGURE 3
Available Cd concentrations in soil and soil amended with biochars. "*" indicates a value to be significantly different to the control (CK) value ($p < .05$).

The properties of biochar including surface area, distribution of surface functional groups, ash content and pH, play important roles during metal adsorption (Jiang et al., 2016). As a consequence of differing physical and chemical properties, the adsorption capacities of the three biochars varied (Figure 1). Complexation of metals, through ion exchange interactions, with ionized surfaces and oxygen-containing functional groups [i.e., carboxyl (–COOH), hydroxyl (–OH), phenol (R–OH) groups] has been suggested as an important mechanism for metal adsorption by biochar (Kołodyńska et al., 2017). In this study, RSB had highest surface area and highest content of surface functional groups, available to prompt interactions with metal ions. Similarly, since the BET surface area and the content of surface functional groups of RHB were lowest among three biochars, the adsorption of Cd^{2+} ion onto RHB was correspondingly lower. In addition, the pH of three biochars also influenced the equilibrium pH and thus the adsorption of Cd^{2+} ions (Supplementary Figure S4). The adsorption of more Cd^{2+} ion onto biochar with increasing pH is consistent with previous reports (Jiang et al., 2016). In the batch experiments, the addition of RSB with highest pH lead to highest equilibrium pH among three biochars (Supplementary Table S4B); this, likely, underpinned the greatest adsorption of Cd^{2+} ions onto RSB. Overall the equilibrium pH in RHB system was lower than RSB or PMB, and its Cd^{2+} ion adsorption was also lower.

When biochar were amended to soil, the increases of soil pH by the addition of three biochars were not significantly different ($p > .05$), and soil CEC were limited changed after biochar application. These outcomes are likely due to the low amendment levels (1.8 and 3.6 t/ha). Nonetheless, all three biochars significantly ($p < .05$) reduced extractable Cd concentrations. It is suggested, therefore, that changes in Cd availability were most likely linked to Cd ion interaction with biochar (rather than changes to the soil chemical environment). Reduced concentrations of available Cd were translated into observed correlated reductions in Cd content in rape plants (Supplementary Table S2). Importantly, the three types of biochar led to different outcomes for Cd-plant interactions. Treatment with RHB was relatively ineffective, while amendment with PMB or RSB resulted in much more effective abatement of soil to plant transfer of Cd. With a doubling in application rates, the decrease of soil available Cd concentrations were increased (on average by approximately extra 10%). This observation suggesting, even at the lowest application rate (1.8 t/ha), that PMB and RSB were effective ameliorants. The literature, in many cases, has reported metal-biochar-soil-plant interactions could result in large decreases in phytoaccumulation of metals into numerous crop types (Mohamed et al., 2017; Zeeshan et al., 2020); while other cases this ameliorative influence has been reported to be minimal (Rees et al., 2014; Zhang et al., 2017; Wang et al., 2019). However, in the present study, RSB and PMB (applied at low-levels: 1.8 and 3.6 t/ha) were established to be effective for the control of Cd phytoaccumulation, while RHB was observed to have only a limited effect.

The performance of these biochars in the batch adsorption experiments and in real soil systems were not consistent, where there was no significant difference between the decreased magnitude of Cd concentrations in rape plants of RSB and PMB

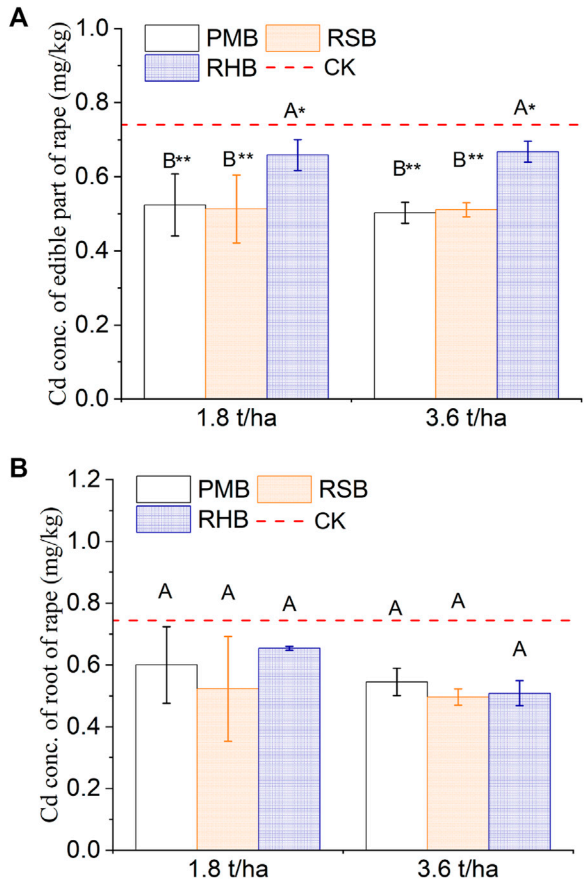

FIGURE 4
Cd concentrations in edible parts **(A)** and roots **(B)** of rape plants grown in soil and soil amended with biochars. "*" indicates a value to be significantly different to the control (CK) value ($p < .05$).

treatments. This outcome is consistent with Uchimiya et al. (2010) who reported biochars produced from broiler litter manure at 350°C (350BL) removed more Ni^{2+} and Cd^{2+} ions than biochars produced at 700°C (700BL); but when applied (at 5%–10% (w/w)) to soil, the 350BL treatment contained higher soluble metal concentrations than the 700BL treated soils. Although the 350BL had a higher adsorption capacity than the 700BL, its lower ability to increase soil pH underpinned the less effective immobilisation of metals in soil by 350BL. Similarly, the pH increase, rather than primary Cd-biochar interaction, has also been proposed by other researchers (Rees et al., 2014). Thus, it is recommended that, before field scale deployment, biochar adsorption capacity should be established in the presence of the soil it is intended to remediate. In addition, given that soil chemical properties (pH and CEC) were largely unchanged, it is suggested that the primary interactions between Cd and the biochars were likely responsible for the outcomes observed.

It is highlighted that in the present research, the soil was not heavily contaminated, which is typical soil pollution condition in farmlands of China. The soil Cd concentration (.38 mg/kg) only just exceeding the regulatory limit of .30 mg/kg (MEP 2018). It is therefore emphasized that the low application rates of biochar were directed at a small excess of Cd in the soil system (this likely underpinned the successful outcomes observed) and that the lower application rate was sufficient to accommodate the excess of Cd. It follows that should prevailing soil Cd concentrations be much higher, such an outcome might not transpire and larger applications of biochar could be needed to accommodate a greater excess of Cd in the soil system. This said, Nie et al. (2018) reported the low level (1.5–3.0 t/ha) application of sugarcane bagasse biochar decreased the concentrations of Cd, Pb and Cu in pak choi by 62%–76%, 17.3%–49.1% and 15%–38%, respectively. In contrast to the present study, the concentrations of Cd, Cu and Pb in this experimental soil were 1.4 mg/kg, 278 mg/kg and 348 mg/kg; Cd being more than 4 times the regulatory limit. Overall, the results of the current research support low-level application (i.e., 1.8 t/ha) of biochar to mitigate the transfer of Cd from soil to rape plants.

It is also highlighted that many of the results reported in the literature relate to biochars that are produced in small quantities in the laboratory (Bashir et al., 2018; Meng et al., 2022). In contrast, the present study considered biochars produced using a larger pyrolysis system having an output capacity of 20 ton per year. Thus, assuming an application rate of 2 t/ha, such a unit could service 10 ha p.a. So, it is emphasised that this scale of production, and low application rates, represents a realistic approach to support the production of biochar in quantities that would allow for meaningful field scale application.

5 Conclusion

Biochars derived from different feedstocks, under identical pyrolysis conditions, showed different adsorption capacities for Cd^{2+} ions. Following amendment to field soil, even at low application rates (1.8 t/ha), all biochars were observed to reduce the bioavailable concentrations of Cd in soil. Biochars derived from pig manure (PMB) or rice straw (RSB) led to much lower Cd concentrations in rape plants when compared to outcomes for rice husk biochar (RHB). This research has validated an approach, wherewith low-level biochar application could efficiently remediate Cd-tainted farmland. These results also highlight the need to trail biochars, in the presence of the soil to be targeted for remediation, before full scale deployment is undertaken. Further field verifications with different biochars at low application rate shall be conducted in different climates with contrasting soil properties and metal concentrations.

Data availability statement

The original contributions presented in the study are included in the article/Supplementary Material; further inquiries can be directed to the corresponding author upon reasonable request.

Author contributions

Conceptualization, YZ and CC; Methodology, YZ and SLIN; Writing-original draft: YZ; Writing-review and editing, YZ, SLIU, BR, FC, and CC. All authors have read and agreed to the published version of the manuscript.

Funding

This work was financially supported by grants from National Key R&D Project (2016YFD0800706), the Science and Technology Project of Xiamen city (3502Z20182001), the STS Program of Fujian-Chinese Academy of Sciences (2021T3006) and the Science and Technology Project of Fujian province (2021N0031).

Acknowledgments

We thank J.J. Fan and Y.W. Hou for supporting in set-up of field trial. We also thank the editors and anonymous experts for their valuable comments.

Conflict of interest

Author SLIU was employed by Zhongke Dingshi Environmental Engineering Co., Ltd.

The remaining authors declare that the research was conducted in the absence of any commercial or financial relationships that could be construed as a potential conflict of interest.

Publisher's note

Supplementary material

The Supplementary Material for this article can be found online at: https://www.frontiersin.org/articles/10.3389/fenvs.2022.1114335/full#supplementary-material

References

Alam, M. S., Gorman-Lewis, D., Chen, N., Flynn, S. L., Ok, Y. S., Konhauser, K. O., et al. (2018). Thermodynamic analysis of Nickel(II) and Zinc(II) adsorption to biochar. *Environ. Sci. Technol.* 52 (11), 6246–6255. doi:10.1021/acs.est.7b06261

AQSIQ (General Administration of Quality Supervision, Inspection and Quarantine of the People's Republic of China) (2009). *Ecological index of arsenic, cadmium, lead, chromium and mercury for fertilizers*. Beijing, China. (GB/T 23349–2009).

Bashir, S., Hussain, Q., Shaaban, M., and Hu, H. (2018). Efficiency and surface characterization of different plant derived biochar for cadmium (Cd) mobility, bioaccessibility and bioavailability to Chinese cabbage in highly contaminated soil. *Chemosphere* 211, 632–639. doi:10.1016/j.chemosphere.2018.07.168

Bian, R., Joseph, S., Cui, L., Pan, G., Li, L., Liu, X., et al. (2014). A three-year experiment confirms continuous immobilization of cadmium and lead in contaminated paddy field with biochar amendment. *J. Hazard. Mater.* 272, 121–128. doi:10.1016/j.jhazmat.2014.03.017

Chen, X. C., Chen, G. C., Chen, L. G., Chen, Y. X., Lehmann, J., McBride, M. B., et al. (2011). Adsorption of copper and zinc by biochars produced from pyrolysis of hardwood and corn straw in aqueous solution. *Biores. Technol.* 102, 8877–8884. doi:10.1016/j.biortech.2011.06.078

Cui, L., Pan, G., Li, L., Bian, R., Liu, X., Yan, J., et al. (2016). Continuous immobilization of cadmium and lead in biochar amended contaminated paddy soil: A five-year field experiment. *Ecol. Eng.* 93, 1–8. doi:10.1016/j.ecoleng.2016.05.007

Gao, Y., Wu, P., Jeyakumar, P., Bolan, N., Wang, H., Gao, B., et al. (2022). Biochar as a potential strategy for remediation of contaminated mining soils: Mechanisms, applications, and future perspectives. *J. Environ. Manag.* 313, 114973. doi:10.1016/j.jenvman.2022.114973

Houba, V. J. G., Lexmond, T. M., Novozamsky, I., and van der Lee, J. J. (1996). State of the art and future developments in soil analysis for bioavailability assessment. *Sci. Total Environ.* 178 (1-3), 21–28. doi:10.1016/0048-9697(95)04793-X

Jeffery, S., Verheijen, F. G. A., van der Velde, M., and Bastos, A. C. (2011). A quantitative review of the effects of biochar application to soils on crop productivity using meta-analysis. *Agric. Ecosyst. Environ.* 144 (1), 175–187. doi:10.1016/j.agee.2011.08.015

Jiang, S., Huang, L., Nguyen, T. A. H., Ok, Y. S., Rudolph, V., Yang, H., et al. (2016). Copper and zinc adsorption by softwood and hardwood biochars under elevated sulphate-induced salinity and acidic pH conditions. *Chemosphere* 142, 64–71. doi:10.1016/j.chemosphere.2015.06.079

Khan, S., Naushad, M., Lima, E. C., Zhang, S., Shaheen, S. M., and Rinklebe, J. (2021). Global soil pollution by toxic elements: Current status and future perspectives on the risk assessment and remediation strategies - a review. *J. Hazard. Mater.* 417, 126039. doi:10.1016/j.jhazmat.2021.126039

Kołodyńska, D., Krukowska, J., and Thomas, P. (2017). Comparison of sorption and desorption studies of heavy metal ions from biochar and commercial active carbon. *Chem. Eng. J.* 307, 353–363. doi:10.1016/j.cej.2016.08.088

Li, S., Wang, M., Zhao, Z., Li, X., and Chen, S. (2019). Use of soil amendments to reduce cadmium accumulation in rice by changing Cd distribution in soil aggregates. *Environ. Sci. Pollut. Res.* 26 (20), 20929–20938. doi:10.1007/s11356-019-05431-4

Liao, Q. L., Liu, C., Wu, H. Y., Jin, Y., Hua, M., Zhu, B. W., et al. (2015). Association of soil cadmium contamination with ceramic industry: A case study in a Chinese town. *Sci. Total Environ.* 514, 26–32. doi:10.1016/j.scitotenv.2015.01.084

Meng, Z., Huang, S., Lin, Z., Mu, W., Ge, H., and Huang, D. (2022). Cadmium long-term immobilization by biochar and potential risks in soils with different pH under combined aging. *Sci. Total Environ.* 825, 154018. doi:10.1016/j.scitotenv.2022.154018

MEP (Ministry of Environmental Protection of the People's Republic of China) (2018). *Soil environmental quality: Risk control standard for contaminated agricultural soils (GB 15618-2018).* Beijing, China.

MEP (Ministry of Environmental Protection of the People's Republic of China) (2014). *Q&A for nationwide soil pollution survey report*. Beijing, China. (In Chinese).

Mohamed, B. A., Ellis, N., Kim, C. S., and Bi, X. (2017). The role of tailored biochar in increasing plant growth, and reducing bioavailability, phytotoxicity, and uptake of heavy metals in contaminated soil. *Environ. Pollut.* 230, 329–338. doi:10.1016/j.envpol.2017.06.075

Nie, C., Yang, X., Niazi, N. K., Xu, X., Wen, Y., Rinklebe, J., et al. (2018). Impact of sugarcane bagasse-derived biochar on heavy metal availability and microbial activity: A field study. *Chemosphere* 200, 274–282. doi:10.1016/j.chemosphere.2018.02.134

O'Connor, D., Peng, T., Zhang, J., Tsang, D. C. W., Alessi, D. S., Shen, Z., et al. (2018). Biochar application for the remediation of heavy metal polluted land: A review of *in situ* field trials. *Sci. Total Environ.* 619-620, 815–826. doi:10.1016/j.scitotenv.2017.11.132

Rajkovich, S., Enders, A., Hanley, K., Hyland, C., Zimmerman, A. R., and Lehmann, J. (2012). Corn growth and nitrogen nutrition after additions of biochars with varying properties to a temperate soil. *Biol. Fertil. Soils* 48 (3), 271–284. doi:10.1007/s00374-011-0624-7

Rees, F., Simonnot, M. O., and Morel, J. L. (2014). Short-term effects of biochar on soil heavy metal mobility are controlled by intra-particle diffusion and soil pH increase: Heavy metal mobility in biochar-amended soils. *Eur. J. Soil Sci.* 65 (1), 149–161. doi:10.1111/ejss.12107

Rehman, M. Z., Rizwan, M., Hussain, A., Saqib, M., Ali, S., Sohail, M. I., et al. (2018). Alleviation of cadmium (Cd) toxicity and minimizing its uptake in wheat (*Triticum aestivum*) by using organic carbon sources in Cd-spiked soil. *Environ. Pollut.* 241, 557–565. doi:10.1016/j.envpol.2018.06.005

Rondon, M. A., Lehmann, J., Ramírez, J., and Hurtado, M. (2007). Biological nitrogen fixation by common beans (*Phaseolus vulgaris* L.) increases with bio-char additions. *Biol. Fertil. Soils* 43 (6), 699–708. doi:10.1007/s00374-006-0152-z

Shen, Z., Zhang, Y., McMillan, O., Jin, F., and Al-Tabbaa, A. (2017). Characteristics and mechanisms of nickel adsorption on biochars produced from wheat straw pellets and rice husk. *Environ. Sci. Pollut. Res.* 24 (14), 12809–12819. doi:10.1007/s11356-017-8847-2

Teng, Y., Jin, W., Lu, S., Wang, Y., Jiao, X., and Song, L. (2014). Soil and soil environmental quality monitoring in China: A review. *Environ. Int.* 69, 177–199. doi:10.1016/j.envint.2014.04.014

Tomczyk, A., Sokołowska, Z., and Boguta, P. (2020). Biochar physicochemical properties: Pyrolysis temperature and feedstock kind effects. *Rev. Environ. Sci. Bio/Technology* 19 (1), 191–215. doi:10.1007/s11157-020-09523-3

Uchimiya, M., Lima, I. M., Thomas, K., Chang, S., Wartelle, L. H., and Rodgers, J. E. (2010). Immobilization of heavy metal ions (Cu^{II}, Cd^{II}, Ni^{II}, and Pb^{II}) by broiler litter-derived biochars in water and soil. *J. Agric. Food Chem.* 58 (9), 5538–5544. doi:10.1021/jf9044217

U. S. Environmental Protection Agency (1986). *Cation-exchange capacity of soils (sodium acetate) (SW846 Method 9081)*. Washington, DC, USA.

Wang, Y., Zhong, B., Shafi, M., Ma, J., Guo, J., Wu, J., et al. (2019). Effects of biochar on growth, and heavy metals accumulation of moso bamboo (*Phyllostachy pubescens*), soil physical properties, and heavy metals solubility in soil. *Chemosphere* 219, 510–516. doi:10.1016/j.chemosphere.2018.11.159

Xiao, R., Wang, P., Mi, S., Ali, A., Liu, X. Y., Li, Y. M., et al. (2019). Effects of crop straw and its derived biochar on the mobility and bioavailability in Cd and Zn in two smelter-contaminated alkaline soils. *Ecotoxicol. Environ. Saf.* 181, 155–163. doi:10.1016/j.ecoenv.2019.06.005

Xiao, W. D., Xuezhu, Y., Qi, Z., De, C., Jing, H., and Na, G. (2018). Evaluation of cadmium transfer from soil to leafy vegetables: Influencing factors, transfer models, and indication of soil threshold contents. *Ecotoxicol. Environ. Saf.* 164, 355–362. doi:10.1016/j.ecoenv.2018.08.041

Yuan, C., Gao, B., Peng, Y., Gao, X., Fan, B., and Chen, Q. (2021). A meta-analysis of heavy metal bioavailability response to biochar aging: Importance of soil and biochar properties. *Sci. Total Environ.* 756, 144058. doi:10.1016/j.scitotenv.2020.144058

Zeeshan, M., Ahmad, W., Hussain, F., Ahamd, W., Numan, M., Shah, M., et al. (2020). Phytostabalization of the heavy metals in the soil with biochar applications, the impact on chlorophyll, carotene, soil fertility and tomato crop yield. *J. Clean. Prod.* 255, 120318. doi:10.1016/j.jclepro.2020.120318

Zhang, R. H., Li, Z. G., Liu, X. D., Wang, B., Zhou, G. L., Huang, X. X., et al. (2017). Immobilization and bioavailability of heavy metals in greenhouse soils amended with rice straw-derived biochar. *Ecol. Eng.* 98, 183–188. doi:10.1016/j.ecoleng.2016.10.057

Zhang, Y. C., Fan, J. J., Fu, M. L., Ok, Y. S., Hou, Y. W., and Cai, C. (2019). Adsorption antagonism and synergy of arsenate (V) and cadmium (II) onto Fe-modified rice straw biochars. *Environ. Geochem. Health* 41 (4), 1755–1766. doi:10.1007/s10653-017-9984-8

Zhang, Y. C., and Luo, W. S. (2014). Adsorptive Removal of heavy metal from acidic wastewater with biochar produced from anaerobically digested residues: Kinetics and surface complexation modeling. *BioResources* 9 (2), 2484–2499. doi:10.15376/biores.9.2.2484-2499

Zhao, L., Cao, X., Mašek, O., and Zimmerman, A. (2013). Heterogeneity of biochar properties as a function of feedstock sources and production temperatures. *J. Hazard. Mater.* 256–257, 1–9. doi:10.1016/j.jhazmat.2013.04.015

Zhu, Y. G., Sun, G. X., Lei, M., Teng, M., Liu, Y. X., Chen, N. C., et al. (2008). High percentage inorganic arsenic content of mining impacted and non-impacted Chinese rice. *Environ. Sci. Technol.* 42 (13), 5008–5013. doi:10.1021/es8001103

Zong, Y., Xiao, Q., and Lu, S. (2021). Biochar derived from cadmium-contaminated rice straw at various pyrolysis temperatures: Cadmium immobilization mechanisms and environmental implication. *Bioresour. Technol.* 321, 124459. doi:10.1016/j.biortech.2020.124459

Zornoza, R., Moreno-Barriga, F., Acosta, J. A., Munoz, M. A., and Faz, A. (2016). Stability, nutrient availability and hydrophobicity of biochars derived from manure, crop residues, and municipal solid waste for their use as soil amendments. *Chemosphere* 144, 122–130. doi:10.1016/j.chemosphere.2015.08.046

Frontiers in Environmental Science

TYPE Original Research
PUBLISHED 01 February 2023
DOI 10.3389/fenvs.2023.1114027

OPEN ACCESS

EDITED BY
Nsikak U. Benson,
Université Claude Bernard Lyon 1, France

REVIEWED BY
Balram Ambade,
National Institute of Technology,
Jamshedpur, India
Hui Wang,
Shenyang University, China

*CORRESPONDENCE
Yusheng Qin,
✉ shengyuq@126.com

SPECIALTY SECTION
This article was submitted
to Soil Processes,
a section of the journal
Frontiers in Environmental Science

RECEIVED 13 December 2022
ACCEPTED 19 January 2023
PUBLISHED 01 February 2023

CITATION
He M, Shangguan Y, Zhou Z, Guo S, Yu H, Chen K, Zeng X and Qin Y (2023), Status assessment and probabilistic health risk modeling of polycyclic aromatic hydrocarbons (PAHs) in surface soil across China.
Front. Environ. Sci. 11:1114027.
doi: 10.3389/fenvs.2023.1114027

Status assessment and probabilistic health risk modeling of polycyclic aromatic hydrocarbons (PAHs) in surface soil across China

Mingjiang He, Yuxian Shangguan, Zijun Zhou, Song Guo, Hua Yu, Kun Chen, Xiangzhong Zeng and Yusheng Qin*

Institute of Agricultural Resources and Environment, Sichuan Academy of Agricultural Sciences, Chengdu, China

Polycyclic aromatic hydrocarbon (PAH) accumulation in topsoil is getting particular concern with the rapid development of urbanization and industrialization, while the overall pollution status and related risk posed by PAHs received limited attentions at the national scale. This study conducted an overview of published data on 16 priority control PAHs by USEPA on the related peer-reviewed 207 research papers between 2000 and 2020 in 30 provinces of China. Based on that, the pollution levels, composition status, spatial distribution pattern, ecological risk, and human health risk posed by soil PAHs were evaluated. Monte Carlo simulation was adopted to model the probabilistic health risk and identify the contributor of such risks. Results demonstrated the concentrations of $\sum_{16}$PAHs in soil varied from “undetected” to 261 μg g^{-1} with a mean value of 0.63 μg g^{-1}, indicating the obvious accumulation of PAHs in topsoil of most provinces in China compared with the guideline value (0.2 μg g^{-1}). The concentrations of $\sum_{16}$PAHs in surface soil of China has obvious regional characteristics. Higher concentrations of soil PAHs are mainly distributed in north, northwest, and eastern regions, especially in Xinjiang, Shandong, Jiangsu, Sichuan, and Guangxi Province. Risk assessment indicates potential ecological and human health risk were posed by soil PAHs, therefore, reducing soil PAHs concentration and exposure frequency are the most effective pathways to protect human health. Despite the fact that risks posed by soil PAHs are generally low, concentrations of PAHs in some sites are relatively high. It is necessary to take effective measures to remediate soil PAHs pollution in certain areas to reduce concentration and associated risks.

KEYWORDS

polycyclic aromatic hydrocarbons, risk assessment, spatial distribution, Monte Carlo, China

1 Introduction

Soil contamination is one of the most concerned issues around the world currently and has attracted particular attentions (Lu et al., 2015; Daso et al., 2016). Pollutants in soil not only have direct harmful effects on ecology, but also pose potential hazard risks to mankind and animals (Salazar et al., 2012; Niu et al., 2013; Lestan, 2017). As reported by the first national soil survey report, the percentage of organic pollutants which exceeded its responding guideline values, ranked second followed by heavy metals (Ministry of Environment Protection and Ministry of Land Resources of the People’s Republic of China, 2014). The polycyclic aromatic hydrocarbon (PAHs) belongs to a group of organic compounds that are composed of more than two condensed aromatic rings, which are carcinogenic, mutagenic, teratogenic, and toxic to living beings (Franco et al., 2008; Ambade and Sethi, 2021). PAHs are widespread in the water, atmosphere, sediments, and soil, and are both from natural sources such as volcanoes and anthropogenic activities such as incomplete combustion of biomass fuels, fossil, and oil spills (Wolska et al., 2012; Yang et al., 2020; Ambade et al., 2022). PAHs tend to retain and accumulate in soil due to their high hydrophobicity. Soil PAHs contamination is getting increasing attention nowadays with a large number reports about high concentrations of PAHs from continuous emission of oil combustion and traffic (Leung et al., 2015; Alves et al., 2016; Chen et al., 2017). To address the overall contamination status, assessment of potential sources, and risks of soil PAHs are vital and essential for soil PAHs pollution remediation.

Risk assessment is the process of estimating the probability of harmful effects posed by contaminants (USEPA, 2016). According to the different end-point receptors, it can be classified into ecological risk and human health risk. Previous studies were mostly focused on the occurrence, source apportionment, and risk assessment of regional soil PAHs (Huang et al., 2014; Yang et al., 2014; Tong et al., 2018). These studies reported the occurrence of soil PAHs regionally, mainly due to human activities such as industrial emission, transportation vehicle, and/or e-waste dismantling. However, existed studies on soil PAHs were largely focused on small regions or areas, limited number of soil samples, or single soil type (Wang et al., 2014; Cai et al., 2017; Zheng et al., 2019). Besides, deterministic (the most likely) values are usually adopted in health risk assessment model of soil PAHs. However, variable of exposure parameters due to the individual differences and PAHs concentration differences from soil spatial heterogeneity would underestimate or overestimate the human health risk from traditional deterministic methods (Yang et al., 2014). Therefore, a comprehensive study taking into account concentration status, pollution level, and induced probabilistic risk modeling of soil PAHs at the national scale was urgent to conduct.

In the present study, a dataset of USEPA 16 priority PAHs in Chinese topsoil was compiled based on peer-reviewed literature. On the ground of the dataset compiled, the objectives of the study were to 1) reveal the overall accumulation and contamination status of PAHs in topsoil of China, 2) present the spatial distribution of soil PAHs concentration, and 3) evaluate the associated ecological and human health risk posed by soil PAHs and model probabilistic health risk by considering variability of exposure parameters. The results would provide basic reference for remediation and risk control of soil PAHs pollution.

2 Methods and materials

2.1 Data collection and development of soil PAHs concentrations dataset

The dataset of PAHs concentrations in topsoil (0–20 cm) was developed based on 14,161 soil samples in 207 research papers published between 2000 and 2020, covering 30 provinces across China (except Hainan, HongKong, Macao, and Taiwan). The keywords "soil PAHs" and "polycyclic aromatic hydrocarbons (PAHs) in soil" were searched on Web of Science, Science Direct, the China Wan Fang database, China Wei Pu Literature, and China National Knowledge Infrastructure Database to find related publications. The papers had to meet the criteria that sampling, analytical methods, quality control were strictly conducted to guarantee the accuracy of the soil PAHs concentrations. The information extracted from each paper included 1) sampling location (province, city, longitude, and latitude), sampling time and depth, number of soil samples; 2) mean value, range of $\sum_{16}$PAHs and mean concentration of the sixteen PAHs congeners. The 16 priority PAHs identified by USEPA were acenaphthylene (ACY), naphthalene (NAP), acenaphthene (ACE), phenanthrene (PHE), fluorene (FL), anthracene (ANT), pyrene (PYR), fluoranthene (FLU), benzo[a] anthracene (BaA), benzo[b] fluoranthene (BbF), chrysene (CHR), benzo[k] fluoranthene (BkF), benzo[a]pyrene (BaP), indeno(1,2, 3-cd)pyrene (IND), dibenzo(a,h) anthracene (DBA), and benzo(g,h,i) perylene (BghiP). Detailed information for each publication are presented in Supplementary Table S1.

2.2 Risk assessment models

2.2.1 Ecological risk assessment

Toxic equivalent concentrations (TEQ_{BaP}) was adopted to characterize ecological risk posed by soil PAHs. TEQ_{BaP} represents the total concentration of transformed individual PAHs congener by the toxic equivalency factor (TEF) (μg kg^{-1}) of BaP (Lin et al., 2013). The TEQ_{BaP} was calculated by the Eq. 1:

$$TEQ_{Bap} = \sum C_i \times TEF_i \tag{1}$$

where C_i means the concentration of PAHs congener i (μg kg^{-1}) and TEF_i is the toxic equivalency factor of PAHs congener i (Samburova et al., 2017). The corresponding TEF of 16 PAHs congeners can be found in Supplementary Table S2.

2.2.2 Human health risk assessment

Human health can be threatened by soil PAHs *via* exposure pathways including oral intake, inhalation, and dermal contact. The USEPA exposure model was adopted to assess the incremental lifetime cancer risk (ILCR) for adults and children exposed by soil PAHs (USEPA, 1989; USEPA, 2009a; USEPA, 2009b). The ILCR through each of the exposure pathways were calculated by the Eqs 2–4:

$$ILCR_{oral} = \frac{CE_s{*}IR_{Ing}{*}\sqrt[3]{\frac{BW}{70}}{*}EF{*}ED}{AT{*}BW{*}10^6} * CSF_{Ing} \tag{2}$$

$$ILCR_{derm} = \frac{CE_s{*}\sqrt[3]{\frac{BW}{70}}{*}EF{*}ED{*}SA{*}AF{*}ABS}{AT{*}BW{*}10^6} * CSF_{Derm} \tag{3}$$

$$ILCR_{inh} = \frac{CE_s{*}IR_{Inh}{*}\sqrt[3]{\frac{BW}{70}}{*}EF{*}ED}{AT{*}PEF{*}BW} * CSF_{Inh} \tag{4}$$

$$ILCR_s = \sum ILCR \tag{5}$$

Where $ILCR_{derm}$, $ILCR_{oral}$, and $ILCR_{inh}$ are the exposure risks of soil PAHs *via* dermal contact, oral intake, and inhalation pathways, respectively (unitless), and $ILCR_s$ is the total human health risk exposed from all the three pathways (unitless). CE_s is TEQ_{BaP} (ug kg^{-1}), BW is the body weight (kg), AT is the average life span (d), IR_{inh} as the soil inhalation rate (m^3 d^{-1}), IR_{ing} represents the soil particle intake rate (mg d^{-1}), ED means the exposure duration (years), SA represents the surface area of dermal exposure (cm^2), EF denotes the exposure frequency (d year^{-1}), AF stands for the adherence factor (mg cm^{-2} h^{-1}), ABS denotes the dermal adsorption fraction (unitless), PEF

TABLE 1 Distribution of collected literature and soil samples of PAHs in China's surface soils.

Region	Province and literature number	Total literature numbers	Soil samples
East China	Jiangsu (19), Shandong (11),Fujian (6), Zhejiang (13),Shanghai (14),Anhui (6), Jiangxi (2)	71	5,958
Northeast China	Liaoning (16), Heilongjiang (3),Jilin (7)	26	974
North China	Beijing (12), Tianjin (14), Hebei (4), Shaanxi (15), Mongolia (2)	47	3,594
Southwest China	Yunnan (1), Tibet (5), Sichuan (3), Guizhou (5), Chongqing (1)	15	809
South China	Guangdong (18), Guangxi (5)	23	963
Northwest China	Shanxi (6), Gansu (3), Xinjiang (3), Ningxia (1), Qinghai (3)	16	580
Central China	Henan (5),Hunan (1),Hubei (3)	9	953

represents the particle emission factor (m^3 kg^{-1}), and CSF_{Ing}, CSF_{Inh}, and CSF_{Derm} are the carcinogenic slope factor for ingestion, inhalation, and dermal contact respectively ($(mg\ kg^{-1}\ d^{-1})^{-1}$).

Determined values of each parameter were used in deterministic risk assessment. *CEs* is the mean values of TEQ_{BaP} in all sampled soil sites, and the value of other parameters used in Eqs 2–4 are listed in Supplementary Table S3.

For probabilistic risk modelling, Monte Carlo (MC) simulation was employed to handle variability in concentrations of PAHs and uncertainty of parameters with 10,000 iterations. Values of *CEs* were chosen from the compiled dataset of sampling sites for each iteration, and extreme values of *CEs* were removed to suit a lognormal distribution. The parameters (*ED, EF, BW, SA*, IR_{Ing} and IR_{Inh}) were probabilistically treated by the defined distribution list in Supplementary Table S4. Other exposure parameters with less variability were still single-point values, as listed in Supplementary Table S3. During the MC simulation, sensitivity analyses was conducted to estimate the contribution of each input parameter to the total variance of probabilistic health risks.

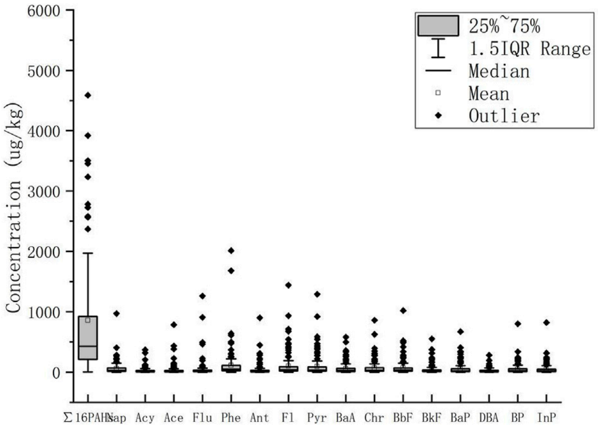

FIGURE 1
Contents of 16 single PAHs and $\sum_{16}$PAHs in surface soil of China.

2.3 Statistical analysis tools

Microsoft Excel 2016 and SPSS 16.0 were employed to perform basic statistical analysis. Figures were made by Origin 2019 Pro (Origin Lab, Northampton, MA). MC simulations and sensitivity analyses were conducted by Oracle Crystal Ball software (11.1.2.4). The spatial distribution maps of soil PAHs concentrations and risks were conducted by ArcGIS 10.7.

3 Results

3.1 Concentration and spatial distribution of PAHs in topsoil of China

The research areas of collected 207 papers distributed in 30 provinces of China (Supplementary Figure S1), which can reflect the overall soil PAHs pollution status nationally. The sampling sites were mainly located in the eastern and northern areas, especially Pearl River Delta, Yangtze River Delta, and the Beijing-Tianjin-Hebei region (Table 1). The concentration of $\sum_{16}$PAHs in each collected literature is listed in Supplementary Table S1. Concentrations of $\sum_{16}$PAHs in the topsoil of China ranged from "undetected" to 261 $\mu g\ g^{-1}$ with a mean value of 0.63 $\mu g\ g^{-1}$. The median value of $\sum_{16}$PAHs was 17.94 $\mu g\ g^{-1}$, which is much higher than the 0.05 $\mu g\ g^{-1}$ of the Dutch government standard of soil PAHs (Agarwal, 2009), indicating PAH pollution in the topsoil was mainly affected by human activities. Figure 1 shows the content distribution of 16 PAHs congers. The 25%–75% interval distribution of 16 PAHs congers concentration ranged from 1.39 to 108.5 $\mu g\ kg^{-1}$. The median concentrations of FL and PYR were 39.7 $\mu g\ kg^{-1}$ and 33.21 $\mu g\ kg^{-1}$, respectively, which were highest among the 16 PAHs congeners. Alternatively, the median concentrations of ACE and ACY were 4.85 $\mu g\ kg^{-1}$ and 6.13 $\mu g\ kg^{-1}$, which were the lowest.

At present, the threshold of soil PAHs pollution is not modulated in China. The pollution classification from Maliszewska-Kordybach (1996) on the base of the total concentrations of PAHs was adopted in this study. Four categories were classified by Maliszewska-Kordybach (1996): heavily contaminated (>1,000 $\mu g\ kg^{-1}$), moderately contaminated (600–1,000 $\mu g\ kg^{-1}$), weakly contaminated (200–600 $\mu g\ kg^{-1}$), and non-contaminated (<200 $\mu g\ kg^{-1}$). Based on the classification, 24.15% of the topsoil in China were categorized as non-contaminated, 39.13% of the soil as weakly contaminated, 14.98% of the soil as moderately contaminated and 21.74% as heavily contaminated. The heavily contaminated soil samples were mainly located in the eastern coastal and southern regions, especially in Yangtze River Delta area, while non-contaminated sites were scattered in across multiples areas of China (Figure 2A).

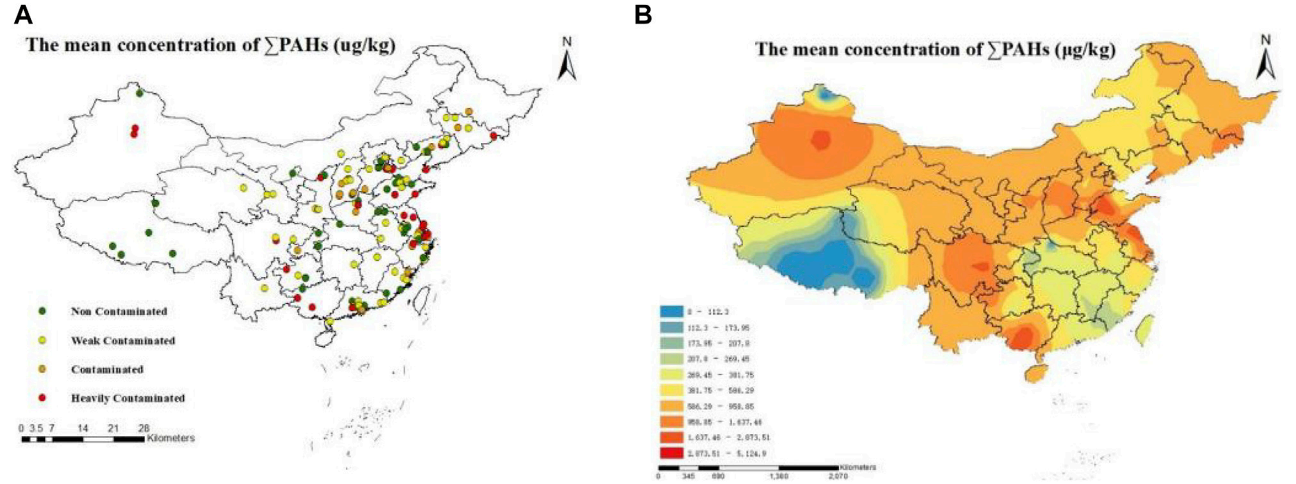

FIGURE 2
The spatial distribution of $\sum_{16}$PAHs concentrations in China from collected data [**(A)**: sampling sites **(B)**: interpolation].

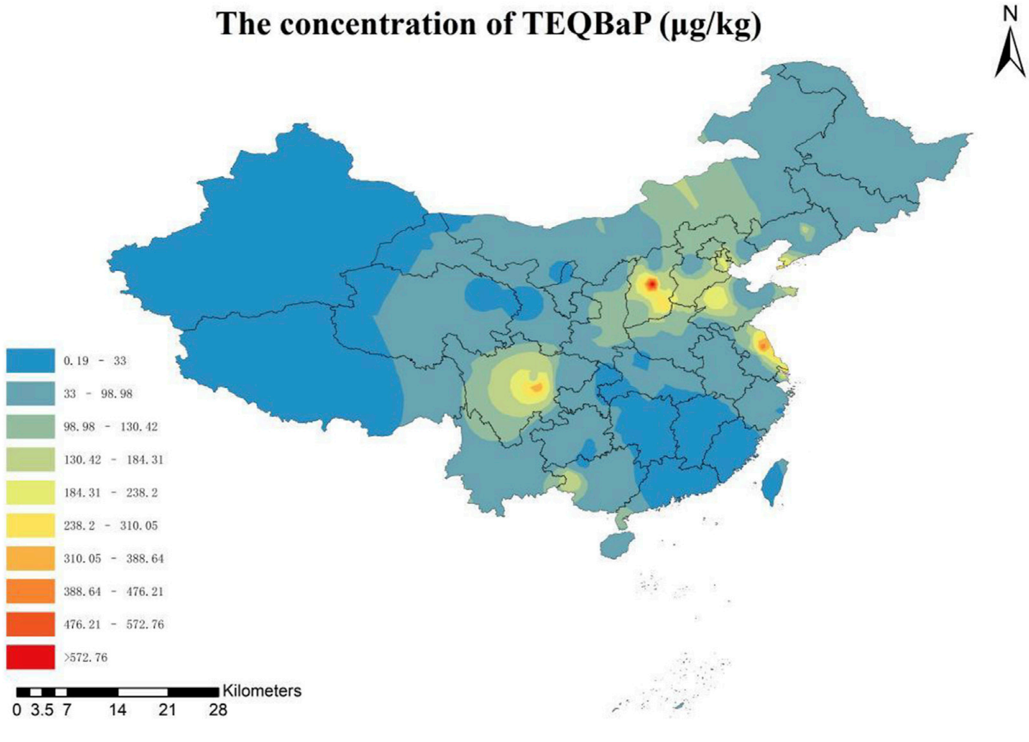

FIGURE 3
The spatial distribution of TEQ_{BaP} in China from collected data.

The concentrations of soil PAHs in China varied greatly among different regions. The median values of $\sum_{16}$PAHs concentration in different regions ranked as: North China (Tianjin, Beijing, Hebei, Shaanxi, Inner Mongolia) (690.3 μg kg^{-1}) > Northeast China (Heilongjiang, Jilin, Liaoning) (497.5 μg kg^{-1}) > East China (Shandong, Jiangsu, Fujian, Zhejiang, Shanghai, Anhui, Jiangxi) (356.47 μg kg^{-1}) >Northwest China (Shanxi, Gansu, Xinjiang, Ningxia, Qinghai) (318.4 μg kg^{-1}) > South China (Guangxi, Guangdong) (318.2 μg kg^{-1}) > Southwest China (Guizhou, Yunnan, Tibet, Sichuan, Chongqing) (217.79 μg kg^{-1}) > Central China (Henan, Hunan, Hubei) (129.5 μg kg^{-1}). The spatial distribution of $\sum_{16}$PAHs in Chinese topsoil was mapped by the Inverse Distance Weight (IDW) interpolation method (Figure 2B). The higher concentrations of $\sum_{16}$PAHs were mainly distributed in north, northwest and east regions, especially Xinjiang, Shandong, Jiangsu, Sichuan, and Guangxi Province, while lower concentrations prevailed in the

TABLE 2 The ILCRs for adults and children *via* three exposure routes.

	Exposure pathway	$ILCR_s$			
		Min	Max	Mean	Median
Adults	Ingestion	9.21E-10	6.02E-06	4.45E-07	1.69E-07
	Inhalation	7.15E-14	4.67E-10	3.45E-11	1.32E-11
	Dermal	1.64E-09	1.07E-05	7.90E-07	3.01E-07
	Total	2.56E-09	1.67E-05	1.23E-06	4.71E-07
Children	Ingestion	7.42E-10	4.85E-06	3.58E-07	1.37E-07
	Inhalation	1.09E-14	7.15E-11	5.28E-12	2.01E-12
	Dermal	9.25E-10	6.05E-06	4.47E-07	1.70E-07
	Total	1.67E-09	1.09E-05	8.05E-07	3.07E-07

western areas, such as Tibet, where industrial activities had lesser effects.

3.2 Risk assessment of soil PAHs

3.2.1 Potential ecological risk assessment

The potential ecological risk posed by soil PAHs was assessed by Toxic equivalent concentrations of BaP (TEQ_{BaP}). Results showed the TEQ_{BaP} of soil PAHs in China ranged from 0.19 to 1,268.01 μg kg^{-1} with a mean value of 93.65 μg kg^{-1}. Overall, 52.98% of the soil samples exceeded the ecological risk guideline value (33 μg kg^{-1}), indicating moderately ecological risks in topsoil of China were posed by PAHs. The spatial distribution map of TEQ_{BaP} of soil PAHs shared similar pattern with concentration (Figure 3). Higher concentrations of TEQ_{BaP} were mainly located in north, southwest, and eastern areas. TEQ_{BaP} of soil PAHs in most regions of China were greater than 33 μg kg^{-1}, especially in Shaanxi, Sichuan, and Jiangsu Provinces.

3.2.2 Human health risk assessment

ILCR model was adopted to assess the human health risk posed by soil PAHs for children and adults. *ILCRs* ranged from 2.56E-09 to 1.67E-05, with a mean value of 1.24E-06, and from 1.67E-09 to 1.09E-05, with a mean value of 8.05E-07 for adults and children, respectively (Table 2). *ILCRs* higher than 10^{-4} is considered as high risk, *ILCRs* lower than 10^{-6} is regarded as no risk, and *ILCRs* range from 10^{-6} to 10^{-4} is considered as potential but acceptable risk posed (USEPA, 2016). The health risk assessment results showed that 35.10% and 20.53% of sampling sites had *ILCRs* exceeding 10^{-6} for children and adults, respectively, with no site having *ILCRs* more than 10^{-4} both for children and adults, which indicate potential human health risks were posed by soil PAHs, but risks were acceptable. Among the three exposure pathways, the *ILCRs* exposed from ingestion and dermal contact were 4–5 orders of magnitude higher than the inhalation pathway. Therefore, ingestion and dermal contact are the dominant pathways of *ILCRs,* while inhalation is negligible. The spatial distribution maps of *ILCRs* of adults and children shared the similar distribution pattern with higher values in north, southwest, central and eastern regions, especially in Shaanxi, Sichuan, and Jiangsu provinces, while lower risks prevailed in west and southeast areas (Supplementary Figure S2).

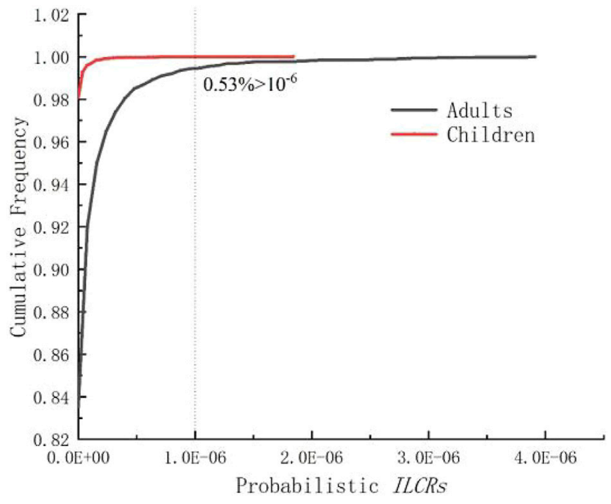

FIGURE 4
Cumulative frequency of probabilistic $ILCR_s$ of adults and children.

3.2.3 MC simulation and sensitivity analyses for probabilistic health risk

The probabilistic health risks of adults and children exposed to soil PAHs were simulated by MC and results are showed in Figure 4. The probabilistic $ILCR_s$ ranged from 2.34 E-11 to 5.61E-05 with a mean value of 6.51E-08for adults, and from 1.35E-12to 3.27E-07 with a mean value of 4.31E-09 for children exposed from soil PAHs through oral intake, dermal contact, and inhalation pathways. Overall, 0.53% of $ILCR_s$ exceeded 10^{-6} for adults, and no $ILCR_s$ exceeded 10^{-6} for children. The results were common with deterministic risk assessment, where potential health risks were posed by surface soil PAHs but risks were acceptable.

The sensitivity of variables to $ILCR_s$ for adults and children was analyzed together with MC (Figure 5). Among the parameters, *EF* (exposure frequency) contributed the most to the total variance of $ILCR_s$, which accounted for 60.0% and 57.1% to $ILCR_s$ for adults and children, respectively. *CEs* contributed the second highest to total variance of $ILCR_s$, followed by IR_{ing}, *BW*, IR_{inh}, and *SA*. The total

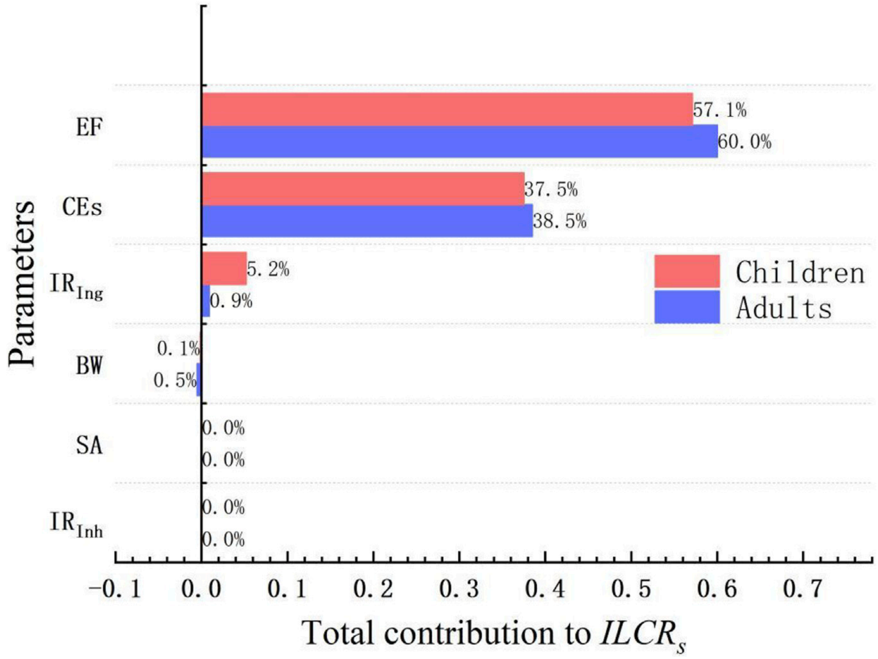

FIGURE 5
Contribution of parameters for probabilistic *ILCRs*.

contributions of *EF* and *CEs* to $ILCR_s$ accounted for 98.5% and 94.6% of the sum of variance for adults and children, respectively. IR_{inh} and *SA* contributed least to the total variance of $ILCR_s$, confirming that inhalation is a negligible pathway for *ILCRs* exposure.

4 Discussion

The PAHs concentrations in soil varied greatly across China. The standard deviation (SD) of soil PAHs concentration was 77,455.85 μg kg^{-1} and coefficient of variation (CV) was 122.98, which reflects strong variety of soil PAHs concentration and huge anthropogenic activities influence (Zhang et al., 2007). According to a former review involving nearly 100 publications, the total concentrations of PAHs in China ranged from 65 to 23,603 μg kg^{-1} with a mean value of 2,802 μg kg^{-1} for urban soil, and 47% of soil were heavily contaminated (Yu et al., 2019). The mean concentration and heavily pollution rate reported by Yu et al. (2019) were both greater than the corresponding values in the present study, mainly because urban soil was influenced by intense anthropogenic activities such as industrial emission and heavy traffic. Sun et al. (2017) reviewed the concentration status of organic contaminants in agricultural soil of China, and their results revealed the concentrations of 16 PAHs ranged from "undetected" to 27,580 ng g^{-1}, with a mean value of 772 ng g^{-1}, which is slightly higher than the present study. Compared to other countries, the mean value of soil PAHs in China in the present study (629.83 μg kg^{-1}) was higher than such locations as of urban soil in Viseu, Portugal (169 μg kg^{-1}) (Cachada et al., 2012) and Belgrade, Serbia (375 μg kg^{-1}) (Crnkovic et al., 2007) but was much lower than the mean concentration of PAHs in the UK (11,930 μg kg^{-1}) (Morillo et al., 2007), urban traffic soils in Delhi, India (4,694 μg kg^{-1}) (Agarwal, 2009), and an e-waste dismantling area in Accra, Ghana (5,627 μg kg^{-1}) (Daso et al., 2016). Pollution levels of soil PAHs all around the world vary greatly, higher concentrations mostly being influenced by anthropogenic activities. Higher soil PAHs concentrations were generally detected in industrial areas and roadsides, while lower levels were found in residential areas (Zhang and Chen, 2017). The PAHs concentrations were also different from various types of sampling sites (Zhang and Chen, 2017). The PAHs concentrations in surface soil in Kunming showed higher values in industrial area and roadside, while lower in green space and education area (Lin et al., 2013). Peng et al. (2016) investigate the distribution of soil PAHs in Beijing with different land uses, results showed soil PAHs concentrations decreased by roadsides, green areas and agricultural areas.

Different migration and enrichment behaviors of PAHs were recorded with different ring numbers (Wild and Jones, 1995). Among the 16 PAHs congeners, FL and PYR had the highest concentrations, while ACE and ACY had the lowest. The finding is consistent with previous studies reported by Zhang and Chen. (2017). Li et al. (2016) analyzed the composition of PAHs in the Yangtze River Delta area, and reported that soil PAHs were dominated by four to five ring PAHs. They mainly related to low saturated vapor pressure, solubility and high K_{ow} coefficient of HMW PAHs, and thus easily absorbed and enriched to soil particles, while LMW PAHs have lower molecular weight, and are easy to volatilize and be degraded by microorganisms (Liu et al., 2011; Dumanoglu et al., 2017). Moreover, PAHs compositions also differed between urban and rural areas. HMW PAHs in urban and suburban areas were usually higher than rural regions mainly due to the different energy types consumed (Wang et al., 2012).

The spatial distribution of soil PAHs in China is heterogenous, where concentrations of soil PAHs in north area was greater than the south. The result was in line with previous studies by Zhang et al. (2019), who reported higher concentrations of soil PAHs in north and northeast region, while lower concentrations in southwest and central areas. There are many factors influencing the concentration and distribution of soil PAHs, such as local economic development, land use, population density, soil organic matter, and traffic conditions (Gao et al., 2012; Wang et al., 2015). Higher concentrations of soil PAHs usually occurred in industry developed areas, and lower in tourist spots (Zhang et al., 2019). In addition to industry and economy development, climate also affect the concentrations of soil PAHs. The relatively low temperature, humidity, and weak ultraviolet radiation of north China decreased microbial and photolysis degradation of soil PAHs (Zhang and Chen, 2017). Identifying potential influencing factors for soil PAHs is essential to control and minimize adverse effects. Generally, the ratios of various PAHs congeners concentration, called diagnostic ratios, are often used to identify between petroleum and combustion sources (Yunker et al., 2002). Diagnostic ratios are used to differentiate origins, by composition and concentration of pollutants produced by different pollution sources (He et al., 2019). In the present study, the ratios of IND/(IND + BghiP) are ranged between 0.028 and 0.992, with a mean value of 0.472. Furthermore, ratios of FLU/(FLU + PYR) are ranged from 0.010 to 0.920 with the mean value of 0.333. As shown in Supplementary Figure S3, most of the soil samples were with the ratios of IND/(IND + BghiP) > 0.2, the ratios of FLU/(FLU + PYR) were scattered distributed between 0.2 and 1, suggesting that soil PAHs in China were mainly resulted from the mix combustion of biomass, petroleum, and coal (Cai et al., 2017). Identical results were also reported by Yu et al. (2019), both indicating coal, biomass, and oil combustion contributed more to soil PAHs distribution. Therefore, the huge amount of coal usage in north China contributes to higher soil PAHs concentrations possibly. The interpolation map of soil PAHs concentration showed the higher values in southwest and northwest area, especially Sichuan and Xinjiang Province, in contrast to the order of median values in different regions. It was possibly due to the limited number of soil samples collected in these areas and the high concentrations of soil PAHs in these samples. Besides, higher concentrations also occurred in Shaanxi and Shandong Province, which might be caused by massive consumption of coal and heavy traffic emissions (Ambade et al., 2021). The mean concentration of soil PAHs in Tibet is relatively low, and the sampling soils were all non-contaminated. As reported by Tao et al. (2011), PAHs in the Tibetan Plateau mostly come from long-range atmospheric transport.

Risk assessment is a valuable tool to characterize the adverse effects of soil pollutants, and quantify exposure risk, both for ecology and human health from soil PAHs, thus providing reference for remediation and management of soil PAHs pollution (Yang et al., 2019; Liu et al., 2021; Li et al., 2022). TEQ_{BaP} of soil PAHs assessment in this study shows that about half of the soil posed ecological risks, which was in accordance with a previous study that about 50% of the TEQ_{BaP} of sampling soils in Shanghai were above the safe level (Wang et al., 2013). Therefore, pollution of soil PAHs should not be ignored in China, remediation measures should be adopted in certain areas to guarantee ecological safety. Soil PAHs not only have direct harmful effects on the environment, but also pose potential risk to human health *via* various exposure pathways. The exposure of humans in contaminated soil usually occurs *via* three pathways, including oral intake, (e.g., incidental hand to mouth intake of soil particle when working or playing on the ground), inhalation and dermal contact with soil particles. As a result, quantifying the risk contribution and identifying the crucial exposure parameters can help provide effective risk control measures towards soil PAHs pollution (Peng et al., 2019). Both deterministic human health risk, where single point value of parameters were adopted, and probabilistic human health risk, where parameters were probability treated, were conducted to quantify the human health risk of soil PAHs in the present study. The results revealed that potential risks were posed to adults and children, but risks were acceptable. The spatial distribution of soil PAHs concentrations showed higher values in Urumqi, where the health risks were relatively low. This was mainly related to the limited number of soil samples collected in this area and the concentration difference of PAHs congeners that resulted in the low value of TEQ_{BaP}. When considering the variability of exposure parameters (EF, ED, BW, SA, IR_{Inh}, and IR_{Ing}), the percentages of *ILCRs* surpassing 10^{-6} for adults and children were both on the decline, confirming that human health risk would be overestimated when single values of parameters were adopted. Similar result was found by Jia et al. (2013), who assessed the risk of naphthalene and benzo(a) pyrene, and found the deterministic risk was four to six folds higher than probabilistic risk. Contrary to that, the deterministic risk assessment of PAHs using the most likely values of exposure parameters and PAHs concentrations were lower than that of the probabilistic risk obtained by MC method (Tong et al., 2018). Probabilistically treated key parameters can provide probability health risk, which is more reliable especially in vast regions, where PAHs concentrations and exposure parameters vary greatly. The sensitivity analysis demonstrated that *EF* and *CEs* were the dominant parameters contributing to the *ILCRs*. Therefore, reducing contact frequency and concentration of soil PAHs are the main and effective method to lower exposure risks.

5 Conclusion

The concentration, composition, spatial distribution, and risks of soil PAHs were systematically analyzed at the national scale based on a robust dataset compiled from literature review. The concentrations of $\sum_{16}$PAHs ranged from “undetected” to 261 μg g^{-1}, with a mean value of 0.63 μg g^{-1} and a median value of 17.94 μg g^{-1}. According to the contamination classification criteria, about 21.74% of the soils were classified as heavily contaminated, 14.98% of the soils were moderately contaminated, 39.13% of the soils were weakly contaminated, and 24.15% of the soils were uncontaminated. Higher concentrations of soil PAHs were located in north and northeast China, and mainly derived from the mix combustion of coal and oil. The TEQ_{BaP} assessment indicated moderate ecological risks were posed by soil PAHs, where higher TEQ_{BaP} were mainly located in Sichuan and Jiangsu provinces. Human health risk assessment results indicated that potential health risks of adults and children were posed by soil PAHs, but risks were acceptable. Sensitivity analysis showed that exposure frequency and concentration of soil PAHs contributed most to the variability of the total risks. Therefore, reducing exposure frequency PAHs concentration from soil by taking remediation actions are effective pathways to protect environmental quality and human health.

6 Limitations and perspectives

We conducted a systematic overview of soil PAHs pollution status and assessed related potential ecological and human health risks at national scale. The data were extracted from previous published literature, and therefore, uncertainties exist inevitably to some extent. Firstly, the sampling time, sampling method, and laboratory analysis of soil PAHs in each publication varies greatly. Nevertheless, the concentrations of soil PAHs in each publication were compared at current time scale. Additionally, the mean concentrations of soil PAHs in each study were used to estimate and interpolate to depict a spatial distribution map. As a result, the actual concentration and induced risks of topsoil PAHs in China could have been underestimated to some extent. Besides, the total concentrations of soil PAHs were used to assess human health risk, while, bioaccessibility and bioavailability of soil PAHs are considered reliable in assessing real exposure risk as reported by Munir Hussain et al. (2011) and Dong et al. (2016). Such scenario could cause an overestimation of human health risks of soil PAHs. Results from this study could enhance the knowledge of soil PAHs contamination status, potential ecological and human health risks across China. However, further work is needed to overcome the existing limitations in this study. Consequently, it would be better to collect soil samples across China at the same time and analyze soil PAHs concentration by same procedure and method to obtain the actual concentration status of soil PAHs in the future. Besides, establishing a pollution classification criterion based on the actual soil properties of China is vital for further contamination assessment and remediation. In addition, assessing human health risk by using bioaccessibility and bioavailability of soil PAHs instead of the total concentrations can help obtain more reliable results. Overall, by combining soil samples, bioaccessibility and bioavailability experiments, probabilistic risk simulation will exert reliable results of soil PAHs contamination status and risk level.

Data availability statement

The raw data supporting the conclusion of this article will be made available by the authors, without undue reservation.

Author contributions

MH: Conceptualization, methodology, manuscript writing. YS: Software, data curation. ZZ: Data curation. SG: Software. HY: Data collection. KC: Data collection. XZ: Review and editing. YQ: Conceptualization and supervision.

Funding

This work was financially supported by the National Natural Science Foundation of China (42107021).

Conflict of interest

The authors declare that the research was conducted in the absence of any commercial or financial relationships that could be construed as a potential conflict of interest.

Publisher's note

Supplementary material

The Supplementary Material for this article can be found online at: https://www.frontiersin.org/articles/10.3389/fenvs.2023.1114027/full#supplementary-material

References

Agarwal, T. (2009). Concentration level, pattern and toxic potential of PAHs in traffic soil of Delhi, India. *J. Hazard. Mat.* 171, 894–900. doi:10.1016/j.jhazmat.2009.06.081

Alves, C. A., Vicente, A. M. P., Gomes, J., Nunes, T., Duarte, M., and Bandowe, B. A. M. (2016). Polycyclic aromatic hydrocarbons (PAHs) and their derivatives (oxygenated-PAHs, nitrated-PAHs and azaarenes) in size-fractionated particles emitted in an urban road tunnel. *Atmos. Res.* 180, 128–137. doi:10.1016/j.atmosres.2016.05.013

Ambade, B., Sethi, S. S., Giri, B., Biswas, J. K., and Bauddh, K. (2022). Characterization, behavior, and risk assessment of polycyclic aromatic hydrocarbons (pahs) in the estuarysediments. *Bull. Environ. Contam. Toxicol.* 108 (2), 243–252. doi:10.1007/s00128-021-03393-3

Ambade, B., and Sethi, S. S. (2021). Health risk assessment and characterization of polycyclic aromatic hydrocarbon from the hydrosphere. *J. Hazard. Toxic. Radioact. Waste.* 25 (2), 50200081–50200111. doi:10.1061/(asce)hz.2153-5515.0000586

Ambade, B., Sethi, S. S., Kurwadkar, S., Kumar, Amit., and Sankar, T. K. (2021). Toxicity and health risk assessment of polycyclic aromatic hydrocarbons in surface water, sediments and groundwater vulnerability in Damodar river basin. *Groundw. Sustain. Dev.* 13, 100553. doi:10.1016/j.gsd.2021.100553

Cachada, A., Pato, P., Rocha-Santos, T., daSilva, E. F., and Duarte, A. C. (2012). Levels, sources and potential human health risks of organic pollutants in urban soils. *Sci. Total Environ.* 430, 184–192. doi:10.1016/j.scitotenv.2012.04.075

Cai, C., Li, J. Y., Di, W., Wang, X. L., Tsang, D. C. W., Li, X. D., et al. (2017). Spatial distribution, emission source and health risk of parent PAHs and derivatives in surface soils from the Yangtze River Delta, eastern China. *Chemosphere* 178, 301–308. doi:10.1016/j.chemosphere.2017.03.057

Chen, Y., Zhang, J., Zhang, F., Li, F., and Zhou, M. (2017). Polycyclic aromatic hydrocarbons in farmland soils around main reservoirs of Jilin province, China: Occurrence, sources and potential human health risk. *Environ. Geochem Hlth.* 40, 791–802. doi:10.1007/s10653-017-0024-5

Crnkovic, D., Ristic, M., Jovanovic, A., and Antonovic, D. (2007). Levels of PAHs in the soils of Belgrade and its environs. *Environ. Monit. Assess.* 125, 75–83. doi:10.1007/s10661-006-9240-7

Daso, A. P., Akortia, E., and Okonkwo, J. O. (2016). Concentration profiles, source apportionment and risk assessment of polycyclic aromatic hydrocarbons (PAHs) in dumpsite soils from Agbogbloshie e-waste dismantling site, Accra, Ghana. *Environ. Sci. Pollut. Res.* 23 (11), 10883–10894. doi:10.1007/s11356-016-6311-3

Dong, Z., Yan, K., Liu, Y., Naidu, R., Duan, L., Wijayawardena, A., et al. (2016). A meta-analysis to correlate lead bioavailability and bioaccessibility and predict lead bioavailability. *Environ. Int.* 92-93, 139–145. doi:10.1016/j.envint.2016.04.009

Dumanoglu, Y., Gaga, E. O., Gungormus, E., Sofuoglu, S. C., and Odabasi, M. (2017). Spatial and seasonal variations, sources, air-soil exchange, and carcinogenic risk assessment for PAHs and PCBs in air and soil of Kutahya, Turkey, the province of thermal power plants. *Sci. Total Environ.* 580, 920–935. doi:10.1016/j.scitotenv.2016.12.040

Franco, S. S., Nardocci, A. C., and Günther., W. (2008). PAH biomarkers for human health risk assessment: A review of the state-of-the-art. *Cad. Saúde Pública* 24 (4), a569–s580. doi:10.1590/s0102-311x2008001600009

Gao, B., Guo, H., Wang, X. M., Zhao, X. Y., Ling, Z. H., Zhang, Z., et al. (2012). Polycyclic aromatic hydrocarbons in PM2.5 in guangzhou, southern China: Spatiotemporal patterns and emission sources. *J. Hazard. Mat.* 240, 78–87. doi:10.1016/j.jhazmat.2012.07.068

He, M. J., Yang, S. Y., Zhao, J., Collins, C., Xu, J. M., and Liu, X. M. (2019). Reduction in the exposure risk of farmer from e-waste recycling site following environmental policy adjustment: A regional scale view of PAHs in paddy fields. *Environ. Int.* 133, 105136. doi:10.1016/j.envint.2019.105136

Huang, D. Y., Liu, C. P., Li, F. B., Liu, T. X., Liu, C. S., Tao, L., et al. (2014). Profiles, sources, and transport of polycyclic aromatic hydrocarbons in soils affected by electronic waste recycling in Longtang, south China. *Environ. Monit. Assess.* 186 (6), 3351–3364. doi:10.1007/s10661-014-3622-z

Hussain, Z., Codling, E. E., Scheckel, K. G., and Chaney, R. L. (2011). *In vitro* and *in vivo* approaches for the measurement of oral bioavailability of lead (Pb) in contaminated soils: A review. *Environ. Pollut.* 159 (10), 2320–2327. doi:10.1016/j.envpol.2011.04.043

Jia, X., Xia, T., Zhong, M., and Liang, J. (2013). Comparing deterministic and probabilistic risk assessment at a coking plant site in China. *Adv. Mat. Res.* 610-613, 798–803. doi:10.4028/www.scientific.net/amr.610-613.798

Lestan, D. (2017). Novel chelant-based washing method for soil contaminated with pb and other metals: A pilot-scale study. *Land. Degrad. Dev.* 28, 2585–2595. doi:10.1002/ldr.2818

Leung, A. O. W., Cheung, K. C., and Wong, M. H. (2015). Spatial distribution of polycyclic aromatic hydrocarbons in soil, sediment, and combusted residue at an e-waste processing site in southeast China. *Environ. Sci. Pollut. Res.* 22 (12), 8786–8801. doi:10.1007/s11356-013-1465-8

Li, J., Wu, D., Xu, Y., Li, X., Wang, X., Zeng, C., et al. (2016). Recent distribution and sources of polycyclic aromatic hydrocarbons in surface soils from Yangtze River Delta. *Environ. Sci.* 37, 253–261. doi:10.13227/j.hjkx.2016.01.033

Li, X. N., Yi, S. Y., Cundy, A. B., and Chen, W. P. (2022). Sustainable decision-making for contaminated site risk management: A decision tree model using machine learning algorithms. *J. Clean. Prod.* 371, 133612. doi:10.1016/j.jclepro.2022.133612

Lin, C., Liu, J., Wang, R., Wang, Y., Huang, B., and Pan, X. (2013). Polycyclic aromatic hydrocarbons in surface soils of kunming, China: Concentrations, distribution, sources, and potential risk. *J. Soil Contam.* 22, 753–766. doi:10.1080/15320383.2013.768201

Liu, G. Q., Yu, L. L., Li, J., Liu, X. A., and Zhang, G. (2011). PAHs in soils and estimated air soil exchange in the Pearl River Delta, South China. *Environ. Monit. Assess.* 173, 861–870. doi:10.1007/s10661-010-1429-0

Liu, J., Wang, Y., Liu, X., and Xu, J. (2021). Occurrence and health risks of heavy metals in plastic-shed soils and vegetables across China. *Agr. Ecosyst. Environ.* 321, 107632. doi:10.1016/j.agee.2021.107632

Lu, Y. L., Song, S., Wang, R. S., Liu, Z. Y., Meng, J., Sweetman, A. J., et al. (2015). Impacts of soil and water pollution on food safety and health risks in China. *Environ. Int.* 77 (1), 5–15. doi:10.1016/j.envint.2014.12.010

Maliszewska-Kordybach, B. (1996). Polycyclic aromatic hydrocarbons in agricultural soils in Poland: Preliminary proposals for criteria to evaluate the level of soil contamination. *Appl. Geochem.* 11, 121–127. doi:10.1016/0883-2927(95)00076-3

Ministry of Environment Protection and Ministry of Land Resources of the People's Republic of China (2014). Nationwide soil pollution survey report. Avaliable At: http://www.zhb.gov.cn/gkml/hbb/qt/201404/t20140417_270670.htm.

Morillo, E., Romero, A. S., Maqueda, C., Madrid, L., Ajmone-Marsan, F., Grcman, H., et al. (2007). Soil pollution by PAHs in urban soils: A comparison of three European cities. *J. Environ. Monit.* 9, 1001–1008. doi:10.1039/b705955h

Niu, L., Yang, F., Xu, C., Yang, H., and Liu, W. (2013). Status of metal accumulation in farmland soils across China: From distribution to risk assessment. *Environ. Pollut.* 176 (5), 55–62. doi:10.1016/j.envpol.2013.01.019

Peng, C., Wang, M., Zhao, Y., and Chen, W. (2016). Distribution and risks of polycyclic aromatic hydrocarbons in suburban and rural soils of beijing with various land uses. *Environ. Monit. Assess.* 188 (3), 1–12. doi:10.1007/s10661-016-5156-z

Peng, H., Chen, Y., Weng, L., Ma, J., Ma, Y., Li, Y., et al. (2019). Comparisons of heavy metal input inventory in agricultural soils in north and south China: A review. *Sci. Total Environ.* 660, 776–786. doi:10.1016/j.scitotenv.2019.01.066

Salazar, M. J., Rodriguez, J. H., Leonardo, N. G., and Pignata, M. L. (2012). Effects of heavy metal concentrations (Cd, Zn and Pb) in agricultural soils near different emission sources on quality, accumulation and food safety in soybean (*glycine max* (L.) merrill). *J. Hazard. Mat.* 10, 244–253. doi:10.1016/j.jhazmat.2012.07.026

Samburova, V., Zielinska, B., and Khlystov, A. (2017). Do 16 polycyclic aromatic hydrocarbons represent PAH air toxicity? *Toxics* 5 (3), 17. doi:10.3390/toxics5030017

Sun, J., Pan, L., Tsang, D. C. W., Zhan, Y., and Li, X. (2017). Organic contamination and remediation in the agricultural soils of China: A critical review. *Sci. Total Environ.* 615, 724–740. doi:10.1016/j.scitotenv.2017.09.271

Tao, S., Wang, W., Liu, W., Zuo, Q., Wang, X., Wang, R., et al. (2011). Polycyclic aromatic hydrocarbons and organochlorine pesticides in surface soils from the Qinghai-Tibetan plateau. *J. Environ. Monit.* 13, 175–181. doi:10.1039/c0em00298d

Tong, R., Yang, X., Su, H., Pan, Y., Zhang, Q., Wang, J., et al. (2018). Levels, sources and probabilistic health risks of polycyclic aromatic hydrocarbons in the agricultural soils from sites neighboring suburban industries in Shanghai. *Sci. Total Environ.* 616-617, 1365–1373. doi:10.1016/j.scitotenv.2017.10.179

USEPA (1989). "Risk assessment guidance for superfund," in *Human health evaluation manual (Part A)* (Washington, DC: US Environmental Protection Agency, Offifice of Emergency and Remedial Response).

USEPA (2009a). *Risk assessment guidance for superfund (RAGS), volume I: Human health evaluation manual (Part E, supplemental guidance for dermal risk assessment) interim*. Washington, DC: EPA.

USEPA (2009b). *Risk assessment guidance for superfund volume I: Human health evaluation manual (Part F, supplemental guidance for inhalation risk assessment)*. Washington, DC: EPA.

USEPA (2016). *Risk assessment guidance for superfund, Volume 1, Human health evaluation manual (Part B, Development of risk-based preliminary remediation goals)*. Washington, DC: EPA. Avaliable At: https://www.epa.gov/expobox_1034 (Accessed February 5, 2017).

Wang, C., Wang, X., Gong, P., and Yao, T. (2014). Polycyclic aromatic hydrocarbons in surface soil across the Tibetan plateau: Spatial distribution, source and air-soil exchange. *Environ. Pollut.* 184, 138–144. doi:10.1016/j.envpol.2013.08.029

Wang, L., Xu, X., and Lu, X. (2015). Composition, source and potential risk of polycyclic aromatic hydrocarbons (PAHs) in vegetable soil from the suburbs of xianyang city, northwest China: A case study. *Environ. Earth Sci.* 75, 56–13. doi:10.1007/s12665-015-4853-1

Wang, X. T., Miao, Y., Zhang, Y., Li, Y. C., Wu, M. H., and Yu, G. (2013). Polycyclic aromatic hydrocarbons (PAHs) in urban soils of the mega city Shanghai: Occurrence, source apportionment and potential human health risk. *Sci. Total Environ.* 447, 80–89. doi:10.1016/j.scitotenv.2012.12.086

Wang, Z., Yang, P., Wang, Y., and Ma, X. (2012). Urban fractionation of polycyclic aromatic hydrocarbons from Dalian soils. *Environ. Chem. Lett.* 10, 183–187. doi:10.1007/s10311-011-0341-3

Wild, S. R., and Jones, K. C. (1995). Polynuclear aromatic hydrocarbons in the United Kingdom environment: A preliminary source inventory and budget. *Environ. Pollut.* 88, 91–108. doi:10.1016/0269-7491(95)91052-M

Wolska, L., Mechlińska, A., Rogowska, J., and Namieśnik, J. (2012). Sources and fate of PAHs and PCBs in the marine environment. *Crit. Rev. Environ. Sci. Technol.* 42, 1172–1189. doi:10.1080/10643389.2011.556546

Yang, J., Sun, P., Zhang, X., Wei, X. Y., Huang, Y., Du, W. N., et al. (2020). Source apportionment of pahs in roadside agricultural soils of a megacity using positive matrix factorization receptor model and compound-specific carbon isotope analysis. *J. Hazard Mate* 403, 123592. doi:10.1016/j.jhazmat.2020.123592

Yang, S. Y., Zhao, J. A., Scott, X., Chris, C., Xu, J. M., and liu, X. M. (2019). Status assessment and probabilistic health risk modeling of metals accumulation in agriculture soils across China: A synthesis. *Environ. Int.* 128, 165–174. doi:10.1016/j.envint.2019.04.044

Yang, W., Lang, Y., and Li, G. (2014). Cancer risk of polycyclic aromatic hydrocarbons (PAHs) in the soils from Jiaozhou Bay Wetland. *Chemosphere* 112, 289–295. doi:10.1016/j.chemosphere.2014.04.074

Yu, H., Li, T., Liu, Y., and Ma, L. (2019). Spatial distribution of polycyclic aromatic hydrocarbon contamination in urban soil of China. *Chemosphere* 230, 498–509. doi:10.1016/j.chemosphere.2019.05.006

Yunker, M. B., Macdonald, R. W., Vingarzan, R., Mitchell, R. H., Goyette, D., and Sylvestre, S. (2002). PAHs in the fraser river basin: A critical appraisal of PAH ratios as indicators of PAH source and composition. *Org. Geochem.* 33, 489–515. doi:10.1016/S0146-6380(02)00002-5

Zhang, P., and Chen, Y. G. (2017). Polycyclic aromatic hydrocarbons contamination in surface soil of China: A review. *Sci. Total Environ.* 605-606, 1011–1020. doi:10.1016/j.scitotenv.2017.06.247

Zhang, X. Y., Sui, Y. Y., Zhang, X. D., Meng, K., and Herbert, S. J. (2007). Spatial variability of nutrient properties in black soil of northeast China. *Pedosphere* 17, 19–29. doi:10.1016/S1002-0160(07)60003-4

Zhang, Y., Peng, C., Guo, Z., Xiao, X., and Xiao, R. (2019). Polycyclic aromatic hydrocarbons in urban soils of China: Distribution, influencing factors, health risk and regression prediction. *Environ. Pollut.* 254, 112930. doi:10.1016/j.envpol.2019.07.098

Zheng, H., Qu, C., Zhang, J., Talpur, S. A., Ding, Y., Xing, X. l., et al. (2019). Polycyclic aromatic hydrocarbons (PAHs) in agricultural soils from ningde, China: Levels, sources, and human health risk assessment. *Environ. Geochem Hlth.* 41, 907–919. doi:10.1007/s10653-018-0188-7

frontiers | Frontiers in Environmental Science

TYPE Original Research
PUBLISHED 03 April 2023
DOI 10.3389/fenvs.2023.1125487

OPEN ACCESS

EDITED BY
Xiaokai Zhang,
Jiangnan University, China

REVIEWED BY
Zhao-Feng Yuan,
Zhejiang University, China
Jie Wang,
Nanjing Agricultural University, China

*CORRESPONDENCE
Nicolas Maurin,
✉ nicolas.maurin@univ-reims.fr

SPECIALTY SECTION
This article was submitted to Soil Processes,
a section of the journal
Frontiers in Environmental Science

RECEIVED 16 December 2022
ACCEPTED 20 March 2023
PUBLISHED 03 April 2023

CITATION
Maurin N, Sayen S and Guillon E (2023), Gas chromatography−mass spectrometry analysis of organic pollutants in French soils irrigated with agro-industrial wastewater.
Front. Environ. Sci. 11:1125487.
doi: 10.3389/fenvs.2023.1125487

Gas chromatography−mass spectrometry analysis of organic pollutants in French soils irrigated with agro-industrial wastewater

Nicolas Maurin*, Stéphanie Sayen and Emmanuel Guillon

Institut de Chimie Moléculaire de Reims (ICMR)-UMR CNRS 7312, Université de Reims Champagne Ardenne, Reims, France

The use of agro-industrial wastewater in the agricultural sector is an interesting practice to save resources but it can bring various contaminants to the receiving soils. In this study 19 organic pollutants [8 polycyclic aromatic hydrocarbons (PAH), 6 BTEX, 4-tert-octylphenol, 4-octylphenol, 4-n-nonylphenol, tributyltin and diethylphtalate] were analyzed by gas chromatography-mass spectrometry (GC-MS) in soils irrigated with agro-industrial wastewater from sugar refinery. The soils were sampled at five different locations to evaluate the contamination heterogeneity. Microwave-assisted extraction (MAE) was performed using methanol and hexane and extraction yields ranged from 44% to 96%. The detection limits of the method were between 1.6 and 64 $\mu g \cdot L^{-1}$ for polycyclic aromatic hydrocarbons, 0.42 $\mu g \cdot L^{-1}$ for diethylphthalate, 0.77 $\mu g \cdot L^{-1}$ for tributyltin and until 9.8 $\mu g \cdot L^{-1}$ for phenol compounds. The highest contaminant concentrations measured in the soil samples, between 0.4 and 1.2 $ng \cdot g^{-1}$, were monitored for polycyclic aromatic hydrocarbons molecules, including napthalene, anthracene, fluoranthene, indeno(1,2,3-c,d)pyrene, benzo[a]pyrene, benzo[b]fluoranthene, benzo[k]fluoranthene, and benzo[ghi]perylene. Toluene, ethylbenzene, xylene isomers accounted from 21 to 66 $ng \cdot g^{-1}$ (mostly toluene). Benzene, 4-tert-octylphenol, 4-octylphenol, 4-n-nonylphenol, tributyltin and diethylphtalate were not detected in soils. The proposed method enables analysis of a wide variety of regulated compounds in a unique preparation step and a unique analytical method. The mean amounts of pollutants were in agreement with measurements or estimates performed in similar contexts.

KEYWORDS

agro-industrial wastewater, soil, gas chromatography, mass spectrometry, organic contaminations, field measurement

1 Introduction

The increasing world population and associated resource consumption make water reuse a significant concern. Human activity uses about 4,600 km^3 of water yearly and a 20% increase is projected for 2050 (Burek et al., 2016). Irrigation, industrial and municipal uses account for 70%, 19%, and 11%, respectively. Hence water reuse, as a water source, represents a mean to reduce wastewater footprint as well as plant nutrients for agriculture. In addition, as wastewater contain nitrogen, phosphorus, potassium and organic carbon, it serves as plant nutrients for agriculture. As these nutrients usually need energy to be produced, recycling water is also a source of energy saving. That's why wastewater from municipal treatment plant or agro-industrial plant as an agricultural resource is used in several countries (Brockmann et al., 2018).

However, due to its previous uses in various activities, wastewater can be loaded with undesired products such as hazardous chemical substances towards human or crop growth. The stability and chemical properties of these organic pollutants result in their accumulation in the topsoil due to its rich organic content (Holoubek et al., 2009). Consequently, many countries have put in place regulations to limit the emission of pollutants in wastewater in order to preserve its quality for reuse. In Table 1 is shown the list of dangerous substances in the environment and the corresponding quantification limits needed to monitor water quality in France in 2014 (Ministère de l'écologie du développement durable et de l'énergie, 2014). It includes five classes of molecules such as polycyclic aromatic hydrocarbons (PAH), alkylphenols, phthalates, organotin and benzene, toluene, ethylbenzene and xylenes (BTEX). Fees are applied on non-domestic wastewater based on pollutant concentrations. Hence, monitoring the output of these substances has become an economical concern for agro-industrial actors reusing wastewater.

In France, contaminants in soils are monitored by the French National Soil Monitoring Network (Réseau de Mesures de la Qualité des Soils—RMQS). Several studies focused on the persistence in soils of PAHs by assessing the impact of atmospheric flux and road transportation (Clément et al., 2015; Gaspéri et al., 2018). BTEX are emitted by vehicle combustion in the atmosphere and then carried by rain into soils by leaching the atmosphere (Popescu and Popescu, 2017). Alkylphenol ethoxylates are found in several goods such as detergents, pesticides, inks, and paper leading to octylphenol and nonylphenol by degradation. They have been detected at high concentrations in soils and few countries have legislation about their concentration in agricultural soils (Llorca-Pórcel et al., 2009; Pérez et al., 2012). Tributyltin is known to be toxic for numerous organisms including humans. Many of industrial or domestic products like fungicides, insecticides, bactericides, wood preservatives and polyvinyl chloride (PVC) stabilizers have been recognized as potential sources of contamination (Champ, 2000). Phthalates have numerous applications such as automotive manufacturing and packaging. Diethylhexyl phthalate may reach up to 50% in PVC composition, and as it is not chemically bound to the polymer, it can be easily released in the environment during PVC production as well as end-product use, storage, or degradation (Heudorf et al., 2007). For these compounds, sludge application is one of the most important sources of agricultural soil contamination (Marcic et al., 2006). Thereby, monitoring the concentration of these pollutants is important to maintain the quality of agricultural soils.

All these contaminants were previously analyzed in soils by mass spectrometry using several extraction methods. PAHs were classically analyzed by gas chromatography coupled with mass spectrometry (GC-MS) (Poster et al., 2006). Their soil extraction was performed using various techniques such as soxhlet extraction, microwave assisted extraction (Wang et al., 2007; Xu and Lee, 2008) and pressurized liquid extraction (Gibson et al., 2005; Martínez Vidal et al., 2009). Alkylphenols can also be analyzed using GC-MS (Gibsons et al., 2005) after soil extraction with pressurized liquid extraction (Andreu et al., 2007) or microwave assisted extraction (Pérez et al., 2012). Heroult et al. (2008) compared several extraction techniques for tributyltin analysis in soils including mechanical stirring, accelerated solvent, microwave and ultrasonic extraction also using GC-MS. Phthalates analysis in soils was performed by liquid or gas chromatography after ultrasonic extraction (Ma et al., 2005) or microwave extraction (Chee et al., 1996; Liang et al., 2010). From these different studies, microwave extraction followed by GC-MS analysis was found to be a reliable analytical method for the monitoring of these pollutants. As for the BTEX class compounds, they are usually extracted from soils *via* headspace chromatography (Ezquerro et al., 2004; Shin, 2012) or liquid-liquid extraction (Khajeh et al., 2014) and to our knowledge no extraction was performed using a microwave oven. Thus it is important to optimize the methods allowing to analyze the whole set of compounds of concern which have various properties in a simple and fast way while respecting the performances required by the legislator.

In this context, this study aims at standardizing the extraction and analysis (quantification) of these different compound families with low detection limits. For this purpose, five soils sampled in different sites irrigated with wastewater from agro-industrial plant were analyzed by GC-MS using microwave-assisted extraction (MAE) targeting the organic substances identified by the French regulation.

2 Materials and methods

2.1 Sample sites

Five sites were sampled to characterize their physico-chemical properties in the Grand Reims area (Figure 1), which is an intercommunal structure located in the Grand Est Region (France) with 300,699 inhabitants in 2019 and a population density of 211/km^2. Agriculture in this area fall into four main activities which are vineyard, beets and alfalfa. Beet cultures are valorized locally in several products such as sugar, ethanol and alcohol. The area of the sampling site is a large beet agricultural zone crossed by active traffic roads, close to the Reims airfield, agricultural facilities and concrete industry. Several villages with a population between 500 and 1,000 inhabitants are surrounding the sites in a 2 km radius in addition to the city of Reims located 5 km west. All these activities may act as indirect sources of pollutants especially combustion residues. The cultures were spread with the effluents of a sugar factory at a 600 m^3·ha^{-1} (60 mm) maximum rate with a minimum of 2 years between each spreading on the same parcel. Land application with such effluents started in 1978. Only the data focusing on the nutritious capacity of the effluents were available. The concentrations of targeted pollutants were not known. Soil samples were provided by the association of agronomic spreading monitoring (ASAE, France). The sampling was focused on the rich organic content layer of the soil where the pollutants can accumulate. The topsoil was collected with a shovel until 25 cm depth and stored in a closed polyethylene bag at 4°C before use. The soils were characterized for particle size distribution without decarbonation, pH, cation exchange capacity (CEC), organic carbon (OC), and $CaCO_3$ contents according to French and International standard methods, following NF X31-107, ISO

TABLE 1 Quantification limits, detection limit, linearity and extraction yield of the method.

Analytes	Quantification limit (LOQ) required by the regulator (ng·g^{-1})	Quantification limit (LOD) (µg·L^{-1})	Quantification limit in soil (LOQ) (ng·g^{-1})	Detection limit in soil (LOD) (ng·g^{-1})	Linearity r^2	Extraction yield ± standard deviation (%)
Benzo(k)fluoranthene	10	3.4	0.37	0.1	0.9999	52 ± 2
Benzo(b)fluoranthene	10	2.4	0.27	0.1	0.9999	50 ± 4
Benzo(a)pyrene	10	1.6	0.18	0.1	0.9999	49 ± 8
Indéno(1,2,3-c,d)pyrene	10	3.6	0.40	0.1	0.9999	49 ± 7
Benzo(g,h,i)perylene	10	3.2	0.35	0.1	0.9999	54 ± 3
Anthracene	10	1.9	0.22	0.1	0.9999	57.3 ± 0.7
Fluoranthene	10	4.6	0.50	0.2	0.9999	62.7 ± 0.8
Naphtalene	10	64	5.0	1.5	0.9997	68 ± 2
Benzene	10	0.3	0.2	0.1	0.9997	79 ± 7
Toluene	50	0.5	0.5	0.1	0.9916	96 ± 2
Ethylbenzene	10	1.6	0.7	0.2	0.9999	81 ± 5
Xylene (o)	10	0.9	0.2	0.1	0.9999	83 ± 6
Xylene (m + p)	10	1.4	0.6	0.2	0.9999	72 ± 2
Diethylphtalate	25	0.42	3.1	0.9	0.9999	90 ± 10
Tributyltin cation	10	0.77	2.5	0.7	0.8797	40 ± 10
∑ Octylphenols	100	—	—		—	—
∑ Nonylphenols	100	—	—		—	—
4-Octylphenol	100	6.7	47.2	14.2	0.9929	90 ± 10
4-tert-octylphenol	100	9,8	68.9	20.7	0.8700	63 ± 8
4-n-nonylphenol	100	7.7	55.5	16.6	0.9762	91 ± 3
∑ 4-nonylphenol	100	—	—		—	—

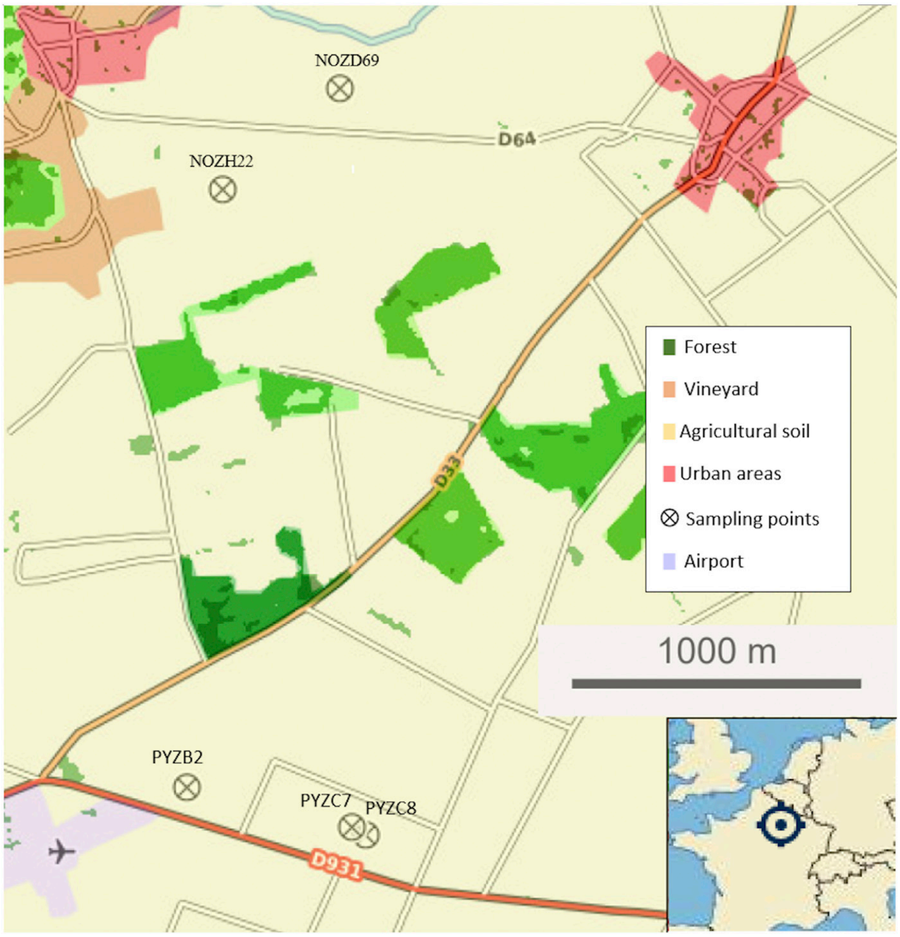

FIGURE 1
Sample locations: the five soil samples are represented by a circled cross (© IGN 2022).

10390, NF X 31-130, ISO 14235, and ISO 10693, respectively (AFNOR, 1995; AFNOR, 1998; AFNOR, 1999; AFNOR, 2003; AFNOR, 2005). Organic matter (OM) content was calculated as follows: % OM = 1.72% OC.

2.2 Chemicals and reagents

Methanol and hexane (HiPerSolv Chromanorm), as well as nylon filter (0.2 μm) syringes and filter supports were purchased from VWR. The standards benzo(k)fluoranthene, benzo(b) fluoranthene, benzo(a)pyrene, indéno(1,2,3-c,d)pyrene, benzo(g,h,i)perylene, anthracene, fluoranthene, naphtalene, benzene, toluene, ethylbenzene, xylene (o,m,p), diethylphtalate, tributyltin, 4-octylphenol, 4-tert-octylphenol, 4-n-nonylphenol were of the highest purity and purchased from Sigma Aldrich.

2.3 Microwave assisted extraction

Soil extraction was performed using a Thermo Scientific Ethos Easy microwave extractor with a Fast-24 rotor. The samples in glass tubes were subjected to a 1,800 W power to reach 110°C in 10 min, this temperature was then maintained during 10 min. PAH and BTEX compounds were extracted from 2 g of soils in 10 mL of hexane; for diethylphtalate, tributyltin and phenolic compounds, 5 g of soils in 10 mL of methanol were used. After microwave extraction the liquid phase was filtered through a nylon membrane and stored in a glass tube. The solvent was then evaporated to dryness in a centrifugal concentrator Genevac HT Series (SP Scientific, Warminster, PA, United States). The manufacturer programs “very low boiling point” and “medium boiling point” were used for hexane and methanol extraction respectively. The temperature was set at 40°C with a rotation speed of 1,400 rpm. The evaporation process started with a decrease in pressure from the atmospheric pressure to full vacuum in 1 h and was maintained for 6 h. The residue was dissolved in 500 μL of methanol and put inside a micro-vial for GC-MS analysis.

2.4 GC-MS analysis

The target compound concentrations were determined using a Thermo Scientific TRACE 1300 GC system coupled to a Thermo

Scientific ISQ Series quadrupole mass spectrometer equipped with an electronic impact source (Low activity). The separation was achieved by injecting 0.5 µL of the sample in a Thermo Scientific TR5-5MS column (30 m, I.D. 0.25 mm, film 0.25 µm). Data were processed with the XCalibur™ 2.2 software. Injection was made in splitless mode. The transfer temperature was set at 250°C with a source at 230°C. The dwell time was set at 0.5 s for each ion. Single Ion Monitoring (SIM) mode was used with ion quantification and identification as listed in Table 2. The temperature program was from 90°C to 300°C with a ramp of 5°C/min and from 40°C during 8 min–300°C with a ramp of 40°C/min for PAH and BTEX, respectively. For the other compounds, it was from 90°C to 300°C with a ramp of 50°C/min. Each soil sample was analyzed three times and a blank extraction without soil was inserted in each extraction batch to check for potential contamination during extraction process.

2.5 Quantification and validation method

The concentrations of target compounds were calculated by an external standard calibration method. A calibration curve with five points was obtained using the pure standard in hexane for HAP and BTEX and methanol for alkylphenol, phtalate and TBT. The limits of quantification (LOQ) was calculated based on the signal to noise approach defined in the ICH Harmonized Tripartite Guideline (2005) by dividing the concentration found in extracted samples by a tenth of the signal-to-noise ratio measured in the chromatogram. Finally, the soil contaminant concentrations were calculated by applying a yield factor on each concentration measured after extraction. The extraction yield factors of adsorbed pollutant were calculated by spiking in triplicate a pristine soil in water with a known amount of each contaminant (100 ng per g of soil) and shaking for 24 h to ensure that equilibrium adsorption is reached. After filtration through a nylon membrane (0.2 µm), the liquid fraction was analyzed. The adsorbed amount (deduced by difference between the introduced concentration (100 ng·g^{-1}) and the remaining concentration after shaking) was extracted from the solid fraction by MAE and analyzed to determine the extraction yield. The method was validated by following exactly the same protocol meaning by spiking in triplicated another pristine soil with a known amout of each contaminant. Then the sampled soil was analyzed using the validated method.

2.6 Statistical analysis

Standard deviation, linearity and coefficient of determination were calculated with Excel 2016 datasheet using build-in function (LINEST and STDEV.S) for linear regression. The LOD and LOQ was calculated with the signal to noise approach according to ICH Harmonized Tripartite Guideline (2005). The noise was determinated graphically on the chromatogram for each compounds then the LOQ was calculated as the equivalent concentration of ten times the noise and the LOD as the equivalent concentration of three times the noise.

3 Results and discussion

3.1 Soil characterisation

The soil physico-chemical properties are reported in Table 3. The five soils were very similar in texture: PYZC8, PYZB2, PYZC7,

TABLE 2 Physico-chemical characteristics of the sampled soils and GPS localization. Perc.

Analytes	Quantification ion (m/z)	Identification ion (m/z)
Benzo(k)fluoranthene	252	224, 198
Benzo(b)fluoranthene	252	224, 174
Benzo(a)pyrene	252	225, 126
Indéno(1,2,3-c,d)pyrene	276	248, 138
Benzo(g,h,i)perylene	276	138, 125
Anthracene	178	152, 126
Fluoranthene	202	152, 126
Naphtalene	128	102, 64
Benzene	78	63, 51
Toluene	91	92, 65
Ethylbenzene	91	106, 77
Xylene (o + m + p)	91	106, 77
Diethylphtalate	149	222, 177
Tributyltin cation	269	269, 267, 213
4-Octylphenol	107	206, 96
4-tert-octylphenol	135	136, 107
4-n-nonylphenol	107	220, 77

TABLE 3 Physico-chemical characteristics of the sampled soils and GPS localization. Percentages of organic matter and $CaCO_3$ are expressed as a weight percentage of dry whole solid. Percentages of sand, silt and clay are expressed as weight percentages of dry mineral solid.

	PYZC8	PYZB2	PYZC7	NOZH22	NOZD69
Clay (%)	20	18	20	26	22
Silt (%)	41	44	46	48	51
Sand (%)	39	38	34	26	27
pH	8.4	8.4	8.4	8.4	8.3
$CaCO_3$ (%)	71	73	67	65	44
Cation exchange capacity (cmol kg^{-1})	10.2	8.1	8.6	9.4	13.4
Organic carbon (%)	3.1	2.9	3.2	3.3	3.3
GPS position	49.20889 4.18359	49.21273 4.16566	49.20916 4.18424	49.24698 4.17198	49.2516 4.17986

and NOZH22 were loam, and NOZD69 was silt loam. They displayed a basic pH (≈8.4) which is characteristic of calcareous soils of the Champagne-Ardenne region and in accordance with their high $CaCO_3$ content (between 44% and 73%). Their OC content was relatively high, ranging between 2.9% and 3.3%, and their CEC was comprised between 8.1 and 13.4 cmol·kg^{-1}. The lack of diversity in soil physico-chemical properties and composition makes extrapolation of data difficult, however a previous study of extractability of organic pollutants using MAE with a wide variety of matrix type has shown that the main soil constituant influencing the extractability of pollutants is total organic carbon (Báez et al., 2003).

3.2 Analytical performance

The performance of the method is summarized in Table 1. Extraction yields ranged from 44% to 96%. The extraction of diethylphtalate, octylphenols, nonylphenols, and toluene was almost quantitative, the one of BTEX compounds ranged from 72% to 96%, while half of the PAH and tributhyltin cation remained adsorbed or lost by degradation during the extraction process. The extraction procedure was intended to be as simple as possible leading in some cases to relatively low extraction yield. However, in each case, the accuracy of the extraction yields was validated by the reproducibility of the extraction allowing an extrapolation of the exact content. In most cases, the LOQ were in the range of a tenth of a ng·g^{-1} (few hundreds of ppt). In the case of phenolic compounds, the LOQ were significantly higher, around 50 ng·g^{-1}. The LOQ values obtained in this paper for the analysis of BTEX and PAH in soils are similar to those reported in previous studies also measured by GC-MS but after solid-phase microextraction (SPME) extraction for BTEX (Franco et al., 2015) or solvent extraction for PAH (Maliszewska-Kordybach et al., 2009). A significant decrease of the detection limits could be reached for alkylphenols by including a derivation step with N-methyltrifluoroacetamide (Zhang et al., 2009) and an alkylation step for tributyltin (Crnoja et al., 2001). Khosravi and Price, 2015 obtained a better quantification limit of less than 1 pg·g^{-1} for diethylphtalate using an ASE-SPE-GC-MS method with a higher volume of sample concentrated and transferred in the injector during the analysis. Although other methods have better quantification limits especially when the methods are specifically designed for a single class of compound adding derivation and purification steps (e.g., for alkylphenols) the advantage of our method is the ability to analyze all the target compounds with a small number of preparation steps thus reducing the global cost of analysis. Nevertheless, this strategy leds to a reduction of the performance for some compounds by balancing selectivity and extraction efficiency but allows to reach the quantification limit fixed by the regulation for the whole list of compounds.

3.3 Concentrations of organic contaminants in soil samples

The results of soil analyses are reported in Table 4. PAH and BTEX (except benzene) were identified in all samples at relatively high concentrations, reaching levels higher than 100 ng·g^{-1} in the case of benzo(b)fluoranthene, indeno(1,2,3-c,d)pyrene, benzo(g,h,i)perylene, and fluoranthene. The total concentration ranged from 406 to 1,237 ng·g^{-1} for $\sum$8PAH and from 21 to 65 ng·g^{-1} for $\sum$BTEX. In France there are no mandatory values defining concentration limits of these pollutants in soil. Concentration limits only exist for ground-water and solid waste. Usually, concentrations are discussed according to the local context or the mean background concentrations. Various field campaigns evidenced the presence of PAH compounds in European soils at amounts depending on the anthropic activities in the area. For example, in Switzerland, concentrations of 98–219 ng·g^{-1} were found in different forest sites (Bucheli et al., 2004), whereas these concentrations could reach 575 ng·g^{-1} in agricultural soils impacted by anthropic activities (Berset and Holzer, 1995). Sometimes, very high contents of PAH were found like in Poland with concentrations reaching 6,680 ng·g^{-1} in soil less than 5 km from the emission source typically industries and urban areas (Maliszewska-Kordybach et al., 2009). In France, a model of the PAH contamination distribution based on 549 uncultivated soil samples throughout the country showed that HAP remained below the detection limits (<5–50 ng·g^{-1}) in most samples (Villanneau et al., 2013). However, in highly contaminated sites (mining, metallurgy and coal burning activities) individual HAP reached 100–1,000 ng·g^{-1}. The

TABLE 4 Mean concentrations of organic contaminants measured in soil samples.

Analytes	PYZC8 (ng·g^{-1})	PYZB2 (ng·g^{-1})	NOZH22 (ng·g^{-1})	NOZD69 (ng·g^{-1})	PYZC7 (ng·g^{-1})
Benzo(k)fluoranthene	63	66	44	28	65
Benzo(b)fluoranthene	118	47	59	0.4	177
Benzo(a)pyrene	81	64	40	43	103
Indéno(1,2,3-c,d)pyrene	254	192	141	148	310
Benzo(g,h,i)perylene	105	125	87	58	114
Anthracene	12	15	10	8	36
Fluoranthene	244	235	164	119	429
Naphtalene	0.7 < LOQ	0.8 < LOQ	11	0.30 < LOQ	4 < LOQ
∑8PAH	880	744	558	406	1,237
Benzene	n.d.	n.d.	n.d.	n.d.	n.d.
Toluene	55	51	31	17	5.8
Ethylbenzene	2.21	2.24	1.8	1.3	1.71
Xylene (o)	1.72	1.9	2.6	1.15	4
Xylene (m + p)	6.3	6.64	7.2	6.31	8.96
Diethylphtalate	n.d.	n.d.	n.d.	n.d.	n.d.
Tributyltin cation	n.d.	n.d.	n.d.	n.d.	n.d.
4-Octylphenol	n.d.	n.d.	n.d.	n.d.	n.d.
4-tert-octylphenol	n.d.	n.d.	n.d.	n.d.	n.d.
4-n-nonylphenol	n.d.	n.d.	n.d.	n.d.	n.d.
∑ 4-nonylphenol	n.d.	n.d.	n.d.	n.d.	n.d.
∑ Octylphenols	n.d.	n.d.	n.d.	n.d.	n.d.
∑ Nonylphenols	n.d.	n.d.	n.d.	n.d.	n.d.

n.d., not detected; LOQ, limit of quantification.

authors evidenced that fluoranthene, pyrene and phenanthrene concentrations where geographically correlated with the contamination levels in the northeastern part of France due to historical industrial activities. The concentrations of each PAH in the contaminated soils were between 15 and 35 ng·g^{-1}. In another study, higher values ranging from 190 to 760 ng·g^{-1} were detected in unamended cropland influenced by urban activity and possibly impacted by direct deposition from agricultural engine particles (Gateuille et al., 2014). In the present study, the individual PAH concentrations measured (n.d to 429 ng·g^{-1}) were in the line with European agricultural soils considering its localization (located in the northeastern part of France and near urban and agricultural areas). In agricultural soil, PAH may impact crops growth or germination and invertebrates reproduction. Exposition studies on terrestrial plants (*Sinapsis alba*, *Trifolium pratense*, and *Lolium perenne*) with several PAHs found EC$_{20}$ values from 30 to 650 µg·g^{-1} for the most sensitive values which is above the total of measured PAH (Sverdrup et al., 2003). Survival and reproduction studies of springtail *Folsomia fimetaria L.*, in contaminated soil showed a typical LC$_{50}$ and EC$_{50}$ of 21 and 11 µg·g^{-1} respectively with no-observed-effect concentration of 8.6 µg·g^{-1} for the most sensitive PAH (Sverdrup et al., 2001) which is also above the total of measured PAH.

Concerning the BTEX, few data are available in the literature concerning their concentration into agricultural soils because they are considered to be mainly present in the atmospheric compartment due to their volatility. BTEX are emitted directly by leakage, stock manipulation or sludge application, but they can reach the soil compartment after their emission into the atmosphere by industry, wastewater treatment plant and vehicle exhausts. For benzene, a predicted environmental concentration of 0.02 ng·g^{-1} based on all the releases into the environment was determined in non-contaminated soils or without direct emission at vicinity (EU, 2008). Taking into account the deposition through the atmosphere, the predicted concentrations in agricultural soils increased in the range 1.21–129 ng·g^{-1} (EU, 2008). In the present study, the benzene concentration in the five studied soils was lower than the quantification limit (0.2 ng·g^{-1}) which was consistent with field studies conducted in uncontaminated soils (Ellison et al., 1997). Concerning toluene, modelisation based on emission calculated from traffic and industry was used to estimate its concentration in air, water and soils at local and regional scale (Hansen et al., 2003).

According to this model the expected background concentration of toluene in agricultural was 0.1 $ng{\cdot}g^{-1}$ and the mean concentration in agricultural soils located near different industrial sites was 7 $ng{\cdot}g^{-1}$. In addition, in the case of field studies without any direct pollution context, toluene soil concentrations of 1 $ng{\cdot}g^{-1}$ and 2.1–5.8 $ng{\cdot}g^{-1}$ were reported in the Netherland (Sloof and Blokzijl, 1987) and in Poland near petrol station or allotment garden (Zygmunt and Namiesnik, 2001), respectively. In this study, the toluene concentration ranged from 5 to 55 $ng{\cdot}g^{-1}$. As for ethylbenzene and xylene data in agricultural soils are very scarce and mostly related to direct spill incident *via* leakage with relative high concentrations in soils. However, using a simple box model, the concentration of ethylbenzene coming from atmospheric depositions was estimated at 0.07 $ng{\cdot}g^{-1}$ in agricultural soils and until 39 $ng{\cdot}g^{-1}$ in local areas (EU, 2007). In our studied soils, the ethylbenzene measured concentrations were in the lowest part of this range (around 2 $ng{\cdot}g^{-1}$); xylene concentrations were between 1 and 9 $ng{\cdot}g^{-1}$ which is relatively low compared to the concentrations detected in United States soils ranging from 1 to 190 $ng{\cdot}g^{-1}$ (Agency for Toxic Substances and Disease Registry (ATSDR), 2007). Thus, according to the cited examples, the measured concentrations of BTEX in the present study is in the same order of level as the measured value in the literature.

The other contaminants, alkylphenols, phthalates and tributyltin were not detected in the studied soil samples. They are surfactants and plasticizers introduced by contaminated wastewater applications or direct deposition from agricultural treatments. Their concentration are thus related to wastewater contamination and agricultural practices. Tributyltin can also be introduced by rainfall leading to very weak concentrations (<1 $ng{\cdot}g^{-1}$ Sn) (Huang et al., 2004). These compounds are known to persist several days before their degradation in well oxygenated soils (Topp and Starratt, 2000; Hoch, 2001) or deeper migration in soils (Sopheak et al., 2015). As the study focused on topsoil, deeper migration in soil cannot be ruled out. Moreover, this study only focused on regulated pollutants without taking into account their degradation products that may impact the ecosystems. Further experiments will be performed, including these degradation products, to assess their occurrence and impact. Alternatively, other data could indicate a historical contamination such as crop health, ecosystem description, soil fertility or soil microbial content. In any case our study shown that no gradient or trace is left on the topsoil.

4 Conclusion

This study aimed at quantifying multiple organic contaminants targeted by the regulation on industrial wastewater management. The main advantage of the proposed method is to minimize the preparation step of the samples and to allow the compound analysis in an only one analytical method, where other methods need several extraction and derivatization steps (with obvious higher performance) with higher costs. The performances (LOQ) reached by the optimized method meet the legislator requirements. Significant quantities of PAH and BTEX were found in sampled agricultural soils. The mean amounts of these compounds were in agreement with measurements or estimates performed in similar contexts. However, a more detailed work is required to improve the understanding of the contamination scope and location. Investigations are needed to quantify source apportionment of the hydrocarbons found in soils as well as their potential accumulation. In contrast, no plasticizer or surfactant was detected suggesting that degradation or migration efficiently removed the potential soil contamination. Also a more detailed study dedicated to the spreading activities would enable to get a better insight into these processes.

Data availability statement

The raw data supporting the conclusion of this article will be made available by the authors, without undue reservation.

Author contributions

Formal analysis and investigation by NM; Conceptualization, Methodology, Writing—original draft preparation review and editing: NM, SS, and EG; Funding acquisition, Resources, Supervision: EG; NM, SS, and EG read and approved the final manuscript.

Funding

This work was supported by the “Seine-Normandie” water agency (AESN).

Acknowledgments

The “Association de Suivi des Epandages Agronomiques” (ASAE, M. Robert) is gratefully acknowledged for providing the soil samples. The “Seine-Normandie” water agency (AESN) is gratefully thanked for its financial support.

Conflict of interest

The authors declare that the research was conducted in the absence of any commercial or financial relationships that could be construed as a potential conflict of interest.

Publisher’s note

References

AFNOR (Association Française de Normalisation) (1999). *Qualité des sols - Méthodes chimiques - Détermination de la capacité d'échange cationique (CEC) et des cations extractibles (NF X31-130)*. Paris: AFNOR. (in French).

AFNOR (Association Française de Normalisation) (2003). *Qualité du sol Détermination de la Distribution Granulométrique des Particules du sol Méthode à la Pipette (AFNOR NF X31-107)*. Paris: AFNOR. (in French).

AFNOR (Association Française de Normalisation) (1995). *Qualité du sol Détermination de la Teneur en Carbonate – Méthode Volumétrique (NF ISO 10693)*. Paris: AFNOR. (in French).

AFNOR (Association Française de Normalisation) (2005). *Qualité du sol Détermination du pH (NF ISO 10390)*. Paris: AFNOR. (in French).

AFNOR (Association Française de Normalisation) (1998). *Qualité du sol Dosage du Carbone Organique par Oxydation Sulfochromique (NF ISO 14235)*. Paris: AFNOR. (in French).

Agency for Toxic Substances and Disease Registry (ATSDR) (2007). *Toxicological profile for Xylenes*. Atlanta, GA: U.S. Environmental Protection Agency. Available at: https://wwwn.cdc.gov/TSP/ToxProfiles/ToxProfiles.aspx?id=296&tid=53.

Andreu, V., Ferrer, E., Rubio, J. L., Font, G., and Picó, Y. (2007). Quantitative determination of octylphenol, nonylphenol, alkylphenol ethoxylates and alcohol ethoxylates by pressurized liquid extraction and liquid chromatography–mass spectrometry in soils treated with sewage sludges. *Sci. Total Environ.* 378, 124–129. doi:10.1016/j.scitotenv.2007.01.024

Báez, M. E., Aponte, A., and Sánchez-Rasero, F. (2003). Microwave-assisted solvent extraction of the herbicide methabenzthiazuron from soils and some soil natural organic and inorganic constituents. Influence of environmental factors on its extractability. *Analyst* 128, 1478–1484. doi:10.1039/B312288C

Berset, J. D., and Holzer, R. (1995). Organic micropollutants in swiss agriculture: Distribution of polynuclear aromatic hydrocarbons (PAH) and polychlorinated biphenyls (PCB) in soil, liquid manure, sewage sludge and compost samples; a comparative study. *J. Environ. Anal. Chem.* 59, 145–165. doi:10.1080/03067319508041324

Brockmann, D., Pradel, M., and Hélias, A. (2018). Agricultural use of organic residues in life cycle assessment: Current practices and proposal for the computation of field emissions and of the nitrogen mineral fertilizer equivalent. *Resour. Resour. Conserv. Recycl.* 133, 50–62. doi:10.1016/j.resconrec.2018.01.034

Bucheli, T. D., Blum, F., Desaules, A., and Gustafsson, Ö. (2004). Polycyclic aromatic hydrocarbons, black carbon, and molecular markers in soils of Switzerland. *Chemosphere* 56, 1061–1076. doi:10.1016/j.chemosphere.2004.06.002

Burek, P., Satoh, Y., Fischer, G., Kahil, M. T., Scherzer, A., Tramberend, S., et al. (2016). "Water futures and solution - fast track initiative (final report)," in *IIASA working paper WP 16-006*. Available at: http://pure.iiasa.ac.at/13008.

Champ, M. A. (2000). A review of organotin regulatory strategies, pending actions, related costs and benefits. *Sci. Total Environ.* 258, 21–71. doi:10.1016/S0048-9697(00)00506-4

Chee, K. K., Wong, M. K., and Lee, H. K. (1996). Microwave extraction of phthalate esters from marine sediment and soil. *Chromatographia* 42, 378–384. doi:10.1007/BF02272126

Clément, N., Muresan, B., Hedde, M., and François, D. (2015). PAH dynamics in roadside environments: Influence on the consistency of diagnostic ratio values and ecosystem contamination assessments. *Sci. Total Environ.* 538, 997–1009. doi:10.1016/j.scitotenv.2015.08.072

Crnoja, M., Haberhauer-Troyer, C., Rosenberg, E., and Grasserbauera, M. (2001). Determination of Sn- and Pb-organic compounds by solid-phase microextraction-gas chromatography-atomic emission detection (SPME-GC-AED) after *in situ* propylation with sodium tetrapropylborate. *J. Anal. At. Spectrom.* 16, 1160–1166. doi:10.1039/B104694M

Ellison, R. J., Larnimaa, K., Margary, S. A., Mata, J. M., Muller, J-M., Peterson, D. R., et al. (1997). *Exposure profile: Gasoline*, 97/52. Brussels: Concawe Report No.

EU (2007). "European union risk assessment report," in *Ethylbenzene*. Available at: https://echa.europa.eu/documents/10162/f9b4577b-c57f-439b-b15a-9e268b1d0a58.

EU (2008). "European union risk assessment report," in *Benzene*. Available at: https://echa.europa.eu/documents/10162/be2a96a7-40f6-40d7-81e5-b8c3f948efc2.

Ezquerro, Ó., Ortiz, G., Pons, B., and Tena, M. (2004). Determination of benzene, toluene, ethylbenzene and xylenes in soils by multiple headspace solid-phase microextraction. *J. Chromatogr. A* 1035, 17–22. doi:10.1016/j.chroma.2004.02.030

Franco, M. S., da Silva, M. R., Santos-Neto, A. J., and Lanças, F. M. (2015). SPME determination of low concentration levels of monoaromatic chemical markers in soils after remediation by supercritical fluid extraction. *Anal. Methods* 7, 4901–4907. doi:10.1039/C5AY00467E

Gaspéri, J., Ayrault, S., Moreau-Guigon, E., Alliot, F., Labadie, P., Budzinski, H., et al. (2018). Contamination of soils by metals and organic micropollutants: Case study of the parisian conurbation. *Environ. Sci. Pollut. Res.* 25, 23559–23573. doi:10.1007/s11356-016-8005-2

Gateuille, D., Evrard, O., Lefevre, I., Moreau-Guigon, E., Alliot, F., Chevreuil, M., et al. (2014). Mass balance and decontamination times of Polycyclic Aromatic Hydrocarbons in rural nested catchments of an early industrialized region (Seine River basin, France). *Sci. Total Environ.* 470–471, 608–617. doi:10.1016/j.scitotenv.2013.10.009

Gibson, R., Wang, M.-J., Padgett, E., and Beck, A. J. (2005). Analysis of 4-nonylphenols, phthalates, and polychlorinated biphenyls in soils and biosolids. *Chemosphere* 61, 1336–1344. doi:10.1016/j.chemosphere.2005.03.072

Hansen, B., Munn, S., Pakalin, S., Luotamo, M., Allanou, R., Pellegrini, G., et al. (2003). *European union risk assessment report toluene*. Available at: https://publications.jrc.ec.europa.eu/repository/handle/JRC24380.

Heroult, J., Zuliani, T., Bueno, M., Denaix, L., and Lespes, G. (2008). Analytical advances in butyl-phenyl- and octyltin speciation analysis in soil by GC-PFPD. *Talanta* 75, 486–493. doi:10.1016/j.talanta.2007.11.053

Heudorf, U., Mersch-Sundermann, V., and Angerer, J. (2007). Phthalates: Toxicology and exposure. *Int. J. Hyg. Environ. Health* 210, 623–634. doi:10.1016/j.ijheh.2007.07.011

Hoch, M. (2001). Organotin compounds in the environment — An overview. *Appl. Geochem.* 16, 719–743. doi:10.1016/S0883-2927(00)00067-6

Holoubek, I., Dušek, L., Sáňka, M., Hofman, J., Čupr, P., Jarkovský, J., et al. (2009). Soil burdens of persistent organic pollutants – their levels, fate and risk. Part I. Variation of concentration ranges according to different soil uses and locations. *Environ. Pollut.* 157, 3207–3217. doi:10.1016/j.envpol.2009.05.031

Huang, J.-H., Schwesig, D., and Matzner, E. (2004). Organotin compounds in precipitation, fog and soils of a forested ecosystem in Germany. *Environ. Pollut.* 130, 177–186. doi:10.1016/j.envpol.2003.12.012

ICH Harmonized Tripartite Guideline (2005). *Validation of analytical procedures: Text and methodology*, Q2.R1

Khajeh, M., Moosavi-Movahedi, A. A., Shakeri, M., Zadeh, F. M., Khajeh, A., and Bohlooli, M. (2014). Dispersive solid phase extraction combined with dispersive liquid–liquid extraction for the determination of BTEX in soil samples: Ant colony optimization–artificial neural network. *J. Chemom.* 29, 245–252. doi:10.1002/cem.2706

Khosravi, K., and Price, G. W. (2015). Determination of phthalates in soils and biosolids using accelerated solvent extraction coupled with SPE cleanup and GC–MS quantification. *Microchem. J.* 121, 205–212. doi:10.1016/j.microc.2015.03.013

Llorca-Pórcel, J., Martínez-Parreño, M., Martínez-Soriano, E., and Valor, I. (2009). Analysis of chlorophenols, bisphenol-A, 4-tert-octylphenol and 4-nonylphenols in soil by means of ultrasonic solvent extraction and stir bar sorptive extraction with *in situ* derivatisation. *J. Chromatogr. A* 1216, 5955–5961. doi:10.1016/j.chroma.2009.06.043

Liang, P., Zhang, L., Peng, L., Li, Q., and Zhao, E. (2010). Determination of phthalate esters in soil samples by microwave assisted extraction and high performance liquid chromatography. *Bull. Environ. Contam. Toxicol.* 85, 147–151. doi:10.1007/s00128-010-0078-x

Ma, L. L., Muir, D., Wang, X. T., and Xu, X. B. (2005). Simultaneous analysis of organic pollutants in soils by gas chromatography and gas chromatography–mass spectrometry. *Int. J. Environ. Anal. Chem.* 85, 89–98. doi:10.1080/03067310512331324736

Maliszewska-Kordybach, B., Smreczak, B., and Klimkowicz-Pawlas, A. (2009). Concentrations, sources, and spatial distribution of individual polycyclic aromatic hydrocarbons (PAHs) in agricultural soils in the eastern part of the EU: Poland as a case study. *Sci. Total Environ.* 407, 3746–3753. doi:10.1016/j.scitotenv.2009.01.010

Marcic, C., Hecho, I. L., Denaix, L., and Lespes, G. (2006). TBT and TPhT persistence in a sludged soil. *Chemosphere* 65, 2322–2332. doi:10.1016/j.chemosphere.2006.05.007

Martínez Vidal, J. L., Garrido Frenich, A., de las Nieves Barco Bonilla, M., Romero-González, R., and Padilla Sánchez, J. A. (2009). Simultaneous extraction of polycyclic aromatic hydrocarbons and polychlorinated biphenyls in agricultural soils by pressurized liquid extraction and determination by gas chromatography coupled to tandem mass spectrometry. *Anal. Bioanal. Chem.* 395, 1551–1562. doi:10.1007/s00216-009-3111-3

Ministère de l'écologie du développement durable et de l'énergie (2014). *Décret n° 2014-1578 du 23 décembre 2014 paru au JO du 26 décembre 2014*. (in French). Available at: https://www.legifrance.gouv.fr/loda/id/JORFTEXT000029958114/.

Pérez, R. A., Albero, B., Miguel, E., and Sánchez-Brunete, C. (2012). Determination of parabens and endocrine-disrupting alkylphenols in soil by gas chromatography--mass spectrometry following matrix solid-phase dispersion or in-column microwave-assisted extraction: A comparative study. *Anal. Bioanal. Chem.* 402, 2347–2357. doi:10.1007/s00216-011-5248-0

Popescu, R. S., and Popescu, L. L. (2017). Assessment of air pollution, by the urban traffic, in university campus of bucharest. *J. Environ. Prot.* 8, 884–897. doi:10.4236/jep.2017.88055

Poster, D. L., Schantz, M. M., Sander, L. C., and Wise, S. A. (2006). Analysis of polycyclic aromatic hydrocarbons (PAHs) in environmental samples: A critical review of gas chromatographic (GC) methods. *Anal. Bioanal. Chem.* 386, 859–881. doi:10.1007/s00216-006-0771-0

Shin, H.-S. (2012). Determination of MTBE, TBA and BTEX in soil by headspace gas chromatography-mass spectrometry. *Bull. Korean Chem. Soc.* 33, 1693–1698. doi:10.5012/bkcs.2012.33.5.1693

Sopheak, N., Sempéré, R., Delmont, A., Paluselli, A., and Ouddane, B. (2015). Occurrence, fate, behavior and ecotoxicological state of phthalates in different environmental matrices. *Environ. Sci. Technol.* 49, 4019–4035. doi:10.1021/es505233b

Sverdrup, L. E., Kelley, A. E., Krogh, P. H., Nielsen, T., Jensen, J., Scott-Fordsmand, J., et al. (2001). Effects of eight polycyclic aromatic compounds on the survival and reproduction of thespringtail Folsomia fimetaria L. (collembolan, isotomidae). *Environ. Toxicol. Chem.* 20, 1332–1338.doi:10.1897/1551-5028(2001)020<1332:eoepac>2.0.co;2

Sverdrup, L. E., Krogh, P. H., Nielsen, T., Kjaer, C., and Stenersen, J. (2003). Toxicity of eight polycyclic aromatic compounds to red clover (Trifolium pratense), ryegrass (Lolium perenne) and mustard (Sinapsis alba). *Chemosphere* 53, 993–1003. doi:10.1016/S0045-6535(03)00584-8

Topp, E., and Starratt, A. (2000). Rapid mineralization of the endocrine-disrupting chemical 4-nonylphenol in soil. *Environ. Toxicol. Chem.* 19, 313–318. doi:10.1002/etc.5620190210

Villanneau, E. E., Saby, N. N., Orton, T. T., Jolivet, C. C., Boulonne, L. L., Caria, G. G., et al. (2013). First evidence of large-scale PAH trends in French soils. *Environ. Chem. Lett.* 11, 99–104. doi:10.1007/s10311-013-0401-y

Wang, W., Meng, B., Lu, X., Liu, Y., and Tao, S. (2007). Extraction of polycyclic aromatic hydrocarbons and organochlorine pesticides from soils: A comparison between soxhlet extraction, microwave-assisted extraction and accelerated solvent extraction techniques. *Anal. Chim. Acta* 602, 211–222. doi:10.1016/j.aca.2007.09.023

Xu, L., and Lee, H. K. (2008). Novel approach to microwave-assisted extraction and micro-solid-phase extraction from soil using graphite fibers as sorbent. *J. Chromatogr. A* 1192, 203–207. doi:10.1016/j.chroma.2008.03.060

Zhang, H., Spiteller, M., Guenther, K., Boehmler, G., and Zuehlke, S. (2009). Degradation of a chiral nonylphenol isomer in two agricultural soils. *Environ. Pollut.* 157, 1904–1910. doi:10.1016/j.envpol.2009.01.026

frontiers | Frontiers in Environmental Science

TYPE Original Research
PUBLISHED 13 April 2023
DOI 10.3389/fenvs.2023.1170427

OPEN ACCESS

EDITED BY
Xing Yang,
Hainan University, China

REVIEWED BY
Yingjie Dai,
Northeast Agricultural University, China
Hongfen Zhu,
Shanxi Agricultural University, China

*CORRESPONDENCE
Joao Arthur Antonangelo,
✉ antonangeloj@apsu.edu

RECEIVED 20 February 2023
ACCEPTED 06 April 2023
PUBLISHED 13 April 2023

CITATION
Antonangelo JA, Zhang H and Sitienei I (2023), Biochar amendment of a metal contaminated soil partially immobilized Zn, Pb, and Cd and reduced ryegrass uptake.
Front. Environ. Sci. 11:1170427.
doi: 10.3389/fenvs.2023.1170427

Biochar amendment of a metal contaminated soil partially immobilized Zn, Pb, and Cd and reduced ryegrass uptake

Joao Arthur Antonangelo[1]*, Hailin Zhang[2] and Isaac Sitienei[1]

[1]Department of Agriculture, Austin Peay State University, Clarksville, TN, United States, [2]Department of Plant and Soil Sciences, Oklahoma State University, Stillwater, OK, United States

Soil heavy metals (HM) contamination threatens soil and water quality, which significantly affects humans and animals. This study focuses on the competitive immobilization of zinc (Zn), lead (Pb), and cadmium (Cd) in soils from a contaminated site using ryegrass (*Lolium perenne*) in a potting experiment amended with biochars. Increased rates of switchgrass- (SGB) and poultry litter-derived biochars (PLB) were applied before ryegrass cultivation. Soil HM phytoavailability and HM concentrations in plant shoots were determined. Multivariate regression models were used to evaluate the influence of several soil chemical attributes on the HM phytoavailability. The increased rates of both biochars reduced the Zn, Pb, and Cd availability ($p < 0.001$). Langmuir models showed that the maximum HM immobilization (I_{MAX}) was 169.2 ± 29.5 mg kg^{-1} for Zn with SGB, and 20 ± 7.4 (Pb) and 1.08 mg kg^{-1} (Cd) with PLB. The extended Langmuir model (EL) showed competitive HM immobilization since there was a decrease in the I_{MAX} of Zn (~90 ± 28 mg kg^{-1} from SGB) and Cd (~0.70 ± 0.21 mg kg^{-1}). Negative values of Pb and Cd immobilization at low rates of SGB indicated an increase in those HM availabilities and preferential immobilization for Zn. The reduced Zn and Pb uptake in ryegrass shoots ranged from 70% to 98% and were optimum at rates of 0.50% ± 0.00%–0.60% ± 0.06% for both biochars, and 1.6% ± 0.4% of SGB for Cd. The stepwise multiple linear regression (SMLR) and partial least squares (PLS) revealed that pH and organic matter (OM) were the most responsible factors for reducing Zn bioavailability while OM was more impactful in decreasing Pb and Cd levels. This suggests that the preferential immobilization for Zn relies on its higher sensitivity to the pH increase. Also, the ubiquitous positive relationship among the metals studied shows that competitive immobilization is ceased at high rates of biochars application. Path analysis (PA) showed that pH and OM were the common contributors from both biochars to simultaneously affect Zn, Pb, and Cd availability regardless of the contrasting physicochemical properties of the two bioproducts. This work proved the potential of applying low rates of two contrasting feedstock-derived biochars to remediate the contaminants and safely grow ryegrass.

KEYWORDS

metals immobilization, biochar (BC), switchgrass, poultry litter, multivariate techniques

1 Introduction

Excessive deposition of HM in the soil caused by human activities is highly hazardous to both the environment and living organisms. Gradual increase in both the level and type of HM has been observed in recent years (da Silva et al., 2022; Su, 2014). Lack of proper chemical remediation interventions as well as phytoremediation could lead to accumulation of HM in the farmlands (Ali et al., 2013; Antonangelo and Zhang, 2019; Yang et al., 2021). Soil quality and its ability to support crops and pasture for animals become compromised at certain higher concentration levels of HM. At these levels, they may even enter the food chain and endanger human health (Abbas et al., 2017; Yang et al., 2021). For instance, Pb is considered one of the most important toxic heavy metal because of its direct effect on humans through water pollution. Drinking Pb contaminated water can cause respiratory, digestive, nervous, blood, urinary and immune system symptoms of acute or chronic poisoning, and may even lead to death (Järup, 2003).

Current advancements in physical, chemical, and biological remediation technologies have greatly enhanced HM's immobilization efforts. Implementation of simple remediation strategies such as using lime, clay, phosphates, silicates, organic compost, etc. have been found to greatly help immobilize heavy metals (Yang et al., 2021). In addition to helping lower HM's level in the soil, implementation of these strategies has benefited soil in many other ways. Soil fertility, pH, cation exchange, etc. have been improved following the application of these soil remediation strategies (Ahmad et al., 2014; Sun et al., 2020). This study will focus on biochar (switchgrass and poultry litter) which are low-cost yet have high efficiency with regards to their effects on soil conditioning (Yang et al., 2021). Biochar is a carbonaceous material derived from different biowastes such as crop straw, wood chips, swine manure, etc. (Ahmad et al., 2014; Fan et al., 2018; Meng et al., 2018; Sun et al., 2020). Unique physicochemical properties of most biochars such as availability, high porosity, low cost, environmentally sustainable and high adsorption performance (Wang et al., 2017; He et al., 2019; Shaheen et al., 2019) makes them highly desirable.

Biochar application increases soil pH (Qiao et al., 2017; Sun et al., 2020; Yang et al., 2021), it can also adsorb various contaminants through ion exchange, precipitation and/or surface complexation (Bradl, 2004; Inyang et al., 2015; Wang et al., 2017). Most recent studies are pointing out the use of advanced technologies to modify biochar and improve its characteristics of soil contaminant immobilization (Liu et al., 2022a; Liu et al., 2022b; Liu et al., 2023) in addition to evaluating the recovery of such bioproducts and their potential reuse, which promotes, even more, the sustainable approach offered by these charcoal products. Of particular interest is its ability to reduce HM bioavailability in the soil (Park et al., 2011; Ahmad et al., 2012; Meng et al., 2018). Biochar has therefore been extensively used in remediation of HM contaminated soils (Zhang et al., 2017; Sun et al., 2020). The effectiveness of biochar in metal immobilization, however, depends on soil physicochemical properties, biochar properties, and metal species (Xie et al., 2015; Zeng et al., 2015; Weng et al., 2017; Meng et al., 2018). The bioavailability of HM has been found to be highly correlated with physicochemical characteristics of soil, including pH, organic matter, redox conditions, etc. (Weng et al., 2017).

It is important to understand the role that soil properties play on the behavior of HM. Fine-textured soils have been found to facilitate rapid metal mobility than coarse-textured soils (Fashola et al., 2020). High organic matter content can enhance metal adsorption thus reducing mobility (He et al., 2019). Acidic conditions can decrease soil cation exchange by increasing metal solubility and thus HM's mobility (Fashola et al., 2020). The solubility of Zn, for example, increases 100-fold for each unit decrease in soil pH (Rengel, 2015). Changes in soil pH have greatly disrupted soil microbial activities by slowing pH-dependent enzymes, altering key nutrients availability, and/or HM's mobility (Kapoor et al., 2015; Fashola et al., 2020).

In this study, the biochars generated from switchgrass (SGB) and poultry litter (PLB) were used to determine their effects on metal phytoavailability in the soil and their concentrations in plant (ryegrass) shoots. Qiao et al. (2017) found that when a biochar composite derived from Chinese herb medicine residue was added to soil, it not only reduced the bioaccumulation of Cd by the cabbage mustard plants but also promoted the growth and development of the plants. The influence of several soil chemical attributes such as pH, organic matter content, etc. on metals' phytoavailability in the soil is also evaluated. This research becomes unique since multimetal contaminated sites must be remediated using a single practice able to immobilize all contaminants simultaneously. Hence, biochars produced from contrasting feedstocks were applied at reasonable rates in a potting experiment so that any potential results might be feasibly tested on a field scale. In the previous work of Antonangelo and Zhang (2021), it was proven low rates of biochar were sufficient to grow ryegrass at the same time Cd concentration was considered safe in ryegrass shoots for cattle grazing. This current work evaluates the competitive immobilization of additional metals to elucidate the viability of applying low rates of either SGB or PLB as multimetal remediation practices.

2 Materials and methods

2.1 Biochar production and properties

The biochars were produced from switchgrass (SGB; *Panicum virgatum*) and poultry litter (PLB) by using high-temperature slow pyrolysis (700°C). The feedstocks obtainment and their conversion into biochar are in Antonangelo and Zhang (2019). The biochar coarse materials were gently ground with a mortar and pastel before being sieved through 1- and 0.25-mm filter/strain for physicochemical analyses and potting experiment, respectively (Antonangelo et al., 2019). The SGB and PLB characterization including several physicochemical properties such as moisture, ash content, particle-size distribution, elemental composition, surface functional groups, chemical attributes, specific surface area (SSA), cation exchange capacity (CEC), and morphology can be found in Antonangelo et al. (2019).

2.2 Soil sampling and analysis

Heavy metal contaminated soil samples were collected from a depth of 0–15 cm in a residential yard near chat piles located in Picher, Ottawa County, Oklahoma using a shovel. Soil sample

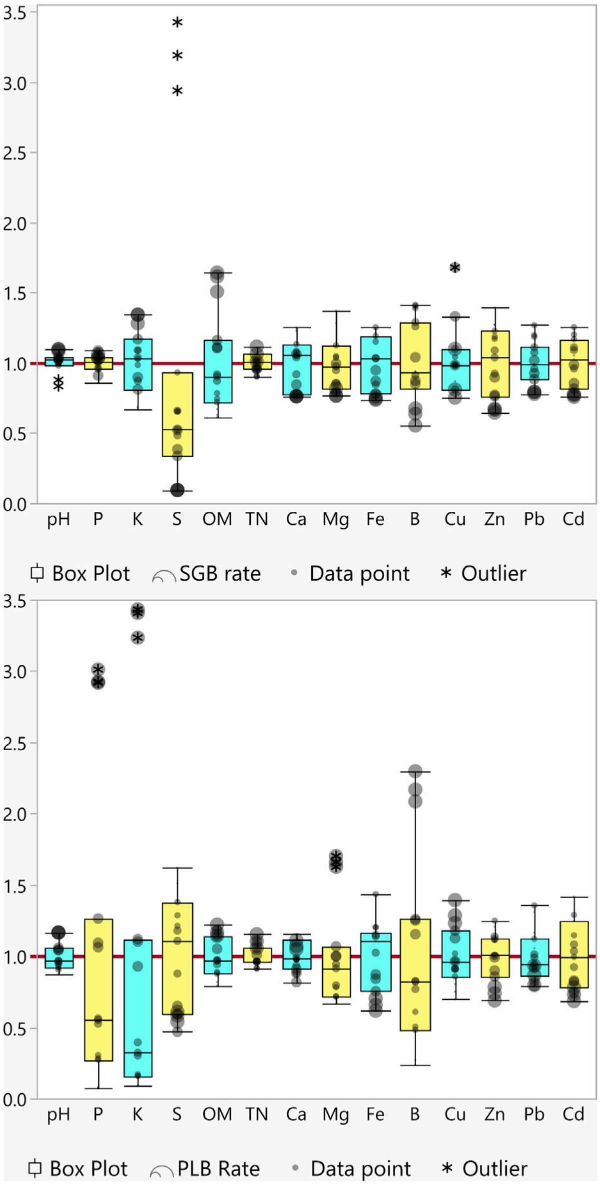

FIGURE 1
Boxplot of soil chemical attributes after switchgrass- and poultry litter-derived biochar application rates, SGB (top) and PLB (bottom). Data were normalized by dividing every measurement by the average of the whole dataset of measurements (*y-axis*). The Red line denotes the average. Boxes span the 25th to 75th data percentile, whiskers represent 1.5 × the interquartile range, and horizontal lines denote the median.

preparation is fully described in Antonangelo and Zhang (2019). Before and after the pot experiment, soil samples were analyzed for DTPA–extractable Cd, Pb, and Zn. The DTPA-extractable heavy metals have been considered the most efficient method to predict their phytoavailability in perennial ryegrass (Antonangelo and Zhang, 2019) and also a reliable extractant for potentially toxic metals in soils (da Silva et al., 2022). Before the potting experiment, the total Cd, Pb, and Zn contents were determined by an inductively coupled plasma-atomic emission spectroscopy, ICP-AES (SPECTRO Analytical Instruments GmbH, Boschstr. 10, 47533 Kleve, Germany) after digestion by concentrated HNO_3 and H_2O_2 using EPA method 3050B (Church et al., 2017). The DTPA-extractable Cd, Pb, and Zn before the potting experiment were respectively 1.84 ± 0.03, 49.9 ± 1.7, and 220.6 ± 9.3 mg kg^{-1}. The total Cd, Pb, and Zn were respectively 9.0 ± 0.6, 233.7 ± 10.8, and 1765 ± 221 mg kg^{-1}. The total Cd content was about tenfold the maximum found in normal Oklahoma soils (Richards et al., 2012; Antonangelo and Zhang, 2021). The threshold of DTPA-extractable Cd was 0.03–0.16 mg kg^{-1} (Wu et al., 2021), which is over tenfold lower than the content found in the Tar Creek soil of this study. The total Zn and Pb contents were about twelvefold and sevenfold, respectively, the maximum found in normal Oklahoma soils (Richards et al., 2012). These reemphasize the immediate need for remediating those metals in the Tar Creek area.

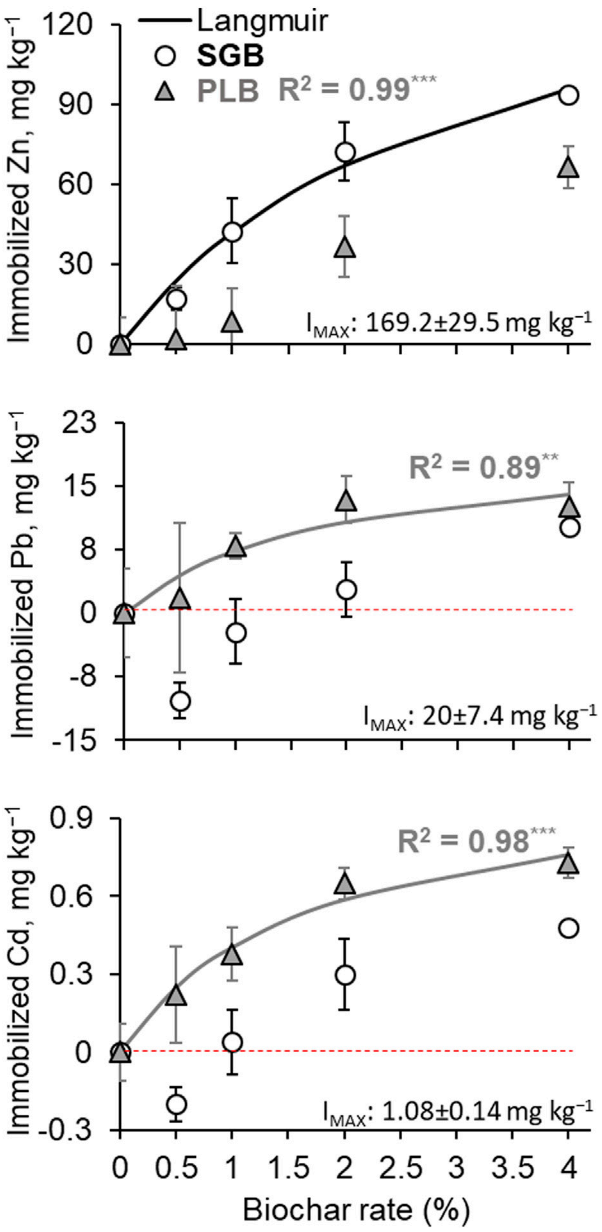

FIGURE 2
Langmuir models used to predict the maximum immobilization of heavy metals. No line means a non-significant fit of the model. Bars represent the standard deviation of the mean ($n = 3$). Points below the red dashed line (negative values) mean that heavy metal becomes more available than the control treatment (0% biochar application). I_{MAX} = maximum immobilization for the fitted model. Values followed by ± are the standard deviation. **: $p < 0.01$; ***: $p < 0.001$. *Simple Langmuir adsorption isotherm equation*: $y = (a*b*x)/(1 + b*x)$

2.3 Potting experiment

Plastic pots received 1,200 g of 2-mm sieved soils and were added 0.0 (control), 0.5, 1.0, 2.0, and 4.0% (w/w) of 0.25-mm sieved SGB and PLB. The mixture was then incubated for 30 days at 75% of field capacity before ryegrass sowing in each pot at the seeding rate of 30 kg ha^{-1}. Ryegrass was grown for 75 days in biochar-amended soils in an environmentally controlled growth chamber. The pots were arranged in a complete randomized block design (CRBD) with 3 replications ($n = 3$). Plots were weekly rotated to eliminate spatial variability in the growth chamber. A detailed description of all procedures conducted during the potting experiment can be found in Antonangelo and Zhang (2019).

2.4 Metal contents in ryegrass

Ryegrass shoots were separated after harvesting, washed with deionized (D.I.) water, and oven-dried at 105°C until constant weight. Dried plant materials were ground using a mechanical

TABLE 1 ANOVA of soil heavy metal immobilization and uptake reduction by ryegrass shoots as a function of increased rates of two feedstock-derived biochars applied separately.

Rate, %	--------------Immobilized, mg kg^{-1}--------------											
	Zn				Pb				Cd			
	SGB		PLB		SGB		PLB		SGB		PLB	
0	0	cA	0	cA	0	abcA	0	cA	0	cA	0	dA
0.5	17.0	bcA	2.1	cA	−10.3	cB	1.8	bcA	−0.20	cB	0.22	cdA
1	42.6	bA	8.4	cB	−2.2	bcB	7.9	abcA	0.04	bcB	0.38	bcA
2	72.4	aA	36.8	bB	2.8	abB	13.4	aA	0.30	abB	0.65	abA
4	93.9	aA	66.5	aB	10.1	aA	12.6	abA	0.48	aB	0.73	aA
Effect test	--------------*p*-value--------------											
Biochar	<0.0001				0.0002				<0.0001			
Rate	<0.0001				<0.0001				<0.0001			
Biochar × Rate	0.06				0.08				0.03			
	--------------Uptake reduction, %--------------											
Rate, %	Zn				Pb				Cd			
	SGB		PLB		SGB		PLB		SGB		PLB	
0	0	dA	0	eA	0	bA	0	bA	0	cA	0	dA
0.5	64.5	cB	67.9	dA	96.7	aA	96.8	aA	46.0	bA	35.4	cB
1	64.2	cB	74.1	cA	96.6	aA	97.0	aA	48.8	bA	37.7	cB
2	67.8	bB	78.4	bA	97.1	aA	97.4	aA	56.5	bA	52.9	bA
4	81.6	aB	85.6	aA	95.9	aA	98.7	aA	78.2	aA	79.9	aA
Effect test	--------------*p*-value--------------											
Biochar	<0.0001				0.66				0.04			
Rate	<0.0001				<0.0001				<0.0001			
Biochar × Rate	<0.0001				0.99				0.25			

SGB, switchgrass-derived biochar; PLB, poultry litter-derived biochar.

For each heavy metal, different lowercase letters in columns and uppercase letters in rows are significantly different at $p < 0.05$ (Tukey).

$\text{Metal immobilization}\left(\frac{mg}{kg}\right) = (\text{Available soil metal content in the control} - \text{Available soil metal content in the biochar treatement rate})$

$\text{Reduced metal uptake } (\%) = ([\text{Tissue metal content in the control} - \text{Tissue metal content in the biochar treatement rate}]/\text{Tissue metal content in the control})*100$

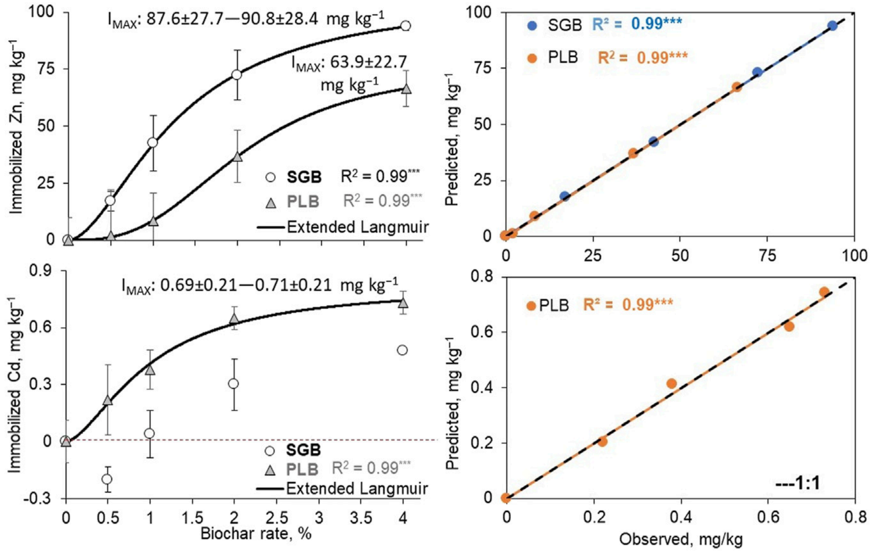

FIGURE 3
Extended Langmuir models used to predict the maximum immobilization of heavy metals as a function of biochar application rates (left), and plot of observed × predicted values from the fitted models (right). No line means a non-significant fit of the model. Bars represent the standard deviation of the mean (n = 3). Points below the red dashed line (negative values) mean that heavy metal becomes more available than the control treatment (0% biochar application). I_{MAX} = maximum immobilization for the fitted model. Values followed by ± are the standard deviation. ***: $p <$ 0.001.*Extended Langmuir adsorption isotherm equation*: $y = (a*b*x[1\hat{-}c])/(1 + bx[1\hat{-}c])$

grinder then analyzed for Cd, Pb, and Zn using nitric acid digestion (as discussed earlier). To determine metal concentrations in plant tissues, 0.5 g of ground plant materials were predigested for 1 h with 10 mL of trace metal grade HNO_3 in the HotBlock™ Environmental Express block digester (Environmental Express, 2345A Charleston Regional Parkway, Charleston, South Carolina 29492, SC, United States), and the digests were then heated to 115°C for 2 h and diluted with D.I. water to 50 mL (Jones and Case, 1990). Finally, the digested samples were filtered and determined for Cd, Pb, and Zn by an ICP-AES.

2.5 Data analysis

2.5.1 Descriptive statistics and ANOVA

Boxplot was plotted after normalizing the whole dataset of measurements (n = 15 for each biochar) to show soil chemical attributes (Antonangelo et al., 2022) affected by switchgrass and poultry litter-derived biochar application rates. The effects of Biochar, Rate, and the interaction Biochar × Rate were tested and a 2-way ANOVA was performed to compare treatment means using the Tukey test ($p < 0.05$).

2.5.2 Langmuir models

Single and extended Langmuir models were used to predict the maximum immobilization of heavy metals as a function of biochar application rates. The heterogeneous extended Langmuir model (EL) was verified because it predicts the adsorption from mixtures and applies the theory of multi-region or multisite adsorption, which is coherent with our study since SGB and PLB have shown several surface functional groups (Antonangelo et al., 2019). Langmuir models were then developed for SGB and PLB separately.

2.5.3 Non-linear regressions

Maximum responsive rates of biochar application to reduced metals uptake were determined by fitting the segmented polynomials linear–plateau (LP) and quadratic–plateau (QP) response models using the NLIN (non-linear) procedure of SAS version 9.4. The models were accepted only when the NLIN convergence criterion method successfully converged and the model was significant ($p < 0.05$). The standard error (SE) of joint points was used to verify if biochars had different maximum responses to increased application rates.

2.5.4 Stepwise multiple linear regression (SMLR)

For Stepwise Multiple Linear Regression (SMLR), all soil chemical attributes were used as independent variables to predict the available metal contents. The SMLR was generated with the whole dataset of measurements in JMP Pro 15 using the backward method. Initially, it incorporates all variables into the model followed by removal of the least important ones (Pelegrino et al., 2021). The remaining variables compose the final SMLR model. In our study, the stopping rule was tested for the *p-value threshold*, *AICc* (Akaike Information Criterion), and *BIC* (Bayesian Information Criterion), and the *AICc* was chosen because it is more appropriate in finding the best model for predicting future observations.

2.5.5 Partial least squares (PLS)

Partial Least Squares Regression (PLSR) was performed using the whole dataset of measurements in JMP Pro 15 to analyze the importance of factors affecting metal availability. PLSR is a

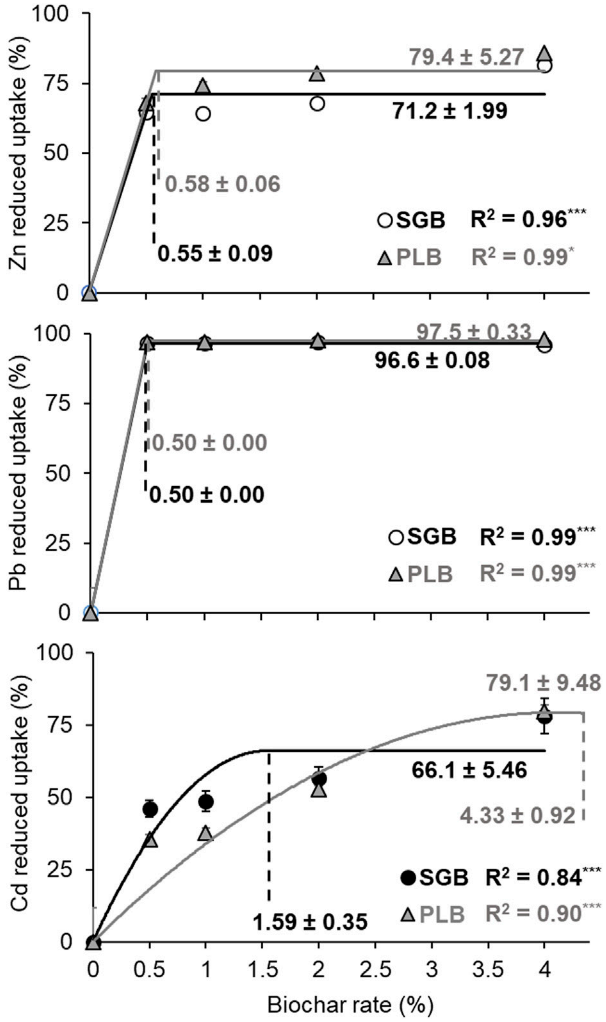

FIGURE 4
The trends of heavy metal uptake reduction by biochar application rates increase. Significant fits to the linear- and quadratic-with-upper-plateau statistical model were obtained. Bars represent the standard deviation of the mean (*n* = 3). *: $p < 0.05$; ***: $p < 0.001$. Values followed by ± are the standard deviation.

multivariate statistical analysis method that integrates the advantages of principal component analysis (PCA), canonical correlation analysis, and multiple linear regression analysis (Yang et al., 2021). It has been widely used to conduct regression analyses with small sample sizes, multiple variables, and multicollinearity among variables (Wold et al., 2001; Fang et al., 2015; Tong et al., 2020). It also uses cross-validation results to determine the number of components and avoids overfitting. The importance of an independent variable is measured by the variable importance in projection (VIP) value (Shi et al., 2013). When VIP > 1 the independent variable is important for predicting the dependent variable; whereas it is less important when V < 0.5 (Shi et al., 2014). The +/− symbols for each of the regression coefficients (RC) in the model indicate the action direction of each independent variable (Onderka et al., 2012). According to Yang et al. (2021), PLSR presents multiple advantages over other methods because it has a stronger interpretative ability for independent variables and its results are more stable and reliable.

For most PLS models, different independent variables (soil chemical attributes) affecting heavy metals availability as well as their direction of effect (positive or negative) were used, as shown in Supplementary Tables S1, S2.

2.5.6 Path analysis

A path analysis (PA) model similar to that performed by Richards et al. (2012) was used to evaluate the relationships between the combined contents of available metals and soil chemical attributes. The selected independent variables of the models were Fe, K, OM, P, and soil pH for SGB; and soil pH and OM for PLB. Direct and indirect effects were obtained with the whole dataset of measurements by using multiple regression of soil chemical attributes on metal contents and

TABLE 2 Equations from the linear- and quadratic-with-upper-plateau statistical models to predict uptake reduction (%) of heavy metals by ryegrass shoots.

Biochar	Plateau model	Zn---------------
SGB	Linear	$y = (0.00 \pm 9.25) + (129 \pm 9.25)x$, when $[x < 0.55 \pm 0.09]$
		$y = (71.2 \pm 1.99)$, when $[x > 0.55 \pm 0.09]$
PLB	Linear	$y = (0.00 \pm 5.91) + (135.8 \pm 16.7)x$, when $[x < 0.58 \pm 0.06]$
		$y = (79.4 \pm 5.27)$, when $[x > 0.58 \pm 0.06]$
		Pb---------------
SGB	Linear	$y = (0.00 \pm 0.47) + (194 \pm 1.09)x$, when $[x < 0.50 \pm 0.00]$
		$y = (96.6 \pm 0.08)$, when $[x > 0.50 \pm 0.00]$
PLB	Linear	$y = (0.00 \pm 0.43) + (193.6 \pm 1.23)x$, when $[x < 0.50 \pm 0.00]$
		$y = (97.5 \pm 0.33)$, when $[x > 0.50 \pm 0.00]$
		Cd---------------
SGB	Quadratic	$y = (3.23 \pm 6.57) + (79.2 \pm 19.6)x + (-24.9 \pm 11.2)x^2$, when $[x < 1.59 \pm 0.35]$
		$y = (66.1 \pm 5.46)$, when $[x > 1.59 \pm 0.35]$
PLB	Quadratic	$y = (8.04 \pm 4.52) + (32.8 \pm 6.4)x + (-3.79 \pm 1.5)x^2$, when $[x < 4.33 \pm 0.92]$
		$y = (79.1 \pm 9.48)$, when $[x > 4.33 \pm 0.92]$

Values followed by ± are the standard deviation.

TABLE 3 Equations from stepwise multiple linear regression models (SMLR) based on the lowest adjusted Akaike information criterion (*AICc*).

Biochar	Zn---------------	R^2
SGB	$(5.2 - [4.6 \times P] - [3.4 \times OM] + [408 \times TN] + [0.34 \times Mg] + [77.2 \times Cd])$	0.99
PLB	$(763 - [109 \times pH] - [0.27 \times S] - [0.06 \times Ca] + [0.47 \times Mg] - [0.77 \times Fe] + [177 \times Cd])$	0.99
	Pb---------------	
SGB	$(0.75 - [0.10 \times Zn] + [40.4 \times Cd])$	0.95
PLB	$(-40.8 + [0.01 \times P] - [0.03 \times S] + [120 \times TN] + [0.78 \times Fe] + [33.4 \times Cd])$	0.99
	Cd---------------	
SGB	$(-0.10 + [0.04 \times P] + [0.03 \times OM] - [3.74 \times TN] - [0.003 \times Mg] + [0.01 \times Zn] + [0.01 \times Pb])$	0.99
PLB	$(-6.4 + [1.02 \times pH] + [0.003 \times S] - [0.003 \times Mg] + [0.006 \times Zn]$	0.99

R^2, coefficient of determination.

The SMLR was generated using the backward method. Initially, it incorporates all variables into the model followed by the removal of the least important ones from the model according to the lowest *AICc*. The remaining variables compose the final SMLR model to predict the heavy metal availability. Results comprise the whole dataset of measurements.

between soil chemical attributes, respectively, using the CALIS procedure of SAS version 9.4.

Graphs were created in Microsoft Excel 2019, PowerPoint, and OriginPro 9.1.

2.5.7 Useful equations

1. Metal immobilization (mg/kg) = (Available soil metal content in the control − Available soil metal content in the biochar treatement rate)
2. Reduced metal uptake (%) = ([Tissue metal content in the control − Tissue metal content in the biochar treatement rate]/Tissue metal content in the control)*100
3. Simple Langmuir adsorption isotherm equation:
   $y = (a^*b^*x)/(1 + b^*x)$
4. Extended Langmuir adsorption isotherm equation:
   $y = (a^*b^*x[1 \overset{\wedge}{-} c])/(1 + bx[1 \overset{\wedge}{-} c])$

Where: a, b, and c are the coefficients of the equation.

3 Results

3.1 Soil chemical attributes and heavy metals

The data distribution for all analyzed variables shows that, regardless of the biochar applied, soil pH and soil organic matter (SOM) increased as biochar application rates increased, and so did some macronutrients such as phosphorus (P) and potassium (K)

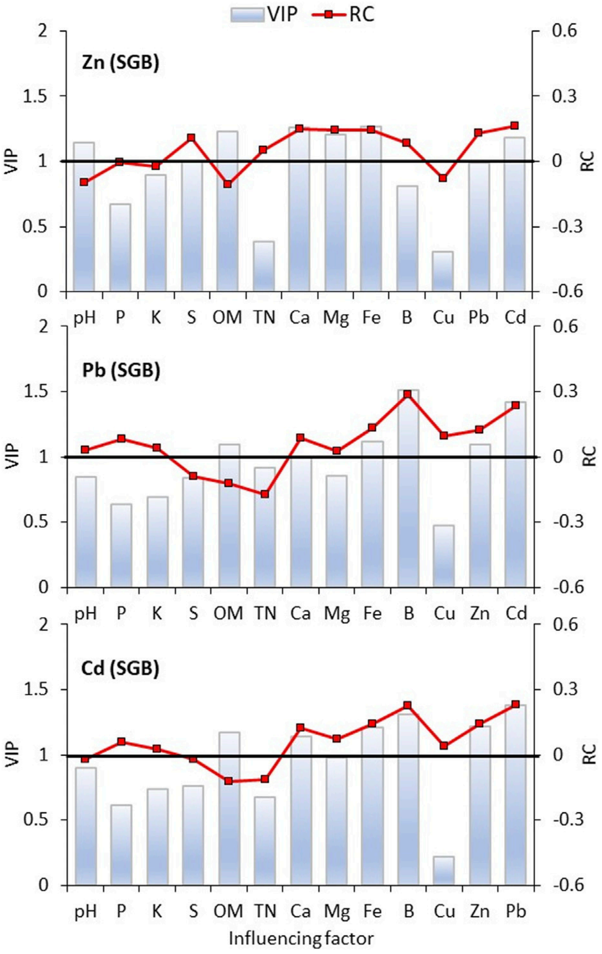

FIGURE 5
Partial Least Square Regression model (PLSR) of factors influencing the content of heavy metals in a soil amended with switchgrass-derived biochar (SGB). VIP is Variable Importance in Projection. When VIP >1, it means that the independent variable is important for predicting the dependent variable; whereas it is less important at VIP <0.5. The regression coefficients (RC) indicate the action direction of each independent variable. Results comprise the whole dataset of measurements.

(Figure 1). Meanwhile, a decrease in the availability of heavy metals (Zn, Pb, and Cd) was observed (Figure 1). As for the other soil chemical attributes the trends were non-uniform thus it was necessary to fully investigate which variables were affecting the metals' availability and how increased biochar rates are affecting metals' immobilization.

3.2 Metal immobilization

The simple Langmuir model was successfully fitted for Zn when SGB was applied and showed a maximum immobilization (I_{MAX}) of 169.2 ± 29.5 mg kg^{-1} (Figure 2). This means that 89.5% of the Zn available can be immobilized when compared to the available content in the control (189.1 ± 10.0 mg kg^{-1} at 0% SGB). Such immobilization potential is estimated to occur when SGB beyond 4% is applied since the ANOVA returned an I_{MAX} of 93.9 mg kg^{-1} for the highest rate of SGB application (4%) (Table 1), which is 49.7% immobilization in comparison to the available Zn content in the control. There was no fit when PLB was applied although an increment in the Zn immobilization is noticed (Figure 2). This is confirmed by ANOVA since the 4% PLB application rate provided the highest immobilization of 66.5 mg Zn kg^{-1}, in comparison to other application rates, which is only 35.2% immobilization as compared to the available Zn content in the control (Table 1). Moreover, from a 1%–4% rate increment, the SGB immobilizes more Zn than PLB (Table 1). This shows that SGB has a higher potential to immobilize Zn although Zn availability decreases as both SGB and PLB application rates increase.

In the case of Pb and Cd, a simple Langmuir model was fitted only with PLB application rates (Figure 2). This was the first indication that SGB has preferable adsorption/immobilization for Zn. Further, negative values of Pb and Cd immobilization at low rates of SGB application indicate that Pb and Cd are becoming more available, then immobilization takes over when increased rates of SGB are applied (Figure 2; Table 1). This reinforces the idea that depending on the feedstock used to

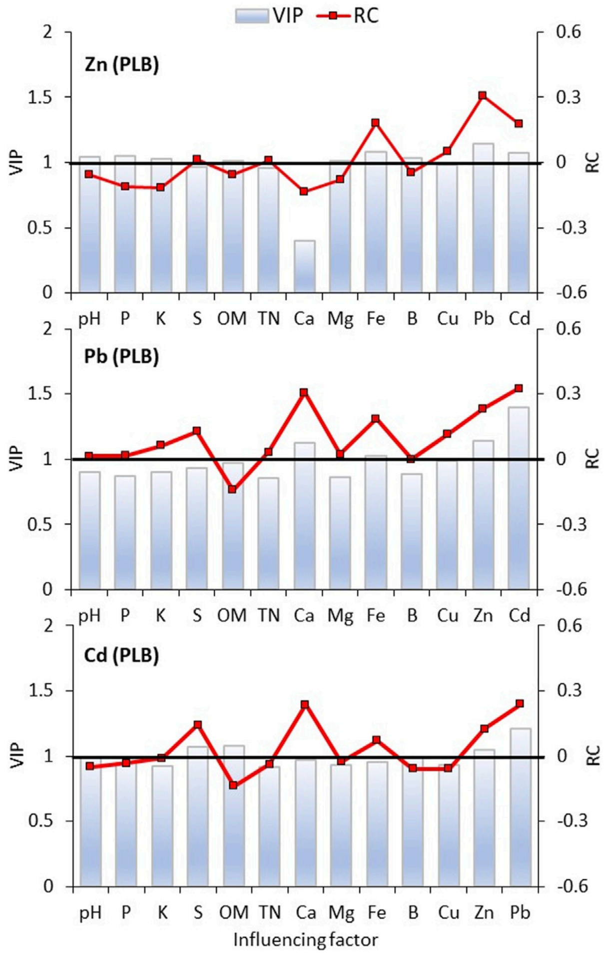

FIGURE 6
Partial Least Square Regression model (PLSR) of factors influencing the content of heavy metals in a soil amended with poultry litter-derived biochar (PLB). VIP is Variable Importance in Projection. When VIP >1, it means that the independent variable is important for predicting the dependent variable; whereas it is less important at VIP <0.5. The regression coefficients (RC) indicate the action direction of each independent variable. Results comprise the whole dataset of measurements.

produce biochar there might be a preference for some metals adsorption in comparison to others when rates of biochar application are low. Such competition is suppressed when more functional groups are available to adsorb metals at higher rates of application.

The I_{MAX} achieved for Pb with PLB application was 20 ± 7.4 mg kg^{-1} (Figure 2), which corresponds to 41.9% immobilization of the Pb available in the control. Such estimation overcome the PLB application rates used in this study since immobilized PLB ranged from 1.8 to 13.4 mg kg^{-1} (Table 1). For Cd, similar results were observed. The I_{MAX} with PLB application was 1.08 ± 0.14 mg kg^{-1} (Figure 2), which corresponds to 65.3% immobilization of the Cd available in the control. This was greater than the ANOVA results showing 0.73 mg kg^{-1} of immobilized Cd (corresponding to 44.2% immobilization) (Table 1). The relationship between observed and predicted metal concentrations from the simple Langmuir models is shown in Supplementary Figure S1.

The extended Langmuir model (EL) successfully fitted for immobilized Zn as a function of increased rates of SGB application and Cd only with PLB addition (Figure 3). The results reinforced the existing competitive immobilization between metals since there was a decrease in the I_{MAX} of Zn (~90 ± 28 mg kg^{-1} from SGB) and Cd (~0.70 ± 0.21 mg kg^{-1} from PLB). Moreover, with the EL, a fit was observed for Zn immobilization with PLB application rates as well (Figure 3). The I_{MAX} obtained was 63.9 ± 22.7 mg kg^{-1} which corresponds to 33.8% immobilization as compared to the amount available in the control. Still, there is greater efficiency of SGB when comparing the I_{MAX} of the EL for Zn immobilization, however, the PLB fit with this model demonstrates the existence of multisite adsorption for Zn since the fit was not successful with the simple Langmuir model. No further conclusion could be drawn for Pb since the EL did not converge for this metal for any of the biochars applied.

3.3 Metal uptake

The linear–with–plateau model successfully converged for Zn reduced uptake and the optimum application rates were

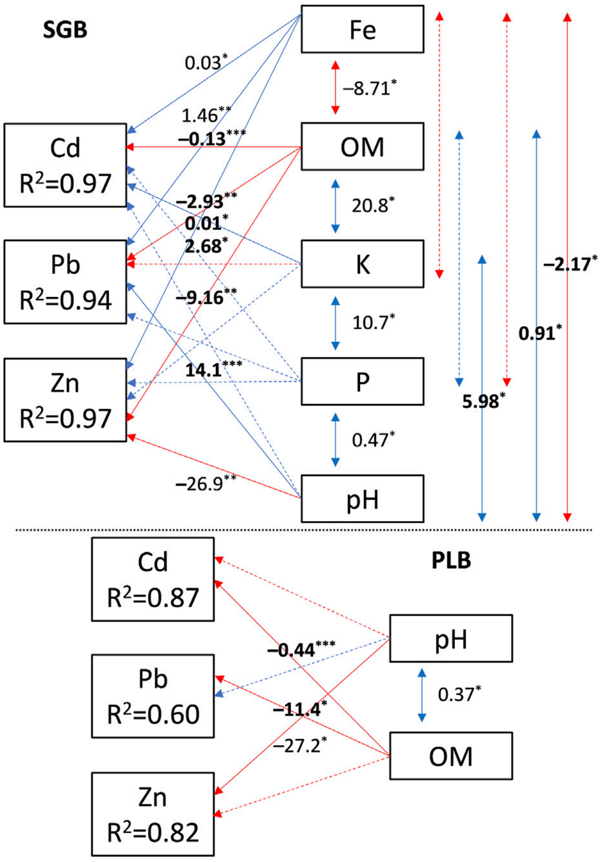

FIGURE 7
Path diagram for the relationship between soil attributes and metals availability. R^2 denotes the coefficient of determination for Squared Multiple Correlations. The direct effects of soil attributes on metals availability are represented by single-headed arrows while the indirect effects of soil attributes are shown by double-headed arrows. Numbers near the arrows are the path coefficients (unstandardized solution). The solid-line path indicates that the effect is significant, and a dashed-line path indicates that the effect has no significance. Blue and red represent positive and negative correlations, respectively. SGB and PLB are switchgrass- and poultry litter-derived biochar, respectively. *: $p < 0.05$; **: $p < 0.01$; ***: $p < 0.001$.

0.55% ± 0.09% and 0.58% ± 0.06%, respectively for SGB and PLB (Figure 4). Those rates correspond to 71.2% ± 1.99% (SGB) and 79.4% ± 5.27% (PLB) of reduced Zn uptake (Figure 4). These results were emphasized with ANOVA, where no reduced uptake increment was observed after 1% of SGB application and 0.5% of PLB application (Table 1). The PLB was better than SGB in terms of reduced uptake for each application rate (Table 1). However, low rates can reduce Zn uptake at its optimum although the metal immobilization keeps increasing as rates of biochar application increase (Table 1; Figures 2, 3). This is also true for Pb because, at 0.5% of both SGB and PLB, the reduced uptake by ryegrass shoots was 96.6% ± 0.08%–97.5% ± 0.33% even though the immobilization was only 3.8% for PLB and Pb was more available than the control for SGB at the same application rate (Table 1).

In the case of Cd, different results were observed. First, the quadratic–with–plateau model was successfully fitted instead of the linear–with–plateau one (Figure 4). Secondly, the optimum application rate for SGB was 1.59% ± 0.35% reducing Cd uptake by 66.1% ± 5.46%; and 4.33% ± 0.08% for PLB, thus overcoming the maximum application rate and reducing Cd uptake by 79.1% ± 9.48% (Figure 4). The reduced Cd uptake by 66.1% ± 5.46% with SGB application falls within the range found by Liang et al. (2022), who observed a reduced Cd concentration in brown rice by 61.2%–65.4% after the application of biochar derived from crop residues.

In both cases (SGB and PLB), the biochar application rates necessary to reduce Cd uptake at its maximum were higher than the rates necessary to reduce the Zn and Pb uptake at their maximum. This may demonstrate that ryegrass has a preferable tolerance for Cd uptake than the other two metals. This is further evidenced by Antonangelo and Zhang (2021), where the transfer of Cd from ryegrass roots to ryegrass shoots was higher than other metals, which was also proved in the work of Ji et al. (2020). All equations from the linear–and quadratic–with–upper–plateau statistical models to predict metal uptake reduction are presented in Table 2.

3.4 Soil chemical attributes affecting metals availability

3.4.1 Stepwise multiple linear regression

From the results of stepwise multiple linear regression (SMLR), it is unquestionable that the soil chemical attributes interfering with the availability of each metal are different when comparing the two biochars given their contrasting characteristics, except for Cd, which gives a positive relationship for Zn and Pb availability regardless of the biochar (Table 3). Considering that results comprise the whole dataset of measurements, which means all the increased rates of biochar application are included, it seems that any possible competition ceases when higher rates of biochar are applied. In that case, it is safe to assume that metals are simultaneously immobilized at 2%+ of SGB and PLB application rates. Besides, Cd availability is explained by a positive relationship with available Zn and Pb (SGB) and only Zn (PLB) (Table 3). The negative relationship between Pb availability and available Zn with SGB application partially explains the preferable immobilization for Zn from SGB, and the considerable negative values of Pb immobilization with low rates of SGB reinforce this assumption (Table 1). This indicates competition between those two metals for immobilization into the same adsorption sites. The relationship between observed and predicted metal concentrations from the SLMR models is shown in Supplementary Figure S2.

Surprisingly, no significant effect of soil organic matter (OM) and soil pH was observed on Pb availability with either the biochars (Table 3). On the other hand, soil OM and pH negatively impacted Zn availability, respectively for SGB and PLB, and positively for Cd (Table 3). The positive relationship of those two soil chemical attributes for Cd availability suggests that, with the preferred immobilization for Zn as a consequence of OM and pH increase, Cd becomes more available since OM and pH are acting directly in reducing Zn availability. However, knowing that OM and pH were substantially responsible for decreasing those metals' availability (Antonangelo and Zhang, 2019), further statistical analyses were performed to elucidate Zn, Cd, and Pb immobilization dynamics.

3.4.2 Partial least squares

The partial least squares (PLS) regression showed that soil OM was a major factor in the immobilization of Zn, Pb, and Cd for both biochars, which is reflected by the negative regression coefficients and the VIP >1.0 (Figures 5, 6). Soil pH did not perform as well as OM for Pb and Cd for any of the biochars application but was effective in immobilizing Zn (Figures 5, 6). In that scenario, one might assume that the preferential immobilization for Zn might rely on its higher sensitivity to the pH increase. The PLS confirmed a positive and significant relationship among the metals studied leading to the conclusion that competition stops when increased rates of biochar are applied. The same is also observed for the relationship between those metals (Zn, Pb, and Cd) and available iron (Fe)—although Fe is not a contaminant in the studied soil (Figures 5, 6).

Even though P and K considerably increased as both SGB and PLB application rates increased (Figure 1), non-effect was observed for those macronutrients over the metals' availability, except for the punctual finding of available Zn with PLB application (Figure 6). This can be partially explained by the substantially greater amount of P and K in the PLB composition in comparison to SGB (Antonangelo et al., 2019), which might negatively affect the Zn levels in the soil to a higher extent than it affects Pb and Cd.

The relationship between observed and predicted metal concentrations from the PLS models is shown in Supplementary Figure S3.

3.4.3 Path analysis

The path analysis (PA) was conducted to verify which soil chemical attributes are interfering simultaneously with the availability of Zn, Pb, and Cd in the contaminated soil. Soil pH and OM are universally impacting the immobilization of those metals disregarding the biochar type (Figure 7). Only those two variables (Soil pH and OM) are affecting the combined contents of Zn, Cd, and Pb when PLB is applied. The significant and negative path coefficient for soil pH and Zn with both SGB and PLB shows a higher sensitivity of Zn to soil pH. This is further illustrated by the non-relationship of soil pH and Cd for any of the biochars and the absent relationship of OM and Zn with the application of PLB (Figure 7). Finally, soil pH did not show any relationship with Pb after PLB application and was positively related to the same metal when SGB was applied (Figure 7).

4 Discussion

4.1 Metals immobilization

The I_{MAX} was possible to determine only for Zn when SGB was applied (Figure 1). A maximum immobilization of 89.5% at a higher rate than the upper end in the range of applied rates (0.5%–4%) shows that SGB has a preference to immobilize Zn. This preferred immobilization for Zn is also reinforced when observing the 0 and 0.5% rates of SGB application because, at such low rates, Pb and Cd have their availability increased given the negative immobilization values (Figure 2; Table 1). In that scenario, Zn is more immobilized, consequently, Pb and Cd become more available. Since the levels of DPTA-extractable Zn were showing a drastic higher content in comparison to normal values found in Oklahoma soils, about twelvefold in contrast to tenfold and sevenfold for Cd and Pb respectively (Richards et al., 2012), it is expected that Zn–OM complexes are formed to a greater extent than Pb/Cd–OM complexes. This preferentially immobilizes Zn when low rates of SGB are applied. It was also observed by Geleto et al. (2022) that the competition among toxic heavy metals for adsorption sites was more intense at higher concentrations of Zn when contrasting biochars were applied. At higher rates of biochar application, the amounts of immobilization are not limited and Cd and Pb availability are reduced when 2%–4% of SGB is applied (Figure 2; Table 1). Indeed, there is competition among Zn, Pb, and Cd when biochar is applied, which is attributed to differences in feedstock properties, nutrient concentration, active functional groups, and pH (Wu et al., 2020).

Zinc is more sensitive to being immobilized by SGB, evidenced by the fact that SGB promoted Zn immobilization to a greater extent than PLB (Figures 2, 3; Table 1). On the other hand, PLB showed a preference for Cd and Pb immobilization although it did not increase Zn availability at low rates of application since no negative values were observed. In that case, we suggest that the mechanisms that PLB offer to immobilize metals go beyond the affinity to adsorption sites.

The extended Langmuir models (EL) also showed that Zn immobilization is more favored with SGB than PLB since the I_{MAX} achieved was ~90 ± 28 mg kg^{-1} for the former and 63.9 ± 28 mg kg^{-1} for the latter (Figure 3). The reason that the EL fitted for Zn as a function of PLB application but the simple Langmuir model did not, rely on the fact that a multi-component adsorption behavior is present in PLB or, in the case of our study, multiple mechanisms for Zn immobilization. In another study, the lower Zn availability was significantly affected by soil pH, EC, P, K, and Mg when PLB was applied, indicating significant adsorption by electrostatic interaction and ion exchange with the biochar surface and/or soil surface exchange sites (Tsai and Chang, 2022).

Considering that the I_{MAX} of Cd after PLB application was lower with the EL (0.70 ± 0.20 mg kg^{-1}) in comparison to the simple Langmuir model (1.08 ± 0.14 mg kg^{-1}) it can be assured that competition between Zn and Cd takes place when the animal manure-derived biochar is applied (Figures 2, 3), mainly because Zn has shown an I_{MAX} of 63.9 ± 28 mg kg^{-1} with PLB application and Pb did not present any relationship with the EL (Figure 3). One reason behind the competition among these metals might be the existence of multi-mechanisms to immobilize Zn and Cd and not Pb when PLB is applied. In that sense, when looking at the simple Langmuir model fitted with PLB, the reduced availability of Cd in comparison to the control was higher (65.3%) while with Pb it was lower (41.9%). The work of Wei et al. (2022) also showed that levels of available DTPA-extractable Cd decreased to a higher extent than DTPA-extractable Pb when biochar was applied. For *Zn×Pb*, the maximum adsorption capacity and strength of adsorption of Pb decreased in the presence of Zn when testing the aging effect of several biochar applications in a sandy calcareous soil (Raeisi et al., 2020).

4.2 Metals uptake

The reduced Zn and Pb uptake in ryegrass shoots ranged from ~70%–98% and were optimum at rates of 0.50% ± 0.00%–0.60% ± 0.06% for both biochars, and 1.6% ± 0.4% of SGB for Cd (Figure 4). Interestingly, from previous results, the HM immobilization achieves the I_{MAX} when higher rates were applied. It means that, even though the HM immobilization increases as rates of biochar increase up to 4%+, the ryegrass uptake ceases at 0.5%–1.5% rates, except for Cd when PLB is applied (Figure 4). Such behavior might be explained by the rhizosphere effect. According to Wang et al. (2022), the rhizosphere effect of wheat accelerated the aging process of biochar, even in the short term, and increased the number of surface functional groups (C=O and O=C–OH) on the aged biochar, in turn, promoting the adsorption capacity of rice husk- and sludge-derived biochar for Cd and Pb. In our study, though, the reduced uptake of Pb was greater than Cd regardless of the biochar (Figure 4). This may be related to a more pronounced rhizosphere effect over Pb in comparison to Cd. Zhu et al. (2022) showed higher microbial Pb fixation and Pb immobilization when a bio-composite produced from wheat straw biochar (pyrolyzed at 700°C) was applied, which sequentially transformed labile Pb into a more stable fraction.

In another study, the 3% application rate of green waste-derived biochars can effectively reduce the uptake of Cd and Pb by *Brassica chinensis* (Houssou et al., 2022). This is within the range found in our study since the reduced uptake by ryegrass reached the plateau when SGB, a green waste-derived biochar, was applied at 0.50 ± 0.00 (Pb) and 1.59 ± 0.35 (Cd) (Figure 4). This higher rate of SGB needed for optimum reduced Cd uptake was the first evidence that ryegrass has more tolerance for Cd absorption than Pb and Zn. Later, with the application of animal manure-derived biochar (PLB), the plateau is reached only at 4.33% ± 0.92% of PLB application, while it was 0.58 ± 0.06 for Zn and 0.50 ± 0.00 for Pb with the same amendment (Figure 4). Thus, ryegrass demonstrates a preferable tolerance for Cd uptake than Zn and Pb.

It is worth to note that nitrogen (N) has a direct relationship with Cd accumulation in ryegrass shoots. First, the higher affinity to Cd^{2+} by the membrane transporter of Italian ryegrass was observed after urea application (increased the Cd uptake) which contributed to the effective Cd accumulation in plant shoots (Ji et al., 2020). Second, ryegrass N and Cd concentrations were strongly related after PLB application at rates of 0.5% and 1%, and the lowest levels of Cd accumulation were observed only at 4% PLB (Antonangelo and Zhang, 2021). It is also noticeable that the total nitrogen (TN) content from PLB is greater than SGB (Antonangelo et al., 2019). Therefore, it is not surprising that the reduced Cd uptake by ryegrass terminates only at the rate of 4.33% ± 0.92% with PLB application (Figure 4).

4.3 Metals availability affected by soil chemical attributes

4.3.1 PLS and SMLR

From the PLS regression, the soil OM was inherently the most important soil attribute that negatively affected the soil HM availability, which was true for both biochars used in this study (Figures 5, 6). The soil OM increased with biochar application rates (Figure 1) partially explains this behavior. There are several direct and indirect effects of soil OM on the bioavailability of metals. To highlight some, dissolved OM is directly involved in the complexation of HM and their removal from the bioavailable fraction. In addition, soil biodiversity and/or microbial communities are increased following soil OM enhancement—thus the effects of microbes on the availability of HMs and their immobilization (Bravin et al., 2012; Seshadri et al., 2015; Sun et al., 2019). In this study, although we were not able to test the microbial community and activity the soil OM increment from the control to the highest rates of SGB and PLB application, strongly suggests that soil biota benefited from biochar application.

Soil pH increment has contributed to decreasing Zn levels no matter which biochar was applied, to reduce available Cd only with PLB application, and had no effect on Pb (Figures 5, 6). This is not in agreement with the previous work of Antonangelo and Zhang (2019), where soil pH increment was one of the most important factors affecting the availability of all those metals, including Pb, regardless of the biochar applied. One reason behind this is the fact that no other soil chemical attributes were considered in the model of Antonangelo and Zhang (2021). Therefore, other variables must be responsible for affecting the dynamics of HM in contaminated soils.

For Zn, the soil pH increase affecting its availability after the application of any biochar shows a higher sensitivity of this metal for soil pH in comparison to other metals. Although both biochars presented a considerable soil pH increment as a function of increased application rates, the buffering capacity of SGB is much lower than PLB (Antonangelo et al., 2019), still it can immobilize Zn. It somehow explains why Zn is more susceptible to soil pH and thus is immobilized by SGB (Figures 2, 3). In the case of Cd, the soil pH effect is only pronounced with PLB application, even considering that pH is the major factor influencing Cd bioavailability (Liang et al., 2022). However, the influence of the increased soil pH by biochar on the immobilization of Cd is dependent on the physicochemical properties of biochar (Wei et al., 2023). In our study, the negative relationship between pH and Cd for PLB is then explained by the greater buffering capacity offered by this biochar in comparison to SGB.

Another trend that was similar for all HM was the positive relationship among them, and between them and available Fe (Figures 5, 6). Since PLS regression comprises the whole dataset of measurements, and thus the increased rates of each biochar application, then it is confirmed that any competition among metals, when immobilization resources are limited (low rates of soil amendment application), is disappeared at high application rates because there will be many immobilization mechanisms to reduce the bioavailability of HM. Positive relationships among DTPA-extractable metals in the soil, after biochar application, were also found elsewhere in the literature (da Silva et al., 2022; Wei et al., 2022; Liu et al., 2022c). Finally, such trends were similarly observed with the SLMR in our study as well (Table 3). Other soil chemical attributes did not exhibit a general trend to explain better the HM availability, so it was necessary to perform path analysis (PA) using the combined availability of all three HMs to determine the overall chemical attributes impacting the simultaneous availability of Zn, Pb, and Cd.

4.3.2 Path analysis

It was confirmed that soil OM is universally impacting the immobilization of those metals disregarding the biochar type (Figure 7). Additionally, when using the combined response variables (Zn + Pb + Cd), soil pH was also impacting metals' availability although trends were different depending on the metals and were not always negative as it was with OM (Figure 7).

The significant inverse path coefficient (–) for soil pH and Zn with both SGB and PLB suggests a higher sensitivity of Zn to soil pH in comparison to other metals, also there is no relationship between soil pH and Cd for any of the biochars and no relationship between soil pH and Pb with PLB application (Figure 7). This means that the pH path moves negatively toward Zn, affecting preferentially its availability. Moreover, the non-relationship of OM and Zn with the application of PLB means higher Zn sensitivity for pH than for OM (Figure 7). Finally, soil pH was positively related to Pb when SGB was applied (Figure 7). This can be justified by the fact that pH increment is immobilizing Zn more than other metals thus Pb is becoming more available, until SOM dictates the Pb immobilization.

It is understandable that OM mainly contributes to the immobilization of all metals when SGB is applied (Figure 7) given its greater total carbon (TC) and lower ash content in comparison to PLB (Antonangelo et al., 2019). Further, the omnipresent positive relationship between Fe and Zn, Pb, and Cd (Figure 7) makes it safe to assume that, since the contents of those heavy metals fall into the toxic levels, OM acts in their complexation rather than non-toxic metals such as Fe, presenting a lower degree of availability. Indeed, in the path OM→Fe→HM, there is a negative relationship ($p < 0.05$) between OM and Fe and a positive relationship between Fe and HM ($0.05 > p < 0.01$) (Figure 7).

Surprisingly, no soil chemical attributes other than pH and OM affected the availability of HM simultaneously with PLB application (Figure 7). This was expected since PLB presented a higher ash content and drastic increase of soil available nutrients, mainly P and K, in comparison to SGB (Figure 7). We assume that lower levels of those nutrients in the soil are enough to cause some threat to HM availability and their slight increment will impact a single metal instead of all of them concomitantly. Both reasons are presented in this study. First, negative effects of P and K were observed only on Zn availability with PLB application when using PLS regression; and non-consistent effects of P, S, and Mg over Zn, Pb, and Cd, depending on the biochar, were shown when performing SLMR. Also, the lower available soil P and K with SGB in comparison to PLB demonstrated a significant effect on the immobilization of all metals when conducting PA (Figure 7). Further research is required to determine key variables in the soil affecting multi-metal immobilization on a global scale after soil organic amendments are applied.

5 Conclusion

In this study, we evaluated the application of biochar from switchgrass and poultry litter in the soil and their effectiveness on metal immobilization and HM concentrations in the plant (ryegrass) shoots. The competitive immobilization of Zn, Pb, and Cd from the Tar Creek superfund site was verified using several multivariate techniques. The simple Langmuir models showed that the maximum HM immobilization (I_{MAX}) was 169.2 ± 29.5 mg kg^{-1} for Zn with SGB application, and 20 ± 7.4 and 1.08 mg kg^{-1} for Pb and Cd, respectively, with PLB application. On the other hand, the extended Langmuir model (EL) showed competitive immobilization between metals since there was a decrease in the I_{MAX} of Zn, from 169.2 ± 29.5 to 90 ± 28 mg kg^{-1} with SGB application, and Cd from 1.08 to 0.70 ± 0.21 mg kg^{-1} with PLB application. The potential of applying low rates such as 0.5%–1% w/w of two contrasting feedstock-derived biochars to remediate the contaminants and safely grow perennial ryegrass was elucidated since Zn, Pb, and Cd uptakes are respectively reduced by ~71.2–79.4%, ~96.6 to 97.5, and ~37.5–50% with that range of both biochars application (Figure 4). Although it is incontestable that OM and soil pH play a significant role in the combined HM immobilization, their direct/indirect mechanisms to do so remain unclear because many other soil chemical attributes may also affect HM dynamics. This study may encourage and serve as a basis for future research performing the similar techniques in more representative soil samples, containing contrasting textures and using both soils naturally contaminated due to anthropogenic activities and soils spiked with known concentrations of several HM. Also, the combined application of HM to soil samples could be compared to those samples receiving only a single metal. In such cases, more accurate results can be achieved when evaluating the many soil chemical attributes affecting HM availability.

Data availability statement

The raw data supporting the conclusion of this article will be made available by the authors, without undue reservation.

Author contributions

JA and HZ contributed to the conception and design of the study. JA organized the database. JA performed the statistical analysis. JA, HZ, and IS wrote the first draft of the manuscript. JA and IS wrote sections of the manuscript. JA contributed to the methodology. JA contributed to visualization. JA contributed to the data validation and data curation. HZ contributed to the resources. JA, HZ, and IS contributed to writing the first draft, reviewing, and editing. HZ contributed to supervision, project administration, and funding acquisition. All authors contributed to the manuscript revision, and read, and approved the submitted version.

Funding

This work was supported by the Oklahoma Agricultural Experiment Station.

Conflict of interest

The authors declare that the research was conducted in the absence of any commercial or financial relationships that could be construed as a potential conflict of interest.

Publisher's note

Supplementary material

The Supplementary Material for this article can be found online at: https://www.frontiersin.org/articles/10.3389/fenvs.2023.1170427/full#supplementary-material

References

Abbas, T., Rizwan, M., Ali, S., Zia-ur-Rehman, M., Farooq Qayyum, M., Abbas, F., et al. (2017). Effect of biochar on cadmium bioavailability and uptake in wheat (triticum aestivum L.) grown in a soil with aged contamination. *Ecotoxicol. Environ. Saf.* 140, 37–47. doi:10.1016/j.ecoenv.2017.02.028

Ahmad, M., Rajapaksha, A. U., Lim, J. E., Zhang, M., Bolan, N., Mohan, D., et al. (2014). Biochar as a sorbent for contaminant management in soil and water: A review. *Chemosphere* 99, 19–33. doi:10.1016/j.chemosphere.2013.10.071

Ahmad, M., Soo Lee, S., Yang, J. E., Ro, H.-M., Han Lee, Y., and Sik Ok, Y. (2012). Effects of soil dilution and amendments (Mussel Shell, Cow Bone, and biochar) on PB availability and phytotoxicity in military shooting range soil. *Ecotoxicol. Environ. Saf.* 79, 225–231. doi:10.1016/j.ecoenv.2012.01.003

Ali, H., Khan, E., and Sajad, M. A. (2013). Phytoremediation of heavy metals—Concepts and applications. *Chemosphere* 91 (7), 869–881. doi:10.1016/j.chemosphere.2013.01.075

Antonangelo, J. A., Souza, J. L., Whitaker, A., Arnall, B., and Zhang, H. (2022). Evaluation of mehlich-3 as a multi-element extractant of micronutrients and sulfur in a soil–ryegrass system amended with varying biochar rates from two feedstocks. *Land* 11, 1979. doi:10.3390/land11111979

Antonangelo, J. A., and Zhang, H. (2019). Heavy Metal phytoavailability in a contaminated soil of northeastern Oklahoma as affected by Biochar Amendment. *Environ. Sci. Pollut. Res.* 26, 33582–33593. doi:10.1007/s11356-019-06497-w

Antonangelo, J. A., Zhang, H., Sun, X., and Kumar, A. (2019). Physicochemical properties and morphology of biochars as affected by feedstock sources and pyrolysis temperatures. *Biochar* 1, 325–336. doi:10.1007/s42773-019-00028-z

Antonangelo, J., and Zhang, H. (2021). Influence of biochar derived nitrogen on cadmium removal by ryegrass in a contaminated soil. *Environments* 8, 11. doi:10.3390/environments8020011

Bradl, H. B. (2004). Adsorption of heavy metal ions on soils and soils constituents. *J. Colloid Interface Sci.* 277, 1–18. doi:10.1016/j.jcis.2004.04.005

Bravin, M. N., Garnier, C., Lenoble, V., Gérard, F., Dudal, Y., and Hinsinger, P. (2012). Root-induced changes in ph and dissolved organic matter binding capacity affect copper dynamic speciation in the rhizosphere. *Geochimica Cosmochimica Acta* 84, 256–268. doi:10.1016/j.gca.2012.01.031

Church, C., Spargo, J., and Fishel, S. (2017). Strong acid extraction methods for "total phosphorus" in soils: EPA method 3050B and EPA method 3051. *Agric. Environ. Lett.* 2, 160037. doi:10.2134/ael2016.09.0037

da Silva, A. P., Silva, A. O., Lima, F. R., Benedet, L., Franco, A., Souza, J. K., et al. (2022). Potentially toxic elements in iron mine tailings: Effects of reducing soil ph on available concentrations of toxic elements. *Environ. Res.* 215, 114321. doi:10.1016/j.envres.2022.114321

Fan, Q., Sun, J., Chu, L., Cui, L., Quan, G., Yan, J., et al. (2018). Effects of chemical oxidation on surface oxygen-containing functional groups and adsorption behavior of biochar. *Chemosphere* 207, 33–40. doi:10.1016/j.chemosphere.2018.05.044

Fang, N., Shi, Z., Chen, F., and Wang, Y. (2015). Partial least squares regression for determining the control factors for runoff and suspended sediment yield during rainfall events. *Water* 7, 3925–3942. doi:10.3390/w7073925

Fashola, M. O., Ngole-Jeme, V. M., and Babalola, O. O. (2020). Physicochemical properties, heavy metals, and metal-tolerant bacteria profiles of abandoned gold mine tailings in Krugersdorp, South Africa. *Can. J. Soil Sci.* 100 (3), 217–233. doi:10.1139/cjss-2018-0161

Geleto, M. A., Forján, R., Arco-Lázaro, E., Covelo, E. F., Marcet, P., and Cerqueira, B. (2022). Influence of pyrolysis temperature and feedstock biomass on cu2+, PB2+, and zn2+ sorption capacity of biochar. *Int. J. Environ. Sci. Technol.* 19, 11857–11866. doi:10.1007/s13762-022-03989-0

He, L., Zhong, H., Liu, G., Dai, Z., Brookes, P. C., and Xu, J. (2019). Remediation of heavy metal contaminated soils by biochar: Mechanisms, potential risks and applications in China. *Environ. Pollut.* 252, 846–855. doi:10.1016/j.envpol.2019.05.151

Houssou, A. A., Jeyakumar, P., Niazi, N. K., Van Zwieten, L., Li, X., Huang, L., et al. (2022). Biochar and soil properties limit the phytoavailability of lead and cadmium by brassica chinensis l. in contaminated soils. *Biochar* 4, 5. doi:10.1007/s42773-021-00126-x

Inyang, M. I., Gao, B., Yao, Y., Xue, Y., Zimmerman, A., Mosa, A., et al. (2015). A review of biochar as a low-cost adsorbent for aqueous heavy metal removal. *Crit. Rev. Environ. Sci. Technol.* 46, 406–433. doi:10.1080/10643389.2015.1096880

Järup, L. (2003). Hazards of heavy metal contamination. *Br. Med. Bull.* 68, 167–182. doi:10.1093/bmb/ldg032

Ji, S., Gao, L., Chen, W., Su, J., and Shen, Y. (2020). Urea application enhances cadmium uptake and accumulation in Italian ryegrass. *Environ. Sci. Pollut. Res.* 27, 34421–34433. doi:10.1007/s11356-020-09691-3

Jones, J. B., and Case, V. W. (1990). Sampling, handling, and analyzing plant tissue samples. *SSSA Book Ser.* 3, 389–427. doi:10.2136/sssabookser3.3ed.c15

Kapoor, V., Li, X., Elk, M., Chandran, K., Impellitteri, C. A., and Santo Domingo, J. W. (2015). Impact of heavy metals on transcriptional and physiological activity of nitrifying bacteria. *Environ. Sci. Technol.* 49 (22), 13454–13462. doi:10.1021/acs.est.5b02748

Liang, T., Zhou, G., Chang, D., Wang, Y., Gao, S., Nie, J., et al. (2022). Co-incorporation of Chinese milk vetch (astragalus sinicus L.), rice straw, and biochar strengthens the mitigation of CD uptake by rice (Oryza sativa L.) *Sci. Total Environ.* 850, 158060. doi:10.1016/j.scitotenv.2022.158060

Liu, L., Li, X., Wang, X., Wang, Y., Shao, Z., Liu, X., et al. (2022a). Metolachlor adsorption using walnut shell biochar modified by soil minerals. *Environ. Pollut.* 308, 119610. doi:10.1016/j.envpol.2022.119610

Liu, L., Wang, X., Fang, W., Li, X., Shan, D., and Dai, Y. (2022b). Adsorption of metolachlor by a novel magnetic illite–biochar and recovery from soil. *Environ. Res.* 204, 111919. doi:10.1016/j.envres.2021.111919

Liu, Q., Huang, L., Chen, Z., Wen, Z., Ma, L., Xu, S., et al. (2022c). Biochar and its combination with inorganic or Organic Amendment on growth, uptake and accumulation of cadmium on lettuce. *J. Clean. Prod.* 370, 133610. doi:10.1016/j.jclepro.2022.133610

Liu, X., Shao, Z., Wang, Y., Liu, Y., Wang, S., Gao, F., et al. (2023). New use for lentinus edodes bran biochar for tetracycline removal. *Environ. Res.* 216, 114651. doi:10.1016/j.envres.2022.114651

Meng, J., Tao, M., Wang, L., Liu, X., and Xu, J. (2018). Changes in heavy metal bioavailability and speciation from a pb-zn mining soil amended with biochars from co-pyrolysis of rice straw and swine manure. *Sci. Total Environ.* 633, 300–307. doi:10.1016/j.scitotenv.2018.03.199

Onderka, M., Wrede, S., Rodný, M., Pfister, L., Hoffmann, L., and Krein, A. (2012). Hydrogeologic and landscape controls of dissolved inorganic nitrogen (DIN) and dissolved silica (DSI) fluxes in heterogeneous catchments. *J. Hydrology* 450-451, 36–47. doi:10.1016/j.jhydrol.2012.05.035

Park, J. H., Choppala, G. K., Bolan, N. S., Chung, J. W., and Chuasavathi, T. (2011). Biochar reduces the bioavailability and phytotoxicity of heavy metals. *Plant Soil* 348, 439–451. doi:10.1007/s11104-011-0948-y

Pelegrino, M. H., Silva, S. H., de Faria, Á. J., Mancini, M., Teixeira, A. F., Chakraborty, S., et al. (2021). Prediction of soil nutrient content via pXRF spectrometry and its spatial variation in a highly variable tropical area. *Precis. Agric.* 23, 18–34. doi:10.1007/s11119-021-09825-8

Qiao, Y., Wu, J., Xu, Y., Fang, Z., Zheng, L., Cheng, W., et al. (2017). Remediation of cadmium in soil by biochar-supported iron phosphate nanoparticles. *Ecol. Eng.* 106, 515–522. doi:10.1016/j.ecoleng.2017.06.023

Raeisi, S., Motaghian, H., and Hosseinpur, A. R. (2020). Effect of the soil biochar aging on the sorption and desorption of pb2+ under competition of zn2+ in a sandy calcareous soil. *Environ. Earth Sci.* 79, 148. doi:10.1007/s12665-020-8891-y

Rengel, Z. (2015). Availability of Mn, Zn and Fe in the rhizosphere. *J. soil Sci. plant Nutr.* 15 (2), 0–409. doi:10.4067/s0718-95162015005000036

Richards, J. R., Schroder, J. L., Zhang, H., Basta, N. T., Wang, Y., and Payton, M. E. (2012). Trace elements in benchmark soils of Oklahoma. *Soil Sci. Soc. Am. J.* 76, 2031–2040. doi:10.2136/sssaj2012.0100

Seshadri, B., Bolan, N. S., and Naidu, R. (2015). Rhizosphere-induced heavy metal(loid) transformation in relation to bioavailability and remediation. *J. soil Sci. plant Nutr.* 15, 0. doi:10.4067/s0718-95162015005000043

Shaheen, S. M., Niazi, N. K., Hassan, N. E. E., Bibi, I., Wang, H., Tsang, D. C. W., et al. (2019). Wood-based biochar for the removal of potentially toxic elements in water and wastewater: A critical review. *Int. Mater. Rev.* 64, 216–247. doi:10.1080/09506608.2018.1473096

Shi, Z. H., Ai, L., Li, X., Huang, X. D., Wu, G. L., and Liao, W. (2013). Partial least-squares regression for linking land-cover patterns to soil erosion and sediment yield in watersheds. *J. Hydrology* 498, 165–176. doi:10.1016/j.jhydrol.2013.06.031

Shi, Z. H., Huang, X. D., Ai, L., Fang, N. F., and Wu, G. L. (2014). Quantitative analysis of factors controlling sediment yield in mountainous watersheds. *Geomorphology* 226, 193–201. doi:10.1016/j.geomorph.2014.08.012

Su, C. (2014). A review on heavy metal contamination in the soil worldwide: Situation, impact and remediation techniques. *Environ. Skeptics Critics* 3 (2), 24. Available at: https://scholar.google.com/scholar_lookup?title=A%20review%20on%20heavy%20metal%20contamination%20in%20the%20soil%20worldwide%3A%20Situation%2C%20impact%20and%20remediation%20techniquesandjournal=Environ%20Skept%20Critandvolume=3andpages=24-38andpublication_year=2014andauthor=Su%2CCandauthor=Jiang%2CLQandauthor=Zhang%2CWJ

Sun, J., Fan, Q., Ma, J., Cui, L., Quan, G., Yan, J., et al. (2020). Effects of biochar on cadmium (CD) uptake in vegetables and its natural downward movement in saline-alkali soil. *Environ. Pollut. Bioavailab.* 32, 36–46. doi:10.1080/26395940.2020.1714487

Sun, X., Li, Z., Wu, L., Christie, P., Luo, Y., and Fornara, D. A. (2019). Root-induced soil acidification and cadmium mobilization in the rhizosphere of Sedum plumbizincicola: Evidence from a high-resolution imaging study. *Plant Soil* 436, 267–282. doi:10.1007/s11104-018-03930-w

Tong, L. S., Fang, N. F., Xiao, H. B., and Shi, Z. H. (2020). Sediment deposition changes the relationship between soil organic and inorganic carbon: Evidence from the Chinese loess plateau. *Agric. Ecosyst. Environ.* 302, 107076. doi:10.1016/j.agee.2020.107076

Tsai, C.-C., and Chang, Y.-F. (2022). Poultry Litter Biochar as a gentle soil amendment in multi-contaminated soil: Quality evaluation on nutrient preservation and contaminant immobilization. *Agronomy* 12, 405. doi:10.3390/agronomy12020405

Wang, B., Gao, B., and Fang, J. (2017). Recent advances in engineered biochar productions and applications. *Crit. Rev. Environ. Sci. Technol.* 47, 2158–2207. doi:10.1080/10643389.2017.1418580

Wang, J., Liu, J., Zhou, J., Chang, L., Shen, Z., Shi, L., et al. (2022). Rhizosphere effect on physicochemical properties and immobilization performance of biochar. *Water, Air, and Soil Pollut.* 233, 438. doi:10.1007/s11270-022-05902-4

Wei, B., Peng, Y., Jeyakumar, P., Lin, L., Zhang, D., Yang, M., et al. (2023). Soil ph restricts the ability of biochar to passivate cadmium: A meta-analysis. *Environ. Res.* 219, 115110. doi:10.1016/j.envres.2022.115110

Wei, T., Li, X., Li, H., Gao, H., Guo, J., Li, Y., et al. (2022). The potential effectiveness of mixed bacteria-loaded biochar/activated carbon to remediate CD, PB co-contaminated soil and improve the performance of Pakchoi Plants. *J. Hazard. Mater.* 435, 129006. doi:10.1016/j.jhazmat.2022.129006

Weng, Z., Van Zwieten, L., Singh, B. P., Tavakkoli, E., Joseph, S., Macdonald, L. M., et al. (2017). Biochar built soil carbon over a decade by stabilizing rhizodeposits. *Nat. Clim. Change* 7 (5), 371–376. doi:10.1038/nclimate3276

Wold, S., Sjöström, M., and Eriksson, L. (2001). PLS-regression: A basic tool of chemometrics. *Chemom. Intelligent Laboratory Syst.* 58, 109–130. doi:10.1016/s0169-7439(01)00155-1

Wu, J., Song, Q., Zhou, J., Wu, Y., Liu, X., Liu, J., et al. (2021). Cadmium threshold for acidic and multi-metal contaminated soil according to Oryza sativa L. cadmium accumulation: Influential factors and prediction model. *Ecotoxicol. Environ. Saf.* 208, 111420. doi:10.1016/j.ecoenv.2020.111420

Wu, P., Wang, Z., Wang, H., Bolan, N. S., Wang, Y., and Chen, W. (2020). Visualizing the emerging trends of biochar research and applications in 2019: A scientometric analysis and review. *Biochar* 2, 135–150. doi:10.1007/s42773-020-00055-1

Xie, T., Reddy, K. R., Wang, C., Yargicoglu, E., and Spokas, K. (2015). Characteristics and applications of biochar for environmental remediation: A review. *Crit. Rev. Environ. Sci. Technol.* 45, 939–969. doi:10.1080/10643389.2014.924180

Yang, P., Hu, Z., and Shu, Q. (2021). Factors affecting soil organic carbon content between natural and reclaimed sites in Rudong Coast, Jiangsu Province, China. *J. Mar. Sci. Eng.* 9, 1453. doi:10.3390/jmse9121453

Zeng, G., Wu, H., Liang, J., Guo, S., Huang, L., Xu, P., et al. (2015). Efficiency of biochar and compost (or composting) combined amendments for reducing CD, Cu, Zn and PB bioavailability, mobility and ecological risk in wetland soil. *RSC Adv.* 5, 34541–34548. doi:10.1039/c5ra04834f

Zhang, R.-H., Li, Z.-G., Liu, X.-D., Wang, B., Zhou, G.-L., Huang, X.-X., et al. (2017). Immobilization and bioavailability of heavy metals in greenhouse soils amended with rice straw-derived biochar. *Ecol. Eng.* 98, 183–188. doi:10.1016/j.ecoleng.2016.10.057

Zhu, X., Li, X., Shen, B., Zhang, Z., Wang, J., and Shang, X. (2022). Bioremediation of lead-contaminated soil by inorganic phosphate-solubilizing bacteria immobilized on biochar. *Ecotoxicol. Environ. Saf.* 237, 113524. doi:10.1016/j.ecoenv.2022.113524

frontiers | Frontiers in Environmental Science

TYPE Original Research
PUBLISHED 15 May 2023
DOI 10.3389/fenvs.2023.1170734

OPEN ACCESS

EDITED BY
Xiaokai Zhang,
Jiangnan University, China

REVIEWED BY
Evrim Elcin,
Adnan Menderes University, Türkiye
Tong Pang,
Chinese Academy of Sciences (CAS),
China
Conghui Liu,
Chinese Academy of Agricultural
Sciences, China

*CORRESPONDENCE
Wei Liu,
✉ liuweics@qlu.edu.cn

RECEIVED 21 February 2023
ACCEPTED 04 May 2023
PUBLISHED 15 May 2023

CITATION
Duan H, Liu W, Zhou L, Han B, Huo S, El-Sheekh M, Dong H, Li X, Xu T and Elshobary M (2023), Improving saline-alkali soil and promoting wheat growth by co-applying potassium-solubilizing bacteria and cyanobacteria produced from brewery wastewater.
Front. Environ. Sci. 11:1170734.
doi: 10.3389/fenvs.2023.1170734

Improving saline-alkali soil and promoting wheat growth by co-applying potassium-solubilizing bacteria and cyanobacteria produced from brewery wastewater

Huijie Duan[1,2], Wei Liu[1,2]*, Lixiu Zhou[1,2], Bing Han[3], Shuhao Huo[4], Mostafa El-Sheekh[5], Haiwen Dong[1,2], Xiaomeng Li[1,2], Tongtong Xu[1,2] and Mostafa Elshobary[5]

[1]Qilu University of Technology (Shandong Academy of Sciences), Shandong Analysis and Test Center, Jinan, Shandong, China, [2]Faculty of Environmental Science and Engineering, Qilu University of Technology (Shandong Academy of Sciences), Jinan, Shandong, China, [3]Liaocheng People's Hospital, Liaocheng, Shandong, China, [4]School of Food and Biological Engineering, Jiangsu University, Zhenjiang, China, [5]Botany and Microbiology Department, Faculty of Science, Tanta University, Tanta, Egypt

Soil salinization is a serious ecological problem. Bacteria and cyanobacteria both have great potential for saline-alkali soil improvement. However, the effect of co-applying bacteria and cyanobacteria on soil improvement and crop growth promotion in saline-alkali soil remains unclear. In this study, the effects of *Paenibacillus sabinae* (potassium-solubilizing bacteria) and *Leptolyngbya* sp. RBD05 (cyanobacteria), produced in brewery wastewater, on soil properties, wheat growth, and wheat stress tolerance were studied by applying them to saline-alkali soil alone or in combination. The study indicated that *P. sabinae* and *Leptolyngbya* sp. RBD05 have important roles in increasing wheat growth, N:P ratio, K:Na ratio, proline content, and superoxide dismutase activity, as well as in slowing the decline of soil nutrient content caused by wheat absorption. Compared to the control group, the co-application had the best effect on soil available K content, wheat dry weight, and wheat root length (increased by 26%, 85%, and 70%, respectively); and it was more conducive to promoting the wheat K:Na ratio (increased by 41%), which would better improve the wheat's saline-alkali stress tolerance. This study provided a new and clean strategy to improve saline-alkali soil quality and promote crop growth by the bacteria and cyanobacteria produced from wastewater treatment.

KEYWORDS

cyanobacteria, potassium-solubilizing bacteria, saline-alkali soil, wastewater, wheat growth promotion

1 Introduction

In recent years, the synergistic treatment of wastewater by bacteria and microalgae (including cyanobacteria) has attracted more and more attention due to its high efficiency (Aditya et al., 2022). But how to make full use of the bacteria and microalgae biomass produced in the wastewater treatment process still needs further development. Generally, the biomass of bacteria and microalgae is usually sent to waste treatment plants as solid waste, which results in significant disposal costs and resource waste. A large amount of wastewater is produced during beer brewing. It is estimated that about 10 L of wastewater were produced for every 1 L of beer (Simate et al., 2011). Unlike industrial wastewater, brewery wastewater contains almost no toxic and harmful substances and contains a lot of nutrients, proteins, minerals, and trace elements (Ashraf et al., 2021). Therefore, the bacteria and microalgae biomass produced in the process of brewery wastewater treatment has great application potential.

There are many saline-alkali fields around the world (Kumar and Sharma, 2020). Soil properties and crop growth are seriously affected by soil salinization (Aycan et al., 2021). It is critical to develop, utilize, and improve saline-alkali land on a global scale to meet the growing food demand. Great achievements have been made by physical and chemical means in the process of saline-alkali soil improvement. However, defects such as a large amount of work and high costs have also been noted (Tejada et al., 2006). The use of microorganisms to improve soil properties, improve the fertilizer utilization rate, and promote the crop growth (Ramadoss et al., 2013), has attracted increasing attention (Renuka et al., 2016). The bacteria and microalgae biomass produced in the process of wastewater treatment might be a good source for saline-alkali soil improvement (Ferreira et al., 2019).

Potassium-solubilizing bacteria (KSB), growing well in wastewater (Wang et al., 2022), can transform the soil insoluble potassium (K) into a soluble state that can be absorbed by plants (Etesami et al., 2017). It is promising to make full use of the potassium-dissolving property of KSB to release mineral K into soil for plant use. In addition, some studies indicated that KSB could secrete plant growth-promoting hormones that promote growth and stress tolerance of plants as well (Sanyal et al., 2020). Ashfaq et al. (2020) reported that the rice plants growth under a saline-alkali environment was improved, the utilization rate of K was increased, and the harmful effect of salt on rice was reduced significantly by the application of *Acinetobacter pittii*. The expression of antioxidase-related genes was enhanced, and the superoxide dismutase (SOD) activity was significantly increased by the application of *Bacillus mojavensis*, which then enhanced corn salt tolerance (Feng et al., 2019). The growth of apple seedlings and the absorption of K by apple seedlings were promoted by the phytohormones produced by *Paenibacillus mucilaginosus* (Chen et al., 2020).

Microalgae, especially cyanobacteria, are photosynthetic autotrophic microorganisms that can survive under harsh conditions and have an effective role in wastewater treatment and soil remediation (Singh et al., 2016). In particular, nitrogen fixation by cyanobacteria has been widely used. Karthikeyan et al. (2007) reported that *Calothrix ghosei* promoted wheat growth by producing somatotropin and fixing atmospheric nitrogen. Microalgae have also received more attention for their role in the remediation of saline-alkali soil. For example, the absorption of salt by *Anabaena* sp. in soil could reduce the impact of salt on plants (Mahanty et al., 2017). The saline-alkali soil fertility could be improved by some nitrogen-fixing microalgae (Li et al., 2019).

Owing to chemical substances exchange, cell signal transduction, and gene transfer between bacteria and microalgae (Aditya et al., 2022), the application of bacteria-microalgae symbiosis for environmental remediation is often better than the application of a single microorganism, particularly in wastewater treatment (Kohler et al., 2007; Zhang et al., 2011). Previous studies have shown that the bacteria and microalgae symbiosis system has been widely used to treat nutrient-rich wastewater, and the microalgae and bacteria system has greater advantages in the nutrient removal of wastewater (Kim et al., 2014). In addition, bacteria could contribute to the flocculation of microalgae, effectively and better harvest microalgae bacterial biomass, and reduce the harvest cost (Lee et al., 2013). The symbiosis of bacteria and microalgae also showed higher efficiency when using biological measures to deal with environmental pollution. Tang et al. (2010) found that the symbiosis of bacteria and algae significantly promoted the degradation ability of oil pollutant-degrading bacteria, especially the ability of biodegradable polycyclic aromatic hydrocarbons (PAHs). The study by Subashchandrabose et al. (2013) also proved the effective use of bacteria and microalgae symbiosis in the degradation of methyl parathion, furan, and other agricultural chemicals. In addition, bacterial communities and microalgae detoxify each other, making bacteria and microalgae have stronger tolerances to higher concentrations of heavy metal content, and therefore the bacteria and microalgae symbiosis has a higher removal rate in the treatment of heavy metal pollution (Muñoz and Guieysse, 2006). Recently, the role of co-application of bacteria and microalgae in soil quality improvement has received increasing attention. For example, the growth and yield of chickpea were significantly improved by the use of *Anabaena–Rhizobium* biofilm (Bidyarani et al., 2016). The use of nitrogen fertilizer could be reduced by the co-use of rhizosphere growth-promoting bacteria and cyanobacteria in normal soil (Rana et al., 2012). The co-application of *Brevundimonas* sp. and *Anabaena* sp. had a positive impact in terms of increasing rice growth and grain yield, as well as improving paddy soil health (Prasanna et al., 2012). However, up to date, the effects of the co-application of bacteria and microalgae on saline-alkali soil improvement and crop growth are still not clear.

In this study, the bacterium (*Paenibacillus sabinae*) and cyanobacterium (*Leptolyngbya* sp. RBD05) produced in the process of brewery wastewater treatment were applied to saline-alkali soil alone or jointly. The goal was to investigate their effects on the chemical properties and nutrient composition of saline-alkali soil, as well as on the growth status and stress resistance of wheat in a saline-alkali environment. This study was expected to provide a clean, sustainable, and green method for the improvement of saline-alkali soil and the further utilization of bacteria and cyanobacteria produced in wastewater treatment.

2 Materials and methods

2.1 The bacteria strain and cyanobacteria strain

The *P. sabinae* (potassium-solubilizing bacterium) and *Leptolyngbya* sp. RBD05 (cyanobacterium) were isolated by

TABLE 1 The main characteristics of brewery wastewater.

Parameter	Unit	Value
Salinity	‰	1.7
pH	—	7.5
COD (chemical oxygen demand)	mg L^{-1}	1,570
DOC (dissolved organic carbon)	mg L^{-1}	512.0
NH_4^+-N	mg L^{-1}	18.30
NO_3^--N	mg L^{-1}	0.66
TN (total nitrogen)	mg L^{-1}	24.50
PO_4^{3-}-P	mg L^{-1}	0.72
TP (total phosphorus)	mg L^{-1}	2.40
Heavy metals	mg L^{-1}	0.00

our laboratory from a wheat field in the Yellow River Delta, China, characterized by coastal saline-alkali soil. In the experiment of treating brewery wastewater (unpublished), it was found that both *P. sabinae* and *Leptolyngbya* sp. RBD05 showed strong salt tolerance (up to 2% salinity level). In addition, *P. sabinae* showed the ability to solve K from K-feldspar, and *Leptolyngbya* sp. RBD05 showed the ability to fix atmospheric N_2. Therefore, it was appropriate to apply these two microorganisms to the saline-alkali soil. A pH meter (PHS-3C, Shanghai Yidian Scientific Instrument Co., LTD) was used to directly measure the pH of brewery wastewater. After the brewery wastewater was filtered by 0.45 μm filter membrane, the DOC (dissolved organic matter) in the brewery wastewater sample was analyzed by a total organic carbon analyzer, and the NO_3-N was determined by high-performance liquid chromatography. According to the national standard of the People's Republic of China, the salinity of brewery wastewater was determined by the gravimetric method (HJ/T 51-1999); the COD (chemical oxygen demand) in water was determined by the standard potassium dichromate method (GB 11914-1989); the NH_4-N was determined by Nath reagent spectrophotometry (HJ 535-2009); the PO_4^{3-}-P was determined by ammonium molybdate spectrophotometry (GB/T 9727-2007); the total nitrogen (TN) was determined by ultraviolet spectrophotometry with potassium persulfate digestion (HJ 636-2012); the total phosphorus (TP) was determined by ammonium molybdate spectrophotometry (GB 11893-89); and the heavy metal content was determined by atomic absorption spectrometry (GB/T 9735-2008). The main characteristics of brewery wastewater are shown in Table 1. *P. sabinae* and *Leptolyngbya* sp. RBD05 were inoculated into sterilized brewery wastewater for culture, respectively. The cultural conditions were as follows: The diurnal-night cycle was 12/12 h, the temperature was 28°C, and the light intensity was 2000 lux. Culture of bacterial solution for 3 days and cyanobacterial solution for 7 days. The brewery wastewater containing *P. sabinae* and *Leptolyngbya* sp. RBD05 was harvested at the log phase by centrifuging at 10,000 rpm for 5 min, the supernatant was removed, and the bacterium and cyanobacterium were then resuspended in sterile deionized water. This process was repeated 3 times to obtain a live inoculum. Part of the live inoculum was sterilized at 121°C for 30 min to obtain the inactivated inoculum.

2.2 Design and analysis of the pot experiments

The wheat pot experiment was divided into the following groups: the *P. sabinae* group (JK), the *Leptolyngbya* sp. RBD05 group (CL), the *P. sabinae* + *Leptolyngbya* sp. RBD05 group (JKCL), and the control group (CK). Fifteen pots were set up in each group. Potting soil comes from the same source as the soil used for screening bacteria and microalgae. The soil was directly used without treatment. The basic soil properties were determined in the same way as the experimental soil samples collected below. The wheat seed source is Datang Seed Industry Co., Ltd., China; the seed number is 20190045. The evenly sized and plump wheat seeds were soaked in 10% alcohol for 3 min, washed with sterile water five times, repeated once, and then set aside for use. The planting depth is 2 cm, and 20 seeds are planted in each pot. The materials used in the experiments and the culture conditions are shown in Table 2. The inoculum volume at the log phase of each pot was as follows: CK (50 mL inactivated *P. sabinae* inoculum and 50 mL inactivated *Leptolyngbya* sp. RBD05 inoculum), JK (50 mL *P. sabinae* inoculum and 50 mL inactivated *Leptolyngbya* sp. RBD05 inoculum), CL (50 mL *Leptolyngbya* sp. RBD05 inoculum and 50 mL inactivated *P. sabinae* inoculum), JKCL (50 mL *P. sabinae* inoculum and *Leptolyngbya* sp. RBD05 inoculum). Inactivated inoculants are added to eliminate errors caused by nutrients introduced into the inoculant solution. The potted plants were placed in a completely random arrangement in a growth chamber (the growth conditions are illustrated in Table2); the pot positions were changed periodically. No fertilizer was added throughout the culture cycle. All pots were watered every 3 days, until they reached field capacity. Field water holding capacity is about 60%. The water content of soil was determined by drying method.

Wheat and soil were collected from five randomly selected pots from each set of 15 parallel samples in each group at 30, 60, and 90 days. The growth status, nitrogen (N), phosphorus (P), potassium (K), sodium (Na), proline content, malondialdehyde (MDA) content, and superoxide dismutase (SOD) activity of wheat were determined. The pH, electrical conductivity (EC), available nitrogen (A-N), available phosphorus (A-P), available potassium (A-K), and available sodium (A-Na) in soil were determined. The determination methods are shown in Table 3.

2.3 Statistical analysis

The result is the mean ± standard error of the five parallel values. One-way analysis of variance (ANOVA) was used to analyze the difference in the same index among different treatments. The same letter (a, b, c, ab, etc.) in the same time group indicated no significant difference using Duncan's test at $p < 0.05$. The correlation among indicators of the same treatment was analyzed by the Pearson correlation coefficient. Data analysis and mapping were performed with IBM SPSS Statistics 26 and Origin 2022 software.

TABLE 2 Material and growth conditions used in the pot experiments.

	Specifications and treatment methods
Pot	The diameter is 13.5 cm, the height is 10 cm, and it contains 1 kg of soil
Saline-alkali soil	Soil was taken from a wheat field in the Yellow River Delta, China. The basic physical and chemical properties of the soil are as follows: 66.38 mg kg^{-1} available N, 61.46 mg kg^{-1} available P, 169.63 mg kg^{-1} available K, 438.06 mg kg^{-1} available Na, pH 7.67, electrical conductivity (EC) 54.6 mS m^{-1}
Wheat seed	Select wheat seeds of the same size for sterilization. The planting depth is 2 cm, and 20 seeds are planted in each pot
Culture temperature	20°C
Illumination	Day/night: 12/12 h; 2000 lux; white light
Bacterium and cyanobacterium inoculum	P. sabinae inoculum contains 7×10^7 colony-forming units mL^{-1}, the concentration of the Leptolyngbya sp. RBD05 inoculation solution is 0.01 g mL^{-1} (calculated based on the dry matter). The brewery wastewater containing P. sabinae and Leptolyngbya sp. RBD05 was harvested at the log phase by centrifuging at 10,000 rpm for 5 min, the supernatant was removed, and the bacterium and microalgae were then resuspended in sterile deionized water. This process was repeated 3 times to form the final inoculum

TABLE 3 Wheat and soil indexes and determination methods.

Soil indexes	Determination methods
Available nitrogen	Alkaline diffusion method Lu (1999)
Available phosphorus	Sodium bicarbonate extraction, molybdenum-antimony anti-spectrophotometry Lu (1999)
Available potassium and sodium	Ammonium acetate extraction, ICP-AES determination Lu (1999)
Electrical conductivity; pH	Water and soil ratio: 5:1, extracted with deionized water, measured by pH and conductivity meters Lu (1999)
Wheat Indexes	Determination methods
Nitrogen	Sulfuric acid–hydrogen peroxide digestion, Nye reagent spectrophotometric determination Wang et al. (2003)
Phosphorus	Sulfuric acid–hydrogen peroxide digestion, molybdenum antimony spectrophotometric determination Wang et al. (2003)
Potassium and sodium	Sulfuric acid–hydrogen peroxide digestion, ICP-AES determination Wang et al. (2003)
Root and stem length	Determination with a ruler
Fresh and dry weight	The fresh weight was weighed directly by electric balance. To determine the dry weight, samples were dried at 70°C for 24 h at a low temperature, and then weighed by electric balance
Proline; Malondialdehyde; Superoxide dismutase	Spectrophotometric determination Bates et al. (1973), Faisal Alharby (2021); Wang et al. (2004)

3 Results and discussion

3.1 Effects of *Paenibacillus sabinae* and *Leptolyngbya* sp. RBD05 on soil chemical properties

3.1.1 Effects on soil A-K and A-Na

Slow-release K compounds could be dissolved by KSB; thereby, the content of soil A-K would increase (Xiao et al., 2017). At 30 days, there was no difference in soil A-K content between the JK and CK groups ($p > 0.05$, Figure 1A). The soil A-K content of the CL and JKCL groups was lower than that of the CK group by 6% and 14% ($p < 0.05$, Figure 1A). It may be that both *P. sabinae* and *Leptolyngbya* sp. RBD05 prolifically increased, which resulted in the enhanced ability of the JK and JKCL groups to release soil A-K at 60 days. The soil A-K content of the JK and JKCL groups was 157.96 and 169.24 mg kg^{-1}, respectively, which was higher than that of the CK group by 16% and 26% (Figure 1A). These results indicated that the soil A-K content was increased by both the application of *P. sabinae* and the co-application of *P. sabinae* and *Leptolyngbya* sp. RBD05, and the co-application of the two microorganisms had a better effect on the soil A-K content than the single application of *P. sabinae*. Liu et al. (2012) showed that *Paenibacillus* sp. had a great K-solubilizing effect, which supported the results of this study. Rossi et al. (2017) reported that some microalgae had a good effect on improving soil nutrients, but most studies focused on their N fixation ability, and no studies have shown that *Leptolyngbya* can increase the A-K content in soil. Our study found that *Leptolyngbya* sp. RBD05 also had a certain improvement effect on the A-K content in soil as discussed

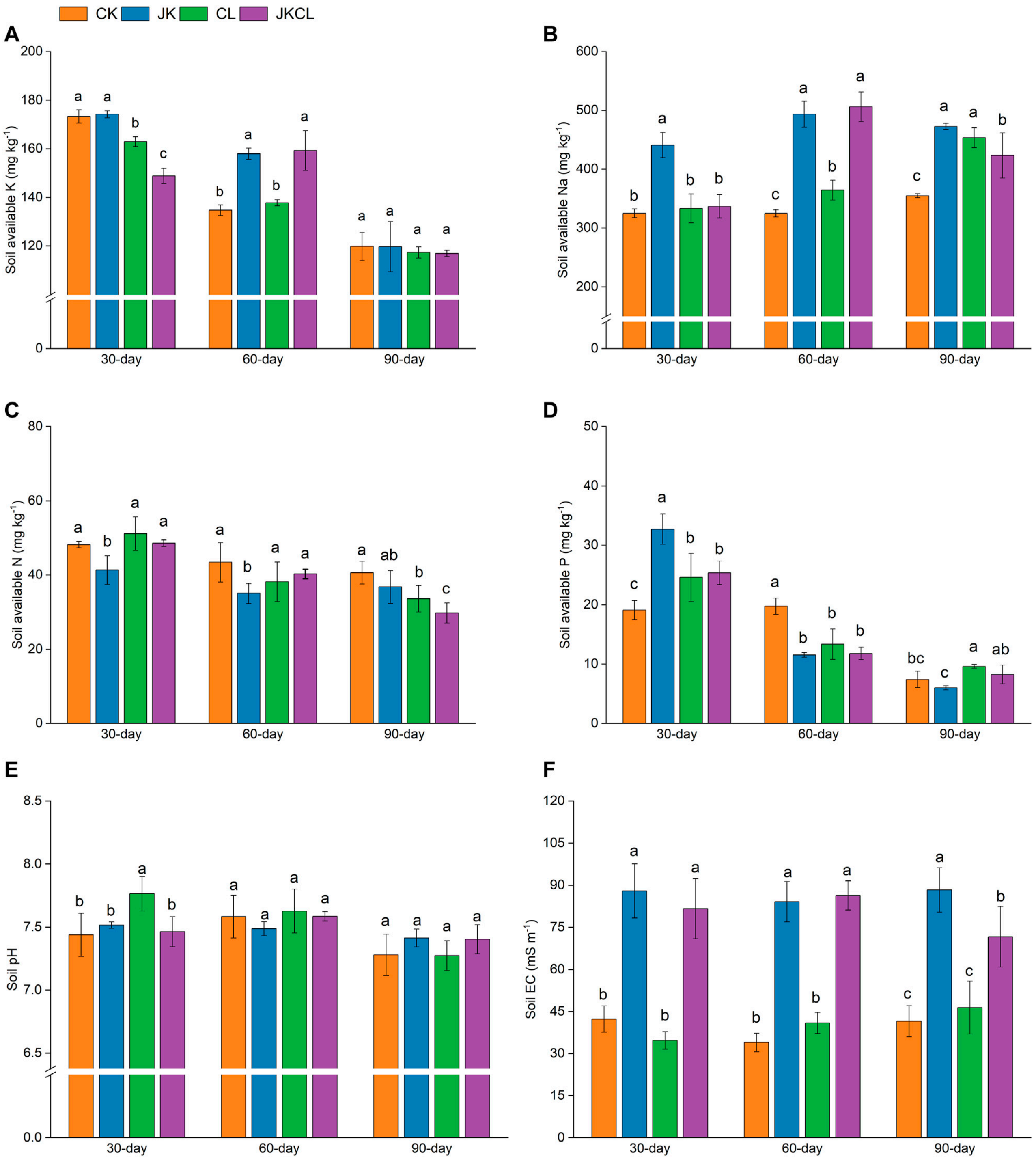

FIGURE 1
Effects of *Paenibacillus sabinae* and *Leptolyngbya* sp. RBD05 on soil available K **(A)**, available Na **(B)**, available N **(C)**, available P **(D)**, soil pH **(E)**, and electrical conductivity **(F)** at different times. CK = the control group, JK = the *Paenibacillus sabinae* group, CL = the *Leptolyngbya* sp. RBD05 group, JKCL = the *Paenibacillus sabinae* + *Leptolyngbya* sp. RBD05 group.

below. The K content of wheat in the treatment groups was not lower than that in the control group (Figure 3A), while the dry weight of the treated wheat groups was heavier (Figure 2D). Therefore, the K absorption of wheat growth from the soil in the treatment groups was higher than that in the control group. The difference of soil A-K content between the four groups was not significant at 90 days ($p >$ 0.05, Figure 1A). These showed that, at 90 days, *P. sabinae* and *Leptolyngbya* sp. RBD05 actually increased the soil A-K content. A comprehensive analysis of all the results on days 30, 60, and 90 showed that the co-application of *P. sabinae* and *Leptolyngbya*

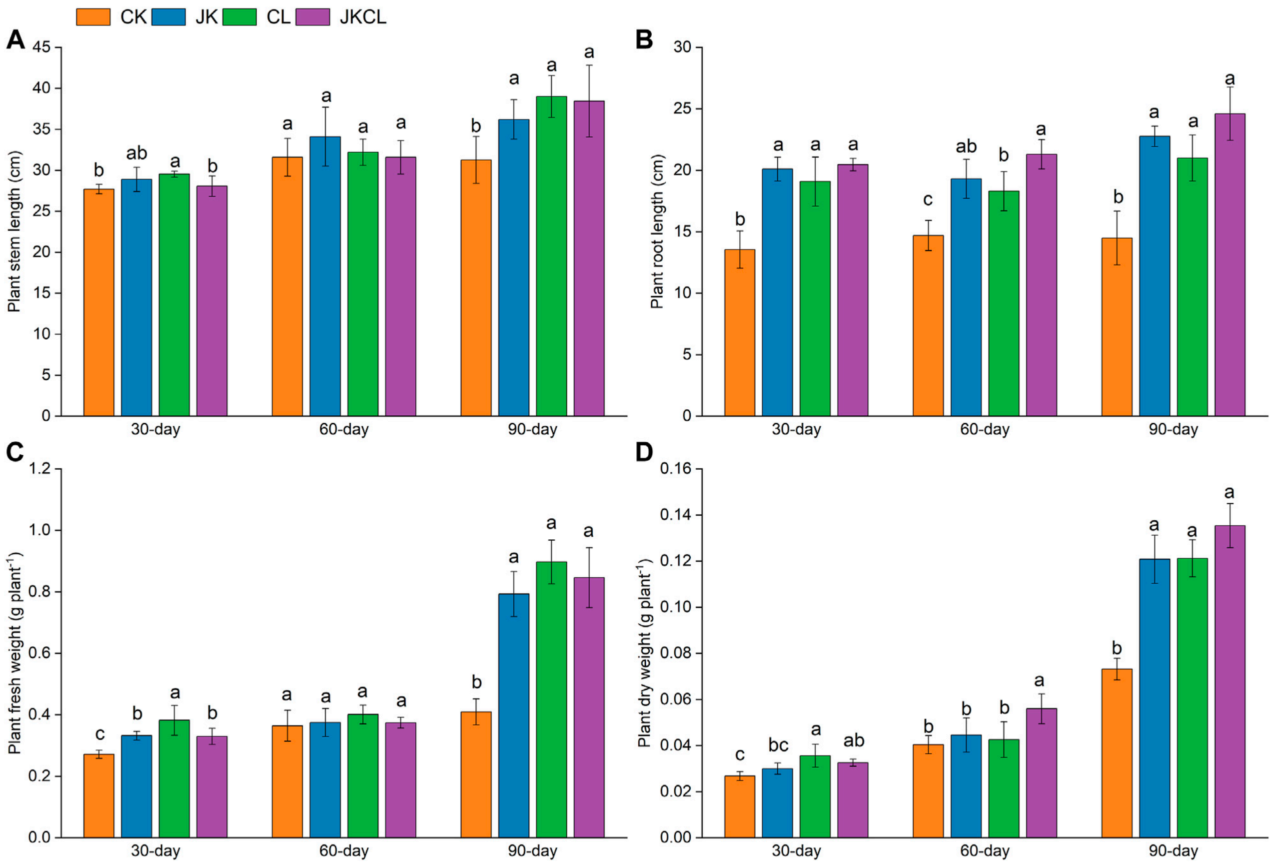

FIGURE 2
Effects of *Paenibacillus sabinae* and *Leptolyngbya* sp. RBD05 on wheat stem length **(A)**, root length **(B)**, fresh weight **(C)**, and dry weight **(D)** at different times. CK = the control group, JK = the *Paenibacillus sabinae* group, CL = the *Leptolyngbya* sp. RBD05 group, JKCL = the *Paenibacillus sabinae* + *Leptolyngbya* sp. RBD05 group.

sp. RBD05 showed a better K dissolution effect than the application of *P. sabinae* or *Leptolyngbya* sp. RBD05 alone. Previous studies have also shown that the application of multiple microorganisms has better effects in improving soil A-K content than one microorganism, which supports the results in this study (Muthuraja and Muthukumar, 2022).

Excessive Na adversely affects plant development and osmotic pressure balance in saline-alkali soil (Rengasamy, 2010). This study found that the soil A-Na content increased with the application of *P. sabinae*. At 30, 60, and 90 days, soil A-Na content in group JK was 440.90, 493.22, and 472.51 mg kg^{-1}, respectively, significantly increased by 36%, 52%, and 33% compared with group CK ($p < 0.05$, Figure 1B), which aggravated the stress of Na on plant growth. At 30 and 90 days, the soil A-Na content of the JKCL group was lower than that of the JK group by 24% and 15%, respectively, at 60 days, there was no significant difference in soil A-Na content between the JK group and the JKCL group ($p < 0.05$, Figure 1B). Studies have shown that cyanobacteria can reduce the A-Na content in soil by fixing Na in their cells or producing exopolysaccharides to adsorb Na (Prasanna et al., 2008). Thus, the co-application of *P. sabinae* and *Leptolyngbya* sp. RBD05 made up for the defect of applying *P. sabinae* alone. At 90 days, the A-Na content in the JKCL group soil was lower than that in the CL and JK groups ($p < 0.05$, Figure 1B). The above results indicated that the co-application of *P. sabinae* and *Leptolyngbya* sp. RBD05 was more conducive to reducing salt stress than a single application. The reason was that when *P. sabinae* and *Leptolyngbya* sp. RBD05 were collaboratively applied, the *P. sabinae* promoted the growth of *Leptolyngbya* sp. RBD05, and made it showing a better ability to fix Na than itself (Li et al., 2019).

3.1.2 Effects on soil A-N and A-P

Nitrogen-fixing microalgae such as *Anabaena doliolum* HH-209, *Cylindrospermum sphaerica*, and *Calothrix elenkinii* and their combinations with other bacteria, all showed good nitrogen-fixing effects in soil (Renuka et al., 2018). Similar to the K consumption by wheat, the N and P consumption by wheat in the soil was also high. However, the A-N content of the CL and JKCL groups did not decrease significantly at 30 and 60 days ($p > 0.05$, Figure 1C), indicating that the application of *Leptolyngbya* sp. RBD05 increased the A-N content in the soil at 30 and 60 days. The growth of wheat accelerated the consumption of soil A-N content. Therefore, at 90 days, the A-N content in soil of the CL and JKCL groups were lower than that of the CK group by 17% and 27%, respectively ($p < 0.05$, Figure 1C). At 30, 60, and 90 days, the A-N content in soil of the JK group was lower than that of the

CK group by 14%, 19%, and 16%, respectively ($p < 0.05$, Figure 1C). This might be because the wheat in the JK group grew better and consumed more soil A-N than that in the CK group, which was boosted by *P. sabinae*. Phosphorus (P) soluble microorganisms can contribute to P release in several ways. Studies have found that some KSB also have a P-dissolving ability (Abou-el-Seoud and Abdel-Megeed, 2012). Our study found that while promoting the release of K in the soil, *P. sabinae* also showed the ability to increase the content of A-P in the soil. At 30 days, the application of *P. sabinae* alone was more beneficial in increasing the A-P content in the soil than the other treatment groups, which was 71% higher than that of the CK group ($p < 0.05$, Figure 1D). Although the application of *P. sabinae* and *Leptolyngbya* sp. RBD05 increased the content of A-P in the soil to a certain extent, the amount required for wheat growth was also high. Therefore, soil A-P content in the three treatment groups decreased at 60 days, and the difference value between the four groups was small at 90 days (Figure 1D). The above results indicated that the co-application of *P. sabinae* and *Leptolyngbya* sp. RBD05 or the application of *P. sabinae* alone could improve the soil A-P content in the early stage (30 days), and the application of *P. sabinae* alone increased the soil A-P content most obviously, but both could not maintain a high level of soil phosphorus content in the middle and later stage (60 and 90 days).

3.1.3 Effects on soil pH and EC

There was little change in soil pH in each group ($p > 0.05$, Figure 1E). This indicated that neither *P. sabinae* nor *Leptolyngbya* sp. RBD05 could significantly affect soil pH.

Soil EC value is an important indicator for monitoring soil health. When the EC value is too high, the soil structure and soil respiration will be adversely affected (Yan and Marschner, 2013). Soil EC will increase to a certain extent if the soil nutrient content increases (Maltas et al., 2022). According to Section 3.1.1 and Section 3.1.2, the application of *P. sabinae* and *Leptolyngbya* sp. RBD05 increased the soil nutrient element content, which increased the EC value in the soil. At 30, 60, and 90 days, the soil EC value of the JK group was higher than that of the CK group by 108%, 148%, and 113%, respectively. The soil EC value of the JKCL group was higher than that of the CK group by 93%, 148%, and 73%, respectively. The soil EC values of the CL and CK group showed little difference (Figure 1F). Although the soil EC in the JKCL group was still higher than that in the CK group at 90 days, it was 23% lower than that at 30 and 60 days, respectively ($p < 0.05$, Figure 1F). However, at 90 days, the EC values of the JK and CL group were higher than those at 30 and 60 days. These results indicated that the EC was reduced by the co-application of *P. sabinae* and *Leptolyngbya* sp. RBD05 over time.

3.2 Effects of *Paenibacillus sabinae* and *Leptolyngbya* sp. RBD05 on the growth and stress resistance of wheat

3.2.1 Effects on wheat growth

The analysis in Section 3.1 showed that, compared with the CK group, the application of *P. sabinae* and *Leptolyngbya* sp. RBD05 could significantly improve the soil environment, which was more conducive to wheat growth. There was little difference in the stem length of wheat in all groups at 30 and 60 days. However, at 90 days, the stem length of wheat in the three treatment groups showed obvious advantages (Figure 2A), indicating that the application of *P. sabinae* and *Leptolyngbya* sp. RBD05 promoted the growth of wheat at the later stage. Majeed et al. (2015) reported that plant development could be improved by the addition of beneficial microorganisms. *P. sabinae* and *Leptolyngbya* sp. RBD05 might secrete plant hormones such as kinetin and auxin to promote wheat growth (Ahmeda et al., 2014; Chen et al., 2020).

The belowground parts of plants are more sensitive to salt than the aboveground parts (Munns and Tester, 2008), and the root development of wheat is obviously affected by salinity (Robin et al., 2016). Compared with the stem length, the promoting effect of each treatment group on the root length of wheat was more significant. At 30, 60 and 90 days, the root length of wheat in each treatment group was higher than that in the CK group. The root growth of the JKCL group was the most obvious, and the root length of JKCL group was the longest at 90 days, which was 70% higher than that of CK group (Figure 2B). This suggested that the co-application of *P. sabinae* and *Leptolyngbya* sp. RBD05 best promoted the root development of wheat, which helped wheat resist saline-alkali stress (Robin et al., 2016). AminiHajiabadi et al. (2021) found that *Bacillus* sp. could promote the wheat root development, which further confirmed the results of this study.

Cyanobacteria usually play an important role in preventing soil erosion and water evaporation, which helps plants to absorb water (Acea et al., 2003). At 30 and 60 days, there was little difference in fresh weight among all groups. At 90 days, the wheat fresh weight in the three treatment groups were all higher than that in the CK group, and the fresh weight in the CL group was the highest, which was 119% higher than that in the CK group (Figure 2C), indicating that the application of *Leptolyngbya* sp. RBD05 alone was more beneficial to wheat water retention. At 30 days, all groups had little difference in dry weight. At 60 days, the dry weight of wheat in the JKCL group was 39% higher than that in the CK group, and there was no significant difference in the dry weight of wheat in other groups except the JKCL group. At 90 days, the dry weight of wheat in the three treatment groups was all higher than that in the CK group. The co-application of *P. sabinae* and *Leptolyngbya* sp. RBD05 had the greatest promoting effect on the dry matter accumulation of wheat, which made the wheat dry weight in the JKCL group the highest, 85% higher than that in the CK group (Figure 2D). In the early stage, the nutrient element demand of wheat was lower, but with the passage of time, the nutrient element demand of wheat increased, and the side effects of stress on wheat were also accumulating. Under the promotion of bacteria and cyanobacteria, the wheat growth status of the treatment group and the control group gradually opened a gap; therefore, at 90 days, the fresh weight and dry weight of wheat between the treatment group and the control group were significantly different. Among them, the co-application of *P. sabinae* and *Leptolyngbya* sp. RBD05 showed the best effect on promoting wheat dry matter accumulation. The reason might be that the bioactivity of bacteria and cyanobacteria could be significantly improved by their cooperation, which was more conducive to promoting plant growth (Prasanna et al., 2012).

3.2.3 Effects on wheat K, Na, and K:Na ratio

K can maintain the homeostasis of osmotic pressure in plants, improve enzyme activity, and reduce damage to plant cells

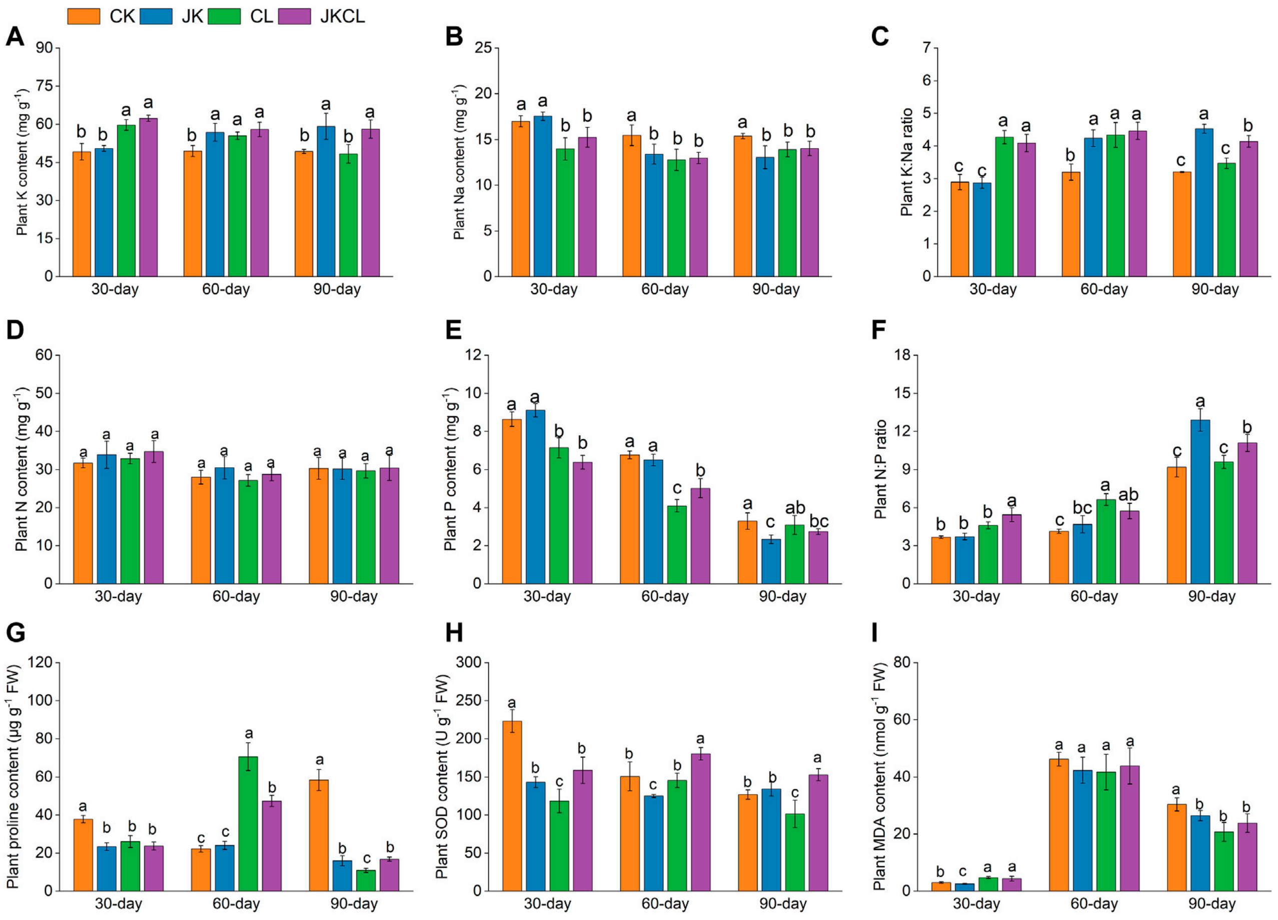

FIGURE 3
Effects of *Paenibacillus sabinae* and *Leptolyngbya* sp. RBD05 on wheat K **(A)**, Na **(B)**, **(K)** Na ratio **(C)**, nitrogen **(D)**, phosphorus **(E)**, N:P ratio **(F)**, wheat proline **(G)**, SOD **(H)**, and MDA **(I)** at different times. CK = the control group, JK = the *Paenibacillus sabinae* group, CL = the *Leptolyngbya* sp. RBD05 group, JKCL = the *Paenibacillus sabinae* + *Leptolyngbya* sp. RBD05 group. FW = fresh weight.

(Assaha et al., 2017). KSB promotes plant growth by dissolving slow-release potassium compounds in soil and secreting auxin while simultaneously promoting plant K absorption (Lin et al., 2002). As shown in Figure 3A, at 30 days, there was little difference between the JK and CK groups in wheat K content. At 60 and 90 days, the wheat K content in the JK group was higher than that in the CK group by 15% and 20%, respectively. The results indicated that although the application of *P. sabinae* alone had no significant effect on increasing the wheat K content at the early stage (30 days), its effect on increasing the wheat K content was significantly enhanced as time extended. The reason might be that the proliferation of *P. sabinae* increased wheat's ability to absorb K from the soil. At 30 and 60 days, the wheat K content in the CL group was significantly higher than in the CK group by 21% and 12%, respectively. At 90 days, there was little difference between the CL and CK groups in wheat K content. These results indicated that with time passing, the promotion effect of *Leptolyngbya* sp. RBD05 alone on wheat K content had a downward trend. The reason might be that *Leptolyngbya* sp. RBD05 is mainly grown on the surface of the soil, and soil salt accumulates on soil surface by transpiration (Tejada et al., 2006), worsening the growth environment of *Leptolyngbya* sp. RBD05 and reducing its activity, which in turn reduced its promoting effect on the K content in wheat. Rana et al. (2012) reported that the co-application of bacteria and cyanobacteria could fully enhance and play their respective advantages. This study found that at 30, 60, and 90 days, the wheat K content in the JKCL group was higher than in the CK group by 27%, 17%, and 18%, respectively. These results indicated that the K content of wheat could be significantly increased at 30, 60, and 90 days by the combination of *P. sabinae* and *Leptolyngbya* sp. RBD05 would effectively maintain the balance of osmotic pressure in wheat (Etesami et al., 2017). Rana et al. (2012) found that the K absorption by wheat was significantly increased by the co-use of rhizosphere growth-promoting bacteria and cyanobacteria, which supported the above results of this study. K deficiency would lead to slow plant growth (Gupta et al., 2015). Therefore, wheat growth in the CK group was worse than in all treatment groups (Figure 2).

Excessive Na in plants could destroy the osmotic pressure balance, leading to physiological drought, and even damaging plant cells (Fang et al., 2021). Grieve and Poss (2000) discovered

TABLE 4 Pearson's correlation coefficients between wheat nutrients.

Treatment	Nutrient	Wheat Na	Wheat K:Na ratio	Nutrient	Wheat P	Wheat N:P ratio
CK	Wheat K	−0.421	0.930**	Wheat N	0.297	−0.135
	Wheat Na		−0.379	Wheat P		−0.940**
JK	Wheat K	−0.439	0.621*	Wheat N	0.503	−0.326
	Wheat Na		−0.942**	Wheat P		−0.940**
CL	Wheat K	−0.188	0.761 **	Wheat N	−0.470	0.382
	Wheat Na		−0.511	Wheat P		−0.902**
JKCL	Wheat K	−0.199	−0.088	Wheat N	0.333	−0.036
	Wheat Na		−0.178	Wheat P		−0.370

*$p < 0.05$. **$p < 0.01$.

an inverse relationship between Na and K in plants, and that the ability of plants to resist salt stress is partly due to the continuous uptake of K by roots, which in turn limits the uptake of Na. The study found that inoculation of exopolysaccharide-producing bacteria under salt stress could limit the absorption of Na by wheat seedlings (Ashraf et al., 2004). Our study revealed that, except there was no significant difference in wheat Na content between the JK and CK groups at 30 days, the wheat Na content in all treatment groups at 30, 60 and 90 days was all lower than that in the CK group, decreasing by 13%–18% (Figure 3B). The results indicated that the Na content of wheat was reduced and the application of *P. sabinae* and *Leptolyngbya* sp. RBD05 alleviated salt stress. The difference was that *Leptolyngbya* sp. RBD05 had more obvious effect at 30 days and 60 days. The reason might be that the soil A-Na of the CL group can be adsorbed by exopolysaccharides secreted by cyanobacteria, thus reducing the absorption of Na by plants (Li et al., 2019).

When the regulation of osmotic pressure and the stability of metabolic function in plants are subjected to a high salt stress level, the plant K:Na ratio will change. A higher plant K:Na ratio can generally ensure that the various physiological functions of plant cells are in a good state, maintaining osmotic balance in plants and protecting enzyme activities (Falhof et al., 2016). Previous studies have reported that both cyanobacteria or KSB could promote the K content of plants and thus increase the K:Na ratio in plants (Rana et al., 2012; Li et al., 2019). In this study, the wheat K:Na ratio in the CL and JK groups was not higher than that in the group CK at 30, 60, and 90 days, but the wheat K:Na ratio in the JKCL group was all higher than that in the CK group by 29%–41% (Figure 3C). Maintaining high K:Na ratio levels could help plants tolerate salt stress (Maathuis and Amtmann, 1999). The results of wheat K:Na ratio further showed that the co-application of *P. sabinae* and *Leptolyngbya* sp. RBD05 was more effective in increasing the wheat K:Na ratio, maintaining the balance of osmotic pressure in wheat, and alleviating salt stress.

Correlation analysis was conducted to analyze the mutual effects among K, Na content and K:Na ratio in wheat. As shown in Table 4, the correlation between the K content and Na content of wheat and the K:Na ratio among the four groups had significant changes. There was a significant positive correlation between the K content and K:Na ratio of wheat in the CK and CL groups ($p < 0.01$). These results indicated that the wheat K:Na ratio in group CK and CL was mainly affected by the wheat K content. The wheat K:Na ratio in the JK group was significantly positively correlated with the wheat K content ($p < 0.05$) and negatively correlated with the wheat Na content ($p < 0.01$), implying that the wheat K:Na ratio in the JK group was affected by the increase of wheat K content and the decrease of wheat Na content. There was no significant correlation between the K and Na contents of wheat and the K:Na ratio in the JKCL group ($p < 0.05$). In addition to regulating the contents of K and Na, plants can also enhance their osmotic potential and regulate the balance of osmotic pressure by accumulating small molecules such as soluble sugars (Kerepesi and Galiba, 2000). The above analysis indicated that the wheat in JKCL group may affect the wheat K: Na through this mechanism.

3.2.3 Effects on wheat N, P, and N:P ratio

N and P are the key factors affecting the growth of plants, and their effects on plant growth are interdependent. An appropriate N:P ratio is more conducive to plant growth and the N:P ratio can be used to indicate whether plant growth is affected or limited by N or P (Güsewell, 2004). Studies have shown that when the N: P ratio in a plant is lower than 14, the plant growth will be limited by N, and when the N: P ratio is higher than 16, the plant growth is limited by P (Güsewell, 2004; Cernusak et al., 2010). In this study, the highest N:P ratio of wheat was 12.91 in the JK group at 90 days (Figure 3F), which was lower than 14, indicating that the N content in saline-alkali soil was limited and the wheat growth was restricted by N.

At 30, 60, and 90 days, there was no difference in the N content of wheat among the four groups ($p > 0.05$, Figure 3D). The differences in the wheat P content among the groups were obvious, and the overall trend of decline was observed with an increase in time. In addition, the wheat P contents in all treatment groups were mostly lower than in the CK group (Figure 3E). This implied that the wheat N:P ratio regulation was mainly due to the decrease in wheat P content under the effects of *P. sabinae* and *Leptolyngbya* sp. RBD05. Pandey et al. (2022) pointed out that plant-related microorganisms could regulate the biosynthesis of plant secondary metabolite, thus promoting the ability of plants to cope with environmental stress. The wheat N:P ratio in all groups in this study showed an overall increasing trend and the application of *P. sabinae* and *Leptolyngbya* sp. RBD05 made the wheat N:P ratio in all treatment groups higher than that in the CK group. At 90 days, the wheat N:P ratio in the JK group was the highest, which was higher than in the CK group by 40% (Figure 3F). These results indicated that the application of *P. sabinae* and *Leptolyngbya* sp. RBD05 both had significant effect on the wheat N: P ratio, and an increase in N: P ratio would then reduce the adverse effect of low N content on wheat growth in the poor saline soil environment (Güsewell, 2004).

The relationship between N and P is always considered to be allometric. When environmental conditions change, plants will store excess nutrients, which may lead to a reduced correlation between changes in nitrogen and phosphorus content in plants (He et al., 2008). As shown in Table 4, the wheat P content in the CK, JK, and CL groups was significantly negatively correlated with the wheat N: P ratio ($p < 0.01$, Table 4), and there was no significant correlation between the wheat N, P content, and wheat N:P ratio in the JKCL group. These results showed that, except in the JKCL group, the wheat N:P ratio in other groups was mainly affected by the change of wheat P content. The effect of the wheat N or P content on wheat N: P ratio was weakened under the joint action of *P. sabinae* and *Leptolyngbya* sp. RBD05.

3.2.4 Effects on wheat proline, SOD, and MDA

Proline is an important amino acid that plays an important role in plant response to abiotic stress. Overproduction of proline in plant cells helps to maintain cell homeostasis, water absorption, osmotic regulation, and REDOX balance to restore cell structure and reduce oxidative damage. In order to cope with saline-alkali stress, plants usually accumulate small organic compounds such as proline to stabilize their osmotic potential (Ahanger et al., 2019; Ghosh et al., 2022). The stressed environment leads to an increase in the content of reactive oxygen species (ROS) content in plants, which can damage the structure of plant cells. SOD activity will increase rapidly to remove ROS, protect the healthy development of plant cells, and reduce the damage to plant cells caused by stressed conditions (Baltruschat et al., 2008; Liu et al., 2018). In addition, when plant cells undergo lipid peroxidation, MDA is usually produced, which is a cytotoxic product and is usually used as an indicator of the degree of plant stress (Liu et al., 2017).

This study found that each treatment group reduced the saline-alkali stress on wheat by promoting K absorption and reducing Na absorption at 30 days (Figure 3), which made the response of wheat in each treatment group to stress weaker than that in the CK group. Therefore, at 30 days, the proline content and SOD activity of the treatment groups were all lower than that of the CK group (Figures 3G, H). At the same time, the MDA content of wheat in all groups was also low, which indicated that the stress had little effect on wheat at this time.

At 60 days, the MDA content in each group increased sharply (Figure 3I), indicating that the stress had intensified (Liu et al., 2017). The proline content in the CL and JKCL groups was significantly higher than that in the other two groups, which were 70.62 and 47.38 $\mu g\ g^{-1}$ FW (fresh weight), and was 218% and 113% higher than that in the CK group ($p < 0.05$, Figure 3G). Hemavathi et al. (2011) reported that the activity of antioxidant enzymes in plants could be increased to a certain extent under the influence of increasing K content. As shown in Figure 3A, the wheat K content in the JKCL group was significantly higher than that in the CK group. A higher wheat K content can improve SOD activity. As a result, the activity of wheat SOD in the JKCL group was higher than that in other groups (Figure 3G). These results indicated that the application of *Leptolyngbya* sp. RBD05 alone or the co-application of *P. sabinae* and *Leptolyngbya* sp. RBD05 had a greater ability to promote proline synthesis and increase the SOD activity in the face of saline-alkali stress.

At 90 days, the MDA content of wheat in all groups decreased, and the difference among treatment groups was not significantly and lower than that observed in the CK group (Figure 3I). However, the proline content of the CK group was significantly higher than that of the other groups (Figure 3G). The accumulation of proline plays a good role in stabilizing the osmotic potential of plants and is also an indicator of the degree of salt stress (Singh et al., 2000). This indicated that the wheat in the CK group was still under high stress at this time, and the increase of proline content mainly regulated the wheat osmotic balance. But the other treatment groups regulated the wheat osmotic balance by increasing the K content and reducing the Na content, as shown in Section 3.2.2.

4 Conclusion

The study showed that the potassium-solubilizing bacterium *P. sabinae* and the cyanobacterium *Leptolyngbya* sp. RBD05 produced in brewery wastewater had the ability to enhance the nutrient level of saline-alkali soil, and promote the stress tolerance and growth of wheat. Among all the treatment groups, the co-application of *P. sabinae* and *Leptolyngbya* sp. RBD05 was more conducive to the increase of the K content in saline-alkali soil, the development of wheat roots, and the improvement of K:Na ratio, proline content and SOD activity of wheat. The application of *Leptolyngbya* sp. RBD05 alone had a more prominent effects on water retention of the wheat plant. The application of *P. sabinae* alone increased soil available P and wheat N:P ratio more obviously. The results of this study provided new ideas for the use of microorganisms to improve crop growth in saline-alkali land and the further utilization of bacteria and cyanobacteria produced in wastewater treatment.

Data availability statement

The original contributions presented in the study are included in the article/supplementary material, further inquiries can be directed to the corresponding author.

Author contributions

HuD: Conceptualization, Formal analysis, Writing—original draft. WL: Data curation, Funding acquisition, Supervision, Writing—review and editing. LZ: Data curation, Methodology. BH and SH: Data curation, Investigation. ME-S and ME: Data curation, Writing—review and editing. HaD and TX: Investigation. XL: Data curation. All authors listed have made a substantial, direct, and intellectual contribution to the work and approved it for publication. All authors contributed to the article and approved the submitted version.

Funding

This work was supported in part by Natural Science Foundation of Shandong Province (ZR2022MC204); Innovation Ability Improvement Project of Small and Medium-sized High-tech Company in Shandong Province (2022TSGC2199); Major Science and Technology Innovation Projects in Shandong Province (2019JZZY010723). Innovation Ability Improvement Project of Small and Medium-sized High-tech Company in Zaozhuang City (2023TSGC15).

Conflict of interest

The authors declare that the research was conducted in the absence of any commercial or financial relationships that could be construed as a potential conflict of interest.

Publisher's note

References

Abou-el-Seoud, I. I., and Abdel-Megeed, A. (2012). Impact of rock materials and biofertilizations on P and K availability for maize (Zea Maize) under calcareous soil conditions. *Saudi J. Biol. Sci.* 19, 55–63. doi:10.1016/j.sjbs.2011.09.001

Acea, M. J., Prieto-Fernández, A., and Diz-Cid, N. (2003). Cyanobacterial inoculation of heated soils: Effect on microorganisms of C and N cycles and on chemical composition in soil surface. *Soil Biol. Biochem.* 35, 513–524. doi:10.1016/S0038-0717(03)00005-1

Aditya, L., Mahlia, T. M. I., Nguyen, L. N., Vu, H. P., and Nghiem, L. D. (2022). Microalgae-bacteria consortium for wastewater treatment and biomass production. *Sci. Total Environ.* 838, 155871. doi:10.1016/j.scitotenv.2022.155871

Ahanger, M. A., Aziz, U., Alsahli, A. A., Alyemeni, M. N., and Ahmad, P. (2019). Influence of exogenous salicylic acid and nitric oxide on growth, photosynthesis, and ascorbate-glutathione cycle in salt stressed Vigna angularis. *Biomolecules* 10, 42. doi:10.3390/biom10010042

Ahmeda, M., Stal, L. J., and Hasnain, S. (2014). The morphology and bioactivity of the rice field cyanobacterium *Leptolyngbya*. *Rev. Biol. Trop.* 62, 1251–1260. doi:10.15517/rbt.v62i3.8657

AminiHajiabadi, A., MoslehArani, A., Ghasemi, S., Rad, M. H., Etesami, H., ShabaziManshadi, S., et al. (2021). Mining the rhizosphere of halophytic rangeland plants for halotolerant bacteria to improve growth and yield of salinity-stressed wheat. *Plant Physiol. Bioch* 163, 139–153. doi:10.1016/j.plaphy.2021.03.059

Ashfaq, M., Hassan, H. M., Ghazali, A. H. A., and Ahmad, M. (2020). Halotolerant potassium solubilizing plant growth promoting rhizobacteria may improve potassium availability under saline conditions. *Environ. Monit. Assess.* 192, 697. doi:10.1007/s10661-020-08655-x

Ashraf, A., Ramamurthy, R., and Rene, E. R. (2021). Wastewater treatment and resource recovery technologies in the brewery industry: Current trends and emerging practices. *Sustain Energy Techn* 47, 101432. doi:10.1016/j.seta.2021.101432

Ashraf, M., Hasnain, S., Berge, O., and Mahmood, T. (2004). Inoculating wheat seedlings with exopolysaccharide-producing bacteria restricts sodium uptake and stimulates plant growth under salt stress. *Biol. Fertil. Soils* 40, 157–162. doi:10.1007/s00374-004-0766-y

Assaha, D. V. M., Ueda, A., Saneoka, H., Al-Yahyai, R., and Yaish, M. W. (2017). The role of Na^+ and K^+ transporters in salt stress adaptation in glycophytes. *Front. Physiol.* 8, 509. doi:10.3389/fphys.2017.00509

Aycan, M., Baslam, M., Asiloglu, R., Mitsui, T., and Yildiz, M. (2021). Development of new high-salt tolerant bread wheat (*Triticum aestivum* L) genotypes and insight into the tolerance mechanisms. *Plant Physiol. Bioch* 166, 314–327. doi:10.1016/j.plaphy.2021.05.041

Baltruschat, H., Fodor, J., Harrach, B. D., Niemczyk, E., Barna, B., Gullner, G., et al. (2008). Salt tolerance of barley induced by the root endophyte *Piriformospora indica* is associated with a strong increase in antioxidants. *New Phytol.* 180, 501–510. doi:10.1111/j.1469-8137.2008.02583.x

Bates, L. S., Waldren, R. P., and Teare, I. D. (1973). Rapid determination of free proline for water-stress studies. *Plant Soil* 39, 205–207. doi:10.1007/BF00018060

Bidyarani, N., Prasanna, R., Babu, S., Hossain, F., and Saxena, A. K. (2016). Enhancement of plant growth and yields in Chickpea (Cicer arietinum L) through novel cyanobacterial and biofilmed inoculants. *Microbiol. Res.* 188–189, 97–105. doi:10.1016/j.micres.2016.04.005

Cernusak, L. A., Winter, K., and Turner, B. L. (2010). Leaf nitrogen to phosphorus ratios of tropical trees: Experimental assessment of physiological and environmental controls. *New Phytol.* 185, 770–779. doi:10.1111/j.1469-8137.2009.03106.x

Chen, Y. H., Yang, X. Z., Li, Z., An, X. H., Ma, R. P., Li, Y. Q., et al. (2020). Efficiency of potassium-solubilizing *Paenibacillus mucilaginosus* for the growth of apple seedling. *J. Integr. Agr.* 19, 2458–2469. doi:10.1016/S2095-3119(20)63303-2

Etesami, H., Emami, S., and Alikhani, H. A. (2017). Potassium solubilizing bacteria (KSB): Mechanisms, promotion of plant growth, and future prospects - a review. *J. Soil Sci. Plant Nut* 17, 897–911. doi:10.4067/S0718-95162017000400005

Faisal Alharby, H. (2021). Using some growth stimuli, a comparative study of salt tolerance in two tomatoes cultivars and a related wild line with special reference to superoxide dismutases and related micronutrients. *Saudi J. Biol. Sci.* 28, 6133–6144. doi:10.1016/j.sjbs.2021.06.062

Falhof, J., Pedersen, J. T., Fuglsang, A. T., and Palmgren, M. (2016). Plasma Membrane H^+ -ATPase regulation in the center of plant physiology. *Mol. Plant* 9, 323–337. doi:10.1016/j.molp.2015.11.002

Fang, S., Hou, X., and Liang, X. (2021). Response mechanisms of plants under saline-alkali stress. *Front. Plant Sci.* 12, 667458. doi:10.3389/fpls.2021.667458

Feng, K., Cai, Z., Ding, T., Yan, H., Liu, X., and Zhang, Z. (2019). Effects of potassium-solubulizing and photosynthetic bacteria on tolerance to salt stress in maize. *J. Appl. Microbiol.* 126, 1530–1540. doi:10.1111/jam.14220

Ferreira, A., Ribeiro, B., Ferreira, A. F., Tavares, M. L. A., Vladic, J., Vidović, S., et al. (2019). Scenedesmus obliquus microalga-based biorefinery – from brewery effluent to bioactive compounds, biofuels and biofertilizers – aiming at a circular bioeconomy. *Biofuel, Bioprod. Bior* 13, 1169–1186. doi:10.1002/bbb.2032

Ghosh, U. K., Islam, M. N., Siddiqui, M. N., Cao, X., and Khan, M. A. R. (2022). Proline, a multifaceted signalling molecule in plant responses to abiotic stress: Understanding the physiological mechanisms. *Plant Biol.* 24 (2), 227–239. doi:10.1111/plb.13363

Grieve, C. M., and Poss, J. A. (2000). Wheat response to interactive effects of boron and salinity. *J. Plant Nutr.* 23, 1217–1226. doi:10.1080/01904160009382095

Gupta, G., Parihar, S. S., Ahirwar, N. K., Snehi, S. K., and Singh, V. (2015). Plant growth promoting rhizobacteria (PGPR): Current and future prospects for development of sustainable agriculture. *J. Microb. Biochem. Technol.* 7, 96–102.

Güsewell, S. (2004). N:P ratios in terrestrial plants: Variation and functional significance. *New Phytol.* 164, 243–266. doi:10.1111/j.1469-8137.2004.01192.x

He, J.-S., Wang, L., Flynn, D. F. B., Wang, X., Ma, W., and Fang, J. (2008). Leaf nitrogen: Phosphorus stoichiometry across Chinese grassland biomes. *Oecologia* 155, 301–310. doi:10.1007/s00442-007-0912-y

Hemavathi, U., C. P., Akula, N., Kim, H. S., Jeon, J. H., Ho, O. M., Chun, S. C., et al. (2011). Biochemical analysis of enhanced tolerance in transgenic potato plants overexpressing d-galacturonic acid reductase gene in response to various abiotic stresses. *Mol. Breed.* 28, 105–115. doi:10.1007/s11032-010-9465-6

Karthikeyan, N., Prasanna, R., Nain, L., and Kaushik, B. D. (2007). Evaluating the potential of plant growth promoting cyanobacteria as inoculants for wheat. *Eur. J. Soil Biol.* 43, 23–30. doi:10.1016/j.ejsobi.2006.11.001

Kerepesi, I., and Galiba, G. (2000). Osmotic and salt stress-induced alteration in soluble carbohydrate content in wheat seedlings. *Crop Sci.* 40, 482–487. doi:10.2135/cropsci2000.402482x

Kim, B.-H., Kang, Z., Ramanan, R., Choi, J.-E., Cho, D.-H., Oh, H.-M., et al. (2014). Nutrient removal and biofuel production in high rate algal pond using real municipal wastewater. *J. Microbiol. Biotechnol.* 24, 1123–1132. doi:10.4014/jmb.1312.12057

Kohler, J., Caravaca, F., Carrasco, L., and Roldán, A. (2007). Interactions between a plant growth-promoting rhizobacterium, an AM fungus and a phosphate-solubilising fungus in the rhizosphere of Lactuca sativa. *Appl. Soil Ecol.* 35, 480–487. doi:10.1016/j.apsoil.2006.10.006

Kumar, P., and Sharma, P. K. (2020). Soil salinity and food security in India. *Front. Sustain Food Syst.* 4. doi:10.3389/fsufs.2020.533781

Lee, J., Cho, D.-H., Ramanan, R., Kim, B.-H., Oh, H.-M., and Kim, H.-S. (2013). Microalgae-associated bacteria play a key role in the flocculation of Chlorella vulgaris. *Bioresour. Technol.* 131, 195–201. doi:10.1016/j.biortech.2012.11.130

Li, H., Zhao, Q., and Huang, H. (2019). Current states and challenges of salt-affected soil remediation by cyanobacteria. *Sci. Total Environ.* 669, 258–272. doi:10.1016/j.scitotenv.2019.03.104

Lin, Q. M., Rao, Z. H., Sun, Y. X., Yao, J., and Xing, L. J. (2002). Identification and practical application of silicate-dissolving bacteria. *Agric. Sci. China* 1, 81–85.

Liu, D. F., Lian, B., and Dong, H. L. (2012). Isolation of *Paenibacillus* sp and assessment of its potential for enhancing mineral weathering. *Geomicrobiol. J.* 29, 413–421. doi:10.1080/01490451.2011.576602

Liu, D., Liu, H., Wang, S., Chen, J., and Xia, Y. (2018). The toxicity of ionic liquid 1-decylpyridinium bromide to the algae Scenedesmus obliquus: Growth inhibition, phototoxicity, and oxidative stress. *Sci. Total Environ.* 622–623, 1572–1580. doi:10.1016/j.scitotenv.2017.10.021

Liu, H., Xia, Y., Cai, W., Zhang, Y., Zhang, X., and Du, S. (2017). Enantioselective oxidative stress and oxidative damage caused by Rac- and S-metolachlor to Scenedesmus obliquus. *Chemosphere* 173, 22–30. doi:10.1016/j.chemosphere.2017.01.028

Lu, R. (1999). *Agricultural chemistry analysis of soil*. Beijing: China Agricultural Science and Technology Press.

Maathuis, F. J. M., and Amtmann, A. (1999). K^+ nutrition and Na^+ toxicity: The basis of cellular K^+/Na^+ ratios. *Ann. Bot.* 84, 123–133. doi:10.1006/anbo.1999.0912

Mahanty, T., Bhattacharjee, S., Goswami, M., Bhattacharyya, P., Das, B., Ghosh, A., et al. (2017). Biofertilizers: A potential approach for sustainable agriculture development. *Environ. Sci. Pollut. R.* 24, 3315–3335. doi:10.1007/s11356-016-8104-0

Majeed, A., Abbasi, M. K., Hameed, S., Imran, A., and Rahim, N. (2015). Isolation and characterization of plant growth-promoting rhizobacteria from wheat rhizosphere and their effect on plant growth promotion. *Front. Microbiol.* 6, 198. doi:10.3389/fmicb.2015.00198

Maltas, A. S., Tavali, I. E., Uz, I., and Kaplan, M. (2022). Monitoring the effects of pH and EC regulated drip fertigation on microbial dynamics of calcareous soil in tomato (Solanum lycopersicum L) cultivation under greenhouse conditions in a Mediterranean climate. *Sci. Hortic.* 306, 111448. doi:10.1016/j.scienta.2022.111448

Munns, R., and Tester, M. (2008). Mechanisms of salinity tolerance. *Annu. Rev. Plant Biol.* 59, 651–681. doi:10.1146/annurev.arplant.59.032607.092911

Muñoz, R., and Guieysse, B. (2006). Algal–bacterial processes for the treatment of hazardous contaminants: A review. *Water Res.* 40, 2799–2815. doi:10.1016/j.watres.2006.06.011

Muthuraja, R., and Muthukumar, T. (2022). Co-inoculation of halotolerant potassium solubilizing Bacillus licheniformis and Aspergillus *violaceofuscus* improves tomato growth and potassium uptake in different soil types under salinity. *Chemosphere* 294, 133718. doi:10.1016/j.chemosphere.2022.133718

Pandey, S. S., Jain, R., Bhardwaj, P., Thakur, A., Kumari, M., Bhushan, S., et al. (2022). Plant probiotics – endophytes pivotal to plant health. *Microbiol. Res.* 263, 127148. doi:10.1016/j.micres.2022.127148

Prasanna, R., Jaiswal, P., and Kaushik, B. D. (2008). Cyanobacteria as potential options for environmental sustainability — Promises and challenges. *Indian J. Microbiol.* 48, 89–94. doi:10.1007/s12088-008-0009-2

Prasanna, R., Joshi, M., Rana, A., Shivay, Y. S., and Nain, L. (2012). Influence of co-inoculation of bacteria-cyanobacteria on crop yield and C–N sequestration in soil under rice crop. *World J. Microbiol. Bio Technol.* 28, 1223–1235. doi:10.1007/s11274-011-0926-9

Ramadoss, D., Lakkineni, V. K., Bose, P., Ali, S., and Annapurna, K. (2013). Mitigation of salt stress in wheat seedlings by halotolerant bacteria isolated from saline habitats. *Springerplus* 2, 6. doi:10.1186/2193-1801-2-6

Rana, A., Joshi, M., Prasanna, R., Shivay, Y. S., and Nain, L. (2012). Biofortification of wheat through inoculation of plant growth promoting rhizobacteria and cyanobacteria. *Eur. J. Soil Biol.* 50, 118–126. doi:10.1016/j.ejsobi.2012.01.005

Rengasamy, P. (2010). Soil processes affecting crop production in salt-affected soils. *Funct. Plant Biol.* 37, 613–620. doi:10.1071/FP09249

Renuka, N., Guldhe, A., Prasanna, R., Singh, P., and Bux, F. (2018). Microalgae as multi-functional options in modern agriculture: Current trends, prospects and challenges. *Biotechnol. Adv.* 36, 1255–1273. doi:10.1016/j.biotechadv.2018.04.004

Renuka, N., Prasanna, R., Sood, A., Ahluwalia, A. S., Bansal, R., Babu, S., et al. (2016). Exploring the efficacy of wastewater-grown microalgal biomass as a biofertilizer for wheat. *Environ. Sci. Pollut. Res.* 23, 6608–6620. doi:10.1007/s11356-015-5884-6

Robin, A. H. K., Matthew, C., Uddin, M. J., and Bayazid, K. N. (2016). Salinity-induced reduction in root surface area and changes in major root and shoot traits at the phytomer level in wheat. *J. Exp. Bot.* 67, 3719–3729. doi:10.1093/jxb/erw064

Rossi, F., Li, H., Liu, Y., and de Philippis, R. (2017). Cyanobacterial inoculation (cyanobacterisation): Perspectives for the development of a standardized multifunctional technology for soil fertilization and desertification reversal. *Earth Sci. Rev.* 171, 28–43. doi:10.1016/j.earscirev.2017.05.006

Sanyal, S. K., Rajasheker, G., Kishor, P. B. K., Kumar, S. A., Kumari, P. H., Saritha, K. V., et al. (2020). "Role of protein phosphatases in signaling, potassium transport, and abiotic stress responses," in *Protein phosphatases and stress management in plants: Functional genomic perspective*. Editor G. K. Pandey (Cham: Springer International Publishing), 203–232. doi:10.1007/978-3-030-48733-1_11

Simate, G. S., Cluett, J., Iyuke, S. E., Musapatika, E. T., Ndlovu, S., Walubita, L. F., et al. (2011). The treatment of brewery wastewater for reuse: State of the art. *Desalination* 273, 235–247. doi:10.1016/j.desal.2011.02.035

Singh, J. S., Kumar, A., Rai, A. N., and Singh, D. P. (2016). Cyanobacteria: A precious bio-resource in agriculture, ecosystem, and environmental sustainability. *Front. Microbiol.* 7, 529. doi:10.3389/fmicb.2016.00529

Singh, S. K., Sharma, H. C., Goswami, A. M., Datta, S. P., and Singh, S. P. (2000). *In vitro* growth and leaf composition of grapevine cultivars as affected by sodium chloride. *Biol. Plant* 43, 283–286. doi:10.1023/A:1002720714781

Subashchandrabose, S. R., Ramakrishnan, B., Megharaj, M., Venkateswarlu, K., and Naidu, R. (2013). Mixotrophic cyanobacteria and microalgae as distinctive biological agents for organic pollutant degradation. *Environ. Int.* 51, 59–72. doi:10.1016/j.envint.2012.10.007

Tang, X., He, L. Y., Tao, X. Q., Dang, Z., Guo, C. L., Lu, G. N., et al. (2010). Construction of an artificial microalgal-bacterial consortium that efficiently degrades crude oil. *J. Hazard Mater* 181, 1158–1162. doi:10.1016/j.jhazmat.2010.05.033

Tejada, M., Garcia, C., Gonzalez, J. L., and Hernandez, M. T. (2006). Use of organic amendment as a strategy for saline soil remediation: Influence on the physical, chemical and biological properties of soil. *Soil Biol. Biochem.* 38, 1413–1421. doi:10.1016/j.soilbio.2005.10.017

Wang, R., Wang, Y., and Chen, H. (2003). *Tobacco chemistry*. Beijing: China Agriculture Press.

Wang, Y. S., Tian, S. P., Xu, Y., Qin, G. Z., and Yao, H. (2004). Changes in the activities of pro- and anti-oxidant enzymes in peach fruit inoculated with Cryptococcus laurentii or Penicillium expansum at 0 or 20 °C. *Postharvest Biol. Tec.* 34, 21–28. doi:10.1016/j.postharvbio.2004.04.003

Wang, Y., Yan, X., Su, M., Li, J., Man, T., Wang, S., et al. (2022). Isolation of potassium solubilizing bacteria in soil and preparation of liquid bacteria fertilizer from food wastewater. *Biochem. Eng. J.* 181, 108378. doi:10.1016/j.bej.2022.108378

Xiao, Y., Wang, X., Chen, W., and Huang, Q. (2017). Isolation and identification of three potassium-solubilizing bacteria from rape rhizospheric soil and their effects on ryegrass. *Geomicrobiol. J.* 34, 873–880. doi:10.1080/01490451.2017.1286416

Yan, N., and Marschner, P. (2013). Response of soil respiration and microbial biomass to changing EC in saline soils. *Soil Biol. Biochem.* 65, 322–328. doi:10.1016/j.soilbio.2013.06.008

Zhang, H., Wu, X., Li, G., and Qin, P. (2011). Interactions between arbuscular mycorrhizal fungi and phosphate-solubilizing fungus (*Mortierella* sp) and their effects on *Kostelelzkya virginica* growth and enzyme activities of rhizosphere and bulk soils at different salinities. *Biol. Fert. Soils* 47, 543. doi:10.1007/s00374-011-0563-3

Frontiers in Environmental Science

TYPE Original Research
PUBLISHED 31 May 2023
DOI 10.3389/fenvs.2023.1154191

OPEN ACCESS

EDITED BY
Xing Yang,
Hainan University, China

REVIEWED BY
Manuel Miguel Jordán,
Miguel Hernández University of Elche,
Spain
Min Chen,
Zhejiang University, China

*CORRESPONDENCE
Aiju Liu,
✉ aijvliu@sdut.edu.cn
Hongliang Liu,
✉ emicrobe@sdut.edu.cn

RECEIVED 30 January 2023
ACCEPTED 12 May 2023
PUBLISHED 31 May 2023

CITATION
Dong M, Wang G, Gul Wazir Z, Liu J, Hou G, Gao X, Chao L, Rong F, Xu Y, Li M, Liu K, Liu A and Liu H (2023), The aggregation effect of organic matter on bauxite residue particles and its improvement mechanism.
Front. Environ. Sci. 11:1154191.
doi: 10.3389/fenvs.2023.1154191

The aggregation effect of organic matter on bauxite residue particles and its improvement mechanism

Mengyang Dong[1], Guizhen Wang[1], Zafran Gul Wazir[1], Jing Liu[1], Guoqin Hou[1], Xinyu Gao[2], Liang Chao[2], Fangxu Rong[1], Yuzhi Xu[2], Mingyue Li[2], Kai Liu[2], Aiju Liu[2]* and Hongliang Liu[3]*

[1]School of Agricultural Engineering and Food Science, Shandong University of Technology, Zibo, China, [2]School of Resources and Environmental Engineering, Shandong University of Technology, Zibo, China, [3]School of Life Sciences and Medicine, Shandong University of Technology, Zibo, Shandong Province, China

Introduction: Understanding organic amendment and the agglomeration of bauxite residue particles is vital to soil amelioration of bauxite residues. In this study, a pot culture experiment was conducted to illustrate the aggregation of organic amendment on bauxite residues particles and its improvement mechanism. The single organic amendment and its combination with soil inoculum were conducted to explore the aggregation effect of organic matter on bauxite residue particles, and its correlations with microbial rehabilitation.

Methods: The dry- and wet-sieving method were used to obtain different sizes of aggregates. The concentrations of soil organic carbon and iron and aluminum (Fe/Al) oxides in the forms extractable by DCB (Fe_d/Al_d) and oxalate (Fe_0/Al_0) were measured. Microbial rehabilitation after 180 days incubation was determined with the methods of Biolog Ecoplate™ and the high-throughput sequencing.

Results and Discussion: The results showed that over 180 days incubation, the alkalinity of bauxite residues was significantly decreased with the organic amendment based on the value of pH, EC and ESP (down to 9.26, 0.61 m/cm and 55.5%, respectively, in HS3). Secondly, organic amendment significantly promoted microbial community establishment and ecological function recovery. Moreover, the MWD value of aggregates also increased to 0.73 mm from the initial 0.32 mm, companied with the increase of the Fe/Al oxidizes. The further Pearson relationship analysis and the characterization of EPMA and SEM indicated that the organic matter and Fe/Al oxides played important roles in cementing fine bauxite residues particles and increasing aggregates stability, while this aggregation process was accelerated by the establishment of microbial ecology in bauxite residues. Therefore, organic amendment was more implication in soil amelioration of bauxite residues other than the directive modifications on alkalinity.

KEYWORDS

bauxite residue, soil amelioration, particle aggregation, iron-aluminum oxides, microbial community

1 Introduction

Aluminum plays a strategic role in economic development and national defense program. The extraction of alumina from bauxite by the Bayer Process is an important process for the production of strategic aluminum (Smart et al., 2016). However, due to the limitation of production technology, a large amount of high alkaline solid waste - bauxite residues is produced during alumina extraction (Kong et al., 2018). Globally, the cumulative inventory of bauxite residue is about 4.60×10^9 t, and the annual production has reached 2.00×10^8 t by 2018 (Zhu et al., 2016d; Xue et al., 2016). Moreover, bauxite residues are characterized by strong saline-alkalinity, heavy metals, fine particles size and poor agglomeration, which cause environmental risk to the surrounding environment and life of residents (Higgins et al., 2017; Di Carlo et al., 2020). Recently, increasing investigations proved that the ecological landscape construction with various organic and inorganic amendments was considered a promising approach for the reclamation of bauxite residues on a large scale and to reduce its potential environmental risks (Courtney et al., 2013; Zhu et al., 2016a; Xue, 2019). However, the characteristics of strong alkalinity, poor aggregate structure, and low organic matter content are still the big challenges facing soil amelioration of bauxite residues, which defines the following reclamation of bauxite residues disposal site (Di Carlo et al., 2019b; You et al., 2019).

In practice, soil aggregates are important to ensure that soil remains structured and consistent, which play a key role in soil water and fertilizer conservation, enzyme activity regulation, and air permeability (Wilpiszeski et al., 2019). So that, the aggregation of bauxite residue clays is a key step to promote the soil amelioration of bauxite residue, although the transformation of bauxite residue into a plant-established soil-like medium, also known as bauxite residue soil amelioration, usually undergoes a series of physical, chemical, and biological processes (Goloran et al., 2017; Xue, 2019). In fact, the optimization of the aggregate structure, improvement of organic nutrients, and microbial restoration are all necessary for soil amelioration of bauxite residues (Tian et al., 2020). However, the aggregation of bauxite residue clays, the same to its alkalinity regulation, is a limiting step for the ecological reclamation of bauxite residues (Jones et al., 2012b; Courtney et al., 2013; Xue et al., 2019e). It showed that the natural weathering could improve the physical structure of bauxite residue (Zhu et al., 2016a), with the aggregate formation and plant growth (Santini and Fey, 2013), but this soil amelioration process could be speeded up with some improvement measures (Bray et al., 2018). For example, Zhu *et al.* (2017) found that the addition of organic matter and Ca^{2+} can reduce bauxite residue's pH, promote the formation and stability of macro aggregate particles in the bauxite residue matrix. The single addition of organic matter also could drive the agglomeration of bauxite residue particles, improve the bauxite residue's structure, and promote microbial rehabilitation and then soil development (Wang et al., 2014; Tian et al., 2020).

In addition, microorganism, as an important part of soil ecosystem, regulating energy flow and material circulation, also plays a key role in soil amelioration of bauxite residue (Ke et al., 2021). It was proved that the rehabilitated microorganisms could produce or excrete various functional metabolites, including organic/inorganic acids, and extracellular polymers, which could neutralize bauxite residues' alkali and bind fine bauxite residues' particles into the larger and stable aggregates (Di Carlo et al., 2020; Redmile-Gordon et al., 2020). This is beneficial to regulate the alkalinity and salinity, increase the agglomeration of micro-particles, and lastly promote the rehabilitation of bauxite residue (Xue et al., 2019f; Ke et al., 2021). Previous studies have shown that the assembly and succession of fungal flora in rehabilitated bauxite residue were also driven by the improvement of texture structure and fertility and the decrease of alkalinity of bauxite residue matrix (Dong et al., 2021). Nevertheless, there is still necessary to give more investigation on the comprehensive improvement of organic amendment on the aggregate formation and microbial community restoration in bauxite residue.

The object of this study is to explore the effect of organic matter addition on the agglomeration of bauxite residue particles, and its correlations with microbial rehabilitation during the bauxite residues amelioration process. The pyroligneous acid extracted from corn stalk was chosen as the organic matter amendment, and the campus soil was used as a microbial source. Soil culture experiment was used to evaluate the soil amelioration effect of organic matter on bauxite residue by analyzing the dynamic changes of salinity, aggregate structure, functional microbial community, and other indexes of the improved matrix with different incubation times. We hope to provide theoretical support for the large-scale ecological disposal of bauxite residue by this study.

2 Materials and methods

2.1 Materials preparation and experimental design

The bauxite residue used in this study was provided by the Shandong branch of Chinalco Limited in Zibo, China (118.05686°E, 36.761111°N). The 0–30 cm samples from the bauxite residue disposal site, and transported to the laboratory in polyethylene bags. After natural air-dried, all samples were passed through a 2 mm sieve for the next analysis and cultural experiment. The organic matter extracted from corn stalk, provided by Aoke New Material Technology Company Limited in Shanghai, China, was used as an organic amendment which ingridents were shown in Supplementary Table S1. The surface soil (0–20 cm) of the campus was used as a microbial inoculum added in bauxite residue. The soil was silty loam with pH 8.51, organic matter 57.1 mg/g, and electrical conductivity 0.11 m/cm.

Seven treatments were prepared: 1) CK, unamended bauxite residues; 2) H1, amended with 1% organic matter; 3) H2, amended with 2% organic matter; 4) H3, amended with 3% organic matter; 5) HS1, amended with 1% organic matter and 5% soil; 6) HS2, amended with 2% organic matter and 5% soil; 7) HS3, amended with 3% organic matter and 5% soil. Triplicates were performed for each treatment. All treatments were placed outside in flowerpots (h × ø: 150 mm × 200 mm) with aerated holes at the bottom, cultured outside and irrigated regularly to maintain a humidity (75% or so of the maximum water holding capacity). At 0, 10, 30, and 180 days of incubation, five samples were collected from each pot and mixed as one sample. Each mixed sample was divided into two parts. One part was air-dried for the physical and chemical properties analysis, while the remaining fresh samples were stored at 4°C for microbial analysis.

2.2 Physico-chemical properties analysis

The pH and electrical conductivity (EC) of bauxite residue samples were determined in the extraction solution of deionized

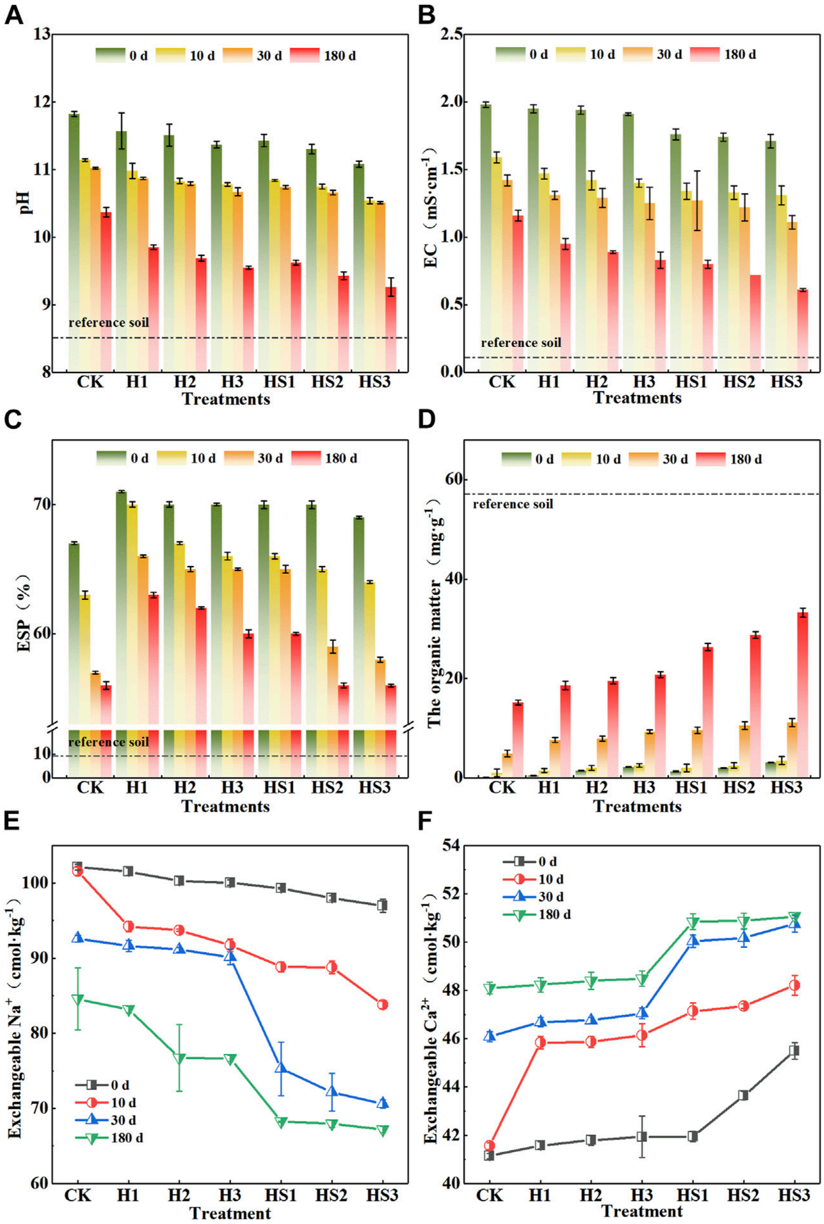

FIGURE 1
Physico-chemical characteristics of different bauxite residue samples **(A)**, pH; **(B)**, EC; **(C)**, ESP; **(D)**, the organic matter; **(E)**, exchangeable Na+ content; **(F)**, exchangeable Ca2+ content.

water with a solid: liquid ratio of 1:5 (Banning et al., 2014). The organic matter was determined by hydrated heat potassium dichromate oxidation-colorimetric method (Wu et al., 2015). The exchangeable cations (i.e., K^+, Na^+, Ca^{2+}, and Mg^{2+}) were extracted by 1 M CH_3COONH_4 (pH 7.0). Free iron oxide (Fe_d) and free alumina (Al_d) were extracted by the dithionite-citrate-bicarbonate (DCB) method, and amorphous iron oxide (Fe_o) and amorphous alumina (Zhu et al., 2018) were extracted by the ammonium oxalate method (Zhu et al., 2016b). The exchangeable cations and the contents of the iron and aluminum oxide in the solution were determined using an Inductively coupled plasma atomic emission spectrometer (ICP-AES, Optima 5300DV, Perkin Elmer). In addition, the cation exchange capacity (Nannipieri et al., 2003) is calculated using the sum of exchangeable cations, and the exchangeable sodium percentage (Vázquez et al., 2020) was calculated by the percentage of exchangeable Na^+ content in total exchangeable cations (Zhu et al., 2016c; Li et al., 2018).

2.3 Microbial community diversity and functional analysis

Biolog EcoPlate™ (Biolog Inc., Hayward, CA, United States) was used to measure the microbial community level physiological profiles

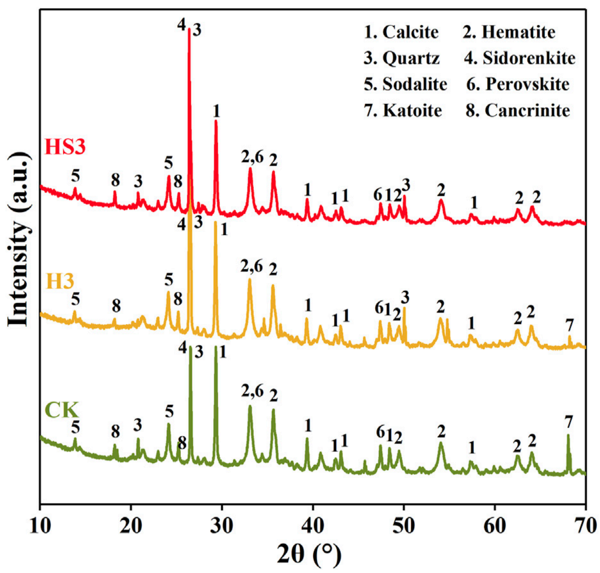

FIGURE 2
XRD patterns of bauxite residue before and after amendment.

(CLPP), and the absorbance data of the plate were measured regularly every 12 h at 590 nm for 7 days. Then the average well color development (AWCD) and microbial functional diversity indexes (Shannon-Wiener (H') and Simpson (D)) were calculated (Feigl et al., 2017).

Microbial community composition and diversity were determined by the high-throughput sequencing. Use the E.Z.N.A. ®Stool DNA Kit (D4015, Omega, Inc., United States) to extract bacterial and fungal DNA from bauxite residue samples according to the instructions. The V3-V4 region of bacterial 16S rDNA was amplified by the polymerase chain reaction (PCR), and the primer sequences were 341F (5′-CCTACGGGNGGCWGCAG-3′) and 805R (5′-GACTACHVGGGTATCTAATCC-3′). The ITS1 gene was amplified by the PCR with primers fITS7 (5′-GTGART-CATCGAATCTTTG-3′) and ITS4 (5′-TCCTCCGCT-TATTGA TATG-3′). The purification and recycling of the PCR products were conducted with AMPure XT beads (Beckman Coulter Genomics, Danvers, MA, United States). And then, Qubit® 2.0 DNA kit was used to accurately quantify the DNA obtained. Illumina Hiseq/Miseq PE300 sequence platform (provided by Hangzhou Lianchuan Biotechnology Co., LTD.) was used for the sequencing analysis of the obtained DNA. High quality sequences were obtained by splicing, filtering, eliminating chimera, and discarding low quality sequences, and used for classification of the operational taxon (OTU), diversity index calculation, and species abundance analysis.

2.4 Aggregate stability analysis

The distribution of aggregates particles size was determined by dry and wet sieving methods respectively (Le Bissonnais, 1996). The mean weight diameter (MWD), geometric mean diameter (GMD), and the proportion of aggregate destruction (PAD) were selected as parameters to evaluate the aggregate stability of bauxite residue. The calculation formulas are as follows:

$$MWD = \sum_{i=1}^{n} \overline{X_i} \times W_i$$

$$GMD = exp\left(\sum_{i=1}^{n} W_i \, ln \, X_i \Big/ \sum_{i=1}^{n} W_i\right)$$

$$PAD\,(\%) = (W_d - W_w)/W_d \times 100$$

Where, X_i is the mean diameter over each particle-size (mm), W_i is the percentage of aggregates in that size range (Six *et al.*), n is the number of sieves, W_d is the proportion of >0.25 mm aggregates in dry sieving (Six *et al.*), W_w is the proportion of >0.25 mm aggregates in wet sieving (Six *et al.*).

2.5 Morphological and mineral composition analysis

Scanning electron microscopy (SEM, Quanta 200 FEG, FEI, American) and electron probe micro-analyzer (EPMA, Oxford INCA Energy 350, United Kingdom) were used to reveal the microstructure and element distribution of different bauxite residue treatments. The mineral composition of different bauxite residue samples was analyzed by X-ray diffraction (XRD, D8 Advance, Bruker, German).

2.6 Data analysis

All raw data were calculated in Microsoft Excel 2019. One-way analyses of variance (ANOVAs) for different treatments using SPSS 19.0. Redundancy analyses (RDAs) were analyzed using Canoco 5. All figures were drawn using Origin 8.0.

3 Results

3.1 Improvement on residues properties

The strong alkalinity, high salt content and nutrient deficiency are the key factors restricting the ecological large-scale disposal of bauxite residues (Wu et al., 2021). As shown in Figures 1A,B, organic amendment process significantly mitigated the alkalinity and salty of bauxite residues as the pH and EC in each amended treatment were lowered compared to the CK treatment, and over 180 days incubation, they were respectively down to 9.26 and 0.61 m/cm in HS3 treatments. However, no significant decrease in ESP was not determined as the organic amendment when compared the CK treatments, although over 180 days incubation the ESP was significantly decreased in each the treatment (Figure 1C). Finally, with the organic amendment, the total organic carbon increased significantly in each organic amended treatments, and it was even up 66.51 mg/kg in HS3 treatment (Figure 1D). Whatever, in comparison, the combined improvement of organic amendment and soil inoculum on bauxite residues is better than that of the single organic amendment, though there was still not rehabilitated to the level of the natural soils.

Different from ESP, organic amendment significantly decreased the content of exchangeable Na^+, and it was down to 67.17 cmol/kg in HS3 after 180 days incubation. In addition, the content of exchangeable

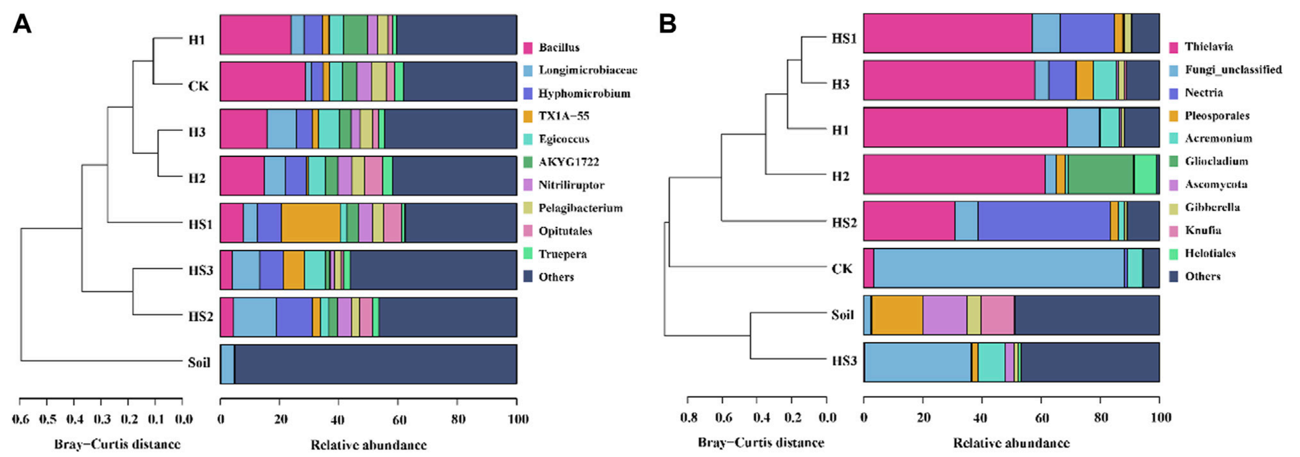

FIGURE 3
Cluster analysis of community compositions of **(A)** bacteria and **(B)** fungi based on the relative abundance.

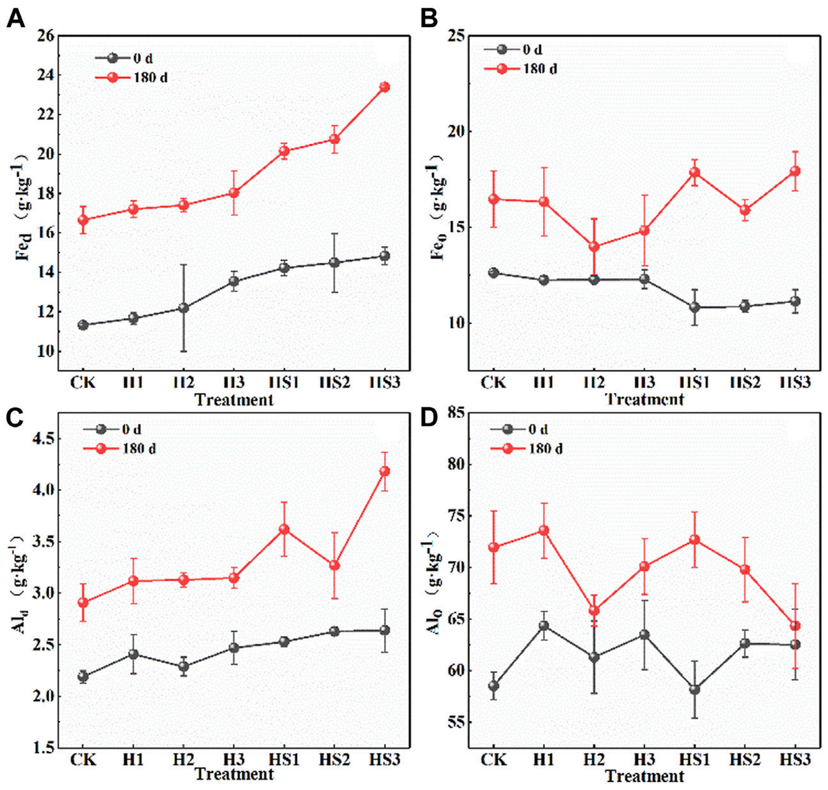

FIGURE 4
Iron-aluminium oxide contents in bauxite residue samples **(A)**, Fed content; **(B)**, Feo content; **(C)**, Ald content; **(D)**, Alo content.

Ca^{2+} showed a continuous increase with the incubation extension, especially in the organic amended treatment. For example, the concentration of exchangeable Ca^{2+} increased from the initial 41.14 cmol/kg to 51.06 cmol/kg in HS3 over 180 days incubation. Moreover, the further XRD analysis indicated that the peak of the alkali mineral phases, such as Calcite ($CaCO_3$) and Katoite ($Ca_3Al_2(SiO_4)(OH)_4$) decreased significantly both in Hs and HS3 treatments (Figure 2). That is, it could speculate that organic amendment decreased the pH, which led to the release of Ca^{2+} from Calcite ($CaCO_3$) and Katoite, etc., the alkali mineral phase. The released Ca^{2+} can not only precipitate with the basic anions of bauxite residue, but also exchange with the bound Na^+ by the bauxite residue particles, which in turn effectively improved the alkalinity of bauxite residues (Xue et al., 2019d).

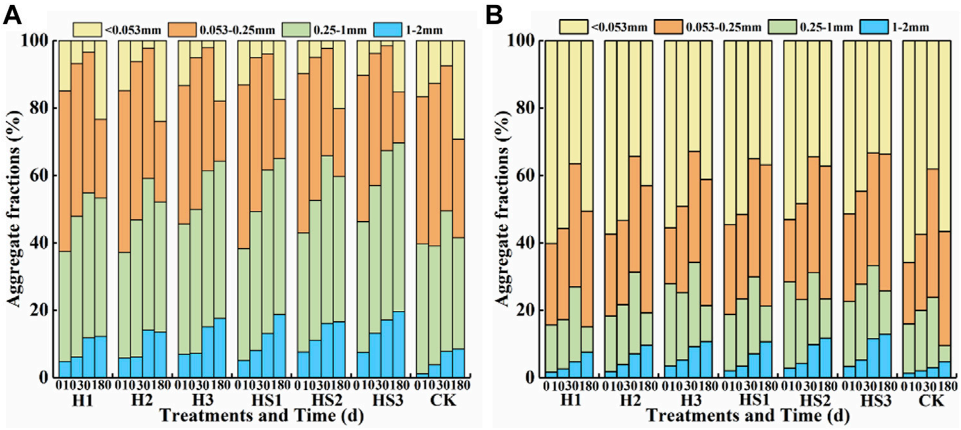

FIGURE 5
Percentage distribution (%) of aggregate sizes (mm) in different residue samples **(A)**, dry sieving; **(B)**, wet sieving.

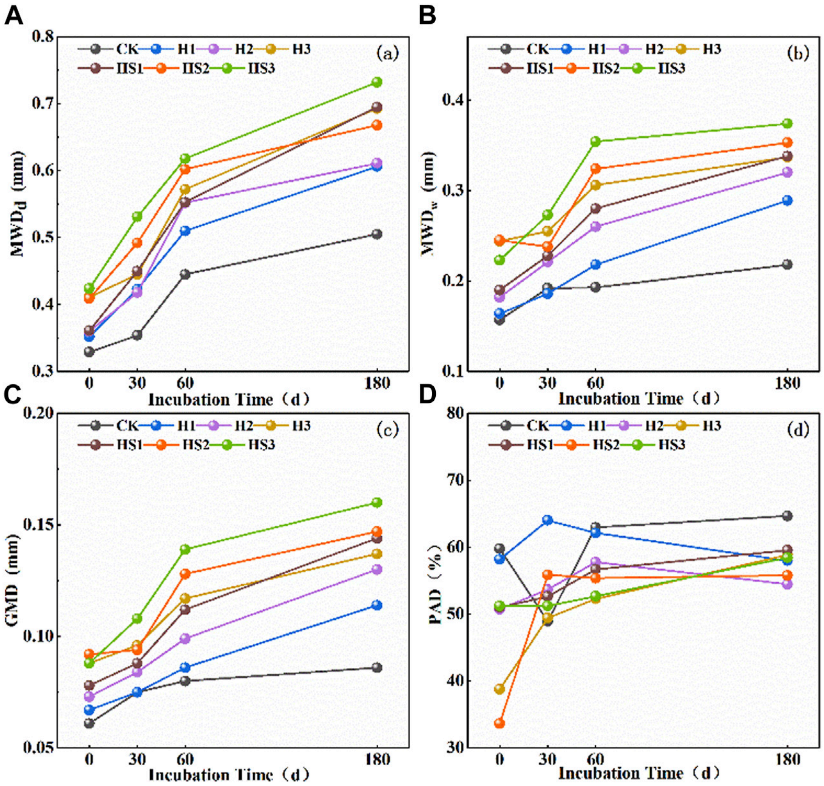

FIGURE 6
Changes in aggregate stability of the treated residues following amendment additions **(A)**, MWDd under dry sieving; **(B)**, MWDw under wet sieving; **(C)**, GMD; **(D)**, PAD in different residue samples.

3.2 Restoration of microbial function and community diversity

The changes of microbial functional diversity in amended bauxite residue were measured by using the community level physiological profile at 0 and 180 days of incubation (Table 1). The microbial activity of fresh bauxite residue was low as the AWCD value was only 0.02. After 180 days incubation, the AWCD and the diversity index (H′ and D), indicating microbial function diversity, were significantly ($p < 0.05$) higher in each amended treatment than those of CK (Table 1), and in the HS treatments, the values of AWCD and H' index was

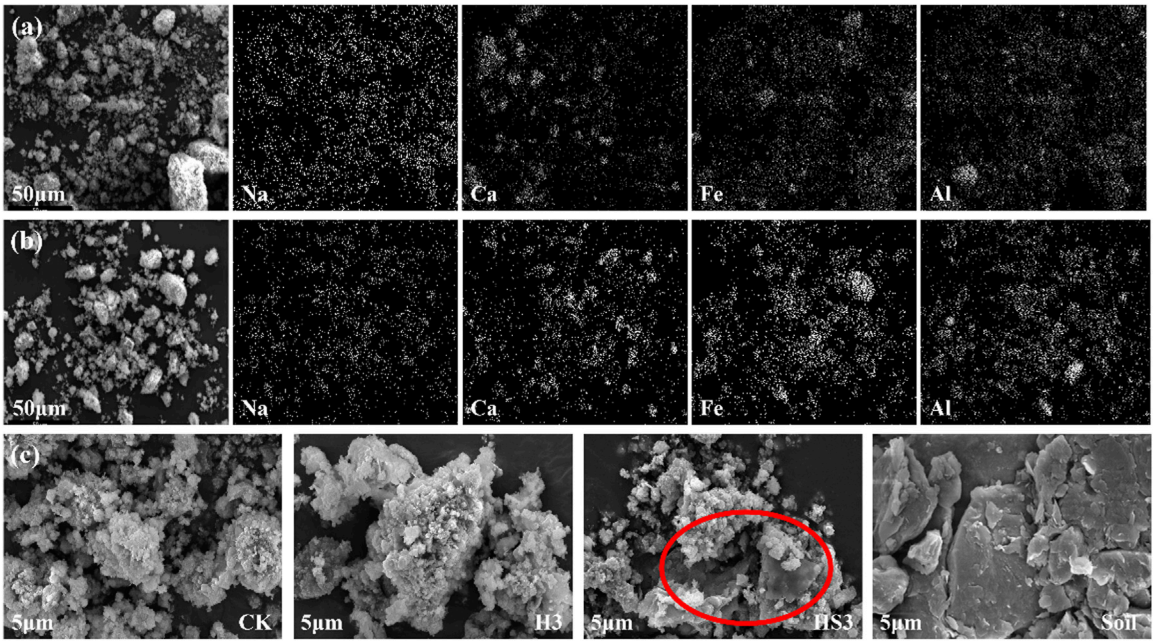

FIGURE 7
The morphology of **(C)** different treatments and elemental mapping images of **(A)** CK and **(B)** HS3.

TABLE 1 Functional diversity index of bauxite residue microbial community.

Index	Fresh bauxite residue	Amended treatment					
		H1	H2	H3	HS1	HS2	HS3
AWCD	0.02c	1.05b	1.06b	1.07b	1.07b	1.11a	1.12a
H'	1.93f	3.12e	3.17c	3.19b	3.14d	3.22a	3.21a
D	0.72b	0.95a	0.96a	0.95a	0.96a	0.96a	0.97a

up to 1.12 and 3.21 respectively, which also significantly higher than the single organic amended treatments. It suggested that the co-addition of soil inoculum was more beneficial to microbial function recovery than the single organic amendment.

The further high-throughput sequencing analysis indicated that organic amendment promotes the rehabilitation of microbial community. Firstly, over 180 days incubation, whatever for bacteria or fungal community, the Chao1 index in organic amended treatments were all significantly ($p < 0.05$) higher than that of CK treatment (Table 2), indicated that organic amendment could significantly improve microbial community richness of bauxite residues, although there was still far from the microbial community richness of natural soils. Moreover, in most cases, the Shannon index or Simpson index in the organic amended treatments were significantly from that in the CK treatment, indicated that a significant increase of microbial community diversity in bauxite residues as the organic amendment. It suggested that organic amendment could make bauxite residues suitable for the colonization of various microorganism. However, different from the improvement effect on the physical and chemical properties of bauxite residues, the promotion of organic amendment and soil inoculum was not significantly better than the single organic amendment for bacterial or fungal community colonization in bauxite residues, according to their indexes of Chao1, Shannon and Simpson (Table 2).

Cluster analysis was performed on the 10 most abundant bacterial and fungal genera in each treatment (Figure 3). The different community composition in bacteria and fungi was determined between the organic amended treatments and the CK treatment. Moreover, in contrast to CK treatment, the abundance of *Bacillus*, *Halomonas*, *Egicoccus*, and *Nitriliruptor,* which are all halotolerant or halophilic to the high salinity-alkali environment (Zhao et al., 2022), were decreased, while some acidogenic strains, such as *Pseudomonas*, *Acidobacteria_unclassified*, and *Acremonium* (Schmalenberger et al., 2013), were increased in the amendment treatments. In short, as the increase of added organic matter, cluster analysis indicated that bacterial and fungal composition at the genus level in the bauxite residue became gradually closer to that of the reference soil (Figure 3).

TABLE 2 Difference of alpha diversity between bauxite residue treatments and the natural soils.

Treatment	Bacteria			Fungal		
	Chao1	Shannon	Simpson	Chao1	Shannon	Simpson
CK	531.9c	6.54c	0.97b	58.0bc	1.05e	0.29c
H1	684.0b	6.87bc	0.97b	45.5c	1.94d	0.46bc
H2	667.5b	7.06b	0.98ab	76.3bc	2.21d	0.51b
H3	764.7b	7.12b	0.97ab	101.4b	2.76c	0.72ab
HS1	736.7b	7.13b	0.98ab	112.4b	2.98c	0.66b
HS2	710.5b	7.17b	0.98ab	117.9b	2.74c	0.64b
HS3	780.2b	7.31b	0.98ab	66.2bc	4.27b	0.91a
Soil	2778.0a	10.50a	1.00a	499.2a	6.11a	0.95a

Note: the letters a, b, c, d, e, f indicates whether there was a significant difference among the bauxite residues' treatments at a 0.05 level by the ANOVA.

3.3 Aggregate size distribution and aggregate stability

Iron and aluminum oxides and organic matter are the basic components of soil complex, which can significantly affect soil structure and aggregates composition through cementation (Six et al., 2004). So that, to illustrate the improvement effect of organic amendment on the aggregation of bauxite residues particles, the present study determined the content of free and amorphous iron and aluminum oxides between the different bauxite residues treatments and their variation along the incubation (Figure 4). As shown in Figures 4A,C, in most cases, organic amendment increased the content of iron and aluminum oxides, especially for the free iron and aluminum oxides, which showed a significantly increase with organic amendment and it was particularly significant over 180 days incubation. However, no significant increase was almost not determined for amorphous iron and alumina with the amendment of organic matter, although there was an obvious increase in most treatments after 180 days incubation (Figures 4B,D).

Accordingly, the aggregation effect of organic amendment on bauxite residues particles was observed in different treatments at each incubation stage (Figure 5). Based on the dry sieve analysis of aggregates, the proportion of >0.25 mm aggregates increased, whilst it decreased markedly for the component of <0.25 mm aggregates, especially for those of <0.05 mm micro-aggregates, in each organic amended treatment; In addition, under wet sieving, the proportion of >0.05 mm aggregates with water stability also increased markedly, especially for macro-aggregates of 1–2 mm. That is, in the CK treatment the aggregates of <0.05 mm accounted for 65.86%, while in the organic amendment treatments, the proportion of 1–2 mm and 0.05–0.25 mm aggregates in HS3 treatment increased to 11.54% and 36.26%, respectively. Moreover, as shown in Figure 6A-C, the MWD and GMD of bauxite residue particles, whatever calculated according to the dry or the wet sieve analysis, all showed a markable increase with the amendment of organic matter and soil inoculum; and with the incubation extension, they increased up to 0.73 mm (MWDd), 0.37 mm (MWD_w) and 0.16 mm (GMD). In addition, after 180 days incubation, the PAD of the aggregates in organic amended treatments showed a markable decrease comparted to the CK treatment (Figure 6D). The results showed that the addition of organic matter had an improvement on aggregation of bauxite residues as well as the water stability of the aggregates, and this improvement with the co-addition of soil inoculum was more significant for the water stability of aggregates.

3.4 Aggregation mechanism of bauxite residue particles

As shown in Figures 6A,B, the distribution of the element Na was distinctly reduced while Ca elements was obviously increased on the particles' surface of the HS3 treatments compared with CK treatment. This is well agreed with the results of the exchange Na^+ and Ca^{2+} (Figures 1E,F) and the XRD results that the peak of the mineral phase Calcite and Katoite decreased in bauxite residues as the organic amendment (Figure 2). Moreover, the EMPA images also indicated that Na was evenly distributed in small particles, while Ca was distributed in large particles (Figures 6A,B). This result might suggest that the increased Ca promoted the aggregation of bauxite residue particles. As for the distribution images of the elements Fe and Al (Figures 6A,B), there was a clear increase with organic amendments (HS3) in contrast to the CK treatment. This is the same to the results of Fe-Al oxides analysis (Figure 4). At the same time, the elements of Al and Fe were more densely distributed on the large aggregates of bauxite residues, especially after treated with organic amendment (Figure 6B), which suggested that organic amendment could promote the formation of the aggregate through the cementation of Fe-Al oxides. The further correlation analysis also proved that the Fe-Al oxides and organic carbon had positive relationships with the aggregates size over >1mm, while were negatively relative to the PAD of aggregates (Supplementary Figure S2).

Figure 6C showed the morphology of bauxite residue particles in different treatments over a 180 days incubation. As shown in Figure 6C, in the unamended bauxite residues (CK), it has a loose microstructure and mainly consists of fine particles and detritus; while for the H3 treatment with a single organic amendment, the flocculation of bauxite residue particles was distinctive in contrast to the CK treatment as the loose large particles became the main component of bauxite residues matrix. Moreover, in HS3 treatment with the organic amendment and soil inoculum, the bauxite residue aggregates began to appear obvious flake structure, and its texture became denser in contrast to the H3 treatments, which was called the formation of large aggregates and began to appear soil-like structure (Li et al., 2019). This gradual improvement in bauxite residues' aggregates from the CK to the H3 and then HS3 suggested that microbial community should play an important role on the agglomeration of bauxite residue particles by the entanglement of hyphae, when considering the closer fungal composition between the HS3 treatments and the reference soils (Figure 3B).

4 Discussion

Despite high alkalinity, the soil amelioration of bauxite residues are also restricted by fine powder particles and poor fertility (Xue et al., 2019c). Therefore, the formation of stable aggregates and accumulation of organic matter were considered to be a key step to the soil amelioration of bauxite residues and the subsequent successful establishment of ecological system (Courtney et al., 2014b). Organic amendment was proved effective to improve the matrix structure of bauxite residues by increasing porosity, and improving aggregate stability (Jones et al., 2012a; Courtney et al., 2013). But few studies illustrated the improvement mechanism of organic amendments on bauxite residues. In the present study, we mainly investigated the promotion of organic amendments on the agglomeration of bauxite residue particles and its possible mechanisms.

Firstly, organic amendment in the present study effectively decreased pH, EC, and ESP of bauxite residue, especially with incubation extension (Figures 1A–C), which is similar to the previous studies (Banning et al., 2011; Haynes and Zhou, 2019). As all known, the high alkalinity and salinity is not a big obstacle to the rehabilitation of bauxite residues (Ruyters et al., 2011; Anam et al., 2019), but also causes great problems on the agglomeration of bauxite residue particles, as the highly active Na^+ could cause the dispersion of the colloidal double layer, and lead to the disintegration of aggregates and the dispersion of clay particles (Kong et al., 2017). At the same time, we determined a more significant decrease of exchangeable Na^+ in bauxite residues with the organic amendment and the distinct increase of exchangeable Ca^{2+} (Figures 1E,F) as well as the changes in mineral phases of bauxite residues (Figure 2). It was proved that the small organic acids from the organic amendment biodegradation could accelerate the dissolution of the alkaline minerals, including Calcite ($CaCO_3$) and Katoite ($Ca_3Al_2(SiO_4)$ $(OH)_4$), in the bauxite residues (Di Carlo et al., 2019a; Di Carlo et al., 2019b), and resulted in the increase of the exchangeable Ca^{2+}, which is beneficial to the aggregation of the fine bauxite residues clays as the clay absorbed Na^+ is removed by the exchanger of Ca^{2+} (Power et al., 2011; Gupta et al., 2019). In the present study, according to the changes of the exchangeable Na^+ and Ca^{2+} with organic amendment and over incubation (Figures 1E,F) as well as the results of XRD (Figure 2), the similar process should have occurred as the organic amendment has various organic acids (Supplementary Table S1), too.

Microorganisms are thought to play important roles in cementing different particles into through the cementing, winding, and wrapping of metabolites (such as extracellular polymers, polysaccharides, *etc.*), mycelium, and dead cells debris (Santini et al., 2015b). Beside of the improvement on bauxite residues' properties, the organic amendment can also increase the nutrient content of the bauxite residue matrix, and then accelerated the colonization of some pioneer microbial strains as well as the further microbial community establishment in the amended bauxite residues (Santini et al., 2015a; Bray et al., 2018), (Courtney et al., 2014a; Yang et al., 2020). In the present study, in contrast to the CK treatment, a significant increase was also found in microbial functional activities (Table 1) and communities' richness and diversity for the organic amendment treatments, especially after 180 days incubation (Table 2). Moreover, with the organic amendment, some reported pioneer organisms, such as the halophilic alkalophilic bacteria *Ascomycota*, *Basidiomycota*, *Actinomycota*, *Proteobacteria,* and *Bacillus* (Liu et al., 2014; Dong et al., 2021), decreased over incubation, and the appearance of some acidogenic organisms, such as *Pseudomonas*, *Acidobacteria_unclassified*, and *Acremonium* (Schmalenberger et al., 2013), compared to the CK treatments. Villar *et al.* (2004) found that the polysaccharide secreted by microorganisms and the winding effect of fungal hyphae made soil particles better aggregate. Studies had shown that microbial decomposition of organic matter produced polysaccharides, which could effectively cemented bauxite residue particles by ionic and hydrogen bonds of free hydroxyl groups (Santini et al., 2015b). So that, stimulating microbial rehabilitation in bauxite residues should be an effective way for organic amendment to promote the agglomeration of bauxite residue particles. This could be proved by the closer bacterial and fungal flora to the reference soils (Figure 3B), companied with the appearance of the soil-like large aggregates in the HS3 treatments (Figure 7B). Qu *et al.* (2019) found that bacteria and fungi could dissolve the fine particles (mainly iron oxide) in bauxite residue, producing the layered structure of bauxite residue.

Soil organic carbon and Fe/Al oxides are the main cementing agents in the formation of soil aggregates (Xue et al., 2019a; Xue et al., 2019b). A significant increase of the total organic carbon and Fe/Al oxides occurred in the organic amended treatments in contrast to the CK treatment (Figure 4), which was all proved to be positive relationship with the aggregates size over >1mm, and negatively relative to the PAD of aggregates (Supplementary Figure S2). This result agreed with the previous studies that the cohesion between aggregates from the SOC and Fe/Al oxides could reduce the breakdown of hydraulic and air pressures to aggregates (Zhao et al., 2017; Pituello et al., 2018; Du et al., 2022). In addition, companied with the transform of the aggregates' morphology from the loose microstructure (CK) to a soil-like structure appearance (HS3) (Figure 7C), there was a markable increase for the distribution of Ca, Fe and Al elements on the aggregate surface (Figures 7A,B). It showed that Ca^{2+} had a good affinity with the soil colloidal surface, which could reduce the dispersion of clays, and promote the flocculation and stability of aggregates (Harris and Rengasamy, 2004; Xue et al., 2021). So that, beside of the directive cohesion between aggregates, Increasing the level of Fe/Al oxides and Ca^{2+} also is principal way for organic amendment to promote the aggregation of fine bauxite residue particles.

5 Conclusion

In the present study, the aggregation effect of organic matter on bauxite residue was investigated with a pot experiment. It was found that, in addition to the improvement on the alkalinity and the promotion on microbial recovery, the proportion and size of bauxite residues' aggregates were significantly increased with organic amendments. Moreover, the further analysis of Fe/Al oxides, EMPA characterization as well as the micromorphology showed that beside of the directive cohesion between aggregates, the increase of Ca^{2+} and Fe/Al oxides should play important roles in the improvement of organic amendment on the agglomeration of bauxite residue particles; and the rehabilitation of microbial community and ecological function could accelerate the large aggregates formation in the organic amended bauxite residues. Based on this study, it could be seen that organic matter amendment was an effective measure for the improvement of bauxite residues aggregates formation.

Data availability statement

The original contributions presented in the study are included in the article/Supplementary Materials, further inquiries can be directed to the corresponding authors.

Author contributions

MD: Data curation, Writing-original draft. ZW, English improvement and modification; GW, JL, GH, XG, LC and FR: Visualization and Investigation. KL, YX, and ML: Reviewing and Validation. HL: Visualization and Editing. AL: Conceptualization, Methodology. All authors contributed to the article and approved the submitted version.

Funding

The work was supported by the National Natural Science Foundation of China (NSFC) under Grant No. 42077129, No.42177403 and No. 41877122; and Natural Science Foundation of Shandong Province under Grant No. ZR2020ZD19 and No. ZR2022YQ34.

Conflict of interest

The authors declare that the research was conducted in the absence of any commercial or financial relationships that could be construed as a potential conflict of interest.

Publisher's note

Supplementary material

The Supplementary Material for this article can be found online at: https://www.frontiersin.org/articles/10.3389/fenvs.2023.1154191/full#supplementary-material

References

Anam, G. B., Reddy, M. S., and Ahn, Y. H. (2019). Characterization of Trichoderma asperellum RM-28 for its sodic/saline-alkali tolerance and plant growth promoting activities to alleviate toxicity of red mud. *Sci. Total Environ.* 662, 462–469. doi:10.1016/j.scitotenv.2019.01.279

Banning, N. C., Phillips, I. R., Jones, D. L., and Murphy, D. V. (2011). Development of microbial diversity and functional potential in bauxite residue sand under rehabilitation. *Restor. Ecol.* 19, 78–87. doi:10.1111/j.1526-100x.2009.00637.x

Banning, N. C., Sawada, Y., Phillips, L. R., and Murphy, D. V. (2014). Amendment of bauxite residue sand can alleviate constraints to plant establishment and nutrient cycling capacity in a water-limited environment. *Ecol. Eng.* 62, 179–187. doi:10.1016/j.ecoleng.2013.10.034

Bray, A., Stewart, D., Courtney, R., Rout, S., Humphreys, P., Mayes, W., et al. (2018). Sustained bauxite residue rehabilitation with gypsum and organic matter 16 years after initial treatment. *Environ. Sci. Technol.* 52, 152–161. doi:10.1021/acs.est.7b03568

Courtney, R., Feeney, E., and O'Grady, A. (2014a). An ecological assessment of rehabilitated bauxite residue. *Ecol. Eng.* 73, 373–379. doi:10.1016/j.ecoleng.2014.09.064

Courtney, R., Harrington, T., and Byrne, K. A. (2013). Indicators of soil formation in restored bauxite residues. *Ecol. Eng.* 58, 63–68. doi:10.1016/j.ecoleng.2013.06.022

Courtney, R., Harris, J. A., and Pawlett, M. (2014b). Microbial community composition in a rehabilitated bauxite residue disposal area: A case study for improving microbial community composition. *Restor. Ecol.* 22, 798–805. doi:10.1111/rec.12143

Di Carlo, E., Boullemant, A., and Courtney, R. (2019a). A field assessment of bauxite residue rehabilitation strategies. *Sci. Total Environ.* 663, 915–926. doi:10.1016/j.scitotenv.2019.01.376

Di Carlo, E., Boullemant, A., and Courtney, R. (2020). Ecotoxicological risk assessment of revegetated bauxite residue: Implications for future rehabilitation programmes. *Sci. Total Environ.* 698, 134344. doi:10.1016/j.scitotenv.2019.134344

Di Carlo, E., Chen, C., Haynes, R., Phillips, I., and Courtney, R. (2019b). Soil quality and vegetation performance indicators for sustainable rehabilitation of bauxite residue disposal areas: A review. *Soil Res.* 57, 419–446. doi:10.1071/sr18348

Dong, M., Shao, Y., Xu, Z., Liu, X., Xu, Y., Hu, X., et al. (2021). Resilience of fungal flora in bauxite residues amended with organic matter and vermiculite/fly ash. *J. Environ. Manage.* 284, 112052. doi:10.1016/j.jenvman.2021.112052

Du, J., Liu, K., Huang, J., Han, T., Zhang, L., Anthonio, C. K., et al. (2022). Organic carbon distribution and soil aggregate stability in response to long-term phosphorus addition in different land-use types. *Soil Tillage Res.* 215, 105195. doi:10.1016/j.still.2021.105195

Feigl, V., Ujaczki, E., Vaszita, E., and Molnar, M. (2017). Influence of red mud on soil microbial communities: Application and comprehensive evaluation of the Biolog EcoPlate approach as a tool in soil microbiological studies. *Sci. Total Environ.* 595, 903–911. doi:10.1016/j.scitotenv.2017.03.266

Goloran, J. B., Phillips, I. R., and Chen, C. (2017). Forms of nitrogen alter plant phosphorus uptake and pathways in rehabilitated highly alkaline bauxite processing residue sand. *Land Degrad. Dev.* 28, 628–637. doi:10.1002/ldr.2630

Gupta, P., Couperthwaite, S. J., Santini, T. C., Pepper, R. A., and Millar, G. J. (2019). Experimental and geochemical modelling investigations on the weathering behaviour of bauxite residue: Effect of pH. *J. Environ. Chem. Eng.* 6, 103509. doi:10.1016/j.jece.2019.103509

Harris, M. A., and Rengasamy, P. (2004). Sodium affected subsoils, gypsum, and green-manure: Inter-actions and implications for amelioration of toxic red mud wastes. *Environ. Earth Sci.* 45, 1118–1130. doi:10.1007/s00254-004-0970-y

Haynes, R., and Zhou, Y. F. (2019). Natural ripening with subsequent additions of gypsum and organic matter is key to successful bauxite residue revegetation. *J. Cent. South Univ.* 26, 289–303. doi:10.1007/s11771-019-4001-2

Higgins, D., Curtin, T., and Courtney, R. (2017). Effectiveness of a constructed wetland for treating alkaline bauxite residue leachate: A 1-year field study. *Environ. Sci. Pollut. Res.* 24, 8516–8524. doi:10.1007/s11356-017-8544-1

Jones, B. E. H., Haynes, R. J., and Phillips, I. R. (2012a). Addition of an organic amendment and/or residue mud to bauxite residue sand in order to improve its properties as a growth medium. *J. Environ. Manage.* 95, 29–38. doi:10.1016/j.jenvman.2011.09.014

Jones, B. E. H., Haynes, R. J., and Phillips, I. R. (2012b). Addition of an organic amendment and/or residue mud to bauxite residue sand in order to improve its properties as a growth medium. *J. Environ. Manag.* 95, 29–38. doi:10.1016/j.jenvman.2011.09.014

Ke, W., Zhang, X., Zhu, F., Wu, H., Zhang, Y., Shi, Y., et al. (2021). Appropriate human intervention stimulates the development of microbial communities and soil formation at a long-term weathered bauxite residue disposal area. *J. Hazard. Mater.* 405, 124689. doi:10.1016/j.jhazmat.2020.124689

Kong, X., Li, M., Xue, S., Hartley, W., Chen, C., Wu, C., et al. (2017). Acid transformation of bauxite residue: Conversion of its alkaline characteristics. *J. Hazard. Mater.* 324, 382–390. doi:10.1016/j.jhazmat.2016.10.073

Kong, X., Tian, T., Xue, S., Hartley, W., Huang, L., Wu, C., et al. (2018). Development of alkaline electrochemical characteristics demonstrates soil formation in bauxite residue undergoing natural rehabilitation. *Land Degrad. Dev.* 29, 58–67. doi:10.1002/ldr.2836

Le Bissonnais, Y. (1996). Aggregate stability and assessment of soil crustability and erodibility: I. Theory and methodology. *Eur. J. Soil Sci.* 67, 11–21. doi:10.1111/ejss.4_12311

Li, Y., Haynes, R. J., Chandrawana, I., and Zhou, Y. F. (2018). Properties of seawater neutralized bauxite residues and changes in chemical, physical and microbial properties induced by additions of gypsum and organic matter. *J. Environ. Manage.* 223, 489–494. doi:10.1016/j.jenvman.2018.06.070

Li, Y. W., Luo, X. H., Li, C. X., Millar, G. J., Li, X. H., and Xue, S. g. (2019). Variation of alkaline characteristics in bauxite residue under phosphogypsum amendment. *J. Central South Univ.* 26, 361–372. doi:10.1007/s11771-019-4008-8

Liu, K., Ding, X., Wang, H. F., Zhang, X., Hozzein, W. N., Wadaan, M. A. M., et al. (2014). Eukaryotic microbial communities in hypersaline soils and sediments from the alkaline hypersaline Huama Lake as revealed by 454 pyrosequencing. *Antonie Leeuwenhoek* 105, 871–880. doi:10.1007/s10482-014-0141-4

Nannipieri, P., Ascher, J., Ceccherini, M. T., Landi, L., Pietramellara, G., and Renella, G. (2003). Microbial diversity and soil functions. *Eur. J. Soil Sci.* 54, 655–670. doi:10.1046/j.1351-0754.2003.0556.x

Pituello, C., Dal Ferro, N., Francioso, O., Simonetti, G., Berti, A., Piccoli, I., et al. (2018). Effects of biochar on the dynamics of aggregate stability in clay and sandy loam soils. *Eur. J. Soil Sci.* 69, 827–842. doi:10.1111/ejss.12676

Power, G., GräFe, M., and Klauber, C. (2011). Bauxite residue issues: I. Current management, disposal and storage practices. *Hydrometallurgy* 108, 33–45. doi:10.1016/j.hydromet.2011.02.006

Qu, Y., Li, H., Wang, X., Tian, W., Shi, B., Yao, M., et al. (2019). Bioleaching of major, rare earth, and radioactive elements from red mud by using indigenous chemoheterotrophic bacterium acetobacter sp. *Minerals* 9, 67. doi:10.3390/min9020067

Redmile-Gordon, M., Gregory, A., White, R., and Watts, C. (2020). Soil organic carbon, extracellular polymeric substances (EPS), and soil structural stability as affected by previous and current land-use. *Geoderma* 363, 114143. doi:10.1016/j.geoderma.2019.114143

Ruyters, S., Mertens, J., Vassilieva, E., Dehandschutter, B., Poffijn, A., and Smolders, E. (2011). The red mud accident in ajka (Hungary): Plant toxicity and trace metal bioavailability in red mud contaminated soil. *Environ. Sci. Technol.* 45, 1616–1622. doi:10.1021/es104000m

Santini, T. C., and Fey, M. V. (2013). Spontaneous vegetation encroachment upon bauxite residue (red mud) as an indicator and facilitator of *in situ* remediation processes. *Environ. Sci. Technol.* 47, 12089–12096. doi:10.1021/es402924g

Santini, T., Kerr, J., and Warren, L. (2015a). Microbial diversity in engineered haloalkaline environments shaped by shared geochemical drivers observed in natural analogues. *Appl. Environ. Microbiol.* 81, 5026–5036. doi:10.1128/aem.01238-15

Santini, T., Kerr, J., and Warren, L. (2015b). Microbially-driven strategies for bioremediation of bauxite residue. *J. Hazard. Mater.* 293, 131–157. doi:10.1016/j.jhazmat.2015.03.024

Schmalenberger, A., Osullivan, O., Gahan, J., Cotter, P. D., and Courtney, R. (2013). Bacterial communities established in bauxite residues with different restoration histories. *Environ. Sci. Technol.* 47, 7110–7119. doi:10.1021/es401124w

Six, J., Bossuyt, H., Degryze, S., and Denef, K. J. S. (2004). A history of research on the link between (micro) aggregates, soil biota, and soil organic matter dynamics. *Soil tillage Res.* 79, 7–31. doi:10.1016/j.still.2004.03.008

Smart, D., Callery, S., and Courtney, R. (2016). The potential for waste-derived materials to form soil covers for the restoration of mine tailings in Ireland. *Land Degrad. Dev.* 27, 542–549. doi:10.1002/ldr.2465

Tian, T., Liu, Z., Zhu, F., Hartley, W., Ye, Y., and Xue, S. (2020). Improvement of aggregate-associated organic carbon and its stability in bauxite residue by substrate amendment addition. *Land Degrad. Dev.* 31, 2405–2416. doi:10.1002/ldr.3609

Vázquez, E., Benito, M., Espejo, R., and Teutscherova, N. (2020). Response of soil properties and microbial indicators to land use change in an acid soil under Mediterranean conditions. *CATENA* 189, 104486. doi:10.1016/j.catena.2020.104486

Villar, M., Petrikova, V., Dıaz-Ravina, M., and Carballas, T. (2004). Changes in soil microbial biomass and aggregate stability following burning and soil rehabilitation. *Geoderma* 122, 73–82. doi:10.1016/j.geoderma.2003.12.005

Wang, C., Tu, Q., Dong, D., Strong, P. J., Wang, H., Sun, B., et al. (2014). Spectroscopic evidence for biochar amendment promoting humic acid synthesis and intensifying humification during composting. *J. Hazard. Mater.* 280, 409–416. doi:10.1016/j.jhazmat.2014.08.030

Wilpiszeski, R. L., Aufrecht, J. A., Retterer, S. T., Sullivan, M. B., Graham, D. E., Pierce, E. M., et al. (2019). Soil aggregate microbial communities: Towards understanding microbiome interactions at biologically relevant scales. *Appl. Environ. Microbiol.* 85, e00324–e00319. doi:10.1128/aem.00324-19

Wu, C., Xia, J., and Duan, Z. (2015). Review on detection methods of soil organic matter(SOM). *Soils* 47, 453–460.

Wu, H., Tang, T., Zhu, F., Wei, X., and Xue, S. (2021). Long term natural restoration creates soil-like microbial communities in bauxite residue: A 50-year filed study. *Land Degrad. Dev.* 32, 1606–1617. doi:10.1002/ldr.3728

Xue, B., Huang, L., Huang, Y., Yin, Z., Li, X., and Lu, J. (2019a). Effects of organic carbon and iron oxides on soil aggregate stability under different tillage systems in a rice–rape cropping system. *CATENA* 177, 1–12. doi:10.1016/j.catena.2019.01.035

Xue, B., Huang, L., Huang, Y., Zhou, F., Li, F., Kubar, K. A., et al. (2019b). Roles of soil organic carbon and iron oxides on aggregate formation and stability in two paddy soils. *Soil Tillage Res.* 187, 161–171. doi:10.1016/j.still.2018.12.010

Xue, S., Ke, W., Zhu, F., Fan, J., Wang, Q., Liu, Z., et al. (2021). Evaluating aggregate stability, surface properties and disintegration behaviour of bauxite residue induced by Ca/Na. *Land Degrad. Dev.* 32, 803–816. doi:10.1002/ldr.3703

Xue, S., Li, M., Jiang, J., Millar, J. G., Li, C., and Kong, X. (2019c). Phosphogypsum stabilization of bauxite residue: Conversion of its alkaline characteristics. *J. Environ. Sci.* 77, 1–10. doi:10.1016/j.jes.2018.05.016

Xue, S. (2019). Soil formation in bauxite residue: The most promising way to large-scale and ecological disposal. *J. Cent. South Univ.* 26, 265–267. doi:10.1007/s11771-019-3999-5

Xue, S., Wu, Y., Li, Y., Kong, X., Zhu, F., William, H., et al. (2019d). Industrial wastes applications for alkalinity regulation in bauxite residue: A comprehensive review. *J. Cent. South Univ.* 26, 268–288. doi:10.1007/s11771-019-4000-3

Xue, S., Ye, Y., Zhu, F., Wang, Q., Jiang, J., and Hartley, W. (2019e). Changes in distribution and microstructure of bauxite residue aggregates following amendments addition. *J. Environ. Sci.* 78, 276–286. doi:10.1016/j.jes.2018.10.010

Xue, S., Ye, Y., Zhu, F., Wang, Q., Jiang, J., and Hartley, W. (2019f). Changes in distribution and microstructure of bauxite residue aggregates following amendments addition. *J. Environ. Sci. (China)* 78, 276–286. doi:10.1016/j.jes.2018.10.010

Xue, S., Zhu, F., Kong, X., Wu, C., Huang, L., Huang, N., et al. (2016). A review of the characterization and revegetation of bauxite residues (Red mud). *Environ. Sci. Pollut. Res.* 23, 1120–1132. doi:10.1007/s11356-015-4558-8

Yang, X., Cheng, L., Huang, X., Zhang, Y., and L Eb Ailly, P. (2020). Incentive mechanism to promote corn stalk return sustainably in Henan, China. *Sci. Total Environ.* 738, 139775. doi:10.1016/j.scitotenv.2020.139775

You, F., Zhang, L. P., Ye, J., and Huang, L. B. (2019). Microbial decomposition of biomass residues mitigated hydrogeochemical dynamics in strongly alkaline bauxite residues. *Sci. Total Environ.* 663, 216–226. doi:10.1016/j.scitotenv.2019.01.317

Zhao, C., Zheng, T., Feng, Y., Xuan, W., Lizhan, Z., Qitiao, H., et al. (2022). Engineered Halomonas spp. for production of l-Lysine and cadaverine. *Bioresour. Technol.* 349, 126865. doi:10.1016/j.biortech.2022.126865

Zhao, J., Chen, S., Hu, R., and Li, Y. (2017). Aggregate stability and size distribution of red soils under different land uses integrally regulated by soil organic matter, and iron and aluminum oxides. *Soil Tillage Res.* 167, 73–79. doi:10.1016/j.still.2016.11.007

Zhu, F., Jingtao, H., Xue, S., Chuan, W., Qiongli, W., and Hartley, W. (2017). Vermicompost and gypsum amendments improve aggregate formation in bauxite residue. *Land Degrad. Dev.* 28, 2109–2120. doi:10.1002/ldr.2737

Zhu, F., Li, X., Xue, S., Hartley, W., Wu, C., and Han, F. (2016a). Natural plant colonization improves the physical condition of bauxite residue over time. *Environ. Sci. Pollut. Res.* 23, 22897–22905. doi:10.1007/s11356-016-7508-1

Zhu, F., Li, Y., Xue, S., Hartley, W., and Wu, H. (2016b). Effects of iron-aluminium oxides and organic carbon on aggregate stability of bauxite residues. *Environ. Sci. Pollut. Res.* 23, 9073–9081. doi:10.1007/s11356-016-6172-9

Zhu, F., Liao, J., Xue, S., Hartley, W., Zou, Q., and Wu, H. (2016c). Evaluation of aggregate microstructures following natural regeneration in bauxite residue as characterized by synchrotron-based X-ray micro-computed tomography. *Sci. Total Environ.* 573, 155–163. doi:10.1016/j.scitotenv.2016.08.108

Zhu, F., Xue, S. G., Hartley, W., Huang, L., Wu, C., and Li, X. F. (2016d). Novel predictors of soil Genesis following natural weathering processes of bauxite residues. *Environ. Sci. Pollut. Res.* 23, 2856–2863. doi:10.1007/s11356-015-5537-9

Zhu, X., Yao, J., Wang, F., Yuan, Z., Liu, J., Jordan, G., et al. (2018). Combined effects of antimony and sodium diethyldithiocarbamate on soil microbial activity and speciation change of heavy metals. Implications for contaminated lands hazardous material pollution in nonferrous metal mining areas. *J. Hazard Mater* 349, 160–167. doi:10.1016/j.jhazmat.2018.01.044